FOR REFERENCE ONLY

ProQuest LLC.
789 East Eisenhower Parkway
P.O. Box 1346
Ann Arbor, MI 48106 – 1346

A Study of Novel Biomaterials Incorporating Silica for Potential Application in Bone Repair.

DAVID EGLIN

A thesis submitted in partial fulfilment of the
requirements of The Nottingham Trent University
for the degree of Doctor of Philosophy.

This research programme was carried out
in collaboration with Smith & Nephew Ltd.

Nottingham

January 2003

Abstract

This thesis is concerned with the synthesis of poly(α-hydroxyacid)-silica composites, the study of their structure and their *in vitro* apatite-forming ability.

Poly(ε-caprolactone) and poly(L-lactic acid)-silica composites were prepared by a bulk, a sol-gel and a new reactive bulk method.

Statistical experimental design was used to study the effect of sol-gel reactants on the crystallinity of the hydroxyl terminated poly(α-hydroxyacids)-silica composites measured by differential scanning calorimetry and powder X-ray diffraction. The materials studied can be described, for a high silica content, as a co-continuous organic and inorganic structure and, for a low silica content, as a dispersed inorganic phase in an organic polymer. Other analytical techniques: infrared spectroscopy, thermal analysis and transmission electron microscopy were also used to study the effects of the silica content in the composite, the effect of poly(α-hydroxyacid) end-group modifications and the effect of procedural modifications on the nature of the prepared materials.

Methods of study of the *in vitro* apatite-forming ability of the composites were developed and compared. Mechanisms of *in vitro* apatite formation and the effect of the materials structure were tentatively elucidated. The study showed that a minimum amount of silica in the composites was necessary to observe *in vitro* apatite-formation and the formation of a silica gel layer on the material surface is probably the important step for the formation of an hydroxyapatite layer.

Finally, a new synthetic route to these composite materials was developed that could potentially lead to useful poly(α-hydroxyacid)-silica materials for medical applications. The mechanical and bioactivity properties of these materials were investigated and compared with those of other biomaterials such as poly(L-lactic acid) and Bioglass ®.

Abbreviations

PCL	Poly(ε-caprolactone)
PLA	Poly(lactic acid)
PDLLA	Poly(D,L-lactic acid)
PLLA	Poly(L-lactic acid)
PGA	Poly(glycolic acid)
TEOS	Tetraethyl orthosilicate
TMOS	Tetramethyl orthosilicate
THF	Tetrahydrofuran
EtOH	Ethanol
MeOH	Methanol
HCl	Hydrochloric acid
T22EH	Tin(II) 2-ethylhexanoate
DSC	Differential scanning analysis
XRD	Powder X-ray diffraction analysis
FTIR	Fourier transform infrared
DRIFT	Diffuse reflectance infrared
TGA	Thermo gravimetric analysis
TEM	Transmission electron microscope
SEM	Scanning electron microscope
EDXA	Energy dispersive X-ray analysis
NMR	Nuclear magnetic resonance
GPC	Gel permeation chromatography
T_m	Melting Temperature
Cr_{DSC}	Crystallinity measured by DSC
RCr_{XRD}	Relative crystallinity index measured by XRD
M_n	Number average molecular weight measured
M_w	Weight average molecular weight measured
Pd	Polydispersity equal to Mw/Mn

HAP	Hydroxyapatite
OCP	Orthocalcium phosphate
TCP	Tricalcium phosphate
SBF	Simulated body fluid
SBP	Static biomimetic process
DBP	Dynamic biomimetic process
ASP	Alternate soaking process

Contents

Biomaterials are materials of natural or synthetic origin that are used to direct, supplement, or replace the functions of living tissues of the human body. Medical practice today utilizes a large number of materials in the form of implants (sutures, bone plates, joint replacements, ligaments, vascular grafts, heart valves, lenses, dental implants, artificial skin, etc) and medical devices (lenses, pacemakers, biosensors, artificial hearts, blood tubes, drugs carrier etc).

These imply that the properties of the materials must respond to the specific need of each application. The following introduction reviews briefly the biomaterials field. Important terms for the comprehension of the key issues of materials used as biomedical devices are defined. Hard and soft tissues will be described briefly; materials for bone repair and specifically internal load-bearing medical devices will be discussed. Biological hard tissues like bone show combinations of strength and toughness that are hard to duplicate with synthetic materials. The composites of organic and inorganic phases with organised microstructures have interesting mechanical properties as well as potential new bioactivity properties. They are the scope of this research. Bio-inspired organic-inorganic hybrid materials could respond to the needs of biomedical applications of today and tomorrow. Finally, the potential use of polymer-silica biodegradable composites as a biomaterial is introduced as well as the actual state of the art.

1.1. Introduction

Biomaterials are materials in contact with living tissue[1]. Their mechanical properties and their interaction with living tissues guide their use as biomaterials. They must not interact adversely with the body, must be sterile, have the required mechanical strength, and degrade or not, to match the properties of the living tissue replaced (bone, skin, etc) to complete the properties required by the medical application. The oldest material used in a medical application has been traced back to the Egyptians. Artificial teeth and fillings have been found in mummies[2]. Until early in the twentieth century, plant, ore, and animal sources were the only materials used in the practice of wound closure and dental repair. In 1788, a porcelain material was specially developed to make artificial teeth. Since then, progress has been phenomenal due to the appearance of new synthetic materials. Metal prosthetic implantations have been carried out since the mid 1920s[3]; as early as the 1930s poly(methyl methacrylate) has been used as a tooth filling[4, 5]. Biomaterials in common use by the general population include contact lenses whose use dates back to the 1950s[4]. The research on new materials was based on trial and error in the early days. Use of technologies has enabled biomedical material researchers to develop a wide range of new, tailored materials that offer the promise to greatly improve the quality of life of many people. The quality of natural tissues is usually a key factor in governing people's quality of life, and because "the quality of life" is something that concerns us all, there is a large amount of research on biomaterials.

First, because the field of biomaterials is relatively new and that scientists from very different specialities, chemists, material scientists, biologists, surgeons, etc, are usually involved in the development of the materials, the terms defining qualitatively the biomaterials are often employed with different meaning. That is why below is listed the definition of the more useful terms used in the field. The definitions below are generally those utilized and employed in the more recent studies and reviews.

1.2. Definitions

Biomaterials are any substance (other than a drug) or combination of substances, synthetic or natural in origin, which can be used for any period of time, as a whole or a part of a system which treats, augments, or replaces any tissue, organ, or function of the body[6].

Bioabsorbable materials are solid polymeric materials or devices, which can dissolve in body fluids without any polymer chain cleavage or molecular mass decrease. An example is the case of slow dissolution of water-soluble implants in body fluids. A bioabsorbable polymer can be bioresorbable if the dispersed macromolecules are excreted[7].

Bioactivity is the characteristic of an implant material that allows it to form a bond with living tissues[8]. For example, bioactive ceramics for bone implants create an environment compatible with osteogenesis (bone growth), with the mineralising interface developing as a natural bonding junction between living and non-living materials.

Biocompatibility is the acceptance of an implant by surrounding tissues and by the body as a whole. Like other important scientific concepts that change over time, the notion of biocompatibility has evolved in conjunction with the continuing development of materials used in medical devices. Until recently, a biocompatible material was essentially thought of as one that would "do no harm". Today, implants should be compatible with the tissues in terms of mechanical, chemical, surface and pharmacological properties. Simply put, biocompatibility is the ability of the implant material to perform with an appropriate host response in a specific application[9].

Biodegradable materials are solid polymeric materials and devices that break down due to macromolecular degradation with dispersion *in vivo* but there is no proof of elimination from the body. Biodegradable polymeric systems or devices can be attacked by biological elements so that the integrity of the system, and in some cases but not necessarily, of the macromolecules themselves, is affected and gives fragments or other degradation by-products. Such fragments can move away from their site of action but not necessarily from the body[10].

Bioerodible materials are solid polymeric materials or devices, which show surface degradation and further resorb *in vivo*. Bioerosion is thus a concept, too, which

reflects total elimination of the initial foreign material and of surface degradation by-products with no residual side effects.

Bioinert materials are materials inert in the physiological environment and should themselves exert no effect on that environment. In other words, there should be no interaction between biomaterials and the host in the latter case implying that the material should be non-toxic, non-irritant, non-allergenic, non-carcinogenic, non-thrombogenic and so on[11].

Bioresorbable materials are solid polymeric materials and devices which show bulk degradation and further resorb *in vivo*; i.e. polymers which are eliminated through natural pathways either because of simple filtration of degradation by-products or after metabolization. Bioresorption is thus a concept, which reflects total elimination of the initial foreign material and of bulk degradation by-products with no residual side effects[12].

Osteoconduction is the ability of a material to guide repair in bone where normal healing will occur if left untreated[13].

Osteoinductive property is the ability of a material to repair in a location that would normally not heal if left untreated[14]. This requires the presence of bone morphogenic (BMP) proteins and other factors that are only present in natural bone. BMP's cause bone cells to multiply and hence increase the rate of bone matrix formation by activating precursor cells to differentiate into osteogenic cells.

Osteoproductive property is the process whereby a biological surface is colonised by osteogenic stem cells free in the defect environment as a result of surgical intervention. An extra- and an intra- cellular response are elicited by a bioactive material at the interface. Osteoproductive materials cause the existing bone cells to produce matrix at an increased rate and enhance the rate of proliferation of already existing osteoprogenitor cells, but do not cause precursor cells to become osteogenic[13, 15].

1.3. Living tissues

1.3.1. The interaction of biomaterials with living tissues

The clinical success of an implant is directly dependent upon the response of the host (living tissue) to the perturbation brought about by the foreign material.
The implant can be accepted or rejected (toxicity) by its living environment. The physical and chemical morphology of the material (bulk and surface) are the key to their biocompatibility. For some applications such as bone or skin replacement, biomaterials must present the property of cell adhesion (bioactive). Such a property is however unacceptable for catheters, where blood can form clots; or in the breast[16], where a fibrous capsule can appear with transformation of aspect and loss of bonding with the living tissue. It is clear that the interface and response of the host tissue to the biomaterial is important for the success of the implant[17]. At the very least the materials should be bioinert, with no negative response from the host tissue (rejection), at the best be bioactive with formation of close bonding.

Generally, tissues are grouped into hard and soft tissues. Bone and tooth are examples of hard tissues, and skin, blood vessels, cartilage and ligaments are a few examples of soft tissues. Only bone will be discussed in length here but other tissues in the body such as skin, cornea, cartilage and membranes are the subject of materials replacement and therefore their biochemical constitution is also important.

1.3.2. Hard tissue - Bone

Bone forms the endoskeleton which supports the human body. It must withstand acute mechanical forces and must be flexible. It has the properties to regenerate itself and therefore heals itself when damaged. It is also an important ion reservoir. The bone is by weight about 60% mineral, 30% organic matrix, 10% water. Bone is also a living tissue and 15% of its weight is due to the cellular content. There are two types of bone, compact or cortical, and cancellous or trabecular bones. The differences between types of bone are their density and their location[18].

The bone architecture and framework is provided by the collagen fibres, with the HA particles located between the fibres (Figure 1.1). The ground substance is formed from proteins, polysaccharides and mucopolysaccharides which act as a cement, filling the spaces between collagen fibres and the mineral phase. In bone, the hydroxyapatite (HAP) ($Ca_{10}(PO_4)_6(OH)_2$) crystals fit in the 37.5 nm gap between the "heads and tails" of the microfibrils. The crystallites are 20 to 40 nm in length and approximately 5 nm

thick, with the long axis orientated along the length of the fibril. These components are important and form the bulk of the bone, but do not provide the real "dynamic" part of the bone. It is the voids that are fluid filled and contain the cells that create (osteoblasts) and resorb (osteoclasts) the surrounding bone, and it is this part of the bone that governs its structure and state of health.

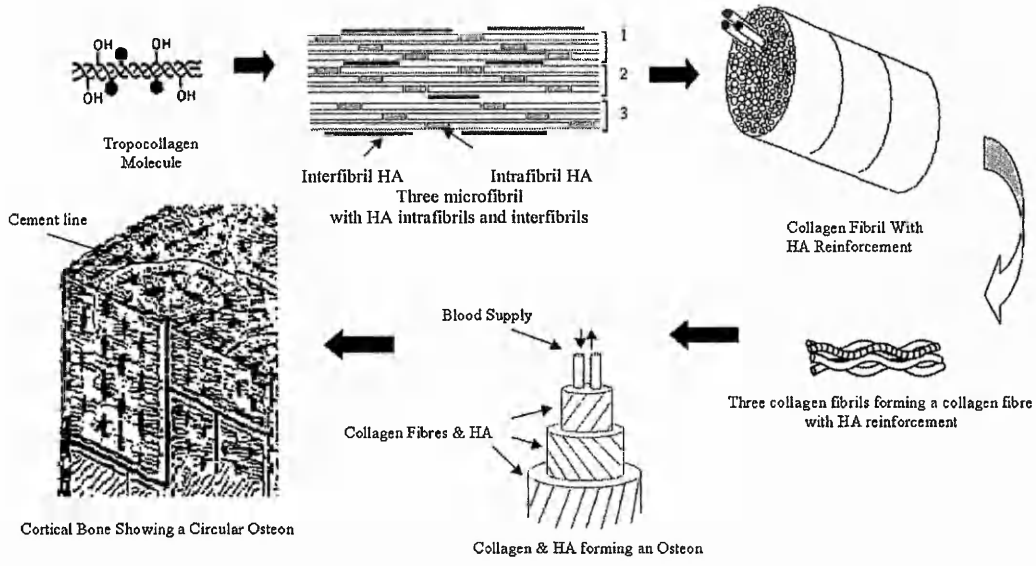

Figure 1.1: Bone schematic morphology[19].

The bone can then be described as a natural composite material with specific nanoscopic morphology which explain its outstanding and anisotropic mechanical properties (Table 1.1).

Table 1.1 : Mechanical properties of biological tissues taken from J. D. Currey [20].

Hard Tissue	**Young's Modulus (Gpa)**	**Tensile Strength (Mpa)**
Cortical bone	3-30	80-150
Cancellous bone	0.1-0.4	5-10
Enamel	84.3	10
Dentine	11.0	39.3
Soft Tissue	**(MPa)**	
Articular Cartilage	10.5	27.5
Ligament	303.0	29.5
Skin	0.1-0.2	7.6

1.4. Materials for Orthopaedic Applications

From a material scientist's point of view, biomaterials can be grouped into five categories, some of them with sub classifications such as biodegradable or non-biodegradable, inert, and bioactive. Two categories are discussed in more detail in the following section; biodegradable synthetic polymers and composite materials. However, most of the materials described in Figure 1.2, have been considered for orthopaedic applications and with success. Table 1.2 lists the modulus and tensile strength of the major materials used in today's biomedical field.

Table 1.2 : Mechanical properties of typical materials[21, 22, 107].

Material	**Modulus (Gpa)**	**Tensile Strength (MPa)**
Stainless steel	190	586
Ti-alloy	116	965
Amalgam	30	58
Alumina	380	300
Zirconia	220	820
Bioglass	35	42
Hydroxyapatite (HAP)	95	50
Polyethylene (PE)	0.88	35
Polymethylmethacrylate (PMMA)	2.55	59
Polyglycolic acid (PGA)	13	310
Poly(L-lactic acid) (PLLA)	10	150
Poly(ε-caprolactone) (PCL)	0.28	13.3
PGA/ PLA	10	150
Polylactic acid (PLA)/ Carbon Fiber (CF)	125	420
PLLA/ HAP	30	92-180
PLA/ Tricalcium Phosphate (TCP)	5.0	52.0

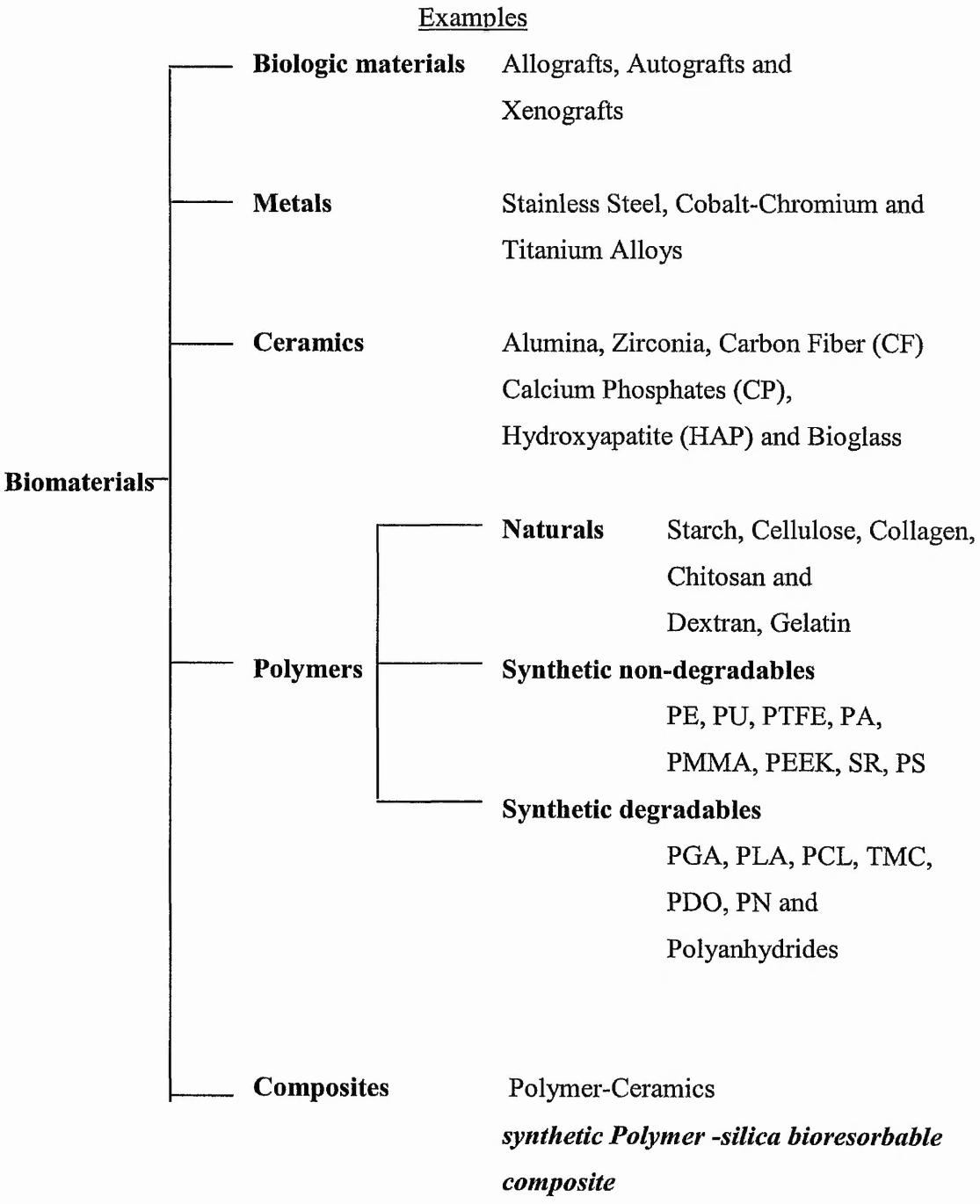

Polyethylene (PE), polyurethane (PU), polytetrafluoroethylene (PTFE), polyacetal (PA), Polymethylmethacrylate (PMMA), polyetheretherketone (PEEK), silicone rubber (SR), polysulfone (PS), poly(glycolic acid) (PGA), poly(lactic acid) (PLA), Poly(ε-caprolactone) (PCL), trimethylene carbonate (TMC), poly(p-dioxanone) (PDO), polyphosphazenes (PN).

Figure 1.2 : Materials used in medical devices[1].

1.4.1. Natural materials

Allograft (graft from dead donor) and autograft (graft from a healthy body part of the patient) materials are the most used natural biomaterials. Their sources, the patient himself or a donor, make them outstanding materials in terms of mechanical properties and biocompatibility[23]. However, they have important drawbacks. The use of allografts is limited by the possibility of an immunological response and the risk of disease transmission[24]. Autografts are restricted by a limited number of donor sites and are associated with additional trauma resulting from the harvesting of tissue. Skin prelevment in patients with severe burns is a well-known example of the use of autografts. Xenografts, grafts from animals, are also currently a field of research, but advances are dependent of the development of better anti-rejection drugs and ethical problems[25].

In this light, man-made materials are still the major field of research for easily available devices, processed and modified to suit the needs of numerous medical applications.

1.4.2. Metals

For many years the guiding principle of synthetic materials development was that the materials should be as chemically inert as possible (body fluids are highly corrosive saline solutions)[11], the devices removable or with a working life higher than the patients life expectancy, and that the materials mechanical properties matched those of the host tissue. Metals were used first for their strength and corrosion resistance[26]. The primary use of inorganic materials such as metals was the repair, replacement, or augmentation of a damaged part of the skeletal scaffold[27]. These materials can bear very high mechanical stress and were relatively inert and resistant. For example, Co-Cr-Mo alloys, stainless steel, and titanium alloys are used as prosthetic joints for hip, knee, shoulder, elbow and wrist repair. Metals are also widely used as dental implants, in heart pacemakers (electrodes), for bone fracture fixation, etc. In spite of their success, the interface instability due to the chemical and mechanical mismatch between metal and host tissue are the cause of possible failure of the bone-implant interface. The body responds to metallic implants by developing a fibrous capsule that isolates the device from the host tissue. The implant can move within the capsule and create local stress concentrations at the interface that lead to loosening, pain and even fracture of the bone

or implant. This happens because metallic implants have moduli of elasticity that are many time larger than those of bone, that means that the implant carries most of the load of the body weight. However bone must be continuously loaded in tension to remain healthy and dense. This problem was called stress shielding[28]. Another problem was that all metals corrode within their fibrous capsule, releasing more or less toxic oxides[29]. Because of the increase of life expectancy and decrease in the average age of patients receiving an implant, the implant lifetime should be extended.

An increase in the interfacial stability or biocompatibility (chemical and mechanical) between biomaterials and host tissue is needed for successful devices. Biocompatibility of orthopedic devices is closely related to cell adhesion to the surface. Surface characteristics of materials, topography, chemistry and surface energy play an essential part in the adhesion and spreading of osteoblasts[30, 31]. For the success of an implant it is critical to establish a good interface between the material and bone tissue with no fibrous tissue[32].

1.4.3. Ceramics

The development of ceramic biomaterials, especially oxides of aluminium and zirconium, eliminated the problem of metallic corrosion of implants. Alumina, for example, was developed especially for hip balls and cups of total femoral prostheses[33]. Zirconia has also been used with success because of its higher toughness and lower modulus of elasticity[11]. However, no improved interfacial stability with the host tissue was acquired over a metal implant. Because of this problem of interfacial stability, new types of ceramic were developed to achieve a stable implant tissue interface; calcium phosphate based ceramics.

Calcium phosphate materials have been extensively studied because of their similarity to the mineral component of bone[34]. As a result, in addition to being non-toxic, they are biocompatible and most importantly they exhibit bioactive behaviour and are integrated in the tissue by the same processes active in remodelling healthy bone. This leads to an intimate physicochemical bond between calcium phosphate implants and bone. The calcium phosphate ceramics are usually obtained either by high temperature processing >500 °C[35] or through a solution mineralization at ambient temperature[36]. Different types of calcium phosphate materials can be prepared with

different bioactivity, degradation and mechanical properties[37]. However, the use of calcium phosphate ceramics as load-bearing biomaterials has a major limitation, due to their poor mechanical behaviour, especially for porous ceramics. Another major drawback is the somewhat unpredictable biodegradation profile of degradable calcium phosphate ceramics such as tricalcium phosphate[38].

Interest in calcium phosphate containing ceramics has been kept alive due to the new attractive bioactive ceramics or Bioglass® prepared by L. L. Hench and co-workers[39, 40, 41]. The first bioactive ceramic reported by L. L .Hench in 1969, was a glass composed of SiO_2, Na_2O, CaO and P_2O_5. The biocompatibility and non-toxicity of these materials has been demonstrated *in vitro* and *in vivo*[42]. Nucleation and growth of bone mineral has been shown to occur at the surface of the ceramic implanted in bone. A comparative study of the Bioglass® in vivo bioactivity with several calcium phosphates ceramics (TCP, HAP, OCP) on soft and hard bone tissues has shown that Bioglass® outclassed all other ceramics[43, 44]. Typical compositions of the bioactive ceramics are SiO_2, CaO, P_2O_5 and Na_2O. Other types of bioactive ceramic-glass have been prepared such as A-W glass[45] and (Fe, Ca)SiO_3 magnetic glass-ceramic[46]. Since the beginning of the 1990's much work has been dedicated to understand the bioactivity of Bioglass® and other bioactive ceramics. The essential active phase is silica, which seems to induce bonding between glass biomaterials and bone tissue[47]. The silica is vital in Bioglass® for the mineralization of bone and formation of a bond with living tissue[48]. Silica induces calcium phosphate nucleation at the interface between the materials and the living tissue[49, 50]. Also *in vivo* implantation of silica gels in mature rabbit bone showed the formation of a calcium phosphate rich layer but no adhesion of the silica gels[51] and the bone. Recently, Xynos et al.[52] reported that bioactive glass dissolution products exert a genetic control over the osteoblast cell cycle and the rapid expression of genes that regulate osteogenesis and the production of growth factors. Also, the exact significance of silica and the mechanisms involved in the mineralization of calcium phosphate by bioactive ceramics is not completely understood, and several mechanisms are still under discussion[53,54,55]. In Figure 1.3 reported from L. L. Hench[40] are the 11 steps necessary for the bone bonding of a bioactive ceramic implanted in bone.

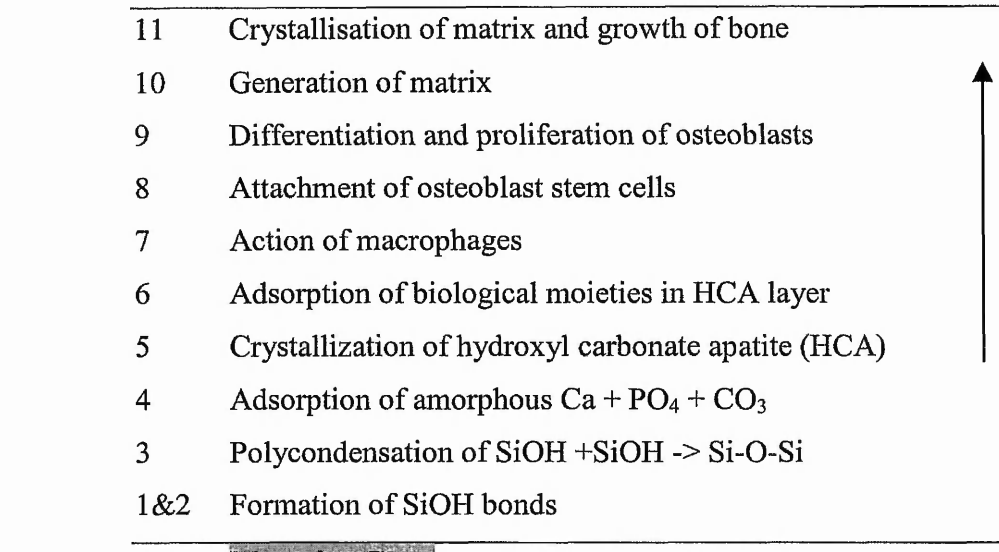

Figure 1.3 : Sequence of interfacial reactions involved in forming a bond between tissue and bioceramics[40].

In Table 1.3 is collected the compositions and degradation times of the more studied calcium phosphate ceramics.

Table 1.3 : Composition, degradation time *in vivo* and solubility constants (Ksp) of calcium phosphate and bioceramic materials at 25°C.

Compounds	**Composition**	**Degradation Time (*in vivo*)**	**p Ksp (25°C)**
Hydroxyapatite (HAP)	$[Ca_{10}(PO_4)_6(OH)_2]$	no resorption or > 2 years	115-117
Octacalcium Phosphate (OCP)	$[Ca_8H_2(PO_4)_6.5H_2O]$	no resorption	96.6-98.6
Tricalcium Phosphate (TCP)	$[Ca_3(PO_4)_2]$	several months	25.5-29.7
Bioglass Melt	SiO_2-P_2O_5CaO-Na_2O system	several years[56]	
Bioglass ® Sol-Gel	SiO_2- P_2O_5CaO-Na_2O system	40% absorption after 1 year[56]	
A-W ceramics	MgO-CaO-SiO_2-CaF_2 system	no resorption after 1 year[57]	

Another type of material; organic polymeric materials have also been studied for biomaterial applications because of the wide properties that can be obtained, notably mechanical and degradation.

1.4.4. Polymeric Materials

1.4.4.1. Synthetic Non Resorbable Polymers

A non-biodegradable or non-resorbable polymer is a polymer which does not undergo significant change in its chemical structure when exposed to the biological environment. Devices such as hard contact lenses, and bone cement are made of poly(methylmethacrylate) (PMMA), a non-biodegradable polymer. Hence researchers started to develop plastic fracture fixation devices from teflon[28], polyacetal[58] and polyester[59].

Other synthetic non-biodegradable polymers have been widely studied and are currently used in medical applications from breast prostheses to drug delivery systems; PMMA, UHMWPE, PVA, silicone, etc.

1.4.4.2. Biodegradable Polymers

The synthesis and characterisation of biodegradable polymers have been extensively reviewed[60]. A recent article from R. Chandra and R. Rustgi[61] reviews the field of biodegradable polymers, both natural and synthetic, together with their applications.

Natural biodegradable polymers

Starch, cellulose, chitin and chitosan are the most common studied polysaccharides. Chitin and chitosan are widely used in health care and cosmetic industries (moisturizing properties) but also in biomedical applications such as artificial skin[62] and absorbable sutures and drug carriers[63]. Polypeptides of animal origin such as gelatin and collagen in industrial, pharmaceutical and biomedical uses are important. Gelatin is an animal protein, water soluble and biodegradable. Biodegradable hydrogels for skin repair and encapsulation of drugs have been developed from collagen and gelatin[64]. The drawback of natural bioresorbable materials especially when extracted from natural products is the poor control over the structure, molecular weight and polydispersity. Therefore the biodegradation and the mechanical control are difficult, and more problematic is the availability of the materials which can be scarce.

Synthetic bioresorbable polymer

Since the development in the early 1970's of the first synthetic resorbable polymer, polyglycolic acid, biodegradable polymers have become increasingly important in biomedical applications. Numerous type of polymers and their use as medical devices have been studied; the poly(p-dioxanones)[65],

the polyhydroxyalkanoates[66], the polyanhydrides[67], the polyphosphazenes[68], the poly(α-hydroxyacids)[69] etc. The poly(α-hydroxyacids) are probably the best characterised and most widely studied biodegradable system[70]. Polyglycolic acid (PGA), polylactic acid (PLA) and poly(ε-caprolactone) (PCL) are the more commonly studied bioresorbable synthetic polyesters in the field of biomaterials[71, 72, 73]. Back in the 1970's, the first poly(α-hydroxyacids) were patented for use as bioresorbable sutures[74]. Since then they have been considered for numerous applications from carrier drugs[67, 75], tissue engineering[76], to orthopaedic applications[77]. For example, poly(glycolic acid)[78] and co-poly(caprolactone-glycolic acid) are used as resorbable sutures. In 1962, polyglycolic acid was developed as the first absorbable suture: Dexon® by American Cyanamid Co[79]. Another example is the use of poly(L-lactide) as plates and screws for internal fixation[77]. A patent for the use of poly(lactic acid) as a resorbable suture material was first filed in 1967[74]. Poly(α-hydroxyacids) have been extensively used as carrier drugs and applications are comprehensively reviewed[77]. Completely resorbable orthopaedic devices are used for treatment of certain bone fractures. Rods made of self-reinforced PGA were commercialised under the name of Biofix® in 1987[80], and in the last decade, several bioresorbable poly(α-hydroxyacids) interference screws have been commercially available[81]. Poly(lactic acid), poly(glycolic acid), poly(ε-caprolactone) and their copolymers are probably the best defined bioresorbable synthetic polymers with regard to their synthesis and degradation performance (Table 1.4)[82].

Hydrolytic degradation of poly(α-hydroxyacids) and all other degradable polymers, is dependent on many factors other than their intrinsic structure, their crystalline order[83], their molecular weight and morphology in general[84], their purity (catalyst traces), their processing[85], sterilization and storage conditions[86], and site of implantation.

Table 1.4 : *In vitro* degradation rate of poly(α-hydroxyacids), in deionised water at 37°C[81, 84].

Poly(α-hydroxyacid)	**Degradation time (months)**
PGA	6 to 12
PDLA	12 to 16
PLLA	> 24
PCL	> 24
PLA-PGA 50/50	1 to 2

The advantage of poly(α-hydroxyacids) over other biodegradable polymers is that the products of degradation released are bioassimilable through metabolic pathways[87]. Mechanical properties of the poly(α-hydroxyacids) (Table 1.5) can be tailored via their morphology control. Increasing their molecular weight and their crystallinity, drastically improved their toughness. Processing also improved the mechanical properties of the materials[88] and self-reinforced polyesters have also been shown to produce high strength devices.

Table 1.5 : Mechanical properties of poly(α-hydroxyacids), hard tissues and metals.

Material	**Tensile strength (MPa)**	**Young's modulus (GPa)**
Cancellous bone	5-10	0.1
Cortical bone	80-150	3-30
Titanium	140	116
Stainless steel	414	171.1
PLLA[(a)89]	75-83	4-5
PDLLA[(b)89]	42-51	
SR-PGA[(c)] (Bionx®)	310	13
SR-PLLA[(d)] (Bionx®)	200	10
PCL[(e)]	13.3	0.28

(a)PLLA; Poly(L-lactic acid), PDLLA; poly(D,L-lactic acid), SR-PGA; self reinforced Polyglycolic acid, SR-PLLA; self reinforced Poly(L-lactic acid), PCL; Poly(ε-caprolactone).

These polymers, poly(α-hydroxyacids), respond to a lot of the medical device imperatives. They are biocompatible, and their bioresorption and mechanical properties can be controlled. However their lack of bioactivity and their limited mechanical properties have been limiting factors for applications where strong bonding is needed with the host tissue.

1.4.5. Composite materials

The aim of making composite materials is to bring out the best of the combined phases. Polymer materials tend to be too flexible and have no osteoconductivity properties. Metals are prone to corrosion and release toxic oxides. Ceramics are often

too brittle and very difficult to fabricate making them poor candidates for load bearing devices. Actually, bone and most human tissues are essentially composite materials. Therefore it makes sense to prepare composites for biomedical applications. The design of a composite material was thought to be a solution to tailoring materials to suit the mechanical and physiological conditions of the host tissue.

Much effort is being devoted to methods of modifying surfaces of existing biomaterials to achieve the desired biological responses[90]. The surface morphology and roughness are altered to influence cell and tissue responses to implants. For example, mineral deposits in bone cell cultures can be altered by surfaces with pits and grooves. Biochemical methods have been used involving immobilization of proteins, enzymes or peptides on the biomaterials for the purpose of inducing specific cell and tissue responses (adhesion, attachment)[31]. Physicochemical methods have been investigated to modify the biomaterials surface chemistry with grafted organic compounds[91, 92] and calcium phosphate materials. This last approach has been considered by several authors; A. G. Stamboulis and co-workers[93] have prepared biodegradable poly(D, L-lactic acid) (PDLLA) coated with Bioglass® and showed the *in vitro* apatite forming ability of the composites. However dissolution, as well as cracking and separation of the coating from the support, remain a concern. This method has also been used with success for load bearing devices such as polymer (PDLLA, PMMA) coated synthetic hydroxyapatite[94]. However, fully degradable materials are not possible using such techniques because the bioactivity property will be lost during the degradation of implant.

1.4.5.1. Inorganic-Organic Composites

S. Ramakrishna and colleagues have recently reviewed the biomedical applications of polymer composite materials[9]. Some of the early studies of composites for biomedical applications have focused on the preparation of carbon-polymer materials, such as CF-epoxy[95], CF-PMMA[96], CF-PEEK[9], etc. Resistance to corrosion and good mechanical properties are qualities of these materials but concern arises about their toxicity. These standard engineering fibres have been used mainly in reinforcement of orthopaedic devices, such as femoral hip stems, knee prostheses and fracture fixation plates. They have not been used in bone analogue materials because of the inability of carbon and inert glass to form any bioactive bonds. It is often desirable, for orthopaedic applications that the biomedical device resorbs. The bone is subject to a gradual increase of stress, then reducing the stress shielding effect. A second beneficial effect is

that no operative procedure is necessary to remove the implant. Bioresorbable polymeric materials have been developed and fulfil those requirements for some limited applications (screw, plate). However, this polymer does not show bioactive properties and it is of poor help for the reconstructing of host tissue. That is why, bioactive resorbable organic polymer-inorganic composites is the next step forward for improved biomaterials. Most of the research effort and development of such bioresorbable and bioactive materials has been concentrated on the preparation of organic polymer-calcium phosphate or polymer-bioactive ceramic materials.

The first bioceramic composites were designed to match the natural components of bone; hydroxyapatite, 45 volume %, and collagen 55 volume %[55]. The replacement of natural HAP in the composite was by particulate HAP produced by a synthetic route and the collagen was replaced by a polyethylene (PE). The resultant blend was initially designed to be used as a bone analogue rather than in load bearing orthopaedic devices. Y. Shikinami et al.[97] and other scientists[98], [99] by mixing calcium phosphate as the filler with a polyester matrix of poly(lactic acid), poly(glycolic acid), poly(ε-caprolactone) and poly(methylmethacrylate), were able to prepare a material with mechanical properties close to, and better than, those of bone, with the composite exhibiting controlled resorption and bioactivity. Several patents exist which describe the preparation and processing of biodegradable polymers filled with calcium phosphate[100, 101]. A material is already on the market and is used under the trademarks Super-Fixsorb® and Super-Fixsorb-MX®. More recently an article from D. Skrtic and co-workers[102] describes the preparation of a methacrylate polymer filled with calcium phosphate. Such materials are currently the object of research focus, notably for their biodegradation behaviour[103, 104], their osteoconductivity[105], their morphology[106], and the effect on their physical properties of the ratio of polymer to filler variation together with their mechanical properties[107]. These polymers and their composites are not suitable for major load-bearing applications, but are suitable for small non-load bearing fracture fixation devices, e.g. finger joint replacement. The interest in this region of biocomposites is very high indeed and apatites or calcium containing-polyester materials are the subject of numerous publications on their structures[108] and their properties[109, 110]. There are two obvious and distinct advantages of these types of materials, 1) as the polymer resorbs there is less stress shielding, and 2) the implant simply dissolves away so there is no need for a second operation, unlike the metal plates

used in fracture fixation. But such an approach has shown limitations such as the failure of some synthetically produced composites to match the natural bone modulus[111]. The present generation of synthetic bioactive composites offer a compromise in mechanical properties compared with living bone. The interface between phases in the synthetic composite is one of the most important limiting factors in long-term performance.

However, it seems for us that the approach could be taken further. In fact, it is known from the literature that silica sol-gels can induce calcium phosphate precipitation *in vivo* and that they are biodegradable. Poly(α-hydroxyacids) are well known bioresorbable polymers with interesting mechanical properties for orthopaedic devices. The idea is to study the possibility of preparing poly(α-hydroxyacid)-silica composites which exhibit biodegradation and osteoconductivity as well as good mechanical properties. These organic polymer and inorganic polymer hybrids have been the subject of interest because they combine both phases at the molecular level and therefore new properties can be obtained, optical and mechanical notably.

The sol-gel method has made possible the incorporation, into a growing inorganic network of metal oxide, of an organic polymer solubilized in a solvent. The sol-gel reaction consists of forming dispersed inorganic materials in solvents through the growth of metal oxide polymers. The chemistry is based on the hydrolysis and condensation of metal alkoxides [$M(OR)_z$, where M= Si, Sn, Ti, Zr, Al,…; OR = alkoxy group, commonly OCH_3 and OC_2H_5]. Other approaches have been evaluated to prepare cross-linked hybrid composites, involving copolymerisation for example. Several reviews deal with the preparation by sol-gel methods of organic-inorganic hybrids[112, 113, 114]. As said earlier, the properties of these new high technology materials are dependent on their structural and chemical composition[115]. Optical properties have been probably the driving interest in the preparation of nano-composites[116] but also improving the mechanical properties of organic polymers[117], self-assembling and layered structures[118]. The techniques to make nano-composites have been developed and could be used for the preparation of new types of biomaterial[119].

1.4.5.2. Biomaterial Application of Silica-Polymer Composites

Silica has been used as a filler in PMMA for dental applications for over two decades[120, 121]. The aim was mostly to improve the mechanical properties of the dental

filling. Nanocomposites with biological components for biological purposes are a more recent interest. Few papers have studied the bio-encapsulation of enzymes and drugs using organic polymer-silica sol-gel composites. For example, a biomaterial drug carrier, such as PMMA-silica composites where proteins and enzymes are entrapped have been prepared by the blending of dispersed silica colloids and polymers[122] and more recently by using a sol-gel procedure[123] and an impregnation method[124]. K. Tsuru and co-workers[125] investigated the bioactivity of organically modified silicates starting from PDMS and TEOS, following a sol-gel procedure developed by J. D. Mackenzie[126] and G. L. Wilkes[127]. They reported that inorganic-organic composite polymers containing silanol groups and Ca(II) ions can be bioactive[128]. However, the elastic moduli of well-known ormosils are still lower in comparison with those of human bone, and rubber like materials have been obtained. The groups of T. Kokubo and T. Nakamura have prepared PDMS-modified $CaO-SiO_2-TiO_2$ hybrids via sol-gel methods[129, 130, 131, 132]. They showed that the incorporation of titanium into PDMS modified $CaO-SiO_2$ hybrids increases the Young's modulus and apatite-forming ability of the hybrids, with particular PDMS contents giving properties almost equal to those of human cancellous bone. The same authors also showed the high apatite-forming ability of PDMS-$CaO-SiO_2$ hybrids in the absence of TiO_2[133]. They examined the *in vitro* bioactivity of the PDMS-silica (TEOS/PDMS weight ratio 60/40) hybrid with and without Ca(II) ions after soaking in a simulated body fluid for 30 days[125]. The deposition of an apatite layer was not observed in calcium free material. However, it was observed that calcium phosphate was precipitated on the surface of polyethylene and ethylene vinyl-alcohol copolymer, coated with silanol groups, in similar conditions[134, 135]. This last year, the Kokubo group published a study of the preparation and *in vitro* bioactivity of SiO_2-CaO-poly(tetramethylene oxide) [PMTO] hybrids[136]. They showed the apatite-forming ability of silica-PTMO hybrids soaked in simulated body fluid. Addition of calcium nitrate to the hybrid increased the apatite precipitation on its surface. The synthesis of bioactive poly(methyl methacrylate)-silica hybrid sol-gels has also been reported by S. H. Rhee and J. Y. Choi[137]. They all concluded that it was possible to prepare homogeneous organic polymer-silica hybrids with apatite-forming ability *in vitro* and interesting mechanical properties. They stated their possible use as new kinds of bioactive bone-repairing materials.

Until recently, very little had been reported on the use of poly(α-hydroxyacid)-silica composites in the biomaterials field. Poly(lactic acid)-silica composites prepared by the impregnation method have been studied as a potential drug carrier but the bioactivity of such a material has not been reported[138]. Poly(ε-caprolactone)-silica sol-gel hybrids have been synthesized and characterized by D. Tian et al.[139, 140, 141]. They characterized these materials using conventional materials techniques[142, 143]. They mostly concentrated on the possibility of controlling the porosity of a silica gel by the preparation of interpenetrating networks and the subsequent degradation of the organic polymer by heating[144]. Preliminary *in vitro* cell cultures and biodegradation tests were reported. The attachment and spreading of fibroblasts on the surface of poly(ε-caprolactone)-silica composites were observed[145]. The apatite-forming ability *in vitro* of comparable materials, PCL-SiO_2-CaO hybrids, had not been reported before 2002[146]. H. Kim demonstrated the huge potential of such hybrid materials[147], poly(α-hydroxyacid)-silica composites, which may lead to potential biomedical applications with good apatite-forming, mechanical and biodegradation properties.

1.5. Aims

The aim of this work was to synthesise and study poly(α-hydroxyacid)-silica composite materials for potential biomedical applications. In the light of the literature available, it was decided to repeat and extend the work carried out notably by R. Jerome's group. Poly(α-hydroxyacid)-silica composites were prepared by a bulk and a sol-gel method. A new reactive bulk procedure was also developed for the preparation of composites. Linear poly(ε-caprolactone) and poly(L-lactic acid), two semi-crystalline poly(α-hydroxyacids), were incorporated in the silica phase. The reactivity of both end-groups was varied. The composites were characterised by thermal analysis, powder X-ray diffraction analysis, infrared spectroscopy and electron microscopy techniques. A statistical design approach was carried out to study the physical properties (crystallinity poly(α-hydroxyacid)) of the sol-gel hybrids and to understand the effect of the reactants on the composite structures.

In vitro hydroxyapatite forming ability of the materials was tested using 3 methods; a dynamic, a static biomimetic process and an alternate soaking process. The *in vitro* osteoconductivity properties of poly(α-hydroxyacid)-silica sol-gels and the effect of the change of the poly(ε-caprolactone) for poly(L-lactic acid), the silica and other reactants content and the reactivity of the end-groups on the poly(α-hydroxyacids) were studied.

Finally, the mechanisms of apatite formation on poly(α-hydroxyacids)-silica materials are discussed in the light of the mechanisms proposed for the bioactive glass-ceramics and silica sol-gels.

1.6. References

[1] C. C. Perry (1998) "Chapter 11: Biomaterials. Chemistry of Advanced Materials: An Overview.", Eds. L. V. Interrante, M. J. Hampden-Smith (Wiley-VCH) 499-562.

[2] M. D. K. Bremner (1939), "The story of dentistry from the dawn of civilization to the present.", (Dental items of interest Publishing Company, Brooklyn, New York) 69.

[3] A. A. Zierold (1924), *Archive of Surgery,* 9, 365.

[4] M. Moukwa (1997), "The development of polymer –based biomaterials since 1920s.", *JOM*, 49, 46-50.

[5] H. Lee (1987), "Advances in Biomaterials." 1st Edition" Ed. S. M. Lee, (Technomic Publishing Co., Lancaster).

[6] D. F. Williams (1987), "Tissue-Biomaterials interactions.", *Journal of Materials Science*, 22(10), 3421-3445.

[7] S. Nyman, J. Lindhe, T. Karring, H. Rylander (1982), "New attachment Following surgical treatment of human periodontal disease.", *Journal of Clinical Periodontology,* 9(4), 290-296.

[8] L. L. Hench (1988), "In bioceramics: Materials characteristics versus In-vivo behavior", Eds. P. Ducheyne, J. Lemons (Annals New York Academy of Sciences, New York) 54-71.

[9] S. Ramakrishna, J. Mayer, E. Wintermantel, K. W. Leong (2001), "Biomedical Applications of polymer-composite materials: A review.", *Composites Science and Technology*, 61, 1189-1224.

[10] G. Scott (1995), "Degradable Polymers: Principles & Applications.", Eds. G. Scott, D. Gilead (Chapman & Hall) 34-85.

[11] D. F. Williams (1998), "Handbook of Biomaterial Properties.", Eds J. Black, G. Hastings (Chapman & Hall) 482.

[12] J. Kahn, R. Langer (1996), "In Biomaterials Science. An Introduction to Materials in Medicine." Eds. B. D. Ratner, A. S. Hoffmann, F. J. Schoen, J. E. Lemons, (Academic Press, San Diego) 64.

[13] L. H. Hench, J. M. Polak (2002), "Third –generation biomedical materials.", *Science*, 295, 1014-1018.

[14] K. J. L. Burg, S. Porter, J. F. Kellam (2000), "Biomaterials developments for bone tissue engineering.", *Biomaterials*, 21, 2347-2359.

[15] A. M. Gatti, T. Yamamuro, L. L. Hench, O. H. Andersson (1993), "In vivo reactions in some bioactive glasses and glass-ceramics granules.", *Cells and Materials*, 3(3), 283-291.

[16] D. W. L. Hukins, J. C. Leahy, K. J. Mathias (1999), "Biomaterials: Defining the mechanical properties of natural tissues and selection of replacement materials.", *Journal of Materials Chemistry*, 9,629-636.

[17] L. L. Hench (1982), "Biomaterials, An interfacial approach.", Eds.L. L. Hench, E. C. Ethridge (Academic Press).

[18] A. L. Boskey (1981), "Current concepts of the physiology and biochemistry of calcification.", *Clinical Orthopaedics and Related Research*, 157, 225-257.

[19] http://www.bg.ic.ac.uk/lectures/Hench/BioComp/

[20] J. D. Curry (1984), "The Mechanical Adaptation of Bones.", (University Press, Princeton).

[21] J. Black, G. Hastings (1998), "Handbook of Biomaterial Properties.", eds. J. Black, G. Hastings (Chapman & Hall).

[22] K. Anselme (2000), "Osteoblast adhesion on biomaterials.", *Biomaterials*, 21, 667-681.

[23] H. S. Sandhu, H. S. Grewal, H. Parvataneni (1999), "Bone grafting by spinal fusion.", *Orthopedic Clinics of North America,* 30,685-698.

[24] T. W. Bauer, G. F. Muschler (2000), "Bone graft materials - An overview of the basic science.", *Clinical Orthopaedics and Related Research,* 371:10–27.

[25] H. Burchardt (1983), "The biology of bone-graft repair.", *Clinical Orthopaedics and Related Research*, 174:28–42.

[26] J. B. Park (1992), "Biomaterials. An introduction. 2nd Edition.", eds. J.B. Park, R.S. Lakes, (Plenum Press, NY).

[27] L. L. Hench (1995), "Chapter 21: Material Chemistry: An emerging discipline" (American Chemical Society) 523-547.

[28] A. J. Tonino, C. L. Davidson, P. J. Klopper, L. A. Linclau (1976), "Protection from stress in bone and its effects.", *The Journal of Bone and Joint Surgery,* 58B(1), 107-113.

[29] O. E. M. Poehler (1983), "In Biomaterials in reconstructive surgery. Degradation of metallic orthopedic implants.", ed. Rubin LR (C.V. Mosby Company, St. Louis) 158-228.

[30] K. D. Chesmel, C. C. Clark, C. T. Brighton, J. Black (1995), "Cellular responses to chemical and morphologic aspects of biomaterial surfaces. II. The biosynthetic and migratory response of bone cell populations.", *Journal of Biomedical Materials Research*, 29, 1101-1110.

[31] M. Lampin, R. Warocquier-Clerout, C. Legris, M. Degrange, M. F. Sigot-Luizard (1997), "Correlation between substratum roughness and wettability, cell adhesion, and cell migration.", *Journal of Biomedical Materials Research*, 36, 99-108.

[32] D. A. Puelo, A. Nanci (1999), "Understanding and controlling the bone-implant interface.", *Biomaterials*, 20, 2311-2321.

[33] S. K. Taylor, P. Serekian, M. Manley (1998), "Wear performance of contemporary alumina-alumina bearing couple under hip joint simulation.", *Proceedings of the 44th Orthopaedic Research Society*, 51.

[34] J. C. Elliot (1994), "Studies in Inorganic Chemistry. 18. Structure and Chemistry of the Apatites and Other Calcium Orthophosphates.", Ed J. C. Elliot (Elsvier).

[35] A. C. Tas, F. Korkusuz, M. Timucin and N. Akkas (1997), "An investigation of the chemical synthesis and high-temperature sintering behaviour of calcium hydroxyapatite (HA) and tricalcium phosphate (TCP) bioceramics.", *Journal of Materials Science: Materials in Medicine*, 8, 91-96.

[36] E. Andronescu, E. Stefan, E. Dinu, C. Ghitulica, (2002), "Hydroxyapatite synthesis.", *Euro Ceramics VII, PT 1-3, Key Engineering Materials,* 206-2: 1595-1598.

[37] H. Y. Yasuda, S. Mahara, T. Nishiyama, Y. Umakoshi (2002), "Preparation of hydroxyapatite/α-tricalcium phosphate composites by colloidal process.", *Science and Technology of Advanced Materials*, 3, 29-33.

[38] J. O. Hollinger, J. Brekke, E. Gruskin, D. Lee (1996), "Role of bone substitutes.", *Clinical Orthopaedics and Related Research,* 324, 55-65.

[39] L. L. Hench, R. J. Splinter, W. C. Allen, T. K. Greenlee (1972), "Bonding mechanisms at the interface of ceramic prosthetic materials.", *Journal of biomedical Materials Research*, 2(1), 117-141.

[40] L. L. Hench (17 July 1995), "Bioactive implants.", *Chemistry and Industry*, 547-550.

[41] L. L. Hench (1995), "Inorganic Biomaterials.", *Materials Chemistry: Advances in Chemistry*, 245, 523-545.

[42] J. Wilson, G. H. Pigott, F. J. Schoen, L. L. Hench (1981), "Toxicology and biocompatibility of bioglasses.", *Journal of Biomedical Materials Research*, 15, 805-817.

[43] H. Oonishi, S. Kushitani, H. Imasaki, K. Sako, H. Ono, A. Tamura, T. Sugihara, L. L. Hench, J. Wilson, E. Tsuji (1995), "Comparative bone formation in several kinds of bioceramic granules.", *Proceedings of the Eighth International Symposium on Ceramics in Medicine. Bioceramics 8.* (Pergamon/Elsevier Science Ltd. Oxford, England) 137.

[44] X. Y. Fujishiro, L. L. Hench, H. Oonishi (1997), "Quantitative rates of in vivo bone generation for bioglass® and hydroxyapatite particles as bone graft substitute.", *Journal of Materials Science: Materials in Medicine,* 8, 649-652.

[45] T. Nakamura, T. Yamamuro, S. Higashi, T. Kokubo, S. Itoo (1985), "A new glass-ceramic for bone replacement. Evaluation of its bonding to bone tissue.", *Journal of Biomedical Materials Research*, 19(6),685-698.

[46] R. P. del Real, D. Arcos, M. Vallet-Regi (2002), "Implantable magnetic glass ceramic based on (Fe, Ca)SiO_3 solid solutions." *Chemistry of Materials*, 14, 64-70.

[47] K. H. Karlsson, K. Froberg, T. Ringbon (1989), "A structural approach to bone adhering of bioactive glasses." *Journal of Non-Crystalline Solids,* 112(1-3), 69-72.

[48] L. L. Hench, J. Wilson (1986), "Ciba Foundation Symposium 121. Silicon Biochemistry.Biocompatibility of silicates for medical use.", (Wiley, Chichester), 231-246.

[49] T. Kokubo (1992), "Bone Bonding. Bioactivity of glasses and glass ceramics.", Eds. Ducheyne, T. Kokubo, Van Blitterswijk (Reed Healthcare Communications) 31-46.

[50] S. Radin, S. Falaize, H. L. Mark, P. Ducheyne (2002), "In vitro bioactivity and degradation behavior of silica xerogels intended as controlled release materials.", *Biomaterials,* 23, 3113-3122.

[51] T. Kitsugi, T. Nakamura, M. Oka, S. B. Cho, F. Miyaji, T. Kokubo (1995), "Bone-bonding behavior of three heat-treated silica gels implanted in mature rabbit bone.", *Calcified Tissue International*, 57, 155-160.

[52] I. D Xynos, A. J. Edgar, L. D. K. Buttery, L. L. Hench, J. M. Polak (2001), "Gene-expression profiling of human osteoblasts following treatment with the ionic products of bioglass.", *Journal of Biomedical Materials Research*, 55, 151-157.

[53] M. M. Pereira, L. L. Hench (1996), "Mechanisms of hydroxyapatite formation on porous gel-silica substrates.", *Journal of Sol-Gel Science and Technology*, 7, 59-68

[54] L. L. Hench (1999), "Forty-fifth mellor memorial lecture. Role of inorganic and theoretical chemistry in ceramics: past, present and future.", *British Ceramic Transactions,* 98(5), 246-250.

[55] K. H. Karlsson (1999), "Bone implants- A challenge to materials science.", *Annales Chirurgiae et Gynaecologiae*, 88, 226-235.

[56] M. Hamadouche, A. Meunier, D. C. Greenspan, C. Blanchat, J. P. Zhong, G. P. La Torre, L. Sedel (2001), "Absorbability of bulk sol-gel bioactive glasses.", *Key Engineering Materials*, 192-195, 593-596.

[57] M. Kobayashi, T. Nakamura, J. Tamura, T. Kikutani, S. Nishiguchi, W. F. Mousa, M. Takahashi, T. Kokubo (1999), "Osteoconductivity and bone-bonding strength of high- and low- viscous bioactive bone cement.", *Journal of Biomedical Materials Research. Applied Biomaterials*, 48 (3), 265-276.

[58] L. Eschbach (2000), "Non resorbable polymers in bone surgery.", *Injury-International Journal of the Care of the Injured*, 31: S22-S27 Suppl.

[59] S. A. Brown, J. Vandergrift (1981), "Healing of femoral osteotomies with plastic plate fixation.", *Biomaterial Medical Devices Artificial Organs,* 9(1), 27-35.

[60] A. J. Domb (1997), "Handbook of biodegradable polymers.", Eds. A. J. Domb, J. Kost, D. M. Wiseman, (Harwood).

[61] R. Chandra, R. Rustgi (1998), "Biodegradable polymers.", *Progress in Polymer Science*, 23, 1273-1335.

[62] L. L. Balassa (1972), "Use of chitin for promoting wound healing.", *United States Patent* 3,632,754.

[63] K. Kurita (1998), "Chemistry and application of chitin and chitosan.", *Polymer Degradation and Stability*, 59(1-3), 117-120.

[64] J. S. Ahn, H.-K. Choi, M. K. Chun, J. M. Ryu, J. H. Jung, Y. U. Kim, C. S. Cho (2002), "Release of Triamcinolone acetonide from mucoadhesive polymer composed of chitosan and poly(acrylic acid) in vitro.", *Biomaterials*, 23, 1411-1416.

[65] J. A. Ray, N. Doddi, D. Regula, J. A. Williams, A. Melveger (1981), "Polydioxanone (PDS), a novel mono-filament synthetic absorbable suture.", *Surgery Gynecology & Obstetrics*, 153(4), 497-507.

[66] J. C. Knowles (1993), "Development of a natural degradable polymer for orthopaedic use.", *Journal of Medical Engineering & Technology*, 17(4), 129-137.

[67] A. H. Shikani, A. J. Domb (2000), "Polymer chemotherapy for head and neck cancer.", *Laryngoscope*, 110 (6), 907-917.

[68] K. E. Uhrich, S. M. Cannizzaro, R. S. Langer (1999), "Polymeric system for controlled drug release.", *Chemical Review*, 99, 3181-3198.

[69] Y. Lemmouchi, E. Schacht, P. Kageruka, R. De Deken, B. Diarra, O. Diall, S. Geerts (1998), "Biodegradable polyesters for controlled release of trypanocidal drugs: In vitro and in vivo studies.", *Biomaterials*, 19, 1827-1837.

[70] D. K. Gilding, A. M. Reed (1979), "Biodegradable polymers for use in surgery-polyglycolic/poly(lactic acid) homo- and copolymers.", *Polymer*, 20, 1459-1464.

[71] M. Vert, G. Schwarch, J. Coudane (1995), "Present and future of PLA polymers.", *Journal of Materials Science–Pure Applied Chemistry,* A32(4), 787-796.

[72] A. U. Daniels, M. K. O. Chang, K. P. Andriano (1990), "Mechanical properties of biodegradable polymers and composites proposed for internal fixation of bone.", *Journal of Applied Biomaterials,* 1, 57-78.

[73] P. Tormala, T. Pohjonen, P. Rokkanen (1998), "Bioabsorbable polymers: materials technology and surgical applications." *Proceeding of the Institution of Mechanical Engineers. Part H- Journal of Engineering in Medicine*, 212(H), 101-111.

[74] E. E. Schmitt, R. A. Polistina (1967), "Surgical Sutures.", *US patent* 3,297,033.

[75] R. A. Jain (2000), "The manufacturing techniques of various drug loaded biodegradable poly(lactide-co-glycolide) (PLGA) devices.", *Biomaterials*, 21, 2475-2490.

[76] D. W. Hutmacher (2000), "Scaffolds in tissue engineering bone and cartilage." *Biomaterials*, 21, 2529-2543.

[77] J. W. Leenslag, A. J. Pennings, R. R. M. Bos, F. R. Rozema (1987), "Resorbable materials of poly(L-lactide). VI. Plates and screws for internal fixation." *Biomaterials*, 8, 70-73.

[78] P. H. Graig, J. A. Williams, K. W. Davis, A. D. Magoun, A. J. Levy, S. Bogdansky, J. P. Jr Jones (1975), "A biologic comparison of polyglactin 910 and polyglycolic acid synthetic absorbable sutures.", *Surgery, Gynecology & Obstetrics,* 141,1-10.

[79] E. E. Schmitt, R. A. Polistina (1969), "Cylindrical prosthetic devices of polyglycolic acid.", *US Patent* 3,620,218.

[80] S. Vainionpää, J. Kilpikari, J. Laiho, P. Helevirta, P. Rokkanen, P. Törmälä (1987), "Strength and strength retention in vitro of absorbable, self-reinforced polyglycolide (PGA) rods for fracture fixation.", *Biomaterials*, 8, 46-48.

[81] G. Schwach, M. Vert (1999), "In vitro and in vivo degradation of lactic acid-based interferences screws used in cruciate ligament reconstruction.", *International Journal of Biological Macromolecules,* 25, 283-291.

[82] M. Vert, G. Schwach, R. Engel, J. Coudane (1998), "Something new in the field of PLA/GA bioresorbable polymers?", *Journal of Controlled release*, 53,85-92.

[83] S. Li (1999), "Hydrolytic degradation characteristics of aliphatic polyesters derived from lactic and glycolic acids.", *Journal of Biomedical Materials Research. Applied Biomaterials,* 48, 342-353.

[84] C. G. Pitt (1992), "Biodegradable polymers and plastics. Non-microbial degradation of polyesters. Mechanisms and modifications.", Eds. M. Vert, J. Feijen, A. Albertsson, G. Scott, E. Chiellini, (Royal Society of Chemistry).

[85] M. Dunne, O. I. Corrigan, Z. Ramtoola (2000), "Influence of particle size and dissolution conditions on the degradation properties of polylactide-co-glycolide particles.", *Biomaterials*, 21, 1659-1668.

[86] S. Li, M. Vert (1995), "Chapter 4: Biodegradation of Aliphatic Polyesters. Degradable Polymers: Principles and Applications." Eds G. Scoot, D. Gilead (Chapman and Hall).

[87] M. S. Taylor, A. V. Daniels, K. P. Andriano, J. Heller (1994), "Six bioabsorbable polymers: In vitro acute toxicity of accumulated degradation products.", *Journal of Applied Biomaterials*, 5, 151-157.

[88] K. P. Andriano, T. Pohjonen, P. Tormala (1994), "Processing and characterization of absorbable polylactide polymers for use in surgical implants.", *Journal of Applied Biomaterials*, 5, 133-140.

[89] S. Vainionpaa, P. Rokkanen, P. Tormala (1989), "Surgical applications of biodegradable polymers in human-tissues.", *Progress in Polymer Science*, 14 (5), 679-716.

[90] K. A. Thomas (1994), "Hydroxyapatite coatings.", *Orthopedics*, 17(3), 267-278.

[91] S. Jin, K. Gonsalves (1999), "Functionalized copolymers and their composites with polylactide and hydroxyapatite.", *Journal of Materials Science: Materials in Medicine*, 10, 363-368.

[92] O. N. Tretinnikov, K. Kato, Y. Ikada (1994), "In vitro hydroxyapatite deposition onto a film surface-grafted with organophosphate polymer.", *Journal of Biomedical Materials Research*, 28, 1365-1373.

[93] A. G. Stamboulis, A. R. Boccaccini, L. L. Hench (2002), "Novel biodegradable polymer/bioactive glass composites for tissue engineering applications.", *Advanced Engineering Materials*, 4(3), 105-109.

[94] A. F. Tencer, V. Mooney, K. L. Brown, P. A. Silva (1985), "Compressive properties of polymer coated synthetic hydroxyapatite for bone grafting.", *Journal of Biomedical Materials Research*, 19, 957-969.

[95] M.S. Ali, G. W. Hastings, T. Rae, N. Rushton, E.R.S. Ross, C. H. Wynn-Jones (1990), "Carbon fiber composite bone plates.", *Journal of Bone and Joint Surgery*, 72-B(4), 586-591.

[96] K. A. Jockisch, S. A. Brown, T. W. Bauer, K. Merritt (1992), "Biological response to chopped-carbon-fiber-reinforced peek.", *Journal of Biomedical Materials Research*, 26, 133-146.

[97] Y. Shikinami, M. Okuno (1999), "Material for osteosynthesis and composite implant material, and production processes thereof.", *US patent* 5,981,619.

[98] R. Zhang, P. X. Ma (1999), "Poly(α-hydroxyl acids)/hydroxyapatite porous composites for bone-tissue engineering. I. Preparation and morphology.", *Journal of Biomedical Materials Research*, 44, 446-455.

[99] M. J. Dalby, L. Di Silvio, E. J. Harper, W. Bonfield (2001), "Initial interaction of osteoblasts with the surface of a hydroxyapatite-poly(methylmethacrylate) cement.", *Biomaterials*, 22, 1739-1747.

[100] Y. Imai, Y. Kakizawa, M. Kamikura (1999), "Biodegradable material and process for the preparation thereof.", *US Patent* 5,955,529.

[101] K. Cooper, C. C. Chen, A. Scopelianos (1998), "Hard tissue bone cements and substitutes.", *US Patent* 5,747,390.

[102] D. Skrtic, J. M. Antonucci, E. D. Eanes, F. C. Eichmiller (2000), "Physicochemical evaluation of bioactive polymeric composites based on hybrid amorphous calcium phosphates." *Journal of Biomedical Material Research*, 53 (4), 381-391.

[103] K. G. Marra, J. W. Szem, P. N. Kunta, P. A. DiMilla, L. E. Weiss (1999), "In vitro analysis of biodegradable polymer blend/hydroxyapatite composites for bone tissue engineering.", *Journal of Biomedical Materials Research*, 47, 324-335.

[104] H. Schliephake, T. Kage (2001), "Enhancement of bone regeneration using resorbable ceramics and a polymer-ceramic composite material.", *Journal of Biomedical Materials Research*, 56, 128-136.

[105] M. Kikuchi, J. Tanaka, Y. Koyama, K. Takahuda (1999), "Cell culture test of TCP/CPLA composite.", *Journal of Biomedical Materials Research. Applied Biomaterials*, 48, 108-110.

[106] N. Ignjatovic, S. Tomic, M. Dakic, M. Miljkovic, M. Plavsic, D. Uskokovic (1999), "Synthesis and properties of hydroxyapatite/poly-L-lactide composite biomaterials.", *Biomaterials*, 20, 809-816.

[107] Y. Shikinami, M. Okuno (1999), "Bioresorbable devices made of forged composites of hydroxyapatites (HA) particles and poly-L-lactide (PLLA): Part I. Basic characteristics.", *Biomaterials*, 20, 859-877.

[108] N. L. Ignjatovic, M. Plavsic, M. S. Miljkovic, L. M. Zivkovic, D. P. Uskokovic (1999), "Microstructural characteristics of calcium hydroxyapatites/poly-L-lactide based composites.", *Journal of Microscopy*, 196(2), 243-248.

[109] L. A. Dos Santos, L. C. De Oliveira, E. C. S. Rigo, R. G. Carrodeguas, A. O. Boschi, A. C. F. De Arruda (1999), "Influence of polymeric additives on the mechanical properties of α-tricalcium phosphate cement.", *Bone*, 25(2), 99S-102S.

[110] H. Maeda, T. Kasuga, M. Nogami, Y. Hibino, K. Hata, M. Ueda, Y. Ota (2002), "Biomimetic apatite formation on poly(lactic acid) composites containing calcium carbonates.", *Journal of Materials Research*, 17(4), 727-730.

[111] L.L. Hench (1995), "Inorganic Biomaterials.", *Materials Chemistry. Advances in Chemistry Series,* 245; 523-547.

[112] Y. Chujo, T. Saegusa (1992), "Organic polymer hybrids with silica gel formed by means of the sol-gel method.", *Advances in Polymer Science*, 100, 11-29.

[113] B. M. Novak (1993), "Hybrid nanocomposite materials-between inorganic glasses and organic polymers.", *Advanced Materials*, 5(6), 422-433.

[114] H. Schmidt, G. Jonschker, S. Goedicke, M. Menning (2000), "The sol-gel process as a basic technology for nanoparticle-dispersed inorganic-organic composites.", *Journal of Sol-Gel Science and Technology*, 19, 39-51.

[115] P. Judeinstein, C. Sanchez (1996), "Hybrid organic-inorganic materials: a land of multidisciplinarity.", *Journal of Materials Chemistry*, 6(4), 511-525.

[116] J. D. Mackenzie (1993), "Nonlinear optical materials by the sol-gel method.", *Journal of Sol-Gel Science Technology*, 1(1), 7-19.

[117] J. Y. Wen, G. L. Wilkes (1996), "Organic/inorganic hybrid network materials by the sol-gel approach.", *Chemistry of Materials.*, 8(8), 1667–1681.

[118] M. Alexandre, P. Dubois (2000), "Polymer-layered silicate nanocomposites: preparation, properties and uses of a new class of materials.", *Materials Science and Engineering*, 28, 1-63.

[119] S. Forster, T. Plantenberg (2002), "From self-organizing polymers to nanohybrid and biomaterials.", *Angewandte Chemie International Edition* , 41(5), 688-714.

[120] S. C. Bayne, H. O. Heymann, E. J. Swift, (1994), "Update on dental composite restorations.", *Journal of the American Dental Association*, 125(6), 687-701.

[121] M. L. Cannon (1988), "in Encyclopaedia of dental devices and instrumentation. Composite resins.", ed. J.G. Webster (Wiley & Sons, New-York).

[122] K. Yoshinaga, K. Kondo, A. Kondo (1997), "Capabilities of polymer-modified monodisperse colloid silica particles as biomaterial carrier.", *Colloid Polymers Science*, 275, 220-226.

[123] Y. Wei, K. Qiu (2000), "Synthesis and biotechnological applications of vinyl polymer-inorganic hybrid and mesoporous materials.", *Chinese Journal of Polymer Science*, 18(1), 1-7.

[124] M. Ahola, J. Rich, P. Kortesuo, J. Kiesvaara, J. Seppala, A. Yli-Urpo (1999), "In vitro evaluation of biodegradable ε-caprolactone-co-D,L-lactide/silica xerogel composites containing toremifene citrate.", *International Journal of Pharmaceutics*, 181, 181-191.

[125] K. Tsuru, C. Ohtsuki, A. Osaka, T. Iwamoto, J. D. Mackenzie (1997), "Bioactivity of sol-gel derived organically modified silicates.", *Journal of Materials Sciences: Materials in Medicine*, 8, 157-161.

[126] J. D. Mackenzie, Y. J. Chung, Y. Hu (1992), "Rubbery ormosils and their applications.", *Journal of Non-Crystalline Solids*, 147&148, 271-279.

[127] G. L. Wilkes, B. Orler, H. H. Huang (1985), "Ceramers: Hybrid materials incorporating polymeric/oligomeric species into inorganic glasses utilizing a sol-gel approach.", *Polymer Preparation*, 26, 300-302.

[128] K. Tsuru, Y. Aburatani, T. Yabuta, S. Hayakawa, C. Ohtsuki, A. Osaka (2001), "Synthesis and in vitro behavior of organically modified silicate containing Ca ions.", *Journal of Sol-Gel Science and Technology*, 21, 89-96.

[129] Q. Chen, F. Miyata, T. Kokubo, T. Nakamura (1999), "Apatite formation on PDMS-modified $CaO-SiO_2-TiO_2$ hybrids prepared by sol-gel process.", *Biomaterials*, 20, 1127-1132.

[130] Q. Chen, F. Miyata, T. Kokubo, T. Nakamura (2000), "Bioactivity and mechanical properties of PDMS-modified $CaO-SiO_2-TiO_2$ Hybrids prepared by sol-gel process.", *Journal of Biomedical Materials Research*, 51, 605-611.

[131] Q. Chen, M. Kamitakahara, M. Miyata, T. Kokubo, T. Nakamura (2000), "Preparation of bioactive PDMS-modified $CaO-SiO_2-TiO_2$ Hybrids by the sol-gel method.", *Journal of Sol-Gel Science and Technology*, 19, 101-105.

[132] Q. Chen, F. Miyata, T. Kokubo, T. Nakamura (2001), "Effect of heat treatment on bioactivity and mechanical properties of PDMS-modified $CaO-SiO_2-TiO_2$ hybrids via sol-gel process.", *Journal of Materials Science. Materials in Medicine,* 12, 515-522.

[133] M. Kamitakahara, M. Kawashita, N. Miyata, T. Kokubo, T. Nakamura (2001), "Bioactivity and mechanical properties of polydimethylsiloxane (PDMS)-$CaO-SiO_2$ hybrids with different PDMS contents.", *Journal of Sol-Gel Science Technology*, 21, 75-81.

[134] H. -M. Kim, M. Uenoyama, T. Kokubo, M. Minoda, T. Miyamoto, T. Nakamura (2001), "Biomimetic apatite formation on polyethylene photografted with vinyltrimethoxysilane and hydrolyzed.", *Biomaterials*, 22, 2489-2494.

[135] A. Oyane, M. Minoda, T. Miyamoto, K. Nakanishi, M. Kawashita, T. Kokubo, T. Nakamura (2001), "Apatite formation on ethylene-vinyl alcohol copolymer modified with silane coupling agent and calcium silicate.", *Key Engineering Materials. Bioceramics 14.*, 192-195, 713-716.

[136] N. Miyata, K. I. Fuke, Q. Chen, M. Kawashita, T. Kokubo ,T. Nakamura (2002), "Apatite formation ability and mechanical properties of PTMO-modified $CaO-SiO_2$ hybrids prepared by sol-gel processing: Effect of CaO and PTMO contents.", *Biomaterials*, 23, 3003-3040.

[137] S. H. Rhee, J. Y. Choi (2002), "Synthesis of bioactive poly(methyl methacrylate)/silica hybrid.", *Key Engineering Materials.*, 218-220, 433-436.

[138] M. Ahola, J. Rich, P. Kortesuo,J. Kiesvaara, J. Seppälä, A. Yli-Urpo (1999), "In vitro evaluation of biodegradable e-caprolactone-co-D, L-lactide/silica xerogel composites containing toremifene citrate.", *International Journal of Pharmaceutics* 181, 181-191.

[139] D. Tian, Ph. Dubois, R. Jerome (1996), "A new poly(ε-caprolactone) containing hybrid creamer prepared by the sol-gel process.", *Polymer*, 37(17), 3983-3987.

[140] D. Tian, Ph. Dubois, R. Jerome (1997), "Biodegradable and biocompatible inorganic-organic hybrids materials I. Synthesis and characterization.", *Journal of Polymer Science. Part A. Polymer Chemistry*, 35, 2295-2309.

[141] D. Tian, S. Blacher, Ph. Dubois, R. Jerome (1998), "Biodegradable and biocompatible inorganic-organic hybrid materials. 2. Dynamic mechanical properties, structure and morphology.", *Polymer*, 39(4), 855-864.

[142] D. Tian, S. Blacher, Ph. Dubois, J. P. Pirard, R. Jerome (1998), "Porous silica obtained from biodegradable and biocompatible inorganic-organic hybrid materials.", *Journal of Sol-Gel Science and Technology*, 13, 415-419.

[143] D. Tian, S. Blacher, J. P. Pirard, R. Jerome (1998), "Biodegradable and biocompatible inorganic-organic hybrids materials. 3. A valuable route to the control of the silica porosity.", *Langmuir*, 14, 1905-1910.

[144] D. Tian, S. Blacher, R. Jerome (1999), "Biodegradable and biocompatible inorganic-organic hybrid materials: 4. Effect of acid content and water content on the incorporation of aliphatic polyesters into silica by the sol-gel process.", *Polymer*, 40, 951-957.

[145] D. Tian, Ph. Dubois, C. Grandfils, R. Jerome, P. Viville, R. Lazzaroni, J. L. Bredas, P. Leprince (1997), "A novel biodegradable and biocompatible ceramer prepared by the sol-gel process.", *Chemistry of Materials*, 9(4), 871-874.

[146] S. H. Rhee, H. M. Kim (2002), "Preparation of a bioactive polycaprolactone/silica nanocomposite.", *Key Engineering Materials*, 218-220, 453-456.

[147] H. M. Kim (2001), "Bioactive ceramics: Challenges and perspectives.", *Journal of the Ceramic Society of Japan*, 109(4), S49-S57.

This chapter describes the synthesis, methods of analysis, sample preparation and conditions of operation for the techniques used in this thesis. In the first part, the material preparation and the analytical methods used to characterize them are described, then the *in vitro* osteoconductivity or apatite forming ability methods as well as the analysis techniques associated are finally presented and discussed. Procedures, measures and data treatments as well as characterisation of poly(α-hydroxyacids) and silica gel are given.

2.1. Preparation of Poly(α-hydroxyacids) and Composites

2.1.1. Materials

α, ω-Hydroxyl poly(ε-caprolactone) (PCL, Mn =2000 g/mole, Pd =2.0) was a gift from Solvay Interox Ltd. ε-Caprolactone, (3S)-cis-3,6-dimethyl-1,4-dioxane-2,5-dione (L-lactide), 1,3-propanediol, 1,4-butanediol, 3-isocyanatopropyltriethoxysilane, 1,4-diazobicyclo(2,2,2)octane (DABCO), tin (II) 2-ethylhexanoate (T22EH), tetraethyl orthosilicate (TEOS), tetramethyl orthosilicate (TMOS) and tetrahydrofuran (THF), toluene were obtained from Aldrich and used as received. Concentrated hydrochloric acid solution (HCl 11.4M), ethanol (EtOH) and methanol (MeOH) were obtained from Fisher. solvents were dried over molecular sieves before use.

2.1.2. Poly(α-hydroxyacids) Synthesis- Ring-Opening Polymerization of Lactones

The poly(α-hydroxyacids) are best described as macromolecules of ester monomer units. The direct condensation reaction of the related carboxylic acids gives low molecular weight polymers because of its reversibility and the backbiting reactions. Therefore it is not a pathway of choice for the controlled synthesis of poly(α-hydroxyacids). These biodegradable polyesters are preferably made by the ring-opening polymerization of their respective cyclic diester dimers or lactones[1] (Figure 2.1).

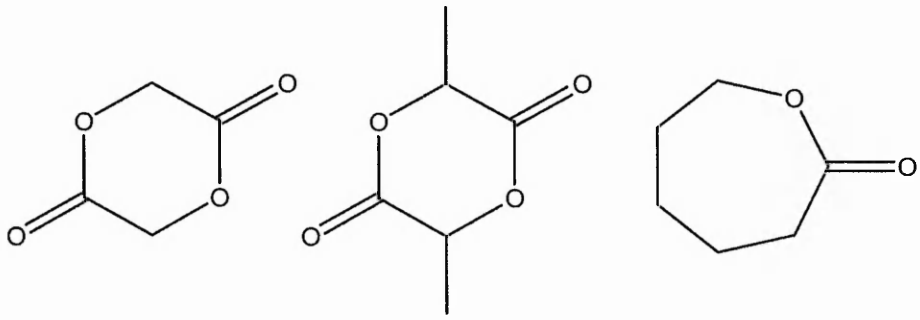

Glycolide Lactide ε-caprolactone

Figure 2.1: Examples of lactones, precursors for the synthesis of common poly(α-hydroxyacids).

Ring opening polymerization reaction (ROP)

The mechanism of the ROP reaction is discussed at more length in the chapter 5 discussing the synthesis mechanisms. The synthesis of poly(α-hydroxyacid) is best described as a metal-mediated ring-opening polymerisation of cyclic esters[2] (Figure 2.2).

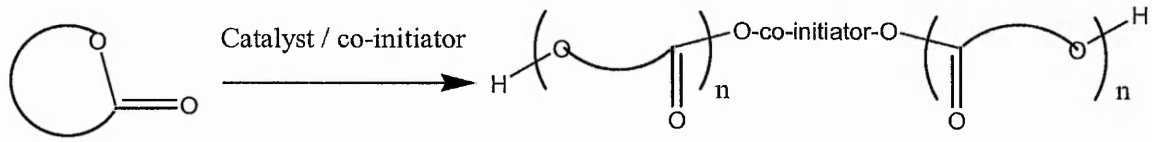

Figure 2.2: General scheme for the ring-opening polymerisation of lactones.

The most commonly used catalyst is tin ethylhexanoate because of its high efficiency and the narrow polydispersity of the polyesters obtained[3]. Catalysts of cyclic esters have been reviewed recently by B. J. O'Keefe and co-workers[4]. P. Dobrzynski and co-workers[5] have also investigated new efficient alternative non-toxic iron based catalysts. A co-initiator or chain-controlling agent is usually added to the ROP reaction. Its role is to speed up the conversion rate of the cyclic esters and to control the final polymer molecular weight as well as its morphology[6]. The co-initiators could be water or an alcohol[6]; propanol, butanol, propane diol, butane diol, etc, and linear polyesters (Figure 2.3) are obtained. The use of a polyols or alcohol terminated polymers allows the synthesis of star or branched polymers[7, 8] and copolymers[9, 10] giving rise to polymers with different structures and properties[11].

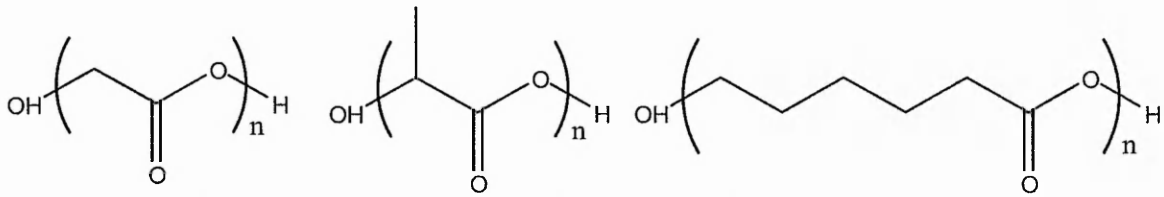

Polyglycolide (PGA) Polylactide (PLA) Poly(ε-caprolactone) (PCL)

Figure 2.3: Linear poly(α-hydroxyacids).

Preparation poly(ε-caprolactone) (PCL)- general procedure

Poly(ε-caprolactone) was prepared in the bulk under an inert atmosphere (Nitrogen) by the ring-opening polymerization of ε-caprolactone or 2-exapenone[12, 13] in the presence of stannous 2-ethyl hexanoate (0.2 % mole) and a desired amount of a co-initiator, either butane or propane diol at 80 °C to 120 °C for 24 to 48 hours. The obtained poly(ε-caprolactone) was dissolved in toluene or tetrahydrofuran and precipitated out by addition of cold methanol and dried under vacuum (0.1 torr) for 24 hours. In the following study butane diol was used as co-initiator except when stated.

Preparation of poly(L-lactic acid)-general procedure

Poly(L-lactic acid) was prepared in the bulk under an inert atmosphere (Nitrogen) by the ring-opening polymerization reaction of L-lactide or (3S)-cis-3,6-dimethyl-1,4-dioxane-2,5-dione[12] in the presence of stannous 2-ethyl hexanoate (0.2 % mole) and a desired amount of a co-initiator, butane diol at 140 °C to 160 °C for 24 to 48 hours. The obtained poly(L-lactide) was dissolved in toluene and precipitated out by addition of cold methanol and dried under vacuum (0.1 torr) for 24 hours.

Modification of the end-groups of poly(α-hydroxyacids)

The α,ω-hydroxyl poly(α-hydroxyacids) had their end-groups modified with reactive functions. The aim was to have end-group functions on the organic polymers more susceptible to reaction with the silanol groups of the silica phase. The alcohol end-groups of the prepared linear poly(α-hydroxyacids) have been modified using 3-isocyanatopropyltriethoxysilane. Figure 2.4 describes the reaction[14].

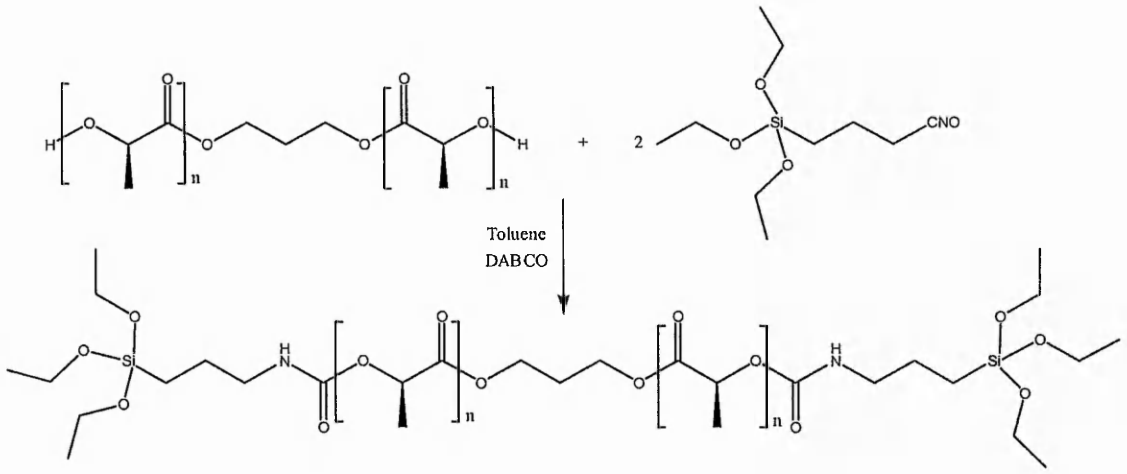

Figure 2.4: Reaction 3-isocyanatopropyltriethoxysilane with poly(L-lactic acid).

General procedure for the preparation of triethoxysilane terminated poly(α-hydroxyacids)[14]

α,ω-Hydroxyl poly(α-hydroxyacids) and 3-isocyanatopropyltriethoxysilane were dissolved in dry toluene in a dried pyrex flask equipped with a rubber septum in a 1: 1.2 molar ratio. 1 mole equivalent of 1,4-diazobicyclo(2,2,2)octane was added as a catalyst. The reaction mixture was stirred and heated at 60 °C for 15 hours. The solution was cooled down to room temperature, precipitated into cold methanol and dried under vacuum (0.1 torr) for 24 hours.

2.1.3. Preparation of Composites

The bulk and sol-gel synthetic routes were explored to make poly(α-hydroxyacid)-silica composites. Having chosen two polymers organic and inorganic whose individual properties may theoretically combine to provide the desired end-use characteristics, the primary requirement was the ability of the polymers to form a blend. A first method used to prepare the α,ω-hydroxyl poly(ε-caprolactone)-silica composite was the bulk method which consisted to the addition of a pre-hydrolysed solution of tetraethyl orthosilicate, ethanol, water and catalyst in melted polyester. The inorganic phase was dispersed in the viscous melted polymer by a strong stirring. This was the more straightforward method, Figure 2.5. For example, an α,ω-hydroxyl poly(ε-caprolactone)-silica composite was prepared by the addition of a silica sol (TEOS\EtOH\H_2O\HCl molar ratio 1/4/4/0.1 mixed for 60 minutes at room temperature) in melted PCL at 80 °C. The mixture was strongly stirred for 1 hour and the mixture cooled down to room temperature.

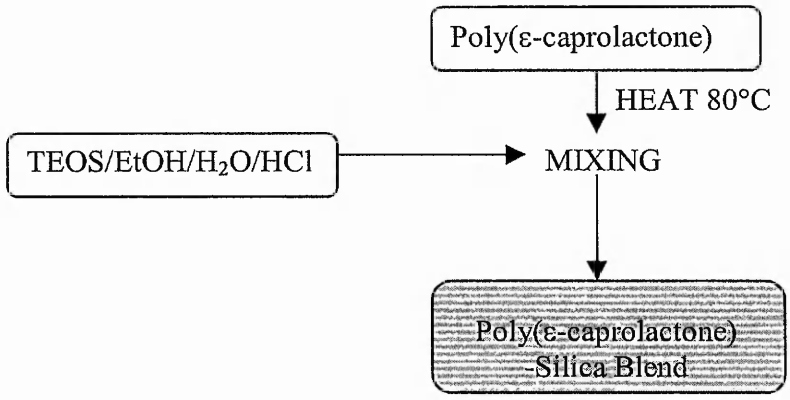

Figure 2.5: Scheme for the poly(ε-caprolactone)-silica blend composite preparation.

Poly(ε-caprolactone)-silica and poly(L-lactide)-silica sol-gel material process

The second method used was the sol-gel procedure. Organically modified silicates constitute an important new family of amorphous solid. Since the successful preparation of these new materials using the sol-gel method[15], there has been an increasing interest in making new organic-inorganic hybrid materials[16]. The sol-gel method consisted of a two-step hydrolysis-condensation reactions process[17], starting with metal alkoxides, typically tetraethoxysilane (TEOS), or tetramethoxysilane (TMOS) as indicated in Figure 2.6.

Step 1: Hydrolysis reaction

$$M(OR)_4 + nH_2O \xrightarrow{\text{catalyst}} M(OR)_{4-n}(OH)_n + nROH$$

Step 2: Condensation reaction

$$\equiv M\text{-}OH + HO\text{-}M\equiv \xrightarrow{\text{catalyst}} \equiv M\text{-}O\text{-}M\equiv + H_2O$$

and/or

$$M\text{-}OH + RO\text{-}M \xrightarrow{\text{catalyst}} M\text{-}O\text{-}M + ROH$$

Figure 2.6: Hydrolysis and condensation reactions involved in the classical sol-gel reaction

The sol-gel process is a very straightforward way to prepare hybrid materials that combine advantageously the reaction of hydrolysis-condensation of metal alkoxides [$M(OR)_4$, M= Si, R= Methyl, Ethyl…] to form a metal oxide network in presence of a organic polymer bearing or not chemical groups such as hydroxyl or alkoxysilane,

reactive in the hydrolysis-condensation reaction. For example, triethoxysilane end-capped poly(tetramethylene oxide) (PTMO)[18] and polydimethylsiloxane (PDMS)[19] – silica hybrid materials have been successfully prepared using the sol-gel process. Others organic polymers without reactive groups such as poly(vinylacetate) and poly(2-methyl-2-oxazoline) have also been incorporated in a silica sol-gel[20]. It has been shown that hydrogen bonds between these organic polymers and silanol functions formed by hydrolysis of tetraalkoxysilane have decisive effect on the formation and final properties of these hybrids[21].

Poly(ε-caprolactone)-silica hybrid sol-gel materials have been studied recently by R. Jerome and co-workers[22]. They have reported the preparation and characterisation of α,ω-hydroxyl and triethoxysilane end-capped poly(ε-caprolactone)-silica materials, Figure 2.7.

Step 1: Hydrolysis reaction tetraalkoxysilane

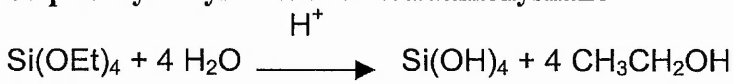

Step 2: Condensation reaction with α,ω-hydroxyl poly(ε-caprolactone)

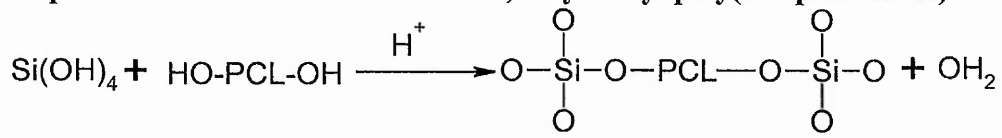

Step 1': Hydrolysis reaction triethoxysilane end-capped poly(ε-caprolactone)

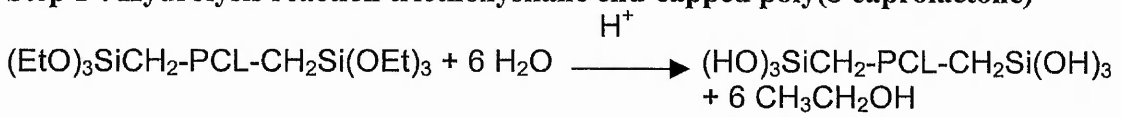

Step 2': Condensation reaction with triethoxysilane end-capped poly(ε-caprolactone)

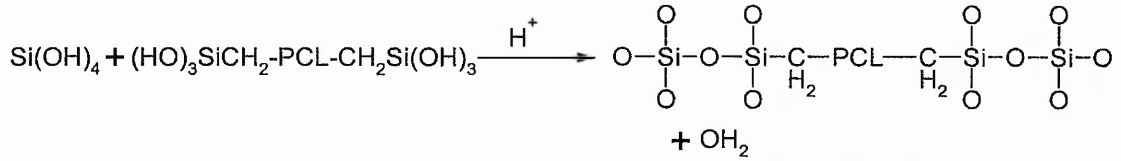

Figure 2.7 : Simplified reaction mechanisms (unbalanced) of α,ω-hydroxyl and triethoxysilane end-capped poly(ε-caprolactone) containing silica sol-gel[14]. (Oxygen linked to on silicon atom (Si-O) could be link to an hydrogen (H), the silica network via an other silicon (Si) or poly(ε-caprolactone) via its terminal end-group).

The hybrid sol-gel materials structure and morphology have been studied in details by the same authors by small angle x-ray diffraction, transmission microscopy and dynamic mechanical spectroscopy[23]. It must be noticed that they have mostly studied the hybrids with poly(ε-caprolactone) weight content around 50% and below. Their SAXS and TEM results indicated that the silica and poly(ε-caprolactone) were intimately interwoven and formed a co-continuous interpenetrated network. The effect on the hybrids morphology of the poly(ε-caprolactone) functional end-groups, the number of functional end-groups per polymer chain, the poly(ε-caprolactone) molecular weight and content, the curing conditions the acid and water content have been studied[23, 24]. The most interesting findings were that increasing the polymer molecular weight and content, the chain polydispersity and decreasing the reactivity and the number of reactive groups resulted a more heterogeneous material[25].

Figure 2.8 shows the preparation of poly(α-hydroxyacids)-silica hybrid materials.

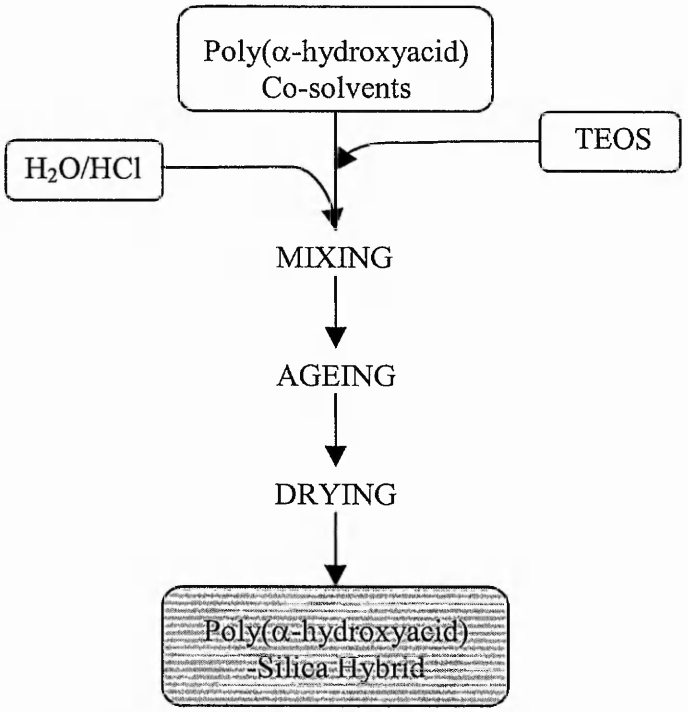

Figure 2.8 : Scheme for poly(α-hydroxyacids)-silica sol-gel hybrid preparation.

Preparation of poly(α-hydroxyacid)-silica sol-gel materials, procedure[14, 26]

Materials were prepared at room temperature using the following procedure: In a dry flask equipped with a magnetic stirrer, the required amount of the poly(α-

hydroxyacid) was added. Then, the co-solvents; either tetrahydrofuran or toluene, ethanol and tetraethyl orthosilicate were added and the mixture stirred until a clear solution was obtained. The desired amount of hydrochloric acid and water were then added and the solution stirred for one hour. Generally the TEOS/Ethanol/water/hydrochloric acid molar ratios were 1/4/4/0.1. The tightly closed flask was then kept in a dessicator at room temperature for 1 to 5 days. Then, the sol-gel was allowed to dry slowly at room temperature for a few days to several weeks. The obtained sol-gel was dried under vacuum (0.1 torr) for 12 hours and a final annealing was performed in an oven for 1 to 2 days at 60 °C to 100°C. Materials were ground in a mortar and stored in a dessicator.

2.2. Analysis

2.2.1. Nuclear Magnetic Resonance Spectroscopy (NMR)

Nuclear magnetic resonance spectroscopy was a valuable method to characterize the organic polymers prepared. Liquid phase ^{1}H and ^{13}C NMR analysis allowed the characterization of organic materials, the conversion rate of the polymerization and the molecular weight of the polymers to be calculated from the values of the quantitative integration of the NMR signals. Solid and liquid phase ^{29}Si NMR analysis were performed for the characterization of the prepared silica sol-gel, and composite materials.

Liquid state ^{13}C, ^{1}H and ^{29}Si NMR spectra were recorded on a Jeol NMR instrument model JNM-GSX200. Samples for ^{13}C, ^{1}H NMR analysis were prepared as follows: 0.5 g of material was dissolved in deuterated chloroform [Avocado] (~ 2.5 ml) with 0.3 % volume of TMS [Aldrich] as an internal standard in a 5 mm diameter NMR glass tube. Usually 16 scans were used for the acquisition of a decoupled proton NMR spectrum with a relaxation time of 1 second. For the acquisition of a ^{13}C NMR spectrum, the relaxation time and the number of scans were respectively set at 1 second and 1024 scans. The liquid state ^{29}Si NMR analysis was conducted to study the speciation of the silica in the hydrolysis-condensation reaction of alkoxysilanes. Reaction samples were withdrawn at required intervals and added quickly to a 10 mm NMR tube equipped with a coaxial 5 mm tube and then frozen in liquid nitrogen to

avoid the evolution of the reaction mixture. The sample tubes were subjected to ^{29}Si NMR analysis at -60 °C using an internal standard acetone-25% TMS.

In the Tables 2.1 to 2.8, the ^{1}H and ^{13}C NMR chemical shift of the poly(α-hydroxyacids) were collected. The Figures 2.10 to 2.14 showed the structure of the prepared polyesters. The solid and liquid state ^{29}Si NMR analysis are presented chapter 5.

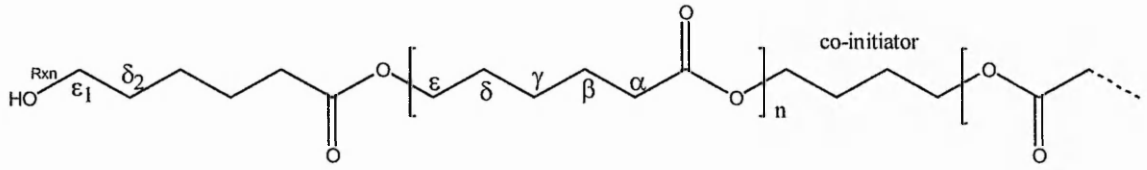

Figure 2.10: Scheme linear α,ω-hydroxyl poly(ε-caprolactone) structure prepared.

Table 2.1: ^{1}H NMR chemical shifts, assignments and coupling constants of α,ω-hydroxyl poly(ε-caprolactone).

Structure	**Chemical shift (ppm), peak multiplicity and ^{2}J (Hz)**	**Ref. [26]**
Hγ	1.40, m	1.40
Hδ, β	1.65, m	1.66
CH_2CH_2O co-initiator	*1.85*	
Hα	2.31, t, 7.42	2.32
Hε$_1$	3.65, t, 6.43	3.64
CH_2CH_2O co-initiator	*4.16*	
Hε	4.06, t	4.07

Table 2.2: ^{13}C NMR chemical shifts and assignments of α,ω-hydroxyl poly(ε-caprolactone).

Structure	**Chemical shift (ppm)**	**Ref. [27], [28]**
Cγ	24.6	26.7
Cβ	25.4	26.7
Cδ	28.7	29.8
Cδ$_2$	32.21	
Cα	34.1	34.8
Cε$_1$	62.6	
Cε	64.4	66.0
C=O	173.5	175.0

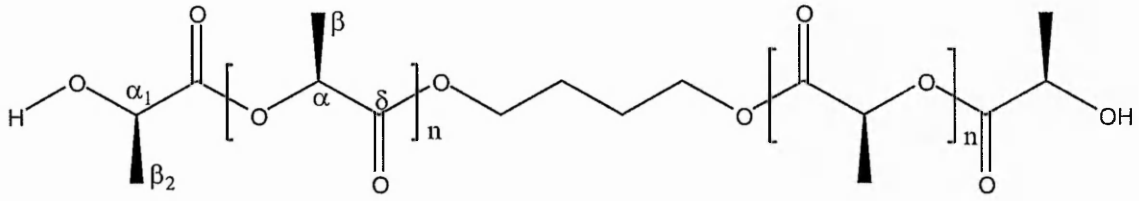

Figure 2.11: Scheme linear α,ω-hydroxyl poly(L-lactic acid) structure prepared.

Table 2.3: ^{1}H NMR assignments, chemical shifts and coupling constant of α,ω-hydroxyl poly(L-lactic acid).

Structure	**Chemical shift (ppm), peak multiplicity and ^{2}J (Hz)**	**Ref.** [35, 29]
Hβ, $H\beta_2$	1.58, d, 6.95	1.46
CH_2CH_2Ocoinitiator	1.85	
CH_2CH_2Ocoinitiator	4.16	
$H\alpha_1$	4.34, q	4.32
Hα	5.17, q, 6.94	5.19

Table 2.4: ^{13}C NMR assignments and chemical shifts of α,ω-hydroxyl poly(L-lactic acid).

Structure	**Chemical shift (ppm)**	**Ref.** [29, 35]
Cβ	16.63	16.70
Cα	69.04	68.95
Cδ	169.89	169.44

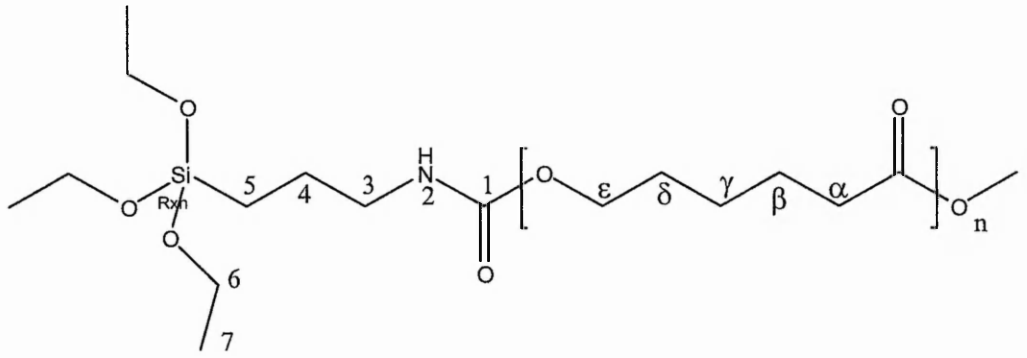

Figure 2.13: Scheme linear triethoxysilane terminated poly(ε-caprolactone) structure prepared.

Table 2.5: ^{1}H NMR chemical shifts, assignments and coupling constants of triethoxysilane terminated poly(ε-caprolactone).

Structure	**Chemical shift (ppm), peak multiplicity and ^{2}J (Hz)**	**Ref.** [26]
H_5	0.60, t	0.64
H_6	1.23	1.24
Hγ	1.40, m	1.40
H_4, Hδ, β	1.60	1.66
H_3	3.12, t	3.18
$H\varepsilon_1$	3.51	3.64
H_7	3.75	3.84
Hε	4.03, t, 6.68	4.07

Table 2.6: ^{13}C NMR chemical shifts, assignments and coupling constants of triethoxysilane terminated poly(ε-caprolactone).

Structure	**Chemical shift (ppm)**
C_7	14.2
C_4	24.3
Cγ	24.6
Cβ	25.5
Cδ	28.4
$C\delta_2$	32.3
Cα	34.2
C_3	60.2
$C\varepsilon_1$	62.6
Cε	64.2
C=O	173.5
C_1	173.8

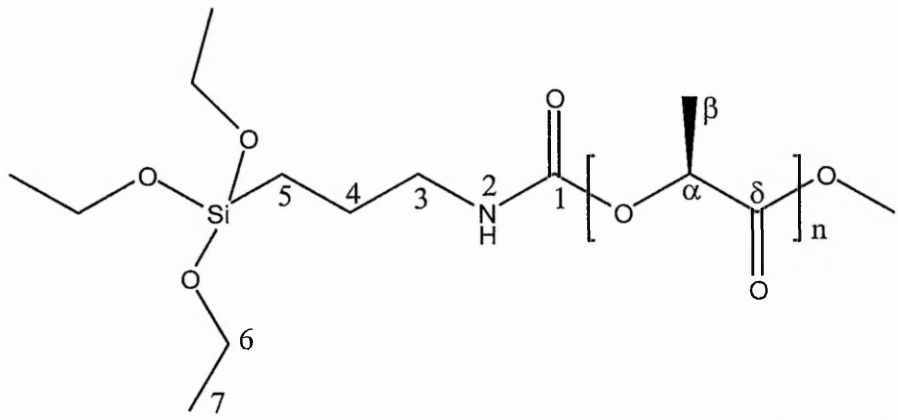

Figure 2.14: Scheme linear triethoxysilane terminated poly(L-lactic acid) structure prepared.

Table 2.7: ^{1}H NMR chemical shifts, assignments and coupling constants of triethoxysilane terminated poly(L-lactic acid).

Structure	**Chemical shift (ppm), peak multiplicity and ^{2}J (Hz)**	**Ref. [30]**
H_5	0.67	0.60
H_7	1.21, t,	1.19
H_4, Hβ	1.48	1.54
H_6	3.77	3.78
H_3	4.37	
Hα	5.10	5.13

Table 2.8: ^{13}C NMR chemical shifts, assignments and coupling constants of α,ω-triethoxysilane terminated poly(L-lactic acid).

Structure	**Chemical shift (ppm)**
Cβ	16.64
C_7	16.86
C_6	18.27
C_4	20.52
C_5	50.21
C_3	66.72
Cα	69.03
Cδ	169.61
C_1	175.13

NMR analyses have shown to be of poor help to understand and defined the sol-gel and bulk composites properties. The composite bulk and sol-gel materials were only partially miscible in solvent (chloroform) and for example the proton and carbon

chemical shifts of the α,ω-hydroxyl poly(ε-caprolactone)-silica bulk and sol-gel composites collected tables 2.9 and 2.10 did not differ significantly from the α,ω-hydroxyl poly(ε-caprolactone). The only difference was the presence of ethanol groups probably coming from the hydrolysis of TEOS. The residual phases were insoluble in usual solvents.

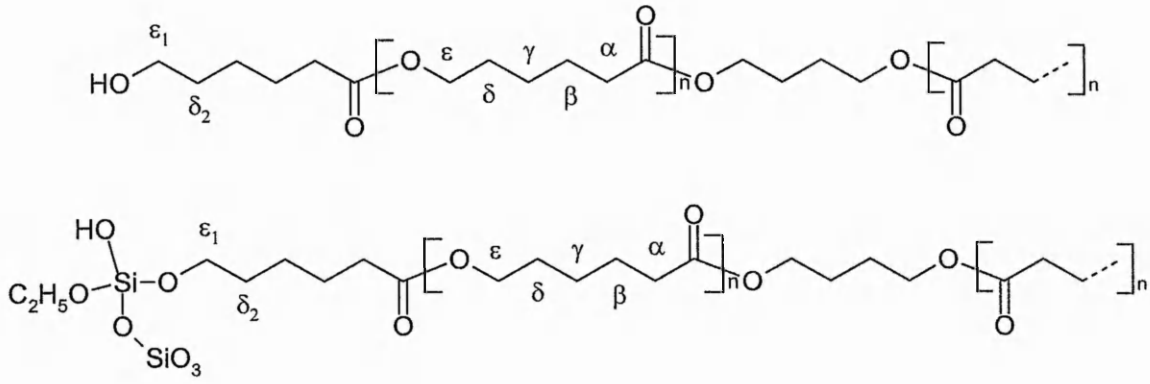

Figure 2.15: Possible structure of α,ω-hydroxyl poly(ε-caprolactone) in bulk and sol-gel composite materials.

The Figure 2.15 shows the possible structure of the hydroxyl end-capped polyester in the composites. It could either have covalent bonding with the silica phase or not[14].

Table 2.9 : ^{1}H NMR chemical shifts and assignments of α,ω-hydroxyl poly(ε-caprolactone)-silica bulk and sol-gel composites.

Structure	**Chemical shift (ppm), peak multiplicity and ^{2}J (Hz)**		
Composite	**Bulk**	**Sol-Gel**	**Poly(ε-caprolactone)**
CH_3CH_2O-	1.24, (t), 6.92	1.24, (dt), 6.90	
Hγ	1.39, m	1.39, m	1.40, m
Hδ, β	1.65, m	1.64, m	1.65, m
CH_2CH_2O co-initiator			*1.85*
Hα	2.30, t, 7.42	2.28, t, 7.42	2.31, t, 7.42
Hε$_1$ and *CH_3CH_2O*	3.82, m, 6.93	3.83, m, 6.91	3.65, t, 6.43
CH_2CH_2O co-initiator			*4.16*
Hε	4.03, t	4.03, t, 6.60	4.06, t

Table 2.10 : ^{13}C NMR chemical shifts and assignments of α,ω-hydroxyl poly(ε-caprolactone)-silica bulk and sol-gel composites.

Structure	Chemical shift (ppm)		
Composite	bulk	Sol-gel	Poly(ε-caprolactone)
$\underline{C}H_3$-CH_2O-	18.0	18.0	
Cγ	24.5	24.4	24.6
Cβ	25.4	25.4	25.4
Cδ	28.2	28.2	28.7
$C\delta_2$, $CH_3\underline{C}H_2O$-	32.2	32.2	32.2
Cα	34.0	34.0	34.1
$C\varepsilon_1$	62.0	63.7	62.6
Cε	64.2	64.1	64.4
C=O	173.4	173.6	173.5

For the triethoxysilane terminated poly(ε-caprolactone)-silica sol-gel composites materials prepared, the ^1H and ^{13}C NMR analysis carried out on the soluble part of the materials did not reveal any information about the possible covalent bonds between the silica and the organic polymer and the spectra obtained and chemical shifts measured similar to those of the polyester prepared described in the previous chapter (Tables 2.9 and 2.10). Poly(L-lactic acid)-silica sol-gel materials prepared as described in the methods chapter were also analysed by ^1H and ^{13}C liquid NMR analysis. The obtained spectra as the composites prepared with the poly(ε-caprolactone). did not showed any significant variations compared to the poly(L-lactic acid) (data not presented). The NMR analysis was poorly conclusive because the materials were partially solubled and therefore the collected spectra did not gave a full picture of the materials. However, it indicated that no or little polymer degradation occurred during the processing, and that residual ethanol was present in the composite materials prepared by sol-gel and bulk processes.

Calculation of the poly(α-hydroxyacid) average number (Mn) from the integration of ^1H NMR signals.

The polyester chain length average number, Mn was calculated by dividing the ^1H NMR peak integrals (I) of the chain methine protons (δ=4.06 ppm) for poly(ε-caprolactone), and methene protons (δ=5.17 ppm) for poly(L-lactic acid) by respectively the integral methane group protons next to the terminal hydroxyl group (δ=3.65 ppm) for poly(ε-caprolactone) and 4.36 ppm for the poly(L-lactic acid) divided by the number of hydroxyl group on the co-initiator used. The result is multiplied by the

molecular weight of the polyester monomer unit (M_w caprolactone = 114.14 g/mol and lactic acid = 89.08 g/mol), then the co-initiator molecular weight, is added to the total (equation 2.1).

$$M_n \text{ Poly}(\alpha\text{-hydroxyacid}) = \frac{I_{CH\ chain}}{(I_{CH\text{-}OH}/\text{number OH on co-initiator})} * M_w \text{ monomer unit} + M_w \text{ co-initiator.}$$

equation 2.1

2.2.2. Fourier Transform Infrared Spectroscopy (FTIR)

Infrared spectroscopy is essentially the study of the interaction of electromagnetic radiation with matter, within the wavenumber region of 12,500 to 20 cm^{-1}. The region from 4000 to 400 cm^{-1} is the mid-infrared region where vibrational and rotational bands are observed[31].

The materials were evaluated by recording their FTIR spectra (KBr pellet technique: 2 mg solid per 200 mg KBr; 4000-400 cm^{-1}) using a Nicolet Magna-IR™ spectrometer 750 with DTGS (KBr) detector, and a KBr beam splitter operating at a resolution of 2 cm^{-1} with 64 scans being accumulated for each sample. FTIR Assignments for the poly(ε-caprolactone) , poly(L-lactic acid) and silica gel are given below.

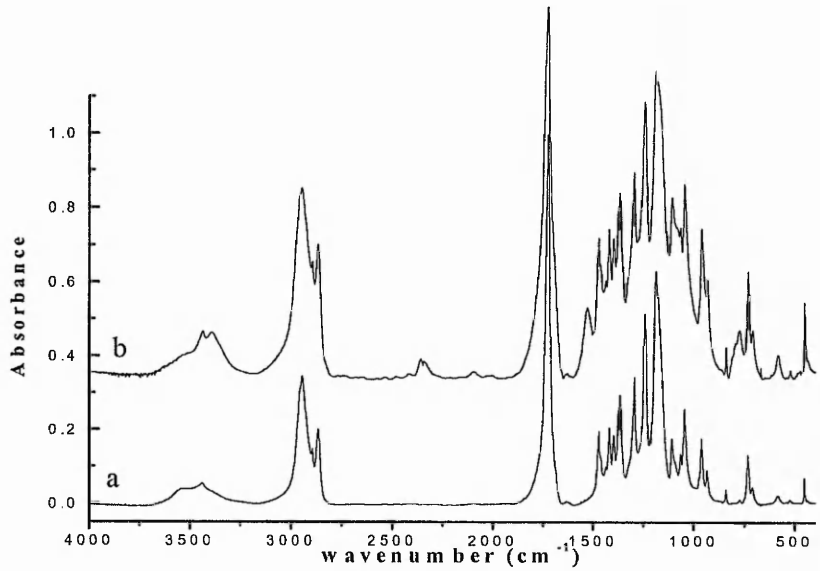

Figure 2.16: Infrared spectra of α,ω-hydroxyl poly(ε-caprolactone) (a) and triethoxysilane terminated poly(ε-caprolactone) (b).

Table 2.11 : IR Absorption frequency (cm^{-1}) and vibrational assignment of α,ω-hydroxyl and α,ω-triethoxysilane terminated poly(ε-caprolactone)[26, 32].

Absorption frequency (cm^{-1})	Structure
3500-3450	-OH H bonded
3350	N-H
2972	CH_3 asymetric stretching
2940	CH stretching
2897	CH_3 symetric stretching
1733	C=O stretching: amorphous PCL
1725	crystalline PCL
1523	Urethane bond
1465	$-CH_2-$ bend
1392	$-CH_3$ bend
1271	C-O-C stretching
1150-1100	C-OH stretching
950±700	CH

α,ω-hydroxyl poly(ε-caprolactone)-silica materials with a poly(ε-caprolactone) weight percent content from 100 to 50 were analyzed by FTIR. The IR spectra are shown Figure 2.17.

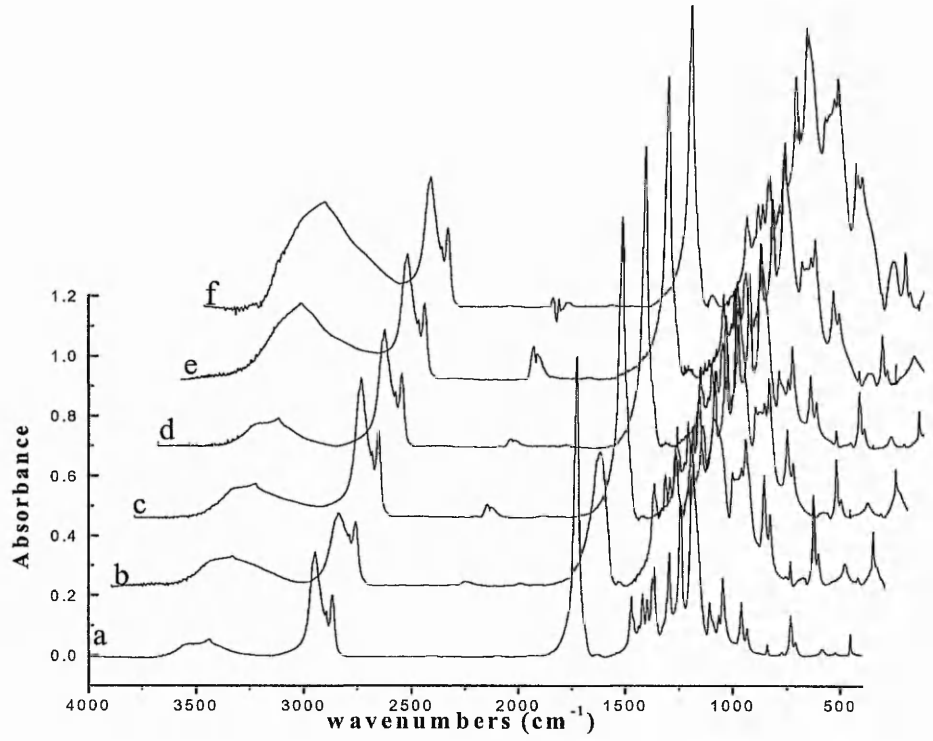

Figure 2.17 : FTIR spectra α,ω-hydroxyl poly(ε-caprolactone) (a) and α,ω-hydroxyl poly(ε-caprolactone)-silica materials prepared following the bulk procedure with a poly(ε-caprolactone) weight % content of 95 (b), 90 (c), 80 (d), 70 (e) and 50 (f).

Figure 2.17 showed the effect of the decreased of poly(ε-caprolactone), equivalent to the increased silica charge on the mid-IR spectra of composite materials prepared by the bulk process. The region between 3000 and 4000 cm^{-1}, corresponded to the fundamental stretching vibrations of different hydroxyl groups. The infrared spectrum in this region is mostly sensitive to vibrations of hydrogen atoms, which due to their low mass have high characteristic frequencies. The signals in this region increased and became broader with the increase of the silica phase. The broadness of this area suggested different local environments for the OH groups; silanol (Si-OH) groups hydrogen-bonded to various extents to nearby silanols and absorbed water which gave the broad absorption centered around 3300 cm^{-1}. This last absorption was assigned to water molecules hydrogen-bonded to the silanol groups. It was confirmed by the presence of a band at about 1630 cm^{-1} assigned to the deformation mode of H_2O molecules, which were probably trapped inside the voids of the composites. A truly isolated silanol group would appear around 3750 cm^{-1}. In the range of 400 cm^{-1} to 1500 cm^{-1}, composite spectra showed several new bands compared to the poly(ε-caprolactone). Of these, the bands located at about 430-450 cm^{-1} (broad), 860-880 cm^{-1} (broad) and 1080-1090 cm^{-1} (broad), were respectively the bond-rocking, the bond-bending and the bond-stretching bands in the SiO_2 lattice (Table 2.12) and their intensity increased with the amount of silica added. A strong peak at 1123 cm^{-1} with a shoulder at 1236 cm^{-1} was due to asymmetric stretching of tetrahedral Si-O units. The 1236 cm^{-1} shoulder was attributed to the LO vibration of the 1123 cm^{-1} asymmetric stretch peak[33].

To resume, the most obvious effect of silica charge in the material spectra were the apparition of vibrations due to the silica lattice and the change in the intensity and the shape of the bond-stretching absorption band of silica with the increase of charge. These facts can be associated with the different degrees of structural disorder in the SiO_2 lattice and increased of silica lattice with the increase of the silica phase. The O-H region observation indicated the presence of Si-OH groups and H_2O adsorbed on silica. It was confirmed by the presence of the band located at about 950 cm^{-1} assigned to the stretching vibrations of silanol groups.

Table 2.12: Typical infrared absorption frequency and vibration assignment for amorphous silica[33].

Absorption frequency (cm^{-1})	Vibration assignment
3745-3750	Isolated single Si-OH group or free hydroxyl group
3650-3660	Isolated pairs of adjacent Si-OH groups mutually hydrogen Bonded
3540-3550	Adjacent pairs of Si-OH groups with hydrogens bonded to each other
3400-3500	Water molecule adsorbed on the above
1100-1250	Si-O-Si Transverse optical (TO) mode of asymmetric bond stretching
850-950	Si-OH vibrational mode (network "defect band")
800	symmetrical stretch of bridging oxygen in Si-O-Si plane
782	TO Mode of symmetric bond-appears only in 4 membered ring
450-520	Si-O-Si rocking/bending vibration

An interesting IR vibration region of the polyesters, Figure 2. 17 is the carbonyl stretching vibration. The frequency of the carbonyl stretching vibration of poly(ε-caprolactone) depends on whether poly(ε-caprolactone) is crystalline or amorphous. The absorption band was reported at 1725 cm^{-1} for crystalline poly(ε-caprolactone)[23] (verified for our samples 1724 cm^{-1}), compared with a band at 1733 cm^{-1} for amorphous poly(ε-caprolactone). A band at 1715 cm^{-1} was observed in the poly(ε-caprolactone)-silica hybrids prepared. This extra vibration signal was attributed to carbonyl having strong hydrogen bonding interactions which results in a shift of the carbonyl absorption toward smaller wavenumber. Identical observation has been reported for the carbonyl absorption of poly(vinylacetate) and poly(methyl methacrylate) when used as part of hybrid silica materials. An indication of the fraction of hydrogen-bonded species (f_b) was tentatively calculated as defined by Coleman et al.[34]. The ratio of the crystalline carbonyl stretching area versus amorphous and hydrogen bonded carbonyl areas was calculated using a peak fitting mathematical software. Gaussian functions were used for the definition of the peak, Figure 2.18.

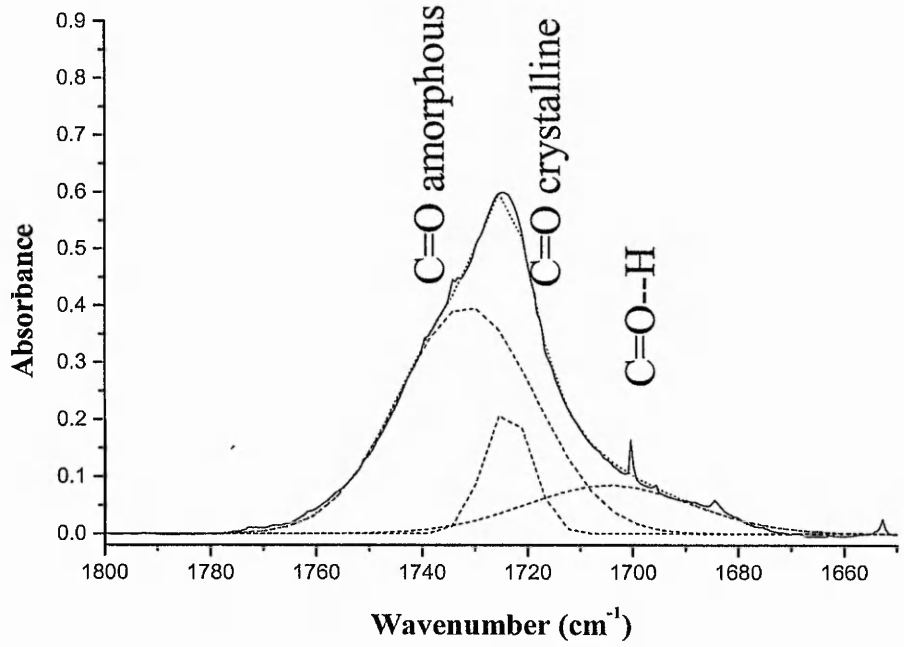

Figure 2.18: the peak fitting of the mid-IR carbonyl stretching region (black line) of α,ω-hydroxyl poly(ε-caprolactone)-silica sol-gel material. The dashed lines correspond to the peaks fitted for the carbonyl groups amorphous (1733 cm^{-1}), crystalline (1725 cm^{-1}) and hydrogen bonded (1705 cm^{-1}). The dotted line corresponds to the overall fitting of the carbonyl stretching region.

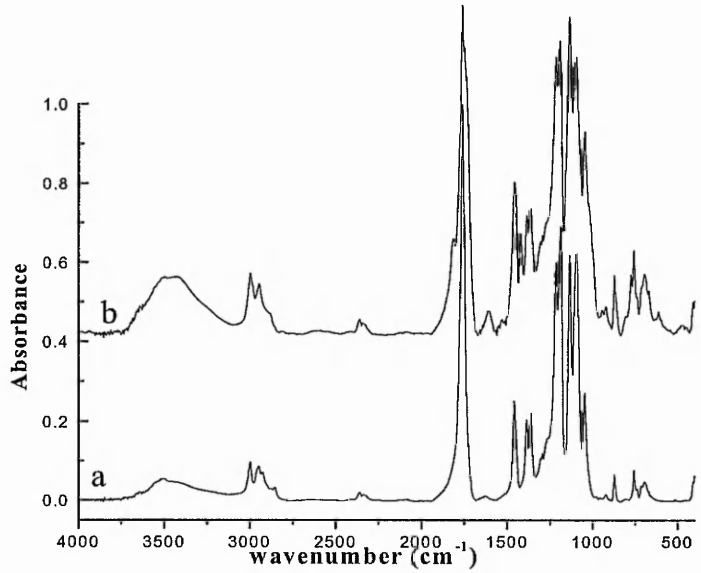

Figure 2.19 : Mid-IR spectra of α,ω-hydroxyl poly(L-lactic acid) (a) and α,ω-triethoxysilane poly(L-lactic acid) (b).

Table 2.13 : Infrared absorption frequency (cm^{-1}) and vibrational assignment of α,ω-hydroxyl and α,ω-triethoxysilane poly(L-lactic acid)[35, 36].

Absorption frequency (cm^{-1})	Structure
3700	OH, alcohol and carboxylic acid
2997	CH_3 asymmetric stretching
2947	CH_3 symmetric stretching
1750-1760	C=O stretching
1215-1185	ν_{as} COC
1100-1090	ν_s COC
1045	ν C-CH_3
760	δ C=O
715-695	γ C=O

The Mid-IR spectra of sol-gel α,ω-hydroxyl and α,ω-triethoxysilane poly(L-lactic)-silica composites were also collected.

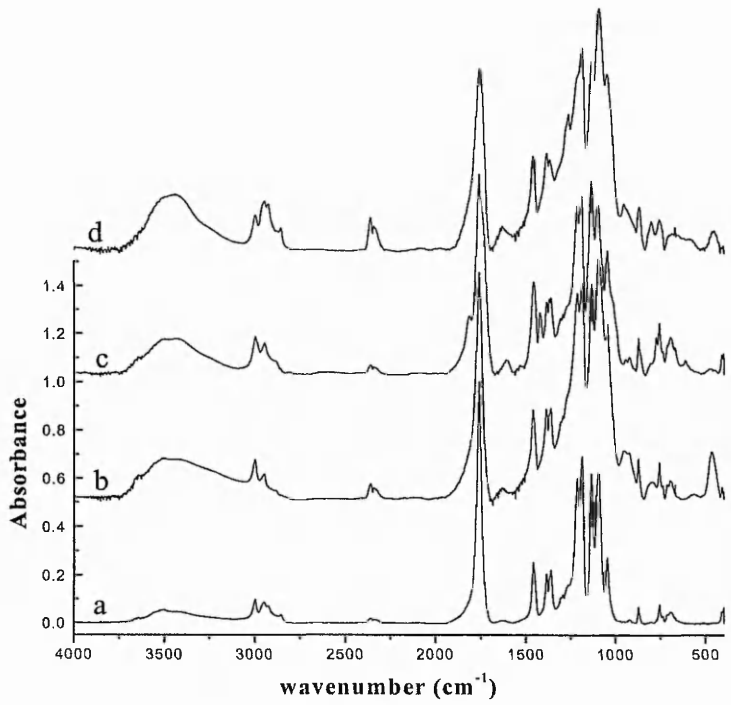

Figure 2.20: Mid-IR spectra of the α,ω-hydroxyl poly(L-lactic acid) (a), the α,ω-hydroxyl poly(L-lactic acid)-silica sol-gel composite with 70% weight content of poly(L-lactic acid) (b), the α,ω-triethoxysilane poly(L-lactic acid) (c) and the α,ω-triethoxysilane poly(L-lactic acid)-silica sol-gel composite with 70% weight content of poly(L-lactic acid) (d).

Figures 2.19 and 2.20 of poly(L-lactic acid)-silica sol-gels showed similarly to the poly(ε-caprolactone)-silica sol-gel materials. At 450 cm^{-1}, 880 cm^{-1} and 1000-1100 cm^{-1}, the broad rocking, bending and stretching bands of the silica lattice (Table 2.12). Also, the bands were very weak for the sol-gel with high poly(L-lactic acid) content, indicating a poorly formed network. The hydroxyl region around 3700 cm^{-1} to 3000 cm^{-1}, showed broad signal with a peak at 3650 cm^{-1} possibly attributed to SiO-H hydroxyl and a very large peak at around 3500 cm^{-1} attributed to adsorbed water. A signal observed at 956 cm^{-1}, confirmed the presence of silanol groups. The carbonyl stretching region from 1723 cm^{-1} to 1780 cm^{-1} showed similarly to the poly(ε-caprolactone) materials a broadening of the signal in composite materials. The symmetric vibration modes A and E_1 active in IR have been reported to give a broad asymmetric band about 1760 cm^{-1} in the poly(L-lactic acid) mid-IR spectra[36]. The attribution and assignment of individual peaks were not successful because, not only the morphology of the poly(L-lactic acid), but also the conformation and configuration gave rise to vibration broadening visible in IR spectroscopy. Therefore, it has not been possible to use the carbonyl stretching vibration of mid-IR data to discussed the "crystallinity" of the poly(L-lactic acid) incorporated in silica.

2.2.3. Gel Permeation Chromatography (GPC)

In GPC, polymer molecules (in a solvent) are delayed in their passage through columns filled with porous particles depending on their ability to penetrate the pores. Larger molecules, unable to penetrate the pores, exit first, and smaller molecules, which pass into the pores, exit later from the columns. Thus the technique grades molecules according to size. Calibration is with well-characterised standard polymers. Calculations of weight average and number average molecular weight lead to polydispersity information.

Samples were dissolved in chloroform and filtered through 0.45 μm PTFE filters prior to analysis. GPC was carried out using the following conditions ; 100 μl of prepared sample was injected in a Phenogel 5 μm linear column from Phenomenex, the eluent (chloroform) flow was set at 1.0 ml/min. The detection RI was set at 35 °C. Calibration was carried out versus polystyrene calibrants supplied by Polymerlabs. Samples were analyzed in duplicate. As polystyrene calibrants were used, the polymers

molecular weights (M_n and M_w) calculated from the chromatogram (Figure 2.21) were expressed as polystyrene equivalents.

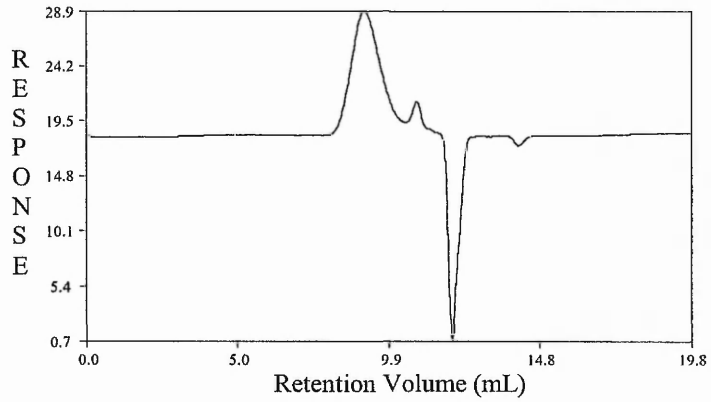

Figure 2.21 : GPC chromatogram of α,ω-hydroxyl poly(ε-caprolactone) prepared by ring-opening polymerisation reaction of ε-caprolactone.

2.2.4. Thermal Analysis

2.2.4.1. Thermo-Gravimetric Analysis (TGA)

In thermogravimetric analysis the mass of a sample is recorded continuously as a function of temperature or time. The resulting plot of mass as a function of temperature (Figure 2.22) provides both qualitative and quantitative information concerning the thermal stability and composition of the initial, intermediate and final compounds of the decomposition. The size of a step in a TGA curve may be used for quantitative analysis if the change can be linked to a particular thermal event such as oxidation, or loss of water. It is possible to encourage or suppress oxidation reactions by controlling the atmosphere (eg. Air, O_2 or N_2) experienced by the sample.

The thermobalance consists of four major components: a precision electro balance and its controller, a furnace and temperature sensors, the programmer and a recorder. Thermal analysis was carried out on a Stanton-Redcroft TG 760 Series instrument. 4 mg to 10 mg of sample was placed in the sample holder (aluminum crucible) and heated in a furnace from 20-900 °C at 10 °C/min in air.

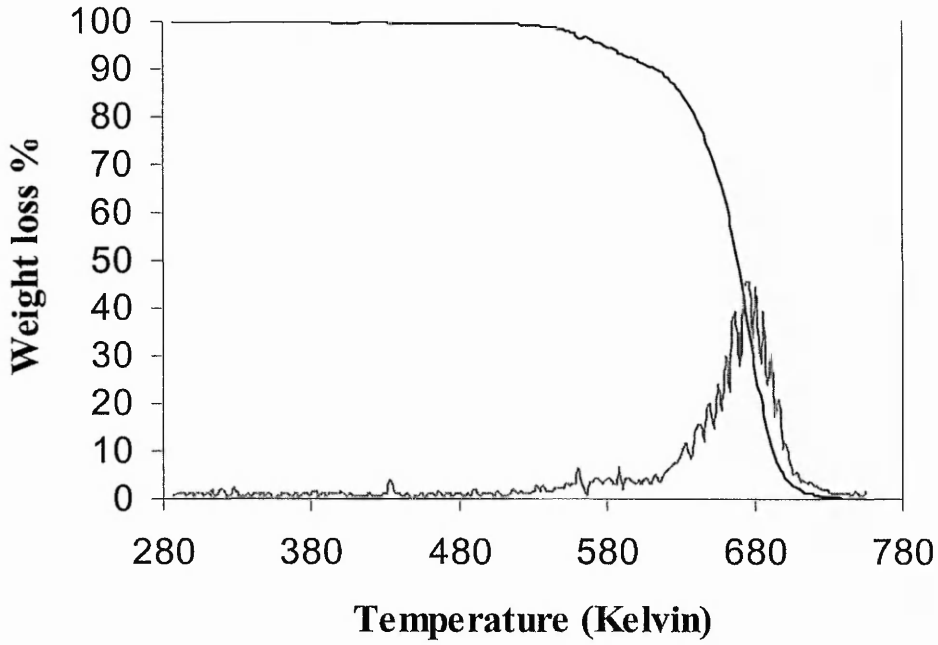

Figure 2.22: TGA curve of α,ω-hydroxyl poly(ε-caprolactone). In black the thermograph and in grey the first derivative.

The degradation temperature Td is obtained from the thermograph derivative maximum, Figure 2.22. Analysis of the degradation profile; steps and slope can also give information on the materials structure.

2.2.4.2. Differential Scanning Calorimetry (DSC)-Power Compensation DSC[37]

The measuring system consists of two microfurnaces, a sample and a reference holder, which contains a temperature sensor and a heat resistor during heating up. The holders are heated and if a temperature difference is detected between them due to a phase change in the sample for example, then energy is supplied until the temperature difference is less than a threshold value typically <0.01 K. The energy input per unit time is recorded as a function of the temperature.

Thermal analysis was performed on 4-8 mg of the composites using a DSC7 differential scanning calorimeter from Perkin-Elmer operating at a heating and cooling rate of 10 °C/min. Temperature and energy calibrations were carried out with indium and tin standards. An initial temperature cycling was used for all samples to eliminate variations due to the individual thermal history of each sample. Samples were first

heated from 25 °C to 200 °C at 10 °C/min, cooled from 200 °C to 25°C at 10 °C/min and subjected to a final heating from 25 °C to 200 °C at 10 °C/min.

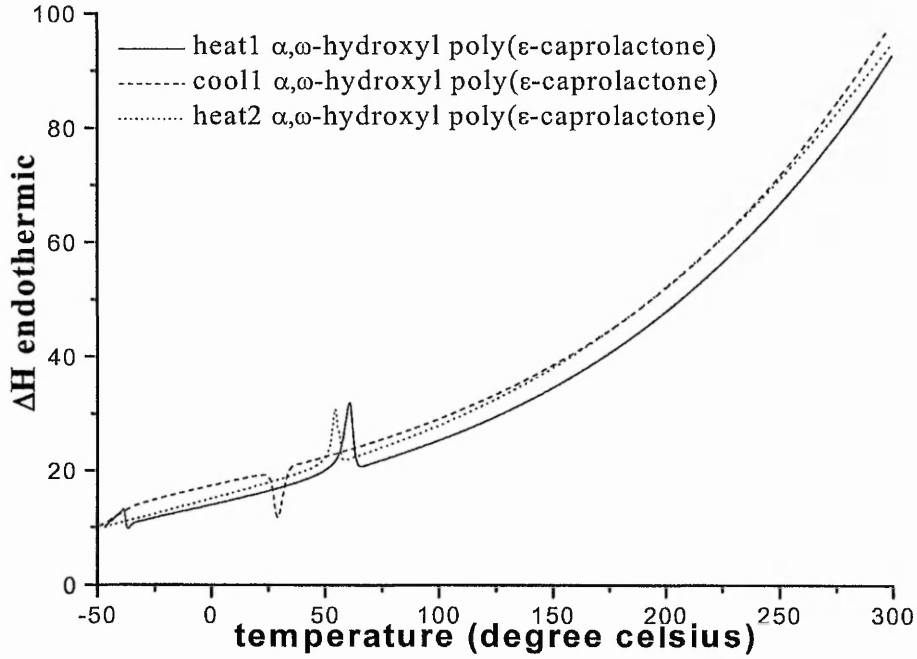

Figure 2.23: DSC thermogram of α,ω-hydroxyl poly(ε-caprolactone).

The DSC thermograms (Figure 2.23) were analyzed and a measure of polymer crystallinity was determinate as follow. The melting point, T_m is determined, for broad melting polymers, by the temperature of the maximum in the (dH/dT) plot near this transition. The enthalpy of melting or melting entropy (ΔH_f) is determined by constructing a baseline above the melting point and extending it to below any cold crystallization phenomena (exothermic peak below T_m and above T_g).

An estimate of the crystallinity of a polymer can be made from the DSC data assuming strict two-state behaviour. The polymer is presumed to be composed of distinct non-interacting amorphous and crystalline regions where reordering of the polymer structure only occurs at the melting temperature of the crystalline components.

The crystallinity of the polymers was calculated using the melting entropy data (ΔH_f) collected from the DSC analysis together with the following equation[38] :

$$Cr_{DSC} = \Delta H_f/(\chi_A * \Delta H_f^\circ) \qquad \textbf{Equation 2.2}$$

ΔH_f is the melting entropy of the sample obtained from the DSC experiment

χ_A is the weight percent of poly(α-hydroxyacid) in the composite sample

$\Delta H_f^\circ{}_{PCL}$ = 135.31 J/g is the melting entropy of poly(ε-caprolactone) when it is 100 % crystalline[39].

$\Delta H_f^\circ{}_{PLLA}$ = 146.00 J/g is the melting entropy of the pure poly(L-lactic acid) when it is 100 % crystalline[40].

$\Delta H_f^\circ{}_{PCLexp}$ = 78.60 J/g is the melting entropy of poly(ε-caprolactone) prepared. PCL Cr_{DSC} = 0.58.

$\Delta H_f^\circ{}_{PLLAexp}$ = 31.54 J/g is the melting entropy of the poly(L-lactic acid) prepared. PLLA Cr_{DSC}= 0.216.

Below, tables 2.14 and 2.15 list some thermal properties of the α,ω-hydroxyl poly(ε-caprolactone) and poly(L-lactic acid).

Table 2.14: Properties of α,ω-hydroxyl poly(ε-caprolactone).

Property	Units	Conditions	Value
Degree of crystalline	Xc %	PCL	semicrystalline
Heat of fusion	ΔH_f kJ.mol^{-1}	PCL complete crystalline	135.31 [39]
		PCL complete crystalline	139.50 [41]
Glass transition temperature T_g	K	PCL	213 [42]
Melting point T_m	K	PCL of various molecular weights	328-333 [42]
Decomposition temperature T_d	K	PCL (M_w=0.5-3 10^5)	573
		M_w =4000	536

Table 2.15: Properties of α,ω-hydroxyl poly(lactic acid) polymers.

Property	Units	Conditions	Value
Degree of crystalline	Xc %	D-PLA	Semicrystalline [43]
		L-PLA	0 ± 37 [44]
		D,L-PLA	Amorphous [44]
Heat of fusion	ΔH_f kJ.mol^{-1}	L-PLA complete crystalline	146 [40]
Glass transition temperature T_g	K	L-PLA of various molecular weights	326-337 [40,45]
		D,L-PLA of various molecular weights	323-330 [46]
Melting point T_m	K	L-PLA of various molecular weights	418-459 [43, 44, 46]
Decomposition temperature T_d	K	L-PLA (M_w=0.5-3 10^5)	508-528 [43]

2.2.5. Powder X-Ray Diffraction Analysis (XRD)

The completely random orientation of individual crystallites in a sample generates cones of diffracted X-ray energy for each individual plane of atoms according to the Bragg equation[47]. $\lambda=2d\sin\theta$, where λ is the wavelength of the radiation, d the spacing between atomic planes and θ the angle between incident and diffracted radiation. The diffraction pattern is scanned by rotating the detector around the specimen. The instrument makes use of the parafocussing effect whereby the focus line of the X-ray tube and that of the counter are held on the line of the circle. This ensures that the x-rays measured are reflected from the surface of the sample and are focused onto the detector. Collection of powder diffraction patterns is made by mixing and grinding the equivalent weight of sample and α-alumina or corundum (α-Al_2O_3), a standard material, to a fine powder and pressing it into a small depression in glass coverslip sample holder. X-ray diffraction was performed on samples using a Hiltonbrooks modified Philips PW1050 Powder diffractometer with Cu-Kα (1.540562 Å) radiation operating at 42.5 KV and 18.00 mA. Samples were scanned over variable ranges between 5 ° to 80 ° of 2θ with a step-size of 0.02 ° and a count time of 8 seconds per step.

Powder XRD patterns are used to qualitatively and quantitatively identify crystalline materials using the JCPDS (Joint Committee on Powder Diffraction Standards) powder diffraction files. Indexing of crystal polymer structures is more difficult than for perfect crystalline structure. The main difference is that polymer crystals cannot be formed in perfect crystals, so single crystal or Laue patterns are not possible. Also, polymer crystals tend to be of low symmetry, orthorhombic or lower symmetry, due to the asymmetry in bonding in the crystalline lattice, i.e. the c-axis contain largely covalent bonds and the a and b axis largely van der Waals interactions or hydrogen bonds. Additionally, the unit cell form factor tends to be fairly complicated in polymer crystals[48]. Polymer crystals display a relatively large number of defects in some cases. This leads to diffraction peak broadening. The powder XRD diffraction pattern of an amorphous silica gel does not show any patterns or peaks. However a diffuse contribution to the background is observed.

Poly(ε-caprolactone) and poly(L-lactic acid) crystallographic data

Figures 2.22 and 2.23 are typical XRD diffraction patterns of α,ω-hydroxyl poly(ε-caprolactone), and poly(L-lactic acid). Tables 2.16, 2.17, 2.18 and 2.19, their respective crystallographic data (lattice, cell dimension, hkl, d-spacing, etc) were collected.

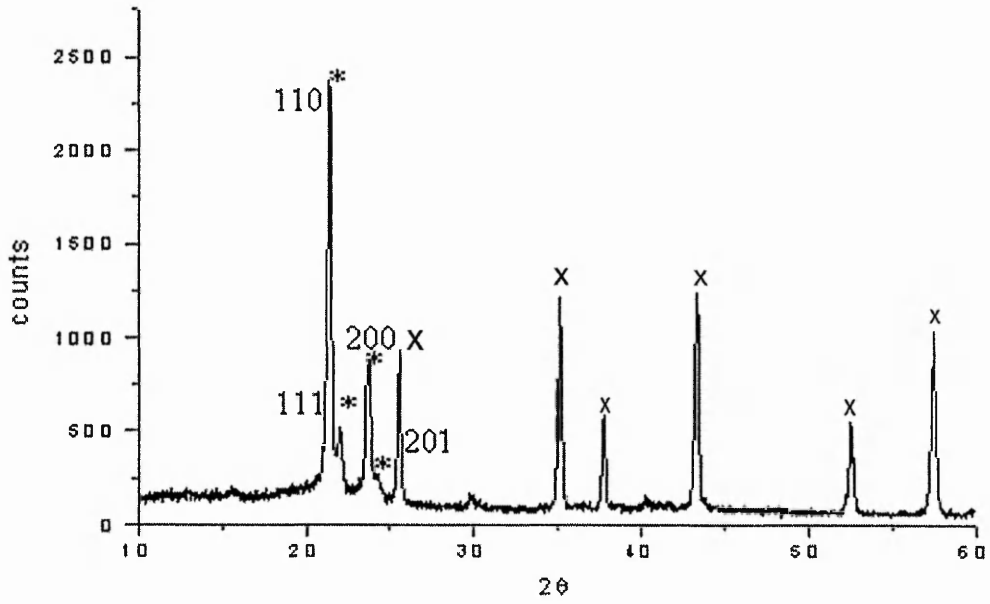

Figure 2.24: α,ω-Hydroxyl poly(ε-caprolactone) [*] and alpha aluminium oxide standard [X] (50 %wt) X-ray diffraction pattern.

Table 2.16: α,ω-Hydroxyl poly(ε-caprolactone), Crystallographic data from the literature.

Lattice	Monomers per unit cell	Cell dimension (Å) a	b	c	Cell angles[(a)]	Ref.
Orthorhombic	4	7.496	4.974	17.30	90	49, 50
	4	7.47	4.98	17.05	90	51

Table 2.17: Angle (2θ), d-spacing and intensity of characteristic peaks observed in the X-ray diffraction pattern of α,ω-hydroxyl poly(ε-caprolactone) with α-Al_2O_3 50 wt% as a standard[52].

No	Angle	Counts	dspacing	Rel I	assignment	hkl
1	21.50(s)	2360	4.130	100	Poly(ε-caprolactone)	110
2	22.14(w)	504	4.012	21	Poly(ε-caprolactone)	111
3	23.84(m)	869	3.729	37	Poly(ε-caprolactone)	112
4	24.46(sh)		3.636		Poly(ε-caprolactone)	201

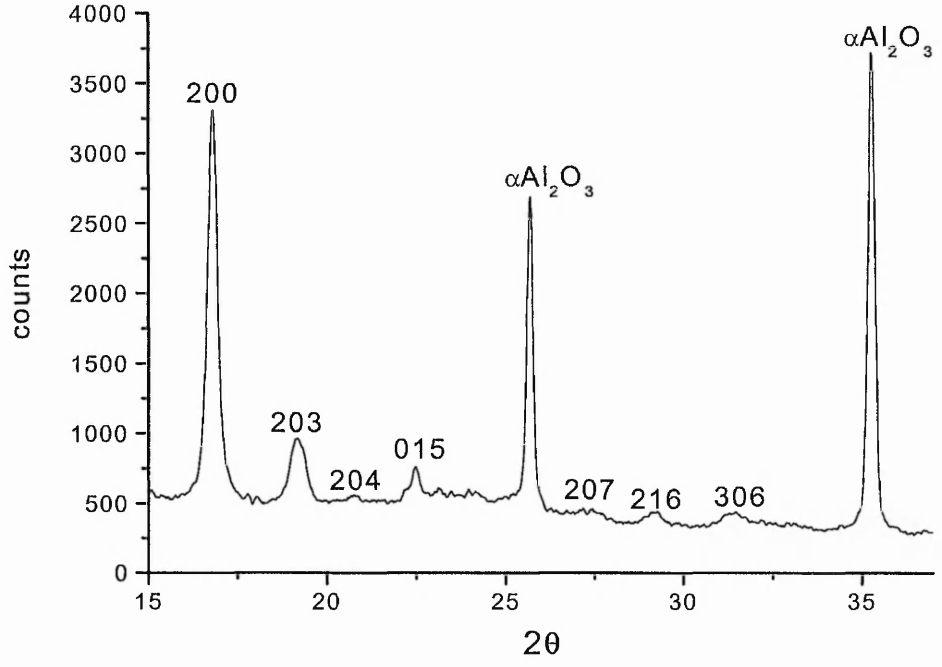

Figure 2.25: α,ω-Hydroxyl poly(L-lactic acid) and alpha aluminium oxide standard (50 %wt) X-ray diffraction pattern.

Table 2.18: Unit cell dimensions of α,ω-hydroxyl poly(L-lactic acid).

Lattice	Monomers per unit cell	Cell dimension (Å) a	b	c	Cell angles[(a)] γ (degree)	Chain conformation ρ_n of helix	
Hexagonal	-	5.9	5.9	-	120		[53]
Orthorhombic	-	10.31	18.21	9.00	90	3_1	[54]
Pseudo-orthorhombic	20	10.34	5.97	-	90	10_3	[53]
Pseudo-orthorhombic	20	10.6	6.1	28.8	90	10_3	[54]
Pseudo-orthorhombic	20	10.7 6	45	27.8	90	10_3	[55]

(a) Cell angles $\alpha = \beta = 90°$.

Table 2.19: Angle (2θ), d-spacing and intensity of characteristic peaks observed in the X-ray diffraction pattern of α,ω-hydroxyl poly(L-lactic acid)[56] with α-Al_2O_3 50 wt% as a standard.

No	Angle Counts	d spacing	Rel I	assignment	hkl
1	16.76(s) 3310	5.285	100	poly(L-lactic acid)	200
2	19.18(m) 530	4.624	16.0	poly(L-lactic acid)	203
3	20.78(w) 40	4.271	1.2	poly(L-lactic acid)	204
4	22.42(w) 188	3.962	5.7	poly(L-lactic acid)	015
5	29.18(w) 200	3.058	6.0	poly(L-lactic acid)	216
6	31.52(w) 236	2.836	7.0	poly(L-lactic acid)	306

The crystallinity of the polyesters was assessed using the powder x-ray diffraction data. The most commonly used method to measure the crystallinity of a solid crystal is by the measure of the Crystallite size (S) from line broadening using the Scherrer equation[47] : $S=K\lambda/b\cos\theta$ **Equation 2.3**

S = average crystallite dimension, λ = Wavelength of X ray beam = 1.5418 Å (Cu Kα), b = Diffraction broadening coefficient = FWHM + instrumental broadening, FWHM = Full Width at Half Maximum, Instrumental broadening set at 0.0 (it is true for crystallite size > at 500 angstroms), θ = Bragg angle, and K = crystallite shape constant, arbitrarily set at 0.89[47].

This method assumes that the polymer consists of perfectly crystalline and amorphous regions (two-phase concept). The powder x-ray diffraction pattern of the poly(α-hydroxyacid)-silica sol-gel composites prepared for the statistical experiments

(chapter 3) had their crystallite size measured. The S value was also calculated for the α-Al_2O_3 standard material. Table 2.20 lists the crystallite size average of α,ω-hydroxyl poly(ε-caprolactone) and α,ω-hydroxyl poly(L-lactic acid) in the composites, the S standard deviation obtained between all the prepared samples (Std b.) and the standard deviation obtained for triplicate measurements of the same sample (Std w.).

Table 2.20 : Crystallite size (S) average of α,ω-hydroxyl poly(ε-caprolactone) (hkl (110), 37 samples) and α,ω-hydroxyl poly(L-lactic acid) (hkl (200), 21 samples) in composites, S standard deviation obtained between all the prepared samples (Std b.) and the average standard deviation obtained for the triplicate measurement of the same sample (Std w.).

Crystallite Size (S)	**Poly(ε-caprolactone)** (Average 35.331°)	**Poly(L-lactic acid)** (Average 24.738°)
Std b.	4.616	0.765
Std w.	0.586	0.473
	Reference α-Al_2O_3 (Average 37.179°)	
Std b.	3.486	1.258
Std w.	1.856	1.258

Table 2.20 showed clearly that the crystallite size variation between the triplicate measurements of the same sample was very large compared to the variation observed between samples with different chemical composition. It was also observed that the crystallite size standard deviations of the reference were also very large. Therefore, this method was not used because of the poor significance of the crystallite size variation observed.

Another method for the measure of the crystallinity more adapted to semi-crystalline polymers is the measure of a relative crystallinity index. The relative crystallinity of the polymers was calculated using the method described by W. O. Statton[57]. The diffraction intensity of an unknown specimen was denoted I_u, and that of crystalline and amorphous specimens as I_c and I_a respectively. The analysis procedure was as follows; after normalization using an internal reference (α-Al_2O_3), the diffraction patterns were smoothed using a Savitzky-Golay filter method. Then the (I_u-I_a) and (I_c-I_a) values were determined at each value of 2θ, and the results plotted graphically with values of (I_u-I_a) as the ordinates and values of (I_c-I_a) as the abscissae. The slope of the plot was the RCr_{XRD} index for the unknown sample (Figure 2.26).

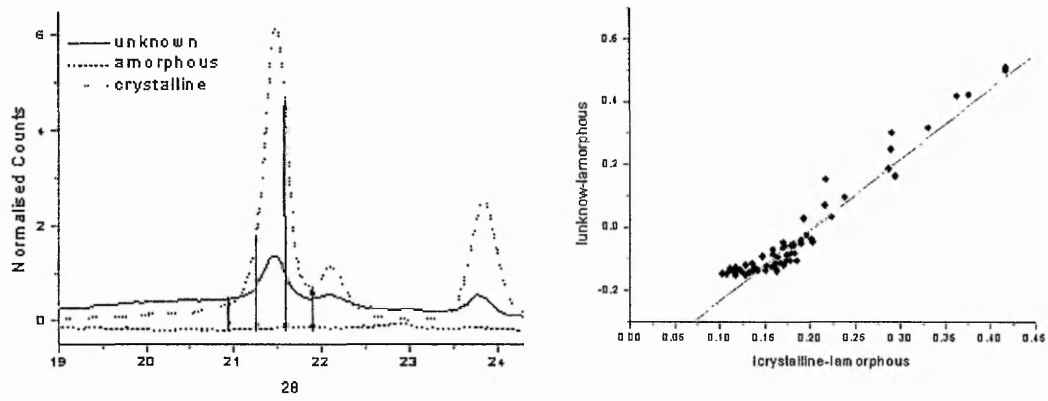

Figure 2. 26 : The graph on the left shows the XRD diffraction patterns of a crystalline, amorphous and unknown crystallinity poly(ε-caprolactone). The graph on the right represents the plot of the values of (I_u-I_a) as the ordinates and values of (I_c-I_a) as the abscissae. The slope of the plot is the RCr_{XRD} index for the poly(ε-caprolactone) with unknown crystallinity.

2.2.6. Statistical experiment

The subject of this paragraph is to introduce the subject of using an experimental design approach in the study of composite materials. Multivariate data analysis experiments and chemometric approaches are increasingly being used in the chemical industry and academia[58]. The spread of these statistical methods corresponds notably to the need to improve and optimise processes for industrial and for the academic scientist introducing more rigorous experimental planning. For example, M. D. Contreras and R. Sanchez applied a factorial design to study the formulation effect on a cosmetic gel[59, 60]. To our knowledge such an approach has not been taken in the field of silica hybrid sol-gel materials. The factorial design approach has, however, been used to good effect in designing syntheses of mesoporous materials including the MCM families[61] and zeolitic materials[62]. Here, It is not intended to discuss in depth the statistical principles behind the experimental design. For more information several textbooks could be studied for familiarization with the theory of statistical methods. For example, the book by R. Christensen[63] examines the application of basic statistical methods up to the design of complex experiments. Others textbooks from B. J. Winer and co-authors, W. G. Cochran and G. M. Cox[64] and finally R. A. Fishers[65] are also recommended for a detailed understanding of the theory. R. C. Graham[66], S. N. Deming & S. L. Morgan[67] and J. C. Miller and co-authors[68] have also edited textbooks especially written for

chemists and analytical chemists with emphasise on the applications of a statistical approach.

The ideal experimentation is an environment in which all variation is systematically related to one or more independent variables, factors or treatments. Then, the experimenter's task would be to describe the mathematical function relating the variables. In reality this is never realized because the object of study is influenced by so many variables that it is impossible to hold them constant. Rather, observation can be conceived as having two major components, one associated with the effects of the variables and another related to the unknown variables, which is called random error. Therefore, the goals of an experiment should yield results in which systematic variation in a variable can be attributed to treatment effects (avoiding bias), and to reduce the random error components of the observations in order to increase the precision with which the treatment effects can be estimated.

The design of experiments is summed up as follows;

1. Have well defined, clear objectives
2. Experimental factors should not be obscured by other variables
3. Experiments should be free of bias
4. Provide a measure of the precision of the experiments
5. Ensure that the precision of the experiments is sufficient to meet the objectives of the experimental program.

A good statistical design authorizes the experimenter to evaluate the combined effect of two or more experimental variables that are used simultaneously. Information obtained from statistical design is more complete than that obtained from a series of single variable/factor experiments, in the sense that designs permit the evaluation of interaction effects. Interaction effects are effect attributable to the combination of variables. This approach also allows for the rationalisation and optimisation of the number of experiments necessary to obtain information on the effects and interaction of variables for an individual treatment. The choice of the particular design utilized is a compromise between information to be gathered and size of the design. There are

several ways to construct an experimental design from a latin square design, complete factorial design, fractional design etc[68]. In designing an experiment, the following principles are important. Randomisation; given the overall plan of the experiment, the final allocation of the treatments to units is performed using a suitable random allocation. This avoids the possibility of a systematic bias in the allocation and gives a basis for the statistical analysis of the experiment. Replication; each treatment should be observed more than once. Replication allows an estimation of the variability of the treatment effect to be measured.

In the following paragraph, factorial designs are introduced. If more than one type of treatment is under consideration, a factorial design consists of looking at all combinations of treatment. The different types of treatment are known as factors and the different values of the factors that are considered in the experiment are known as levels. For example, the treatment combination in a 2*2 factorial experiment can be represented schematically as follows.

		Levels of factor B		
		b_1	b_2	
	means			
Levels of factor A	a_1	ab_{11}	ab_{12}	$1\cdot$
	a_2	ab_{21}	ab_{22}	$2\cdot$
	means	$\cdot 1$	$\cdot 2$	$\cdot\cdot$

a_1 and a_2 designate the levels of factors **A**; b_1, b_2 designate the levels of factor **B**; ab_{11}, ab_{12}, ... are the treatment conditions in the factorial design. This can be generalized to larger designs for example a 2*3 factorial design.

		Levels of factor B			
		b_1		b_2	
Levels of factor C		c_1	c_2	c_1	c_2
Levels of factor A	a_1	abc_{111}	abc_{112}	abc_{121}	abc_{122}
	a_2	abc_{211}	abc_{212}	abc_{221}	abc_{222}

a_1 and a_2; b_1 and b_2; c_1 and c_2 designate the levels of respectively factors **A**, **B** and **C**; abc_{111}, abc_{112}, ... are the treatment conditions in the three-factorial design.

The structural model provides a theoretical rationale for the magnitude of these individual observations. Some of the assumptions that will be made for the purpose of estimation and analysis in two and three-factor experiments are summarized by the following structure models. For larger factorial designs with more factors and levels, the models are made similarly. The models assume that the factorial effect as well as the experimental error are additive and that an observation is a linear function of the factorial effects and the experimental error. Each term is supposed independent of the others.

The general model for a randomised complete 2 factorial design is

$$y_{ij} = \mu + A_i + B_j + AB_{ij} + \varepsilon_{ijk} \qquad \textbf{Equation 2.4}$$

In this model (equation 2.3) , y_{ij} is an observation made in the experiment under the treatment combination ab_{ij}. μ is the grand mean of all observations and is constant for all observation. ε_{ijk} is the random error which is associated with all the uncontrolled factors that potentially contribute to the experimental error. A_i, B_j, AB_{ij} are the main effects and the two-interaction effect. This model assumes that the factorial effects as well as the experimental error are additive.

For a 2*3 factorial design the model function can be written;

$$y_{ijk} = \mu + A_i + B_j + C_k + AB_{ij} + AC_{ik} + BC_{jk} + ABC_{ijk} + \varepsilon_{ijk} \qquad \textbf{Equation 2.5}$$

From the data obtained in the experiment, the analysis of variance is carried out. The objective of the analysis of variance is to investigate the effect of the various factors on the variability of the data and to determine which part of the variation in a population is due to the systematic reasons (called factors A, B, … or interactions) and which is due to random effects[69]. This consists of a decomposition of the treatment sums of square (SS) and degree of freedom (*df*), then the means squares (MS) are computed. Finally a test of significance is carried out, appropriate F ratios ($MS_{treatment}/MS_{error}$) are determined and the null hypothesis, H_0 tested. The hypothesis H_0: there is an effect of the treatment/ factor on the observations,

$X = \mu + \text{Treatment} + \varepsilon'$. In Table 2.21 is collected the analysis of variance calculations for a two-factorial design.

Table 2.21: Analysis of variance for a two-factorial design.

Source	***df***	**SS**	**MS**
A	a_i-1	$bN\Sigma_i(\ _i - \ ..)^2$	$bN\Sigma_i(\ _i - \ ..)^2/(a_i-1)$
B	b_j-1	$aN\Sigma_j(\ _{.j} - \ ..)^2$	$aN\Sigma_j(\ _{.j} - \ ..)^2/(b_j-1)$
AB	$(a_i-1)(b_j-1)$	$N\Sigma_{ij}(\ _{ij} - \ _{i.} - \ _{.j} + \ ..)^2$	$N\Sigma_{ij}(\ _{ij} - \ _{i.} - \ _{.j} + \ ..)^2/(a_i-1)(b_j-1)$
Error	a_ib_iN-1	$N\Sigma_{ij}(\ _{ij} - \ ..)^2$	$N\Sigma_{ij}(\ _{ij} - \ ..)^2/(a_ib_iN-1)$

For a three-factor experiment, the definitions of the degree of freedom, sums of squares, means squares, F ratio for main effects, interactions and experimental error are summarized in Table 2.22.

Table 2.22 : Analysis of variance for a three-factorial design[70].

Source	***df***	**SS**	**MS**	**F**
A main effect	a_i-1	$SS_A = b_j c_k n\Sigma(_{i\ldots} - \ldots.)^2$	$MS_A = SS_A / (a_i-1)$	$F_A = MS_A/MS_e$
B main effect	b_j-1	$SS_B = a_i c_k n\Sigma(_{\cdot j\cdot\cdot} - \ldots.)^2$	$MS_B = SS_B / (b_j-1)$	$F_B = MS_B/MS_e$
C main effect	c_k-1	$SS_C = a_i b_j n\Sigma(_{\cdot\cdot k\cdot} - \ldots.)^2$	$MS_C = SS_C / (c_k-1)$	$F_C = MS_C/MS_e$
AB interaction	$(a_i-1)(b_j-1)$	$SS_{AB} = c_k n\Sigma\Sigma(_{ij\cdot\cdot} - _{i\ldots} - _{\cdot j\cdot\cdot} + \ldots.)^2$	$MS_{AB} = SS_{AB}/(a_i-1)(b_j-1)$	$F_{AB} = MS_{AB}/MS_e$
AC interaction	$(a_i-1)(c_k-1)$	$SS_{AC} = b_j n\Sigma\Sigma(_{i\cdot k\cdot} - _{i\ldots} - _{\ldots k} + \ldots.)^2$	$MS_{AC} = SS_{AC}/(a_i-1)(c_k-1)$	$F_{AC} = MS_{AC}/MS_e$
BC interaction	$(b_j-1)(c_k-1)$	$SS_{BC} = a_i n\Sigma\Sigma(_{\cdot jk\cdot} - _{\cdot j\cdot\cdot} - _{\cdot\cdot k\cdot} + \ldots.)^2$	$MS_{BC} = SS_{BC}/(b_j-1)(c_k-1)$	$F_{BC} = MS_{BC}/MS_e$
ABC interaction	$(a_i-1)(b_j-1)(c_k-1)$	$SS_{ABC} = n\Sigma\Sigma\Sigma(_{ijk\cdot} - _{ij\cdot\cdot} - _{i\cdot k\cdot} - _{\cdot jk\cdot} + _{i\ldots} + _{\cdot j\cdot\cdot} + _{\cdot\cdot k\cdot} - \ldots.)^2$	$MS_{ABC} = SS_{ABC}/(a_i-1)(b_j-1)(c_k-1)$	$F_{ABC} = MS_{ABC}/MS_e$
Experimental error	$a_i b_j c_k(n-1)$	$SSe = \Sigma\Sigma\Sigma\Sigma(_{ijk} - _{ijk\cdot})^2$	$MSe = SSe/a_i b_j c_k(n-1)$	
Total	$a_i b_j c_k n-1$	$SStot = \Sigma\Sigma\Sigma\Sigma(_{ijk} - \ldots.)^2$	$MSe = SSe/a_i b_j c_k(n-1)$	

In the case of factorial experiments, the treatment sum of square and degrees of freedom may be partitioned into main effects for the factors, and interactions between factors. For the factorial designs with higher numbers of factors and values, the analysis of variance treatments are similar. The calculations are often then carried out using dedicated software. The results are presented as variance tables with the P value and a table of the coefficient and strength of effect values. The results are also easily read in the form of a graph plotting each factor and interactions of effect as a function of the P-value multiplied by the strength of the effect. Factorial designs are especially useful for describing qualitative and quantitative factors, factors that are measured on interval or ratio scales[67]. Because the factors are quantitative, the results have some predictive ability. However, for a full factorial design there is no replication so it is impossible to estimate the purely experimental error. Repeated centre points can be added to the factorial design. This allows an estimation of the experimental error and also validates the linearity of the equation model. Further, the factorial designs can be fractioned when interaction effects are known or assumed to be negligible. It is very often verified for interaction effects above or equal to three. This type of design is called a fractional design.

2.3. *In vitro* Apatite-Forming Ability or Osteoconductivity Tests

In vitro osteoconductivity tests have been developed to respond to the need to predict and understand the behavior of glasses and ceramics inside the human body. Bioactive materials are capable of promoting bond-tissue formation at their surface and bond to surrounding living tissue. Bond-tissue creation seems to be produced by carbonate hydroxyapatite layer formation on their surface, when in contact with physiological fluids. The solution parameters of pH, temperature and ionic concentration have a large effect on the precipitation of calcium phosphate from solutions containing Ca^{2+} and HPO_4^{2-} ions. This discussion is concerned only with the heterogeneous precipitation of calcium phosphate induced by silica-polyester materials. That is why, it is important to establish the conditions for which calcium phosphate precipitation induced by specific substrates only occurs (Figure 2.27).

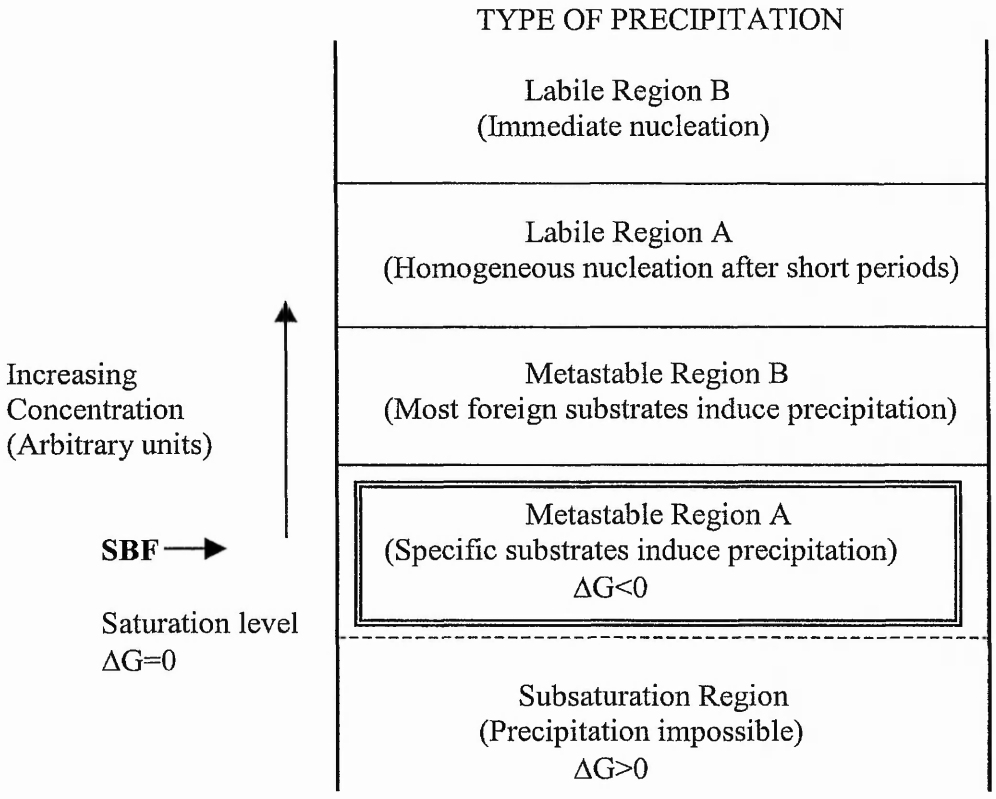

Figure 2.27 : Effect of solution ion concentration on precipitation[71].

These mechanisms of calcium phosphate layer formation on bioactive materials will be discussed in length in the chapter dedicated to the osteocondctivity results. The formation of the apatite-like layer occurs not only inside the body but also *in vitro* when the material is soaked in solutions simulating the human plasma (pH, ionic composition, etc)[72]. Some of the solutions used for the *in vitro* assays are: tris-buffer[73], newborn bovine serum[74] and cell culture media. In 1990, Kokubo and co-workers proposed the use of a simulated body fluid (SBF)[75], a cellular aqueous solution with an ion concentration and pH almost equal to those of human blood plasma. The SBF solution itself contains Ca^{2+} and HPO_4^{2-} ions and others ions (Table 2.23). It can be used to perform the *in vitro* bioactivity assessment of a wide variety of materials.

Table 2.23 : Ionic composition of SBF and human blood plasma (mM)[76].

	Na^+	K^+	Mg^{2+}	Ca^{2+}	Cl^-	HCO_3^-	HPO_4^{2-}	SO_4^{2-}
SBF	142.0	5.0	1.5	2.5	147.8	4.2	1.0	0.5
Plasma	142.0	5.0	1.5	2.5	103.0	27.0	1.0	0.5

A solution of simulated body fluid (SBF) was prepared from an ameliorated procedure of S. B. Cho and al.[77]. The preparation of a reproducible simulated body fluid was important to obtain repeatability of the precipitation of calcium phosphate on materials. The simulated body fluid was prepared using bottles and flasks, which were all washed with neutral detergent and deionised water. First, 700ml of deionised water was put in 1 litre polyethylene bottle and stirred with a magnetic teflon stirrer and the reagent-grade chemicals given in Table 2.24 were added to the water one by one in the order given, after each reagent had completely dissolved. The temperature of the solution in the bottle was adjusted to 37 °C with a water bath, and the pH of the solution was finally adjusted to pH 7.4 by 1 M hydrochloric acid solution solution (few drops). Then the solution was transferred from the polyethylene bottle to a glass volumetric flask. Deionised-water was added to adjust the total volume of the solution to 1 litre, and the flask was shaken. The solution was transferred from the flask to a polyethylene bottle, and used directly to avoid ageing. The SBF could also be stored in a refrigerator at 5 °C for few weeks.

Table 2.24: Simulated body fluid (**SBF**): Materials and composition.

Order	Name Reagent (Mw)	g/l
1	NaCl (58.44) [Aldrich 99%]	7.9953
2	Na_2HCO_3 (84.01) [BDH 99%]	0.3530
3	KCl (74.55).[BDH 99.5]	0.2237
4	$K_2HPO_4.3H_2O$ (228.23) [BDH 99%]	0.2282
5	$MgCl_2,6H_2O$ (203.30) [BDH 99%]	0.3049
6	1 mol/dm^3 HCl	40ml
7	$CaCl_2$ (147.02) [BDH 99%]	0.3677
8	Na_2SO_4 [BDH 99.5%]	0.071
9	$(CH_2OH)_3CNH_2$ Tris buffer [Sigma]	6.057

Material disk for *in vitro* osteoconductivity tests were prepared as follow. Samples were cast in a DRIFT sample cup (∅ 13 mm, h 2 mm) or pressed onto an Infrared die (∅ 13 mm) under 10 Tonnes for 5 minutes. Usually, between 0.1 to 0.2 gm of material was used for each disk. The disks were washed with deionised water before use.

Two protocols have been performed using the SBF solution. The first one called the static biomimetic process (SBP) and the second, the dynamic biomimetic process (DBP). A third protocol was developed, using supersaturated calcium and phosphate solutions, called alternate soaking process (ASP).

2.3.1. Static Biomimetic Process

Static *in vitro* assays were performed following the protocol described by Greenspan and co-workers[78] and still the most commonly used[79, 80, 81]. The disks were soaked horizontally or kept in a vertical position using a platinum scaffold in 20 ml of simulated body fluid covered to prevent SBF loss and kept at 37 °C. Samples were withdrawn at required intervals, washed gently with deionised water, and dried in an oven at 40 °C for 2 days. Figure 2.28 represents the static biomimetic process.

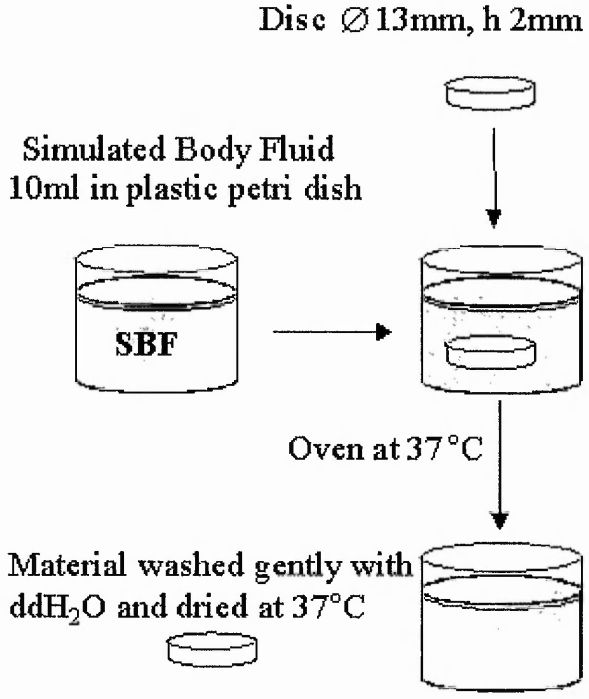

Figure 2.28 : Static biomimetic process (SBP).

2.3.2. Dynamic Biomimetic Process (DBP)

Dynamic *in vitro* assays were performed following the protocol described by Vallet-Regi and co-workers[81]. DBP was performed by soaking the disks in SBF solution at 37 °C, using a platinum scaffold to keep them in vertical position. The SBF was introduced in the assay container at the same rate as it was removed, keeping the volume constant; around 30 ml, during the test. This operation was carried out using a peristaltic pump with a flow rate of 0.2 ml/min. The selection of the flow value was a compromise between other authors' protocols[81, 82] and technical possibility. Samples were withdrawn, washed gently with deionised water, and dried in the oven at 40 °C for 2 days. Figure 2.29 represents the dynamic biomimetic process.

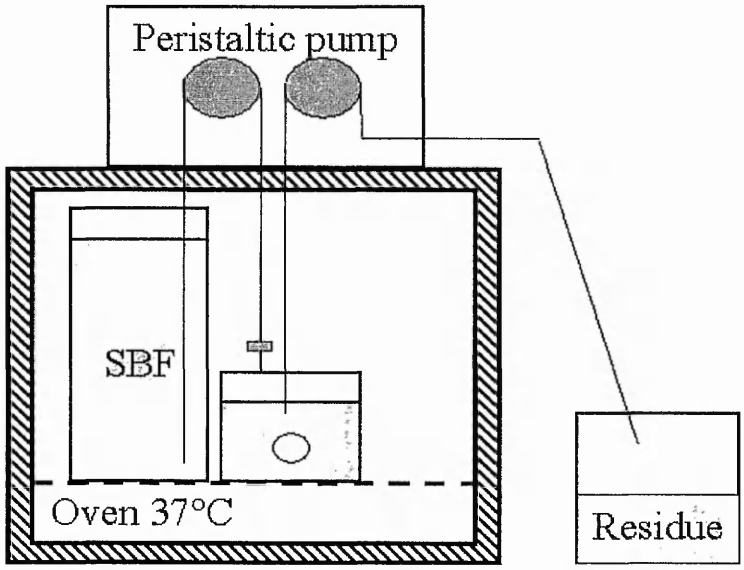

Figure 2.29 : Dynamic biomimetic process (DBP).

2.3.3. Alternate Soaking Process (ASP)

This procedure differs from the above in that it does not attempt to mimic the fluid surrounding the implanted materials. The drawbacks of the above processes are that they take a long period of time to form apatite[83, 84]. The aim of the alternate soaking of the materials in a calcium and phosphate solutions was to precipitate calcium phosphate materials on the material surfaces quickly (with in hours). It is a process based on the wet preparation of hydroxyapatite[85]. The schematic representation of the ASP process is given in Figure 2.30.

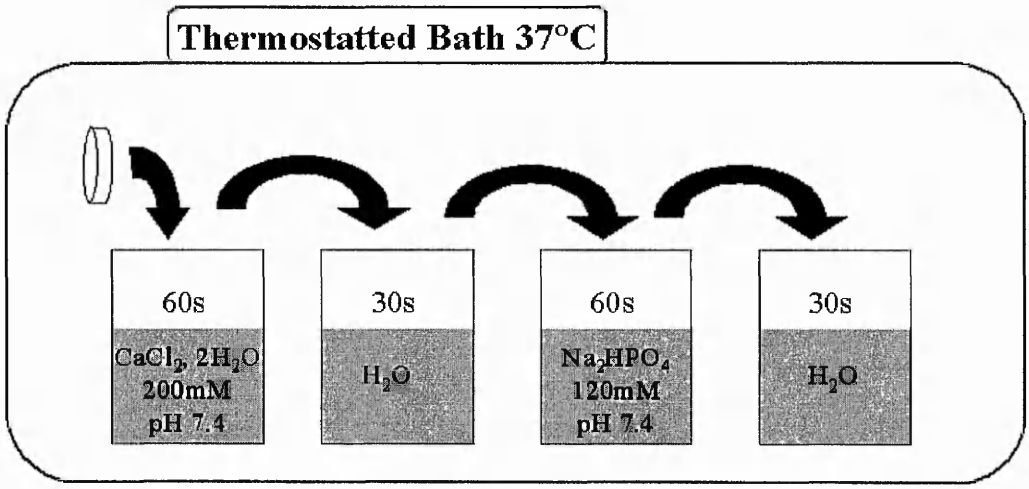

Figure 2.30 : Alternate soaking process (ASP).

The procedure was adapted from several published works[86, 87, 88]. The first step consists of soaking a disk of the chosen material in 500 ml of a 200 mM $CaCl_2$, 2 H_2O solution buffered with tris-HCl [Sigma] pH 7.4 at 37 °C for 60 seconds, followed by washing in deionised water (500 ml) at 37 °C for 30 seconds. The second step consists of the subsequent soaking of the disk in 500 ml of 120 mM Na_2HPO_4/HCl (pH 7.4) aqueous solution at 37 °C for 60 seconds and then washing in 500 ml deionised water for 30 seconds. A combination of the two steps was defined as one ASP cycle. After the chosen number of ASP cycles, the disks were dried at 37 °C for 24 hours.

The *in vitro* assay, when bioactive materials are in contact with any of these solutions, three phenomena occur: release of ions (silicon species), pH modifications and growth of an apatite like layer on the material surface. Therefore the assessment of the processes taking place is based on monitoring and characterizing the modification in the fluid and on the materials surface. The characterization methods for the fluid are the molybdenum blue assay to measure the release of silicic acid, and pH measurement. The characterization methods for the material surface are a calcium assay, electron microscopy (TEM and SEM-EDX), diffuse reflectance infrared (DRIFT).

2.4. Diffuse Reflectance Infra-red Spectroscopy (DRIFT)

The DRIFT analytical technique has been used for the study of apatite formation[89] on the surface of materials. It is a non-destructive technique suitable for powdered and solid samples. Basically, when infrared radiation is directed onto the surface of a solid sample, two types of reflected energy are observed. One is diffuse reflectance and the other is specular reflectance. Diffuse reflectance is the radiation, which penetrates into the sample and then re-emerges. Samples are generally mixed with KBr, but can also be used alone after roughening the surface with abrasive paper to increase the proportion of diffuse radiation. Spectra obtained are different from the conventional transmission infrared spectra. A mathematical function (Kubelka-Munk) is use to compensate for the decrease in peak intensities at high wavelengths. Also the peaks are often less sharp than in transmission spectra and distortions such as inverted or derivative signal shapes can be observed. The last mentioned are called Restrahlen bands and depend on particle size, sample packing and concentration. Figure 2.31 presented the FTIR and DRIFT spectra of the same poly(ε-caprolactone) sample.

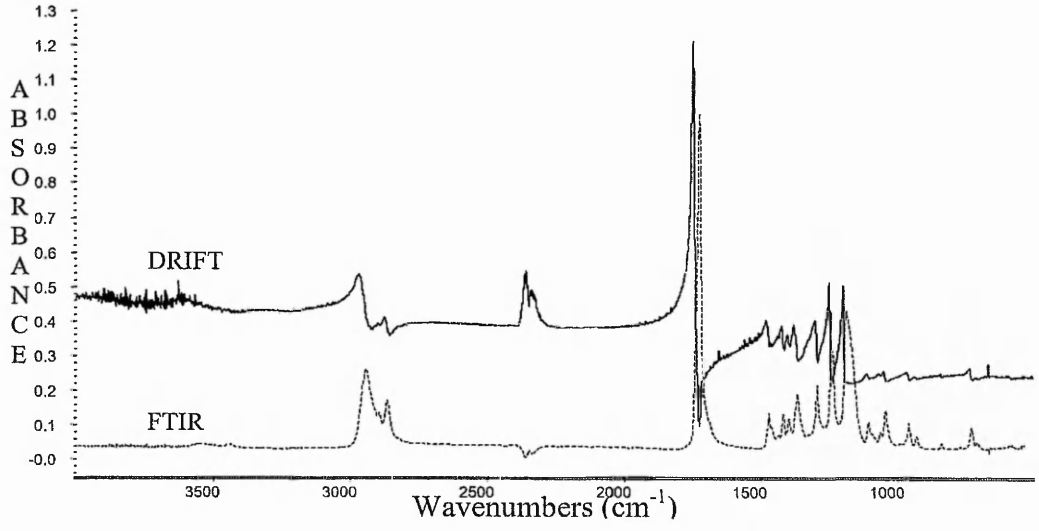

Figure 2. 31 : DRIFT and FTIR spectra of α,ω-hydroxyl poly(ε-caprolactone).

3.5. Electron Microscopy

Electron microscopes were developed due to the limitations of light microscopes which are limited by the physics of light to 500x or 1000x magnification and a resolution of 0.2 micrometers. The transmission electron microscope (TEM) was the first type of electron microscope to be developed and is patterned exactly on the light transmission microscope except that a focused beam of electrons is used instead of light to "see through" the specimen. It was developed by Max Knoll and Ernst Ruska in Germany in 1931.The first scanning electron microscope (SEM) was developed in 1942 with the first commercial instruments available around 1965. Its late development was due to the electronics involved in "scanning" the beam of electrons across the sample. Electron microscopes (EMs) function exactly as their optical counterparts except that they use a focused beam of electrons instead of light to "image" the specimen and gain information as to its structure and composition. The basic steps involved in all EMs:

1. A stream of electrons is formed (by the electron source) and accelerated toward the specimen using a positive electrical potential
2. This stream is confined and focused using metal apertures and magnetic lenses into a thin, focused, monochromatic beam.
3. This beam is focused onto the sample using a magnetic lens
4. Interactions occur inside the irradiated sample, affecting the electron beam

These interactions and effects are detected and transformed into an image. The above steps are carried out in all EMs regardless of type.

Transmission electron microscopy (TEM) analyses were performed using a JEOL 2010 TEM with a tungstene or LaB_6 electron gun filament operating at an accelerating voltage of 200 keV. The TEM was calibrated to check the camera length using an aluminum standard. As the d-spacing are already known, diffraction patterns were obtained at the camera length to be used with samples and a back calculation performed to obtain the exact length. For a crystalline material such as calcium phosphate materials, the sample was ground to a fine powder. A suspension of the powder was prepared in an inert solvent (ethanol or acetone). The suspension was dropped onto a 3 mm diameter copper support grid coated with polyvinyl formal (formvar) and sputtered with a thin film of carbon and allowed to dry in air before

examination. For the composite materials the samples were prepared as above or embedded in a resin. The resin was prepared as follow; 2 parts volume of TAAB 812 [TAAB] an epoxy resin, 1.2 part volume of dodecenyl succinic anhydride [TAAB] and 1 part volume of methyl nadic anhydride were added and mixed for 20 minutes at room temperature. Then, 0.8 part volume of benzyl dimethylamine (accelerator) [TAAB] was added and the mixture stirred for 20 more minutes. The materials samples were soaked with the prepared resin and put under vacuum for 60 minutes. The samples were collected and put in plastic molds and the mold volume top up with the resin. The prepared molds were then put in an oven at 50-60 °C under vacuum (0.01 torr) for 48 hours to allow the resin to solidify. Slides were prepared using a glass knife.

Scanning electron microscopy (SEM) analyses were carried out on a Jeol JSM6400 instruments using low accelerating voltages of 5 keV and 10 keV respectively to avoid accumulation of electronic charge on the materials and their destruction. Solid samples were put on a double-sided adhesive tape mounted onto a flat-topped alminium stub. After mounting the specimens onto the stubs, they were sputter coated with either a gold, aluminium or carbon thin film to prevent the specimen charging up in the electron beam using. Coating were performed on an Edwards S150B sputter coater equipped with an Edward carbon system with the gas pressure less than $3x10^{-1}$ mbar and the current about 40 mA. The purpose of this film was to allow the current to leak away avoiding charging of the specimen surface and degradation of the quality and resolution of the SEM image. The choice of film type was driven by the need to have quantitative micro-analysis. In fact, the gold line $K\beta_1$=2.149 keV overlapped the phosphorous line $K\alpha_1$= 2.02 keV and the silica $K\alpha_1$=1.74 keV line. Therefore, aluminium ($K\alpha_1$=1.49 keV) or even better carbon ($K\alpha_1$=0.282 keV) were more suitable coating materials for SEM sample preparation and quantitative micro-analysis.

Scanning electron microscopes are often coupled with Energy dispersive X-ray micro-analysers (EDXA). The energetic electron beam - sample interactions generate X-rays that are characteristic of the elements present in the sample. Detectibility limits can be as low as 0.2% for the higher atomic number elements. EDXA analysis can also quantify the elements it detects. A quantitative analysis can be performed by a standardless analysis procedure. A standardless analysis quantifies the elements by

calculating the area under the peak of each identified element and after taking into account the accelerating voltage of the beam to produce the spectrum, the computer performs calculations to create sensitivity factors that will convert the area under the peak into weight or atomic percent. EDXA analysis was carried out on SEM samples using a PGT X-ray microanalysis system mounted on Jeol JSM6400 at a 20 keV accelerating voltage. Usually, elemental composition data were obtained and means calculated from at least 5 EDXA measurements over different parts of the sample surface.

2.6. Colorimetric assays

2.6.1. Determination of Silicic Acid Concentration by the Molybedenum Blue Assay

Numerous chemical methods exist for the determination of silica concentration such as atomic absorption and silicamolybdate, respectively for concentrations higher than 0.1 % and 1 to 0.1 ppm[17]. The method is based on the ability of silicic acid to form a yellow heteropoly acid, silico-12-molybdic acid, with molybdate ions in an acidic solution[90]. Silicomolybdic acid can readily be reduced in an acidic medium to give a blue α silicomolybdous acid[91]. The optical density is then monitored at a wavelength of 810nm and concentration of silicic acid related to the absorbance of light using a calibration curve. This technique is more sensitive than the yellow silicomolybdate method as a much stronger absorbance is obtainable with a small concentration of orthosilicic acid. It must be noticed that polysilicic acid will not completely dissociate to form monosilicic acid and is therefore undetectable by this method.

The molybdenum blue assay method was as follows. For the calibration, 1-10ml of a silica stock solution (10 ppm with respect to SiO_2) [BDH, silicate standard, originally 1000 ppm as SiO_2] was made up to 16 ml with distilled deionised water. To this was added 1.5 ml of a molybdate solution containing 20 $g.L^{-1}$ ammonium molybdate tetrahydrate [Aldrich, 98%] and 60 $ml.L^{-1}$ concentrated hydrochloric acid [Fisons A.R., 35.5-37.5%]. After 10 minutes (±0.5 minute), 7.5 ml of a reducing solution, containing 20 $g.L^{-1}$ oxalic acid [Aldrich ACS 99%], 6.67 $g.L^{-1}$ 4-methylaminophenol sulphate [Aldrich 98%], $4g.L^{-1}$ anhydrous sodium sulfite [HBL] and 100 $ml.L^{-1}$ concentrated sulfuric acid [Fisons AR 98%], was added to the assay

solution, left two hours at room temperature to develop the blue colour, before being read at 810 nm on a Unicam UV/Vis spectrometer. This produced a linear calibration over the concentration range used (Figure 2.32).

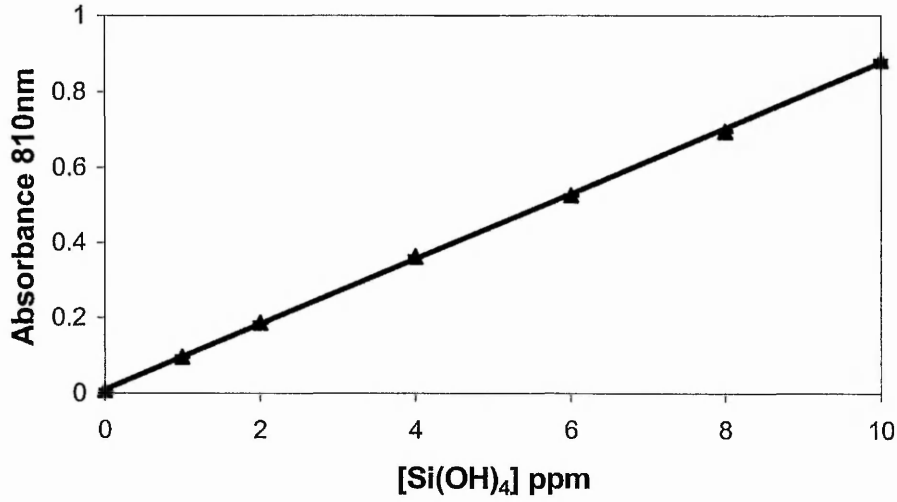

Figure 2. 32 : Typical calibration curve for molybdenum blue assay. Linear regression equation; Y= 0.0867X+0.0105, R^2= 0.9998, standard deviation = 0.003.

For the samples analysis, between 0.25 ml to 1 ml of the unknown silicic acid concentration solution was mixed with deionised water and made up to 16 ml. To this was added 1.5 ml of a molybdate solution. After 20 minutes, 7.5 ml of a reducing solution was added to the assay solution before being read at 810 nm on UV/Vis spectrometer after 2 hours to allow the coloration to fully develop. The coloration was stable for at least 24 hours.

2.6.2. Determination of the Calcium Precipitation by the Cresolphtalein Complexone Assay

The presence of calcium phosphate materials at the surface of the materials can be qualitatively assessed by EDX analysis. However direct quantification of the calcium-phosphate material precipitates on of the materials surface for comparison of the apatite forming ability of the composites was not straightforward. The method chosen was to dissolve in a strong acidic solution, the calcium phosphate materials precipitated on the material discs and to measure the amount of calcium dissolved in the collected acidic solution.

Cresolphtalein complexone assay; the procedure for the determination of calcium concentration is based on the interaction of the cation with suitable chromogenic agents. The chromogenic reagent is the o-cresolphtalein complexone which reacts with the calcium in an alkaline medium (pH ~ 10-12) to form a purple complex with an absorbance maximum at 575 nm. The quantitative measurement of the calcium concentration is based on the intensity of the 575 nm wavelength observed using a UV-vis spectrometer. A Sigma calcium kit® assay was used with ready prepared solutions. The procedure consisted first of combining 1 part of the calcium binding reagent solution (o-cresolphtalein complexone + 8-hydroxyquinoline) with 1 part of calcium buffer (2-amino-2-methyl-1,3-propanediol + stabilizers) in plastic container. 1 ml of the calcium reagent working solution was added to a 2 ml plastic cuvette at room temperature and 10 µl of samples added. The solution was mix gently. After 5 to 10 minutes and before 30 minutes (time of color stability) the absorbance value at 575 nm was measured. Calibration was carried out for each prepared calcium reagent solution with at least 10 points from 0 to 150 ppm calcium concentration (Figure 2.33). The calibration solutions were 1 N HCl solutions and calcium was added as the $CaCl_2$ salt. By using an acidic solution for the calibration curves, the aim was to perform calibration and analysis of data in similar conditions such that the measurements of the calcium concentrations were meaningful.

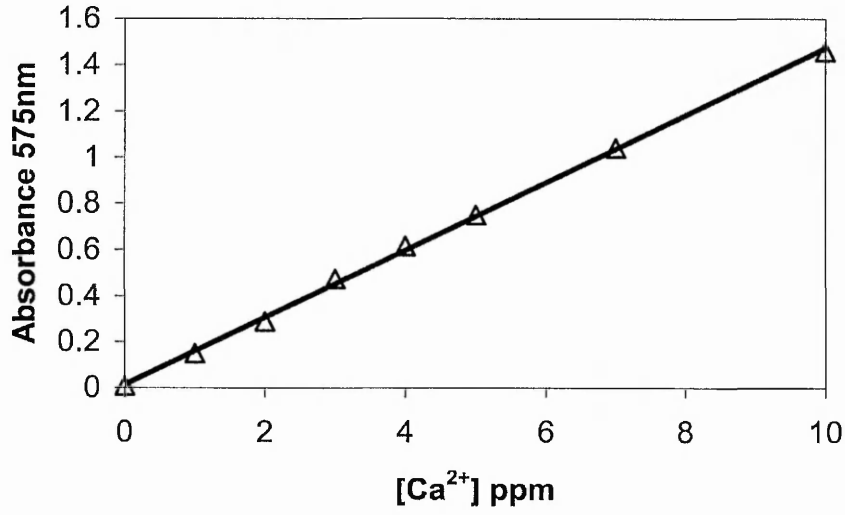

Figure 2. 33: Typical calibration curve for o-cresolphtalein complexone assay. Linear regression equation; $Y= 0.146X+0.0132$, $R^2= 0.9992$.

2.7. References

[1] D. E. Perrin, J. P. English, (1997), "Handbook of Biodegradable Polymers", Eds. A. J. Domb, J. Kast, D. M. Wiseman (Harwood Academic) 3-27.

[2] H. R. Kricheldorf, (2000), "Tin-initiated polymerizations of lactones: Mechanistic and preparative aspects.", *Macromolecular Symposia*, 153, 55-65.

[3] A. Duda, S. Penczek, A. Kowalski, J. Libiszowski (2000), "Polymerizations of epsilon-caprolactone and L,L-dilactide initiated with stannous octoate and stannous butoxide - A comparison.", *Macromolecular Symposia.*, 153, 41-53

[4] B. J. O'Keefe, M. A. Hillmyer, W. B. Tolman (2001), "Polymerization of lactide and related cyclic esters by discrete metal complexes.", *Journal of the Chemical Society-Dalton Transactions,* 2215-2224.

[5] P. Dobrzynski, J. Kasperczyk, H. Janeczek, M. Bero (2002), "Synthesis of biodegradable glycolide/L-lactide copolymers using iron compounds as initiators.", *Polymer*, 43 (9), 2595-2601.

[6] A. Schindler, Y. M. Hibionada, C. G. Pitt (1982), "Aliphatic polyesters. III. Molecular weight and molecular weight distribution in alcohol-initiated polymerization of ε-caprolactone.", *Journal of Polymer Science: Polymer Chemistry Edition*, 20, 319-326.

[7] Y. J. Du, A. J. Nijenhuis, C. Bastiaansen, P. J. Lemstra (1995), "New approaches to ring-opening polymerization-Evidences of step transfer polymerization.", *Macromolecular Report*, A32(7), 1061-1069.

[8] J. A. Burdick, L. M. Philpott, K. S. Anseth (2001), "Synthesis and characterisation of tetrafunctional lactic acid oligomers: A potential in situ forming degradable orthopaedic biomaterial.", *Journal of Polymer Science A: Polymer Chemistry*, 39, 683-692.

[9] D. Cohn, T. Stern, M. F. González, J. Epstein (2002), "Biodegradable poly(ethylene oxide)/ poly(ε-caprolactone) multiblock copolymers." *Journal of Biomedical Materials Research*, 59, 273-281.

[10] M. Messori, M. Toselli, F. Pilati, L. Mascia, C. Tonelli (2002), " Synthesis and characterization of silica hybrids based on poly(ε-caprolactone-b-perfluoropolyether-b-ε-caprolactone).", *European Polymer Journal*, 38, 1129-1136.

[11] H. Korhonen, A. Helminen, J. V. Seppälä (2001), "Synthesis of polylactides in the presence of co-initiators with different numbers of hydroxyl groups.", *Polymer*, 42, 7541-7549.

[12] W.P. Ye, F.S. Du, J.Y. Jin, J.Y. Yang, Y. Xu (1997), "In vitro degradation of poly(caprolactone), poly(lactide) and their block copolymers: Influence of composition, temperature and morphology.", *Reactive and functional polymers*, 32 (2), 161-168.

[13] A. Duda, S. Penczek, A. Kowalski, J. Libiszowski (2000), "Polymerizations of ε-caprolactone and L, L-dilactide initiated with stannous octoate and stannous butoxide. A comparison.", *Macromolecular Symposia,* 153, 41-53.

[14] D. Tian, Ph. Dubois, R. Jerome (1996), "A new poly(ε-caprolactone) containing hybrid creamer prepared by the sol-gel process." *Polymer*, 37(17), 3983-3987.

[15] G. L. Wilkes, B. Orler, H. Huang (1985),"Ceramers-Hybrid incorporating polymeric oligomeric species into inorganic glasses utilizing a sol-gel approach.", *Abstract of Paper of the American Chemical Society*, 190(SEP), 109-POY.

[16] B. M. Novak (1993), "Hybrid nanocomposite materials. Between inorganic glasses and organic polymers.", *Advanced Materials*, 5(6), 422-433.

[17] R. K. Iler (1979), "The Chemistry of Silica.", (John Wiley & Sons, New York).

[18] A. B. Brennan, G. L. Wilkes (1991),"Structure property behavior of sol-gel derived hybrid materials. Effect of a polymeric acid catalyst.", *Polymer*, 32(4),733-739 .

[19] H. H. Huang, B. Orler, G. L. Wilkes (1987), "Structure property behavior of new hybrid materials incorporating oligomeric species into sol-gel glasses. 3. Effect of acid content, tetraethoxysilane content and molecular-weight of poly(dimethylsiloxane).", *Macromolecules*, 20(6), 1322-1330.

[20] C. J. T. Landry, B. K. Coltrain, B. K. Brady (1992), "In situ polymerization of tetraethoxysilane in poly(methyl methacrylate)- Morphology and dynamic mechanical properties.", *Polymer*, 33(7), 1486-1495.

[21] J. J. Fitsgerald, C. J. T. Landry, J. M. Pochan (1992), "Dynamic study of molecular relaxations and interactions in microcomposites prepared by in situ polymerization of silicon alkoxides.", *Macromolecules*, 25(14), 3715-3722.

[22] D. Tian, Ph. Dubois, R. Jerome (1996), "A new poly(ε-caprolactone) containing hybrid creamer prepared by the sol-gel process.", *Polymer*, 37(17), 3983-3987.

[23] D. Tian, S. Blacher, Ph. Dubois, R. Jerome (1998), "Biodegradable and biocompatible inorganic-organic hybrid materials. 2. Dynamic mechanical properties, structure and morphology.", *Polymer*, 39(4), 855-864.

[24] D. Tian, S. Blacher, R. Jerome (1999), "Biodegradable and biocompatible inorganic-organic hybrid materials; 4. Effect of acid content and water content on the incorporation of aliphatic polyester into silica sol-gel process.", *Polymer*, 40, 951-957.

[25] D. Tian, S. Blacher, J. P. Pirard, R. Jerome (1998), "Biodegradable and biocompatible inorganic-organic hybrid materials. 3. A valuable route to the control o the silica porosity.", *Langmuir*, 14, 1905-1910.

[26] D. Tian, Ph. Dubois, R. Jerome (1997), "Biodegradable and biocompatible inorganic-organic hybrid materials. I. Synthesis and characterization.", *Journal of Polymer Science. Part A: Polymer Chemistry*, 35, 2295-2309.

[27] J. Wang, M. K. Cheung, Y. Mi (2002), "Miscibility and morphology in crystalline/amorphous blends of poly(caprolactone)/poly(4-vinylphenol) as studied by DSC, FTIR, and ^{13}C solid state NMR.", *Polymer*, 43, 1357-1364.

[28] H. Kaji, F. Horii (1997), "One- and two-dimensional solid-state C-13 NMR analyses of the solid structure and molecular motion of poly(epsilon-caprolactone) isothermally crystallized from the melt.", *Macromolecules*, 30, 5791-5798.

[29] J. L. Espartero, I. Rashkov, S. M. Li, N. Manolova, M. Vert (1996), "NMR analysis of low molecular weight poly(lactic acid)s.", *Macromolecules*, 29, 3535-3539.

[30] A. Helminen, H. Korhonen, J. V. Seppälä (2001), "Biodegradable cross-linked polymer based on triethoxysilane terminated polylactide oligomers.", *Polymer*, 42, 3345-3353.

[31] P. B. Coleman (1993), "Practical sampling technique for infrared analysis.", (CRC press).

[32] E. J. Moskala, D. F. Varnell, M. M. Coleman (1985), "Concerning the miscibility of poly(vinylphenol) blends-FTIR Study.", *Polymer*, 26, 228-234.

[33] A. Burneau, J. P. Gallas (1998), "Chapter 3A. Vibrational spectroscopies. The surface properties of silicas.", Ed. A. P. Legrand (Wiley & Sons, Chichester) 147-227.

[34] M. M. Coleman, J. F. Graf, P. C. Paintez (1991), "Specific Interactions and the Miscibility of Polymer Blends. Vibrational spectroscopy and the hydrogen bond.", (Lancaster) 276-290.

[35] J. Rak, J. L. Ford, C. Rostron, V. Walters (1985), "The preparation and characterization of poly(D, L-lactic acid) for use as a biodegradable drug carrier.", *Pharmaceutica Acta Helvetiae*, 60 (5-6), 162-169.

[36] G. Kister, G. Cassanas, M. Vert (1998), "Effect of morphology, conformation and configuration on the IR and Raman spectra of various poly(lactic acid)s." *Polymer*, 39(2), 267-273.

[37] G. Hohne, W. Hemminger, H. J. Flammersheim (1996), "Differential Scanning Calorimetry. An Introduction for Practitioners." Eds. G. Hohne, W. Hemminger, H. J. Flammersheim (Springer Verlag).

[38] T. Hatakeyama, F. X. Quinn (1999), "Thermal Analysis: Fundamentals and Applications to Polymer Science", 2nd ed. (John Wiley & Sons, New-York) 105-106.

[39] Lundberg, R. D., J. V. Koleske, and K. B. Wischmann (1969), *Journal of Polymer Science. Part A-1*, 7 2,915.

[40] K. Jamshidi, S.-H. Hyon, Y. Ikada (1988), "Thermal characterization of polylactides.", *Polymer* 29 (12), 2229-2234.

[41] V. Crecenze, G. Manzini, G. Calzolari, C. Borri (1972), "Thermodynamics of fusion of poly-β-propiolactone and poly-ε-caprolactone. Comparative analysis of the melting of aliphatic polylactone and polyester chains.", *European Polymer Journal*, 8, 449-463.

[42] G. L. Brode, J. V. Koleske (1973), "Lactone polymerisation and polymer properties. Polymerization of heterocycles.", eds. O. Vogl, J. Furukawa (Marcell Dekker, New-York).

[43] I. Engelberg, J. Kohn (1991), "Physicomechanical properties of degradable polymers used in medical applications. A comparative study.", *Biomaterials,* 12 (3), 292-304.

[44] D. K. Gilding, A. M. Reed (1979), "Biodegradable polymers for use in surgery-polyglycolic/polylactide acid homo-and copolymers: 1.", *Polymer* 20, 459-469.

[45] A. Celli, M. Scandola (1992), "Thermal properties and physical ageing of poly(L-lactic acid).", *Polymer,* 33(13), 2699-2703.

[46] P. Van De Witte, P. J. Dijkstra, J. W. A. Van Den Berg, J. Feijen (1996), "Phase behavior of polylactides in solvent-non solvent mixtures.", *Journal of Polymer Science Part B, Polymer Physics,* 34(15), 2553-2568.

[47] H. P. Klug, L. E. Alexander (1952)," X-ray Diffraction Procedures for polycrystalline and amorphous materials.", eds H. P. Klug, L. E. Alexander (John Wiley and Sons).

[48] L.E.Alexander (1979), "X-ray Diffraction Methods in Polymer Science.", eds. L.E.Alexander, Robert E.Krieger (Publishing Company, New York).

[49] H. Kaji, F. Horii (1997), "One- and two- dimensional solid-state ^{13}C NMR analyses of the solid structure and molecular motion of poly(ε-caprolactone) isothermally crystallized from the melt." *Macromolecules*, 30, 5791-5798.

[50] H. Bittiger, R.H. Marchessault, W.D.N. Niegish, (1970), "Crystal structure of poly(ε-caprolactone).", *Acta Crystallographica Section B: Structural Crystallography and Crystal Chemistry*, 26, 1923-1927.

[51] T. Hayashi, K. Nakayama, M. Mochizuki, T. Masuda (2002), "Studies of biodegradable of poly(hexano-6-lactone) fibers. Part 3. Enzymatic degradation in vitro.", *Pure Applied Chemistry*, 74(5), 869-880.

[52] S. Jiang, X. Ji, L. An, B. Jiang (2001), "Crystallization behavior of PCL in hybrid confined environment.", *Polymer*, 42, 3901-3907.

[53] B. Kalb, A. J. Pennings (1980), "General Crystallization Behavior of Poly(L-lactic acid).", *Polymer* 21, 607-612.

[54] W. Hoogsteen, A. R. Postema, A. J. Pennings, G. Tenbrinke, P. Zugenmaier (1990), "Crystal structure, conformation and morphology of solution-spun poly(L-lactide) fibers.", *Macromolecules,* 23(2), 634-642.

[55] P. De Santis, A. J. Kovacs (1968),"Molecular conformations of poly(S-lactic acid).", *Biopolymers* 6, 299-306.

[56] D. Brizzolara, H. J. Cantow, K. Diederichs, E. Keller, A. J. Domb (1996), "Mechanism of the stereocomplex formation between enantiomeric poly(lactides)s.", *Macromolecules*, 29, 191-197.

[57] W. O. Statton (1963), "An X-ray crystallinity index method with application to poly(ethylene terephthalate).", *Journal of Applied Polymer Science*, 7:803-815.

[58] R. Brereton (8 March 2002), "Applications of chemometrics.", *The Alchemist*, http://www.chemweb.com/alchem/articles/1014822038074.html.

[59] M. D. Contreras, R. Sanchez (2002), "Application of a factorial design to the study of specific parameters of a Carbopol ETD 2020 gel. Part I. Viscoelastic parameters.", *International Journal of Pharmaceutics*, 234, 139-147.

[60] M. D. Contreras, R. Sanchez (2002), "Application of a factorial design to the study of the flow behavior, spreadability and transparency of a Carbopol ETD 2020 gel. Part II.", *International Journal of Pharmaceutics*, 234, 149-157.

[61] G. Oye, J. Sjoblom, M. Stocker (2000), "A multivariate analysis of the synthesis conditions of mesoporous materials.", *Microporous and Mesoporous Materials,* 34, 291-299.

[62] N. Rueda, R. Bacaud, P. Lanteri and M. Vrinat (2001), "Factorial design for the evaluation of the influence of preparation parameters upon the properties of dispersed molybdenum sulfide catalysts.", *Applied Catalysis A: General,* 215 (1-2), 81-89.

[63] R. Christensen (1996), "Analysis of variance, design and regression. applied statistical methods.", ed. R. Christensen (Chapman & Hall).

[64] W. G. Cochran, G, M. Cox (1968), "Experimental designs. 2nd Edition. ", (Wiley and Sons, London).

[65] R. A. Fisher (1990), "Statistical methods, experimental design, and scientific inference." Ed. J. H. Bennett, (Oxford university Press).

[66] R. C. Graham (1993), "Data analysis for the chemical sciences." (VCH Publishers Inc.).

[67] S. N. Deming, S. L. Morgan (1993), "Data handling in science and technology-Volume 11. Experimental design: A chemometric approach. 2nd Ed." (Elsevier).

[68] J. C. Miller, J. N. Miller (1993), "Statistics for analytical chemistry. 3rd edition.", (Ellis Horwood Limited).

[69] M. Meloun, J. Militky, M Forina (1992), "Chemometrics for analytical chemistry. Volume 1: PC aided statistical data analysis." (Ellis Horwood Limited).

[70] H. M. Wadsworth (1990), "Handboook of statistical methods for engineers and scientists.", Ed. H. M. Wadsworth (McGraw Hill Publishing Co.).

[71] R. E. Wuthier (1984), "Metal ions in biological systems. V17 Calcification of vertebrate hard tissues.", Ed. H. Sigel, (M. Dekker).

[72] L. L. Hench (1991), "Bioceramics; from concept to clinic.", *Journal of the American Ceramics Society*, 74 (7), 1487-1510.

[73] C. G. Pantano, A. E. Clark, L. L. Hench (1974), "Multilayer Corrosion Films on Bioglass Surfaces.", *Journal of American Ceramic Society*, 57 (9), 412-415.

[74] S. Radin, P. Ducheyne, B. Rothman, A. Conti (1997), "The effect of in vitro modeling conditions on the surface reactions of bioactive glass.", *Journal of Biomedical Materials Research,* 37 (3), 363-375.

[75] T. Kokubo, H. Kushitani, S. Sakka, T. Kitsugi, T. Yamamuro (1990), "Solutions able to reproduce in vivo surface-structure changes in bioactive glass-ceramic A-W3.", *Journal of Biomedical Materials Research*, 27 (6), 721-734.

[76] K. Tsuru, M. Kokubo, S. Hayakawa, C. Ohtusuki, A. Osaka (2001), "Kinetics of apatite deposition of silica gel dependent on the inorganic ion composition of simulated body fluids.", *Journal of the Ceramic Society of Japan*, 109(5), 412-418.

[77] S. Cho, K. Nakanashi, T. Kokubo, N. Soga, C. Ohtsuki, T. Nakamura, T. kitsugi, T. Yamamuro (1995), "Dependence of apatite formation on silica gel on its structure: effect of heat treatment.", *Journal of American Ceramic Society*, 78(7), 1769-1774.

[78] D. C. Greenspan, L. L. Hench (1976), "Chemical and Mechanical Behavior of Bioglass Coated Alumina.", *Journal of Biomedical Materials Research*, 10 (4), 503-509.

[79] M. Vallet-Regi, I. Izquierdo-Barba, A. J. Salinas (1999),"Influence of P2O5 on crystallinity of apatite formed in vitro on surface of bioactive glasses.", *Journal of Biomedical Materials Research*, 46 (4), 560-565.

[80] M. Vallet-Regi, A. M. Romero, V. Ragel, R. Z. LeGeros (1999), "XRD, SEM-EDS, and FTIR studies of in vitro growth of an apatite-like layer on sol-gel glasses.", *Journal of Biomedical Materials Research*, 44 (4), 416-421.

[81] A. Ramila, M. Vallet-Regi (2001), "Static and dynamic in vitro study of a sol-gel glass bioactivity.", *Biomaterials*, 22, 2301-2306.

[82] P. Siriphannon, Y. Kameshima, A. Yasumori, K. Okada, S. Hayashi (2002), "Comparative study of the formation of hydroxyapatite in simulated body fluid under static and flowing systems.", *Journal of Biomedical Materials Research*, 60, 175-185.

[83] T. Taguchi, A. Kishida, M. Yanagi, T. Shimotakahara, T. Aikou, M. Akashi (1996), "Preparation of hydrogel-hydroxyapatite composite and evaluation of its biocompatibility.", *Bioceramics*, 9, 375-378.

[84] T. Taguchi, A. Kishida, M. Akashi (1998), "Hydroxyapatite formation on/in poly(vinyl alcohol) hydrogel matrices using a novel alternate soaking process.", *Chemistry Letters*, 711-712.

[85] R. N. Correia, M. C. F. Magalhaes, P. A. Marques, A. M. R. Senos (1996), "Wet synthesis and characterization of modified hydroxyapatite powders.", *Journal of Materials Science. Materials in Medicine*, 7 (8), 501-505.

[86] T. Karita, K. Imachi, T. Taguchi, A. Kishida, M. Akashi (2000), "In vitro Calcification model Part 1: Apatite formation on segmented polyurethane containing silicone using and alternate soaking process.", *Journal of Bioactive and Compatible Polymers*, 15, 72-84.

[87] T. Karita, K. Imachi, T. Taguchi, M. Akashi, K. Sato, J. Tanaka (2000), "In vitro Calcification model Part 2: Apatite formation on segmented polyurethane thin films by using an alternate soaking process: The effect of adsorbed serum proteins on calcification.", *Journal of Bioactive and Compatible Polymers*, 15, 230-244.

[88] K. Suzuki, T. Yumura, M. Mizuguchi, T. Taguchi, K. Sato, J. Tanaka, M. Akashi (2001), "Apatite-silica gel composite materials prepared by a new alternate soaking process." *Journal of Sol-Gel Science and Technology*, 21, 55-63.

[89] S. Cho, F. Miyaji, T. Kokubo, K. Nakanashi, N. Soga, T. Nakamura (1996), "Apatite formation on various silica gels in a simulated body fluid containing excessive calcium ion.", *Journal of the Ceramic Society of Japan*, 104(5), 399-404.

[90] L. V. Myshlyaeva, V. V. Krasnoshchekov (1974), "Analytical Chemistry of Silicon", (John Wiley & Sons, Chichester, translation J. Schmorak).

[91] J. D. H. Strickland (1952), "The preparation and properties of silicomolybdic acid. I. The properties of alpha silicomolybdic acid.", *Journal of the American Chemical Society*, 74, 862-876.

The studies presented in this chapter are about the poly(α-hydroxyacid)-silica composites. The composite materials have been prepared by two different methods; sol-gel and bulk. Statistical design experiments were carried out on the effect of the reactants on α,ω-hydroxyl poly(ε-caprolactone) and poly(L-lactic acid)-silica sol-gels. The polyesters crystallinity in composites was characterised by two techniques, powder X-ray diffraction and differential scanning calorimetry analysis. An understanding of the degree of poly(α-hydroxyacid) crystallinity was important since the crystallinity affects physical properties such as storage modulus, permeability, density, and melting point and consequently the polymer biodegradation and bioactivity properties. While most of these manifestations of crystallinity can be measured, a direct measure of degree of crystallinity provides a fundamental property from which these other physical properties can be predicted as well as the confinement of the polyesters in the silica phase and consequently the formation of homogeneous composites[1]. The effect of the bulk and sol-gel methods on the composites structure and the modification of the hydroxyl end-groups by triethoxysilane chemical groups on the poly(ε-caprolactone) and poly(L-lactic acid) have been investigated.

3.1. Statistical Design Applied to Poly(α-hydroxy acid)-Silica Sol-Gel Composites. Effects of Reactants on Poly(α-hydroxy acid) Crystallinity

The use of a factorial experimental design method allowed the rationalisation and optimisation of the number of experiments necessary to obtain information on the effects and interaction of variables for an individual synthesis procedure. The choice of the particular designs utilised in these studies was a compromise between information to be gathered and size of the design. In the current case, the aims were to investigate the effect and interaction of reactants on the incorporation of α,ω-hydroxyl poly(ε-caprolactone) and α,ω-hydroxyl poly(L-lactic acid) into organic-inorganic sol-gel composite materials. In the factorial design approach, it is postulated that the measured properties of the considered system can be expressed as a polynomial function of experimental parameters and interactions[2].

Choice of variables and levels were crucial. For the present studies, it was not the intention to look at the effect of physical factors such as temperature, stirring,

gelation and annealing times, as these effects have already been partially studied and have been reported elsewhere[3]. These parameters were therefore kept constant for all experiments and the effects of the relative concentrations of the chemical reactants on the structure of the polyester phase were investigated.

For the α,ω-hydroxyl poly(ε-caprolactone)-silica sol-gel material, a full 2^5 factorial design with five-repeated central points was chosen because it allowed the estimation of the experimental error, validates the equation model (curvature) and permitted the observation the effect of the interaction of variables. Each set of experimental conditions was called a run. The number of runs performed was 37. For the α,ω-hydroxyl poly(L-lactic acid)-silica sol-gel composites, a 2^5 fractional design (equivalent to half of a 2^5 factorial design) with five-repeated central point was chosen. Such a statistical design assumes that the measured properties of the considered system can be expressed as a first order polynomial function, and 3, 4 and 5-interactions are aliased[2]. The limited information available in the literature on the synthesis conditions for similar hybrid materials and the preliminary experiments done, allowed the definition of the maximum and minimum levels between which variations of the α,ω-hydroxyl poly(ε-caprolactone) and poly(L-lactic acid) physical state could be expected to be observed.

3.1.1. Choice of Factors, Levels, Experimental Matrix and Measured Responses

The following five factors (variables) were selected for the α,ω-hydroxyl poly(ε-caprolactone)-silica sol-gels: the molar ratios of: TEOS (tetraethyl orthosilicate)/PCL (α,ω-hydroxyl poly(ε-caprolactone)), EtOH (ethanol)/TEOS, THF (tetrahydrofuran)/TEOS, H_2O (water)/TEOS and HCl (hydrochloric acid)/TEOS. The maximum and minimum limits for the TEOS/PCL molar ratio were chosen following preliminary experiments (not presented here), such that variation of poly(ε-caprolactone) crystallinity could be observed. The minimum limit and the maximum limit for the TEOS/PCL molar ratio were set at 19.35 or 70 % total weight of poly(ε-caprolactone) and 3.226, corresponding to 95 % total weight of poly(ε-caprolactone) in the final materials. The minimum level and the maximum level for the HCl (catalyst)/TEOS and H_2O/TEOS and EtOH/TEOS molar ratios were set at 0.025 and 0.1

(HCl/TEOS) 4 and 8 (H_2O/TEOS) and 4 and 8 respectively according to our own previous studies of sol-gel materials[4] and studies performed by others on similar systems[5, 6]. For the remaining factor, THF/TEOS molar ratios, the maximum levels have been set arbitrarily at 8 and the minimum levels set as 4[4]. The table 3.1 lists the limits of all factors used in this first experimental model.

Table 3.1 : Range of variation of the parameters introduced in the design of the experimental matrix for the α,ω-hydroxyl poly(ε-caprolactone)-silica sol-gel composites .

Factor (molar ratio)	Minimum level	Maximum level
TEOS/PCL	3.226	19.35
THF/TEOS	4	8
EtOH/TEOS	4	8
H_2O/TEOS	4	8
HCl/TEOS	0.025	0.1

The experimental matrix (Table 3.2) was designed considering a full 2^5 experiment with 5 central points for 5 factors with two levels of variance. Minitab software was used to prepare and analyse the factorial design experiment. The experiment run order was randomised to avoid any significant effect from the operator.

Table 3.2 : 2^5 Factorial central design, experimental matrix and results of XRD and DSC analysis (RCr_{XRD} and Cr_{DSC}) for the α,ω-hydroxyl poly(ε-caprolactone)-silica sol-gel composites.

Std Order	Run Order	TEOS /PCL	THF/ TEOS	EtOH/ TEOS	H_2O/ TEOS	HCl/ TEOS	RCr XRD	Cr DSC
5	1	3.226	4	8	4	0.0250	0.482	0.541
30	2	19.350	4	8	8	0.1000	0.056	0.000
6	3	19.350	4	8	4	0.0250	0.137	0.176
4	4	19.350	8	4	4	0.0250	0.380	0.350
21	5	3.226	4	8	4	0.1000	0.287	0.435
36	6	11.288	6	6	6	0.0625	0.374	0.180
12	7	19.350	8	4	8	0.0250	0.415	0.463
24	8	19.350	8	8	4	0.1000	0.014	0.146
16	9	19.350	8	8	8	0.0250	0.358	0.438
7	10	3.226	8	8	4	0.0250	0.561	0.525
31	11	3.226	8	8	8	0.1000	0.309	0.502
33	12	11.288	6	6	6	0.0625	0.220	0.246
8	13	19.350	8	8	4	0.0250	1.000	0.258
25	14	3.226	4	4	8	0.1000	0.400	0.393
35	15	11.288	6	6	6	0.0625	0.655	0.341
11	16	3.226	8	4	8	0.0250	0.952	0.563
2	17	19.350	4	4	4	0.0250	0.266	0.360
14	18	19.350	4	8	8	0.0250	0.362	0.429
9	19	3.226	4	4	8	0.0250	0.409	0.561
18	20	19.350	4	4	4	0.1000	0.008	0.028
20	21	19.350	8	4	4	0.1000	0.187	0.281
1	22	3.226	4	4	4	0.0250	0.546	0.551
37	23	11.288	6	6	6	0.0625	0.150	0.191
15	24	3.226	8	8	8	0.0250	0.533	0.559
29	25	3.226	4	8	8	0.1000	0.407	0.489
27	26	3.226	8	4	8	0.1000	0.365	0.519
26	27	19.350	4	4	8	0.1000	0.259	0.426
3	28	3.226	8	4	4	0.0250	0.645	0.558
13	29	3.226	4	8	8	0.0250	0.506	0.557
34	30	11.288	6	6	6	0.0625	0.260	0.405
19	31	3.226	8	4	4	0.1000	0.413	0.503
32	32	19.350	8	8	8	0.1000	0.014	0.000
28	33	19.350	8	4	8	0.1000	0.271	0.387
17	34	3.226	4	4	4	0.1000	0.385	0.499
22	35	19.350	4	8	4	0.1000	0.000	0.000
23	36	3.226	8	8	4	0.1000	0.391	0.452
10	37	19.350	4	4	8	0.0250	0.550	0.507

The following five factors were selected for the α,ω-hydroxyl poly(L-lactic acid)-silica sol-gels study: TEOS (tetraethyl orthosilicate)/PLLA (poly(L-lactic acid)), Toluene/PLLA, EtOH (ethanol)/TEOS, H_2O (water)/TEOS and HCl (catalyst)/TEOS molar ratios, Table 3.3. The maximum and minimum limits for the TEOS/PLLA molar ratio were set at 3.226 and 19.35 as for the poly(ε-caprolactone)-silica sol-gel composite design. The maximum and minimum levels for the catalyst (HCl)/TEOS and H_2O/TEOS molar ratios were set at 0.025 and 0.1 (HCl/TEOS) and 4 and 8 (H_2O/TEOS) respectively. The limits of the Toluene/PLLA molar ratio were set so as to obtain a clear homogeneous solution when mixing PLLA, TEOS and EtOH. For the remaining factor, EtOH/TEOS molar ratios, the maximum level has been set arbitrarily at 8 as there was no information (to our knowledge) in the literature relating the effect of this variable on the behaviour of poly(L-lactic acid) in composites and the minimum level set respectively as 4 as often used for silica sol-gel processing[6].

Table 3.3 : Range of variation of the parameters introduced in the design of the experimental matrix for the α,ω-hydroxyl poly(L-lactic acid)-silica sol-gel materials.

Factor (molar ratio)	Minimum level	Maximum level
TEOS/PLLA	3.226	19.35
Toluene/PLLA	150	300
EtOH/TEOS	4	8
H_2O/TEOS	4	8
HCl/TEOS	0.025	0.1

The experimental matrix, Table 3.4 was designed considering a fractional 2^5 experiment with 5 central points for 5 factors with two levels of variance. Minitab software was used to prepare and analyse the factorial design experiment. The experiment run order was randomised to avoid any significant effect from the operator.

Table 3.4 : 2^5 centred fractional design, experimental matrix with factors (molar ratios) and results of XRD and DSC analysis (RCr_{XRD} and Cr_{DSC}) for the α,ω-hydroxyl poly(L-lactic acid)-silica sol-gel composites.

Std Order	Run Order	TEOS/ PLLA	Toluene /PLLA	EtOH/ TEOS	H_2O /TEOS	HCl /TEOS	RCr XRD	Cr DSC[(a)]
21	1	11.288	225	6	6	0.0625	0.452	0.370
8	2	19.350	300	8	4	0.0250	0.813	1.000
7	3	3.226	300	8	4	0.1000	0.205	0.561
5	4	3.226	150	8	4	0.0250	0.273	0.607
1	5	3.226	150	4	4	0.1000	0.558	0.569
3	6	3.226	300	4	4	0.0250	0.804	0.618
4	7	19.350	300	4	4	0.1000	0.233	0.498
19	8	11.288	225	6	6	0.0625	0.483	0.480
13	9	3.226	150	8	8	0.1000	0.946	0.587
18	10	11.288	225	6	6	0.0625	0.526	0.458
16	11	19.350	300	8	8	0.1000	0.674	0.212
10	12	19.350	150	4	8	0.1000	0.075	0.050
14	13	19.350	150	8	8	0.0250	0.000	0.000
12	14	19.350	300	4	8	0.0250	0.201	0.503
17	15	11.288	225	6	6	0.0625	0.493	0.488
6	16	19.350	150	8	4	0.1000	0.490	0.286
11	17	3.226	300	4	8	0.1000	1.000	0.639
15	18	3.226	300	8	8	0.0250	0.884	0.656
2	19	19.350	150	4	6	0.0250	0.456	0.383
22	20	11.288	225	6	6	0.0625	0.498	0.381
20	21	11.288	225	6	6	0.0625	0.571	0.445
9	22	3.226	150	4	8	0.0250	0.435	0.589

(a) the Cr_{DSC} data were normalised for a better comparison with the RCr_{XRD} and to recognize outliers.

The aim of these experiments was to observe the effect of the reactants on the incorporation and homogeneity of the polyester and silica phases in the sol-gel composites. The polymers crystallinity measured by FTIR, DSC and XRD analysis were the chosen measured responses. The treatment of the powder X-ray diffraction and the differential scanning calorimetric analyses data and the preparation of sol-gel materials have been described in chapter 2.

3.1.2. Results of the Statistical Design for the α,ω-hydroxyl Poly(ε-caprolactone)-Silica Sol-Gel Composites

First, it must be noted that the level of confidence or α-level used for the treatment of the statistical data was set at 0.05, and that the discussion of the results and the conclusions drawn from them are only relevant within the limits of the experiments. Results of a Ryan-Joiner test applied to the α,ω-hydroxyl poly(ε-caprolactone) RCr_{XRD} values table 3.2 for the calculated response within the whole range of factor variation indicated that the experimental data followed a normal distribution. Thus all the XRD data were suitable for statistical analysis using the 2^5 central factorial design.

Table 3.5 : Analysis of variance and estimated effects and coefficients for α,ω-hydroxyl poly(ε-caprolactone) RCr_{XRD}.

Source	**DF[a]**	**Seq SS[b]**	**Adj SS**	**Adj MS[c]**	**F[d]**	**P[e]**
Main Effects	5	1.06636	1.06636	0.213272	5.92	**0.008**
2-Way Interactions	10	0.19750	0.19750	0.019750	0.55	0.821
3-Way Interactions	10	0.26179	0.26179	0.026179	0.73	0.688
Curvature	1	0.00660	0.00660	0.006603	0.18	0.678
Residual Error	10	0.35999	0.35999	0.035999		
Lack of Fit	6	0.20305	0.20305	0.033841	0.86	0.586
Pure Error	4	0.15694	0.15694	0.039236		
Total	36	1.89224				

Term	**Strength[f]**	**Coef[g]**	**SE Coef[h]**	**T**	**P**
Constant		0.3709	0.03354	11.06	0.000
TEOS/PCL	-0.2071	-0.1036	0.03354	-3.09	**0.011**
THF/TEOS	0.1093	0.0546	0.03354	1.63	0.134
EtOH/TEOS	-0.0646	-0.0323	0.03354	-0.96	0.358
H_2O/TEOS	0.0290	0.0145	0.03354	0.43	0.675
HCl/TEOS	-0.2710	-0.1355	0.03354	-4.04	**0.002**

(a) degree of freedom, (b) SS= sum of square, (c) MS = mean square, (d) F= (MS factor)/(MS error), (e) P =p-value statistical significance of the corresponding F-statistic, (f) relative strength of the effect, (g) coefficients to construct the equation representing the relationship between the response and the factors, (h) standard error of the coefficient.

First the p-values (P) in the analysis of variance Table 3.5 were used to determine which of the effects in the model were statistically significant. The curvature was not significant at the 0.05 level of confidence (P equal to 0.678) and therefore the data fitted the assumption of linearity in the model. The 2 and 3-way interaction effects were looked at first in the model because a significant interaction could influence the interpretation of the main effects. The 2 and 3-way interaction effects were not significant at the 0.05 level of confidence. There was evidence of the effect of individual factors (P main effects equal to 0.008). The estimated strength effects and coefficients for α,ω-hydroxyl poly(ε-caprolactone) RCr_{XRD} (Table 3.5) allowed identification of the relative strength of the main effects. The absolute value of the effect determines its relative strength: the higher the value, the greater the effect on the response. The sign of the effect determines which factor setting results in a higher response measurement: A positive sign indicates that the high factor setting results in a higher response than the low setting (i.e. increase of the α,ω-hydroxyl poly(ε-caprolactone) RCr_{XRD}) and a negative sign indicates that the low factor setting results in a higher response than the higher setting (decrease of the α,ω-hydroxyl poly(ε-caprolactone) RCr_{XRD}). The table 3.5 showed the significance ($P<0.05$) of the following individual effects in decreasing order of strength; HCl/TEOS > TEOS/PCL. Increase of the HCl/TEOS and TEOS/PCL molar ratios decreased the RCr_{XRD} value (effect strength values respectively equal at –0.2710 and –0.2071).

A representative set of data obtained from the differential scanning calorimetry analysis of α,ω-hydroxyl poly(ε-caprolactone) silica hybrid materials is given in Figure 3.1.

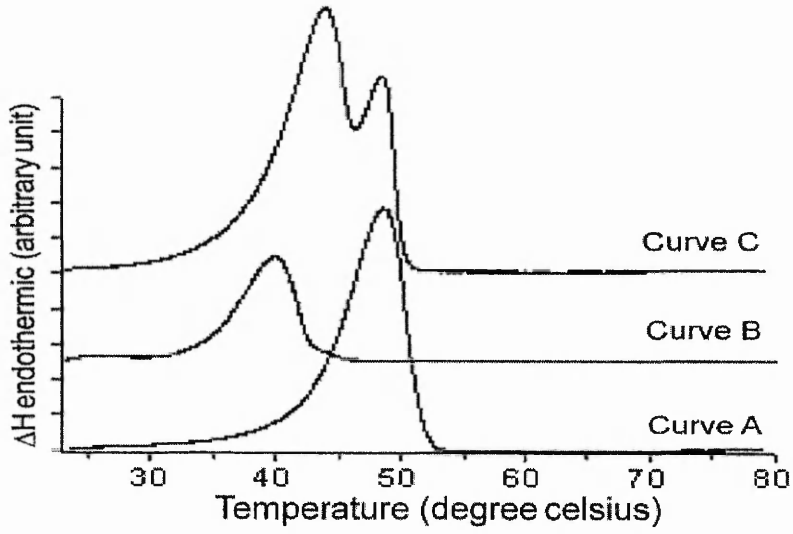

Figure 3.1 : DSC curves obtained from A, TEOS/PCL, EtOH/TEOS, THF/TEOS, H_2O/TEOS and HCl/TEOS molar ratios equal respectively to 3.226, 4, 8, 4 and 0.025 (low:low:high:low:low); B: 19.35, 4, 8, 4 and 0.025 (high:low:high:low:low); C: 3.226, 4, 8, 8 and 0.1 (low:low:high:high:high)

Curve A was obtained from a material with TEOS/PCL, EtOH/TEOS, THF/TEOS, H_2O/TEOS and HCl/TEOS molar ratios equal respectively to 3.226, 4, 8, 4 and 0.025 (low:low:high:low:low). The endothermic peak at 49.0 °C represents the melting entropy of poly(ε-caprolactone) in the composite (melting point of pure poly(ε-caprolactone) ~ 60.0 °C). Curve B was obtained for a composition identical to the previous material except that the TEOS/PCL molar ratio was set equal to 19.35 (high:low:high:low:low). The endothermic peak showed a shift of the maximum temperature (T_m= 37.5 °C) compared to curve A. Curve C was obtained from a material with the composition 3.226 TEOS/PCL, 4 EtOH/TEOS, 8 THF/TEOS, 8 H_2O/TEOS

and 0.1 HCl/TEOS (low:low:high:high:high). Two peaks were observed, one with a T_{m1} of 49.0 °C and a second with T_{m2} of 39.0 °C.

The Cr_{DSC} data collected, minus outliers, followed a normal distribution as described by the Ryan-Joiner test and were therefore suitable for statistical analysis.

Table 3.6: Analysis of variance and estimated effect and coefficient for α,ω-hydroxyl poly(ε-caprolactone) Cr_{DSC}.

Source	**DF[a]**	**Seq SS[b]**	**Adj SS**	**Adj MS[c]**	**F[d]**	**P[e]**
Main Effects	5	0.77449	0.77449	0.154898	19.43	**0.000**
2-Way Interactions	10	0.14875	0.14875	0.014875	1.87	0.170
3-Way Interactions	10	0.06411	0.06411	0.006411	0.80	0.631
Curvature	1	0.05884	0.05884	0.058842	7.38	**0.022**
Residual Error	10	0.07971	0.07971	0.007971		
Lack of Fit	6	0.04156	0.04156	0.006926	0.73	0.655
Pure Error	4	0.03815	0.03815	0.009537		
Total	36	1.12591				

Term	**Strength[f]**	**Coef[g]**	**SE Coef[h]**	**T**	**P**
Constant		0.3893	0.01578	24.66	0.000
TEOS/PCL	-0.2474	-0.1237	0.01578	-7.84	**0.000**
THF/TEOS	0.0345	0.0173	0.01578	1.09	0.300
EtOH/TEOS	-0.0901	-0.0451	0.01578	-2.86	**0.017**
H_2O/TEOS	0.0706	0.0353	0.01578	2.24	**0.049**
HCl/TEOS	-0.1460	-0.0730	0.01578	-4.63	**0.001**

(a) degree of freedom, (b) SS= sum of square, (c) MS = mean square, (d) F= (MS factor)/(MS error), (e) P =p-value statistical significance of the corresponding F-statistic, (f) relative strength of the effect, (g) coefficients to construct the equation representing the relationship between the response and the factors, (h) standard error of the coefficient.

First the p-values (P) in the analysis of variance table (Table 3.6) were used to determine which of the effects in the model were statistically significant. The curvature was significant at the 0.05 level of confidence (P equal to 0.022) and therefore the DSC data did not fit the assumption of linearity in the model. However, the design results were interpreted as for the XRD data. The 2 and 3-way interaction effects were not significant at the 0.05 level of confidence (P>0.05). There was evidence of the effect of individual factors (P equal to 0.000). The estimated strength effects and coefficients for

PCL Cr_{DSC} (Table 3.6) allowed identification of the relative strength of the main effects. The TEOS/PCL, HCl/TEOS, EtOH/TEOS, and H_2O/TEOS molar ratios had an effect on Cr_{DSC}.

FTIR analysis was carried out on the prepared composites but did not provide quantitative information relating the crystallinity of the poly(ε-caprolactone) component of the hybrid material to the synthesis conditions due to too many overlapping peaks. However, the technique was able to provide information on the presence of specific interactions between the organic and inorganic phases[7]. Samples prepared for this present study gave spectra with contributions to the carbonyl-stretching region from amorphous and crystalline polymer peaks at 1733 cm^{-1} and 1725 cm^{-1} respectively and contributions from hydrogen bonded interactions at around 1705 cm^{-1}. Qualitative information only was obtained.

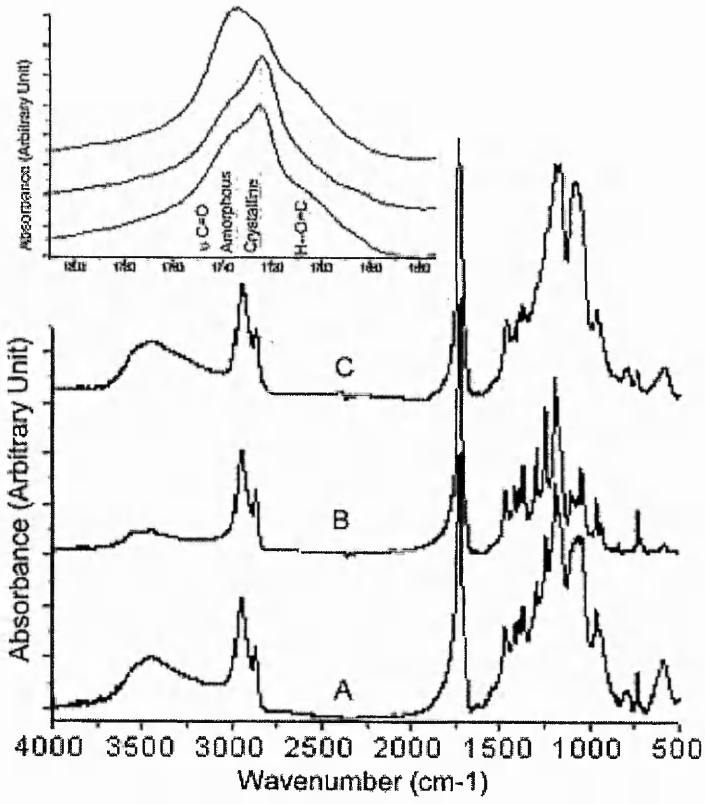

Figure 3.2 : FTIR spectra of hybrid materials, TEOS/PCL, EtOH/TEOS, THF/TEOS, H_2O/TEOS and HCl/TEOS molar ratios of spectrum A: 19.35, 4, 8, 8, 0.1(high,low,high,high,high); B: 3.226, 4, 8, 8, 0.1(low,low,high,high,high) and C: 19.35, 4, 8, 4, 0.025 (high,low,high,low,high) and inset of the carbonyl stretching area.

The spectra obtained from three representative hybrid materials prepared with the following molar ratios of TEOS/PCL, EtOH/TEOS, THF/TEOS, H_2O/TEOS and HCl/TEOS; A: 19.35, 4, 8, 8, 0.1(high,low,high,high,high); B: 3.226, 4, 8, 8, 0.1(low,low,high,high,high) and C: 19.35, 4, 8, 4, 0.025 (high,low,high,low,high) were presented in Figure 3.2. The carbonyl-stretching region was enlarged for a better view of the area, see inset. Comparison of the carbonyl stretching region of the spectra for samples A and B showed that increasing the TEOS/PCL molar ratio increased the contribution of the amorphous carbonyl and hydrogen bonded carbonyl signals to the spectrum. Comparison of the spectra from samples A and C showed that increasing the HCl/TEOS molar ratio increased the amorphous component of the carbonyl stretching area to the detriment of the signal from crystalline regions.

3.1.3. Results of the Statistical Design for the α,ω-Hydroxyl Poly(L-lactic acid)-Silica Sol-Gel Composites

Results of a Ryan-Joiner test applied to the poly(L-lactic acid) RCr_{XRD} values (Table 3.4) for the calculated response within the whole range of factor variation indicated that the experimental data followed a normal distribution. Thus all the XRD data were suitable for statistical analysis using the statistical model.

Table 3.7: Analysis of variance for α,ω-hydroxyl poly(L-lactic acid) RCr_{XRD}.

Source	DF[a]	Seq SS[b]	Adj SS	Adj MS[c]	F[d]	P[e]
Main effect	5	0.48110	0.48110	0.096220	58.14	0.000
2-Way Interactions	10	1.07529	1.07529	0.107529	64.97	0.000
Curvature	1	0.00000	0.00000	0.000004	0.00	0.965
Residual Error	5	0.00827	0.00827	0.001655		
Pure Error	5	0.00827	0.00827	0.001655		
Total	21	1.56467				

(a) degree of freedom, (b) SS= sum of square, (c) MS = mean square, (d) F= (MS factor)/(MS error), (e) P =p-value statistical significance of the corresponding F-statistic.

Table 3.8: Estimated effects and coefficients for α,ω-hydroxyl poly(L-lactic acid) RCr_{XRD}.

Term	Effect[f]	Coef[g]	SE Coef[h]	T	P
Constant		0.5029	0.01017	49.45	0.000
TEOS/PLLA	**-0.2704**	**-0.1352**	**0.01017**	**-13.29**	**0.000**
Toluene/PLLA	**0.1976**	**0.0988**	**0.01017**	**9.72**	**0.000**
EtOH/TEOS	0.0654	0.0327	0.01017	3.21	0.024
H_2O/TEOS	0.0479	0.0239	0.01017	2.35	0.065
HCl/TEOS	0.0394	0.0197	0.01017	1.94	0.111
TEOS/PLLA*Toluene/PLLA	0.0274	0.0137	0.01017	1.35	0.236
TEOS/PLLA*EtOH/TEOS	**0.1876**	**0.0938**	**0.01017**	**9.22**	**0.000**
TEOS/PLLA*H_2O/TEOS	**-0.3084**	**-0.1542**	**0.01017**	**-15.16**	**0.000**
TEOS/PLLA*HCl/TEOS	-0.0389	-0.0194	0.01017	-1.91	0.114
Toluene/PLLA*EtOH/TEOS	0.0191	0.0096	0.01017	0.94	0.390
Toluene/PLLA*H_2O/TEOS	0.1281	0.0641	0.01017	6.30	**0.001**
Toluene/PLLA*HCl/TEOS	-0.1869	-0.0934	0.01017	-9.19	**0.000**
EtOH/TEOS*H_2O/TEOS	0.1329	0.0664	0.01017	6.53	**0.001**
EtOH/TEOS*HCl/TEOS	0.0469	0.0234	0.01017	2.30	0.069
H_2O/TEOS*HCl/TEOS	**0.2544**	**0.1272**	**0.01017**	**12.51**	**0.000**
Ct Pt		0.0009	0.01947	0.05	0.965

(f) relative strength of the effect, (g) coefficients to construct the equation representing the relationship between the response and the factors, (h) standard error of the coefficient.

First the p-values (P) in the analysis of variance table (Table 3.7) were used to determine which of the effects in the model were statistically significant. The curvature was not significant at the 0.05 level of confidence (P equal to 0.965) and therefore the data fitted the assumption of linearity in the model. The 2-way interaction effects were looked at first in the model because a significant interaction could influence the interpretation of the main effects. The 2-way interaction effects were significant at the 0.05 level of confidence. There was evidence that the effect of a factor depends on the level of another factor. The estimated effects and coefficients for the α,ω-hydroxyl poly(L-lactic acid) RCr_{XRD} (Table 3.8) allowed identification of the relative strength of the main effects and interaction effects. The absolute value of the effect determines its relative strength: the higher the value, the greater the effect on the response. The sign of the effect determines which factor setting results in a higher response measurement: A positive sign indicates that the high factor setting results in a higher response than the

low setting (i.e. increase of the PLLA RCr_{XRD}) and a negative sign indicates that the low factor setting results in a higher response than the higher setting (decrease of the PLLA RCr_{XRD}). Only the effects and interaction effects with absolute strength effect greater than 0.1 are discussed. Those with lower strength effects were not considered for the following discussion on the materials crystallinity as although the results were statistically significant, the extent of the effect on the structure and properties of the materials was considered to be small. The results presented in Table 4 showed significance of the following two-way interaction effects and individual effects in decreasing order of strength; TEOS/PLLA*H_2O/TEOS > TEOS/PLLA > H_2O/TEOS*HCl/TEOS > Toluene/PLLA > TEOS/PLLA*EtOH/TEOS > Toluene/PLLA*HCl/TEOS > EtOH/TEOS*H_2O/TEOS > Toluene/PLLA*H_2O/TEOS molar ratios. Increase of the TEOS/PLLA molar ratio decreased the RCr_{XRD} value (effect value –0.2704). Moreover, the 2-way interaction effects analysis showed a synergic effect between TEOS/PLLA and H_2O/TEOS molar ratios and further decreased RCr_{XRD} with increase of both molar ratio settings. Other 2-way interaction effects in Table 3.8 were similarly analysed.

A representative set of data obtained from the differential scanning calorimetry analysis of α,ω-hydroxyl poly(L-lactic acid) silica sol-gel materials is given in Figure 3.3.

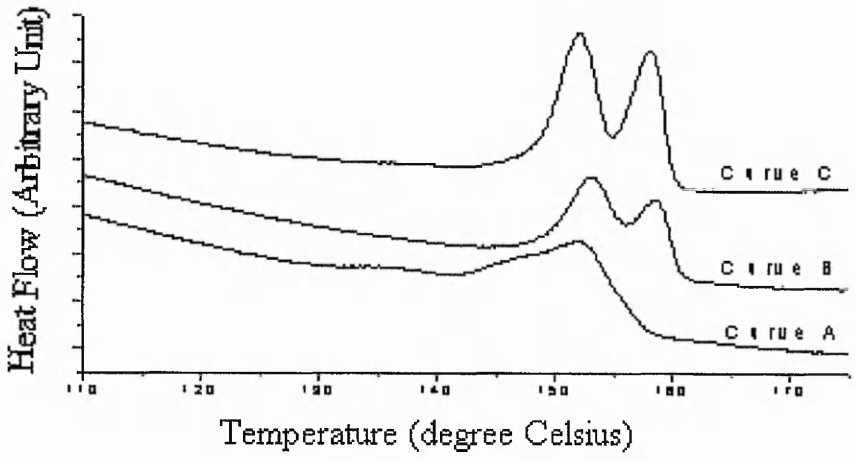

Figure 3.3 : DSC curves of the pure PLLA (curve A) and the hybrid materials prepared with the following molar ratios of TEOS/PLLA, Toluene/PLLA, EtOH/TEOS, H_2O/TEOS and HCl/TEOS; curve B: 3.226, 300, 8, 8, 0.025(low,high,high,high,low) and curve C: 19.35, 150, 8, 8, 0.025(high,low,high,high,low).

Figure 3.3 shows typical DSC curves of the pure α,ω-hydroxyl poly(L-lactic acid) (curve A) and the composite materials prepared with the following molar ratios of TEOS/PLLA, Toluene/TEOS, EtOH/TEOS, H_2O/TEOS and HCl/TEOS; curve B: 3.226, 300, 8, 8, 0.025(low,high,high,high,low) and curve C: 19.35, 150, 8, 8, 0.025(high,low,high,high,low). The hybrid DSC curves showed two endothermic peaks suggesting that the α,ω-hydroxyl poly(L-lactic acid) was in two physical states. One phase where PLLA was free T_m~153 °C and one PLLA phase entrapped or interacting with the silica matrix T_m~160 °C. The DSC data were treated using equation 2.2 and the results presented in Table 3.4. Results of a Ryan-Joiner test applied to the α,ω-hydroxyl poly(L-lactic acid) Cr_{DSC} values for the calculated response within the whole range of factor variation indicated that the experimental data followed a normal distribution. Thus all the DSC data were suitable for statistical analysis. The results of the statistical model are presented in Tables 3.9 and 3.10.

Table 3.9 : Analysis of variance for α,ω-hydroxyl poly(L-lactic acid) Cr_{DSC}

Source	**DF[a]**	**Seq SS[b]**	**Adj SS**	**Adj MS[c]**	**F[d]**	**P[e]**
Main effect	5	0.54789	0.54789	0.109578	43.55	0.000
2-Way Interactions	10	0.38640	0.38640	0.038640	15.36	0.000
Curvature	1	0.01000	0.01000	0.010002	3.98	0.103
Residual Error	5	0.01258	0.01258	0.002516		
Pure Error	5	0.01258	0.01258	0.002516		
Total	21	0.95687				

(a) degree of freedom, (b) SS= sum of square, (c) MS = mean square, (d) F= (MS factor)/(MS error), (e) P =p-value statistical significance of the corresponding F-statistic.

Table 3.10 : Estimated effects and coefficients for α,ω-hydroxyl poly(L-lactic acid) Cr_{DSC}.

Term	Effect[f]	Coef[g]	SE Coef[h]	T	P
Constant		0.4849	0.01254	38.67	0.000
TEOS/PLLA	**-0.2367**	-0.1184	0.01254	-9.44	**0.000**
Toluene/PLLA	**0.2020**	0.1010	0.01254	8.05	**0.000**
EtOH/TEOS	0.0075	0.0038	0.01254	0.30	0.777
H_2O/TEOS	**-0.1607**	-0.0804	0.01254	-6.41	**0.001**
HCl/TEOS	**-0.1193**	-0.0596	0.01254	-4.75	**0.005**
TEOS/PLLA*Toluene/PLLA	**0.1715**	0.0857	0.01254	6.84	**0.001**
TEOS/PLLA*EtOH/TEOS	0.0085	0.0043	0.01254	0.34	0.748
TEOS/PLLA*H_2O/TEOS	**-0.1898**	-0.0949	0.01254	-7.57	**0.001**
TEOS/PLLA*HCl/TEOS	**-0.0908**	-0.0454	0.01254	-3.62	**0.015**
Toluene/PLLA*EtOH/TEOS	0.0352	0.0176	0.01254	1.41	0.219
Toluene/PLLA*H_2O/TEOS	-0.0060	-0.0030	0.01254	-0.24	0.820
Toluene/PLLA*HCl/TEOS	**-0.0975**	-0.0487	0.01254	-3.89	**0.012**
EtOH/TEOS*H_2O/TEOS	**-0.0890**	-0.0445	0.01254	-3.55	**0.016**
EtOH/TEOS*HCl/TEOS	-0.0350	-0.0175	0.01254	-1.40	0.222
H_2O/TEOS*HCl/TEOS	0.0543	0.0271	0.01254	2.16	0.083
Ct Pt		-0.0479	0.02401	-1.99	0.103

(f) relative strength of the effect, (g) coefficients to construct the equation representing the relationship between the response and the factors, (h) standard error of the coefficient.

The curvature was not significant at the 0.05 level of confidence (P equal 0.103). Therefore, the data fitted the assumption of a linear model, Table 3.9. The 2-way interaction effects were significant at the 0.05 level of confidence (p-value 0.004). Table 3.10 showed the significance of the following two-way interaction effects and individual effects in a decreasing order of strength; TEOS/PLLA, Toluene/PLLA, TEOS/PLLA*H_2O/TEOS, TEOS/PLLA*Toluene/PLLA, H_2O/TEOS, HCl/TEOS, Toluene/PLLA*HCl/TEOS, TEOS/PLLA*HCl/TEOS and EtOH/TEOS*H_2O/TEOS molar ratios. Increasing the TEOS/PLLA, H_2O/TEOS and HCl/TEOS molar ratios decreased the Cr_{DSC} value; the effect value are respectively –0.2367, -0.1607 and -0.1193. Increasing the Toluene/PLLA molar ratio decreased the Cr_{DSC} value; effect equal to 0.2020. The Analysis of the 2-way interaction effects, Table 3.10 showed a significant synergetic effect between TEOS/PLLA and H_2O/TEOS molar ratios. The strength effect absolute value of combined variable, 0.3084 was superior to the addition

of the individual strength effects |-0.2704 + 0.0479|. The negative sign of the effect indicated the negative effect of the two way-interaction on the Cr_{DSC}. Other significant 2-way interaction effects in Table 3.10 had all a negative effect value except for the TEOS/PLLA*Toluene/TEOS.

3.1.4. Discussion of Statistical Experiments

The results of the two statistical designs are summarized in Figures 3.4 and 3.5. The value of the strength of effect on the crystallinity of the polyesters measured by XRD and DSC data multiplied by one minus the significance or P value was plotted for each effect. The plot gives a graphical representation of the "weight" of the molar ratio variations on the value of the hydroxyl terminated poly(ε-caprolactone) and poly(L-lactic acid) crystallinity as measured by XRD and DSC. For example for the study of the α,ω-hydroxyl poly(ε-caprolactone)-silica sol-gels, EtOH/TEOS molar ratio had a significant effect on Cr_{DSC}. The P value was equal to 0.017 and the strength value to -0.0901. Similarly for TEOS/PCL molar ratio the P value and strength were equal to 0.000 and -0.2474 respectively from the table 3.6. The strength*(1-P value) calculated were respectively for EtOH/TEOS and TEOS/PCL molar ratios; -0.015 and –0.2474 indicating that TEOS/PCL molar ratio has a much more important effect than the EtOH/PCL molar ratio. Only the most important effects observed by both XRD and DSC responses are discussed.

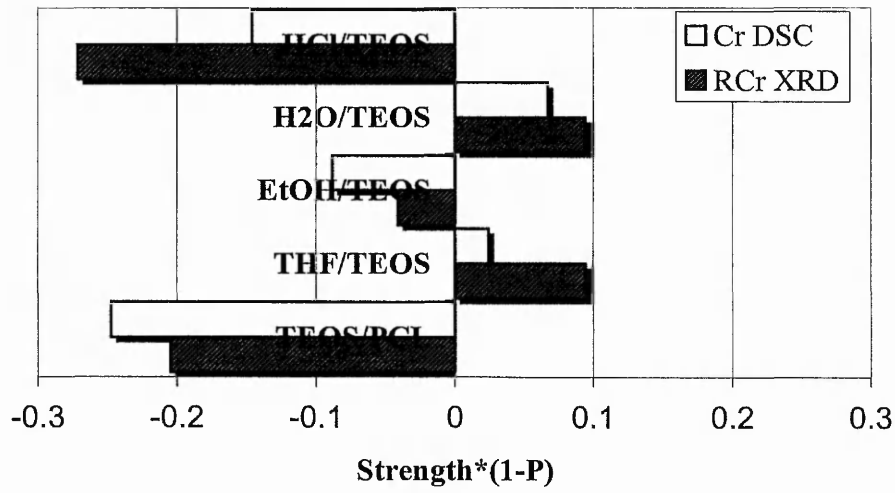

Figure 3.4 : Box plot of strength*(1-P) for each individual variable for α,ω-hydroxyl poly(ε-caprolactone) RCr_{XRD} and Cr_{DSC} design results.

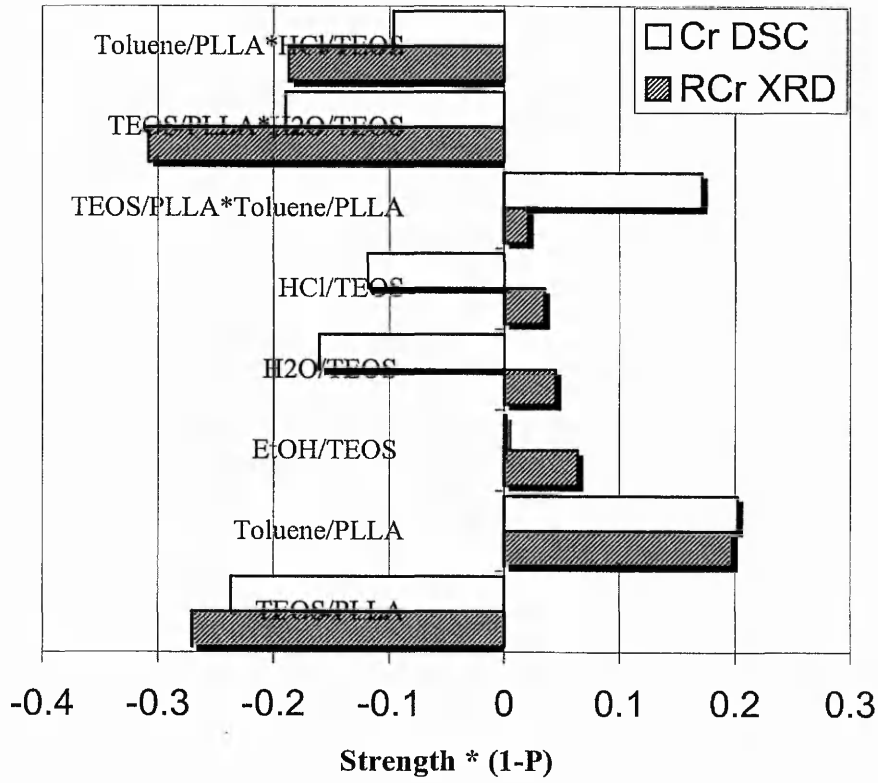

Figure 3.5 : Box plot of strength*(1-P) for each individual variable and most important two-way interaction effect of α,ω-hydroxyl poly(L-lactic acid) RCr_{XRD} and Cr_{DSC} design results.

The data collected by powder X-ray diffraction and differential scanning calorimetry analysis and treated by the factorial design were in accordance with the limited results published by S. Jiang and co-workers[1].

The statistical designs applied to the X-ray diffraction and calorimetry data, Figure 3.4 and tables 3.6 and 3.7 showed that increasing the TEOS/PCL molar ratio decreased the value of the α,ω-hydroxyl poly(ε-caprolactone) RCr_{XRD}, and Cr_{DSC} at the 0.05 α-level as reported by S. Jiang et al. for the α,ω-hydroxyl poly(ε-caprolactone)-silica sol-gel hybrids[1]. The factorial design also showed that increasing the HCl/TEOS molar ratio decreased the poly(ε-caprolactone) crystallinity values in these composites. This last result was in accordance with the dynamic thermal and SAXS analysis of R. Jerome et al.[5, 13]. As the study presented was carried out with varying one variable at a time, the same authors did not determine whether acid catalysis had a decisive effect on the hydrolysis reaction rather than on the polycondensation reaction of the tetraethyl orthosilicate. The statistical model provided the following new results; in the limits of the experiments and at the 0.05 level of confidence, the variable H_2O/TEOS molar ratio had little or no effect nor did the interaction H_2O/TEOS*HCl/TEOS on the α,ω-hydroxyl poly(ε-caprolactone) RCr_{XRD} and Cr_{DSC} values and therefore, the significance of this was that the increase in catalyst content has a more important effect on the condensation rate of tetraethyl orthosilicate in the composite sol-gel rather than on the hydrolysis rate of tetraethyl orthosilicate. This was in accordance with the idea of the development of co-continuous phases with confined organic polymers within inorganic phase. Hydrogen bonding between α,ω-hydroxyl poly(ε-caprolactone) and silica has been thought to have a retarding effect on their phase separation and thus the aggregation of the inorganic constitutive component[8]. The results of this study show that even if such an effect exists during the formation of the sol-gel, the structure or order of the α,ω-hydroxyl poly(ε-caprolactone) in silica hybrid materials was mostly dictated by the physical constraints of putting the organic polymer into the open silica network.

For the FTIR analysis a strict quantitative treatment of the carbonyl stretching signal was not possible. Therefore, FTIR peak fitting results were not used in the statistical model. However, they were still of interest for the observation and supplementation of the data obtained via the other analysis methods used. The results of the mid-IR analysis of α,ω-hydroxyl poly(ε-caprolactone)-silica sol-gel were in accordance with the other analysis methods in that increasing the TEOS/PCL molar ratio and the HCl/TEOS molar ratio, led to a more developed silica network and a less ordered poly(ε-caprolactone) polymer network. Further discussions concerning the hydrogen bonding carbonyl-stretching region were more hazardous and were not entered into the statistical designs treatments.

For the statistical study of the α,ω-hydroxyl poly(L-lactic acid)-silica sol-gels, there was evidence of the TEOS/PLLA molar ratio effect on RCr_{XRD} and Cr_{DSC}, indicating the confinement of the macromolecular chains in the silica matrix and thus better incorporation of the polyester within the silica phase as observed for the poly(ε-caprolactone)-silica sol-gels[7]. Effect of the Toluene/PLLA molar ratio and the two-way interactions TEOS/PLLA*H_2O/TEOS and Toluene/PLLA*HCl/TEOS molar ratios on RCr_{XRD} and Cr_{DSC} values were also observed, Figure 3.5. The increase of solvent (toluene) volume increased the poly(L-lactic acid) crystallinity measured by XRD and DSC. The increase of the molar ratios interaction TEOS/PLLA*H_2O/TEOS and Toluene/PLLA*HCl/TEOS decreased the poly(L-lactic acid) RCr_{XRD} and Cr_{DSC} values. At the 0.05 level of confidence, the variables H_2O/TEOS and HCl/TEOS and Toluene/PLLA*TEOS/PLLA molar ratios had little effect on the poly(L-lactic acid) RCr_{XRD} but a significant effect on Cr_{DSC} values, Figure 3.5. There were some discrepancies in the statistical design between the two analysed responses. These variations could either originate from the accuracy of the XRD and DSC analysis and treatments, or the unrelated sense of the crystallinity as measured by XRD and DSC techniques. It must be noted that the DSC results did not fit properly the equation model of the design and the Cr_{DSC} values did not vary linearly within the limits of the studied variables.

However, it was clear that the co-solvent; toluene had a strong influence on the crystalinity of the α,ω-hydroxyl poly(L-lactic acid). The solvents, toluene, and ethanol, controlled the solubility of the poly(L-lactic acid) and water and the occurrence of a more or less rapid phase separation in the reaction medium[4]. These phenomena must also influence strongly the progress of the silica network formation.

Consequently, the increase of polyester crystallinity with the increase of the toluene/PLLA molar ratio and the toluene/PLLA*TEOS/PLLA molar ratios was related to the organic and inorganic phases separation within the composite, and in fact it was observed that at high toluene content demixing of phases occurred for some of the prepared sol-gels. The toluene/PLLA molar ratio also influenced the sol-gel process as effect of the interactions toluene/PLLA*HCl/TEOS and toluene/PLLA* TEOS/PLLA were observed. It is well know that the strength of an acid and the rate of the TEOS hydrolysis-condensation reactions are influenced by the solvents used[9].

Table 3. 11 : Dielectric constant and dipole moment for the solvents used in the sol-gel experiments[9].

Solvent	ε_r [(a)]	μ (10^{-3}Cm)[(b)]
Water	78.30	5.9
Ethanol	24.55	5.8
THF	7.58	5.8
Toluene	2.38	1.0

[(a)] dielectric constant or relative permittivity, [(b)] dipole moment

For example, the hydrolysis-condensation of tetraethyl orthosilicate catalysed by hydrochloric acid is speeded up by the use of alcohols with decreasing dielectric constant[8]. The simultaneous increase of toluene/PLLA and HCl/TEOS molar ratios decreased the α,ω-hydroxyl poly(L-lactic acid) crystallinity. It is then reasonable that toluene with a low dielectric constant (Table 3.11) compared to water disturbed the water sphere of solvation around the hydrochloric acid and consequently the enhancement of the strength of the acid and the rate of the catalytic hydrolysis-

condensation reactions of tetraethyl orthosilicate were observed. The increase of the rate of formation of the silica gel prevented the demixing of the organic and inorganic phases and caused the decrease of the polyester crystallinity observed.
The increase of toluene/PLLA and TEOS/PLLA molar ratios increased the poly(L-lactic acid) crystallinity. This is probably explained by the fact that oligomeric silica species tended to be poorly soluble in toluene and precipitate out. Increasing the amount of TEOS and co-solvent without changing the amount of polyester which stabilized the oligomeric species in solution via hydrogen bonding, permitted the precipitation of silica and therefore decreased the confinement of the organic and inorganic phases and increased poly(L-lactic acid) crystallinity.

Finally, the interaction H_2O/TEOS*TEOS/PLLA molar ratios had a negative effect on the crystallinity of the poly(L-lactic acid). The explanation of the effect of water content was not straightforward. The water content controlled in part the solubility of the poly(L-lactic acid) as a part of the solvent media; toluene, ethanol, water, but it also hydrolyzed tetraethyl orthosilicate and therefore its concentration affected the kinetic of the hydrolysis reaction and the formation of the whole sol-gel.

To conclude, both statistical studies showed that the TEOS/polyester molar ratio had the most important effect of the variables studied using either the hydroxyl terminated poly(ε-caprolactone) or poly(L-lactic acid). Strict comparison of the two statistical studies was not possible because of the different solvents used; tetrahydrofuran for the poly(ε-caprolactone) and toluene for the poly(L-lactic acid). This was due to the poor solubility of the poly(L-lactic acid) in tetrahydrofuran. The tetrahydrofuran and toluene have different solvating properties (Table 3.11) and the concentration of solvents used was different for each design. This may have been the reason for the observation of a strong effect of the toluene on α,ω-hydroxyl poly(L-lactic acid) and the weak effect of the tetrahydrofuran variation on the α,ω-hydroxyl poly(ε-caprolactone) crystallinity. An interesting follow up experiment would be the study of the effect of different polyesters (PCL, PLLA, PDLLA, PGA) on the structure of the sol-gel hybrids using an identical co-solvent, toluene .

The statistical design gave useful information on the behaviour and the incorporation of a poly(α-hydroxyacids) within a silica phase formed by the sol-gel process. Obviously, increasing the amount of silica phase increased the confinement of the poly(α-hydroxyacids). The fine tuning of the relative amount of co-solvent and water in the reaction system was important to avoid demixing of phases as was observed for the α,ω-hydroxyl poly(L-lactic acid)-silica sol-gels. The extent of polyester incorporation in the silica sol-gel depended on the HCl/TEOS and H_2O/TEOS molar ratios. The condensation reaction of the tetraethyl orthosilicate has been shown to have a dominant effect in the incorporation of α,ω-hydroxyl poly(ε-caprolactone) in silica. The use of a design method was a very interesting statistical tool for the observation and understanding of the effect of reactants and their interactions in the sol-gel process.

3.2. Effect and Comparison of the Preparation Methods and Reactive End-Groups on Poly(α-hydroxyacid)-Silica Composite Structures

Several analytical techniques were used to characterise the prepared composite materials. Infrared spectroscopy, thermal analyses, powder X-ray diffraction (wide angle) and transmission electron microscopy.

3.2.1. Mid-Infrared Analysis

The Figure 3.7 shows the Mid-IR spectra of α,ω-hydroxyl poly(ε-caprolactone) and α,ω-hydroxyl poly(ε-caprolactone)-silica materials prepared by the sol-gel method.

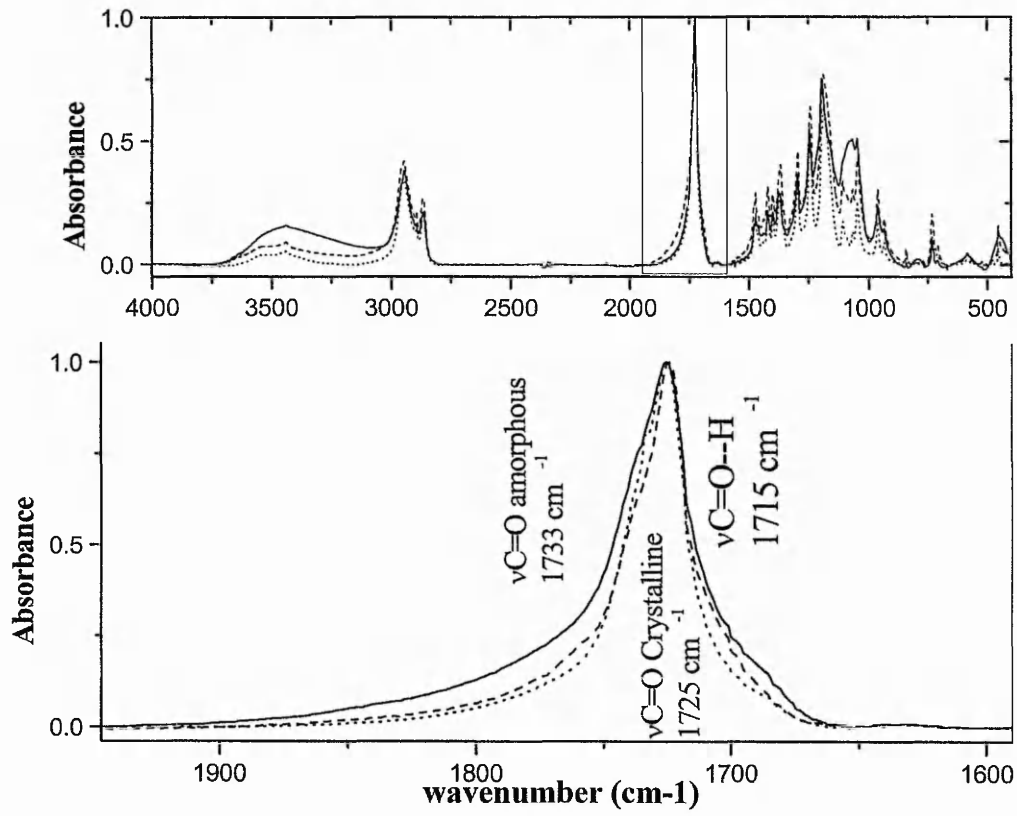

Figure 3.7: Mid-IR spectra α,ω-hydroxyl poly(ε-caprolactone) (dotted line) and α,ω-hydroxyl poly(ε-caprolactone)-silica materials prepared following the sol-gel procedure with a poly(ε-caprolactone) weight % content of 90 (dashed line) and 70 (black line), below a window of the carbonyl stretching region.

The α,ω-hydroxyl poly(ε-caprolactone)-silica sol-gel IR spectra, Figure 3.7 showed that with the addition of the silica in the sol-gel materials, bands assignable to the silica lattice[8] appeared; the broad bands of Si-O rocking, bending and stretching at 440 cm^{-1}, 860 cm^{-1} and 1190 cm^{-1} respectively were apparent. These bands were very weak in intensity when the poly(ε-caprolactone) weight in the bulk and sol-gel composites was equal to or greater than 80%. This indicated a poorly formed silica network. R. Jerome and al.[10] have characterised their hybrid poly(ε-caprolactone)-silica composites prepared by the sol gel process using FTIR analysis. The FTIR spectra of the sol gel and bulk process prepared hybrids in this study were in accordance with the previously published results.

For the bulk and sol-gel methods of sample preparation, in IR spectra the ν C=O hydrogen bond was observed. The average value of the hydrogen-bonded carbonyl stretching frequency at 1705 cm^{-1} was lower than the expected value of 1715 cm^{-1} reported by R. Jerome and co-workers[10], indicating stronger hydrogen bonding than previously reported. A possible explanation, for the shift of the stretching carbonyl hydrogen bonded to lower wavenumber was, that a strong inter-association exists between the carbonyl groups of the poly(ε-caprolactone) and the hydroxyl groups of an acceptor molecule[11]. These suggested that hydrogen bonding in these materials involves water and/or ethanol (observed by ^1H NMR analysis) present in the composites as well as silanol groups present at the surface of the silica phase[12]. It is possible that different annealing times between our experiments and those reported[13] were the reason for the presence of residual solvent in the composites and consequently the shift in wavenumber for the band arising from the carbonyl hydrogen bonded.

The ratio of the crystalline carbonyl stretching area versus amorphous and hydrogen bonded carbonyl areas was calculated using peak fitting mathematical software (Gaussian function)[12] and are presented in the Table 3.12 below for α,ω-hydroxyl poly(ε-caprolactone), α,ω-hydroxyl poly(ε-caprolactone)-silica bulk and α,ω-hydroxyl poly(ε-caprolactone)-silica sol-gel composites with 80% weight content of polyester.

Table 3.12 : Ratio of areas of ν C=O Crystalline/(Amorphous + Hydrogen bond) for α,ω-hydroxyl poly(ε-caprolactone)-silica composite materials prepared using the sol-gel and bulk processes.

Processes	**Poly(ε-caprolactone) weight%**	**Ratio area νC=O Cryst./(Amorph. + H-Bond.)**
Poly(ε-caprolactone)	100	1.178 ±0.1
Bulk	80	0.3835 ±0.011
Sol-gel	80	0.329 ±0.02

Table 3.12 shows that α,ω-hydroxyl poly(ε-caprolactone) in the composite materials had a smaller ratio of the carbonyl stretching crystalline/ (amorphous + H-bonded) signals than for the poly(ε-caprolactone) alone. The poly(ε-caprolactone)

crystallinity decreased when it was incorporated in a silica phase. Using the bulk process, the ν C=O ratio calculated was significantly higher than for the sol-gel process for a similar polyester content.

The percentage of ester group of the α,ω-hydroxyl poly(ε-caprolactone) involved in hydrogen bonding was calculated by dividing the ν C=O hydrogen bonded peak area by the total ν C=O region fitting as performed by R. Jerome[10]. However as already discussed, this figure was not a true value of the hydrogen bonding in the composite because the relative intensity of the peaks are not quantitative[11]. The percentage of ν C=O hydrogen bonding found for α,ω-hydroxyl poly(ε-caprolactone)-silica sol-gel, bulk processes and triethoxysilane terminated poly(ε-caprolactone)-silica sol-gel composites was equal to 11.7 % ± 1.1, 10.3 % ± 3.3 and 19.3% ± 1.0 respectively. The last value was in accordance with the reported value of 20 % in the literature[13]. The percentage of ν C=O hydrogen bonded values for α,ω-hydroxyl poly(ε-caprolactone)-silica sol-gel and bulk processes were lower than for the triethoxysilane terminated poly(ε-caprolactone) and no significant variation was observed between the bulk and sol-gel processes.

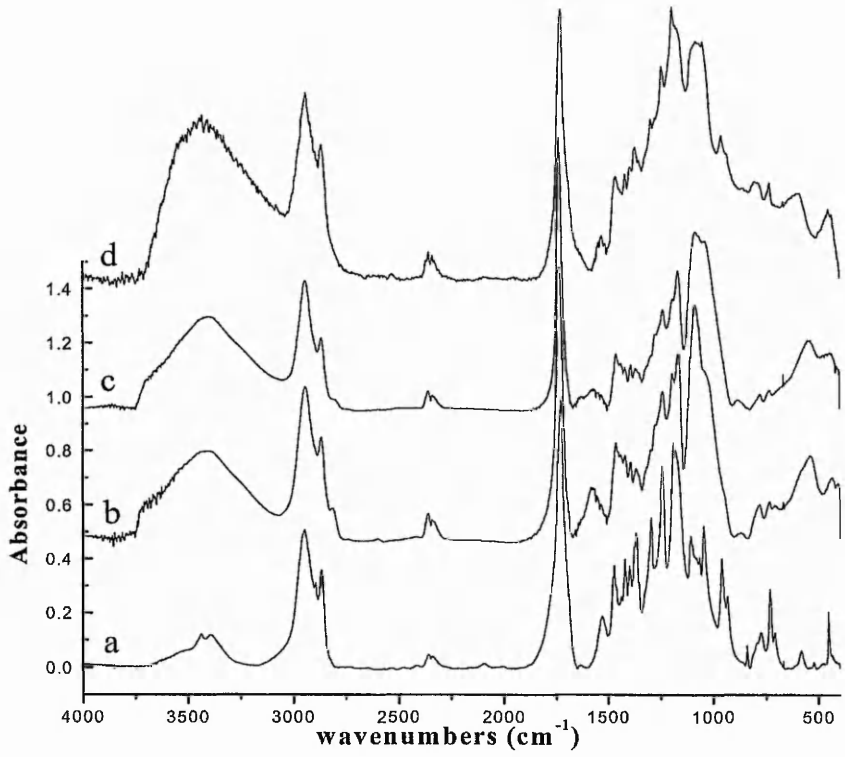

Figure 3.8: Mid-IR spectra of triethoxysilane terminated poly(ε-caprolactone) (a) and triethoxysilane terminated poly(ε-caprolactone)-silica composites prepared by the sol-gel procedure with a poly(ε-caprolactone) percent weight content of 90 (b), 80 (c) and 70 (d).

Figure 3.8 shows the mid IR spectra of the triethoxysilane terminated poly(ε-caprolactone)-silica sol-gel materials. As already seen for the α,ω-hydroxyl poly(ε-caprolactone)-silica sol-gel materials, broad signals are attributable to the silica network vibrations at 445 cm^{-1}, 883 cm^{-1}, 1084 cm^{-1}, respectively, for the Si-O rocking, bending and stretching vibrations in silica matrix. It was also noticed that the signal in the hydroxyl vibration area from 3700 cm^{-1} to 3200 cm^{-1} increased and became broader with increasing the amount of silica. The urethane bond at around 1523 cm^{-1} was observed in all the materials, but more interestingly, the carbonyl stretching signal broadened with increase of the silica phase in the sol-gel composites, and therefore as for the α,ω-hydroxyl poly(ε-caprolactone)-silica composites prepared by bulk and sol-gel processes the crystalline/(amorphous+ H-bonded) carbonyl stretching ratios were

calculated for different polymer content and are reported in the Figure 3.9 with the α,ω-hydroxyl poly(ε-caprolactone)-silica bulk and sol-gel materials prepared.

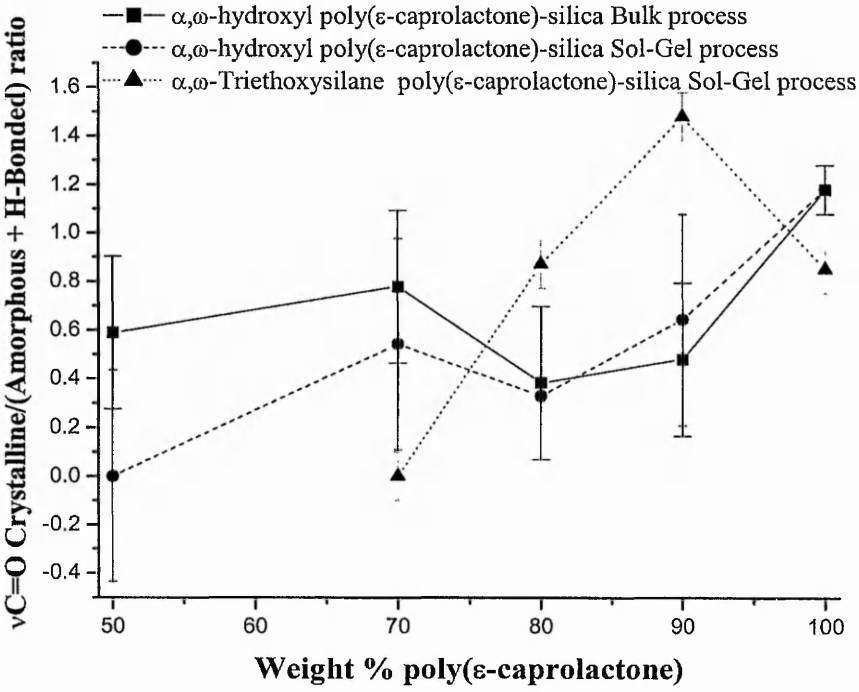

Figure 3.9: Plots of the crystalline/(amorphous + hydrogen bonded) carbonyl stretching vibration peaks ratio as a function of the poly(ε-caprolactone) weight percent for the α,ω-hydroxyl poly(ε-caprolactone)-silica bulk (dark line) and sol-gel (dashed line) materials and the triethoxysilane terminated poly(ε-caprolactone)-silica sol-gel (dotted line) materials.

The decrease of the poly(ε-caprolactone) weight content in all the composite materials decreased the crystalline/ (amorphous + Hydrogen bonded) ν C=O ratio. At a α,ω-hydroxyl poly(ε-caprolactone) weight percent content of 70 and lower, the sol-gel composite had a ν C=O ratio lower than the bulk material. This indicated that the decrease of the crystalline signal compared to the amorphous and hydrogen bonded signals was more important for the sol-gel than for the bulk composites. The effect of the reactive end groups on the ν C=O ratio of the linear poly(ε-caprolactone) was not

apparent at high polymer content but below 70 % weight content the ν C=O ratio was lower for the triethoxysilane terminated than for the hydroxyl terminated polyester in composites prepared by the sol-gel method.

3.2.2. Powder X-ray Diffraction Analysis

Figures 3.10 and 3.11 show the powder X-ray diffractographs of α,ω-hydroxyl poly(ε-caprolactone) and the α,ω-hydroxyl poly(ε-caprolactone)-silica bulk and sol-gel materials with several polymer weight contents. The diffractograms were all normalized using the peak intensity at 2θ equal to 35.30° for the α-aluminium oxide standard added in equal amount to the material sample. It can be seen that similar traces were obtained and that the more evident characteristics were the diminution and broadening of the polyester X-ray peaks.

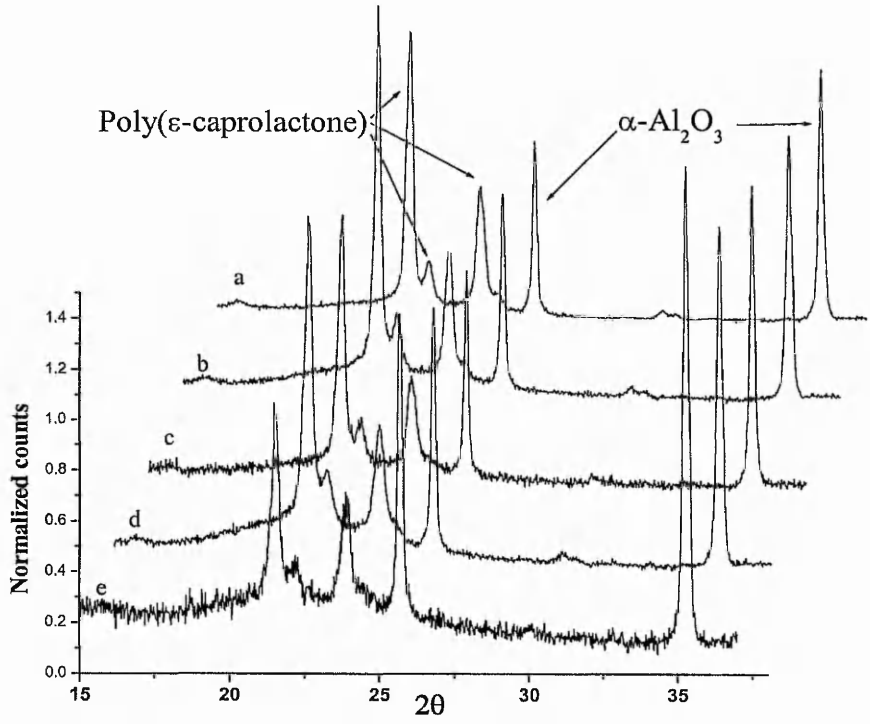

Figure 3.10: Powder X-ray diffractograms of α,ω-hydroxyl poly(ε-caprolactone) (a) and α,ω-hydroxyl poly(ε-caprolactone)-silica materials prepared following the bulk procedure with a poly(ε-caprolactone) weight % content of 95 (b), 90 (c), 80 (d) and 70 (e).

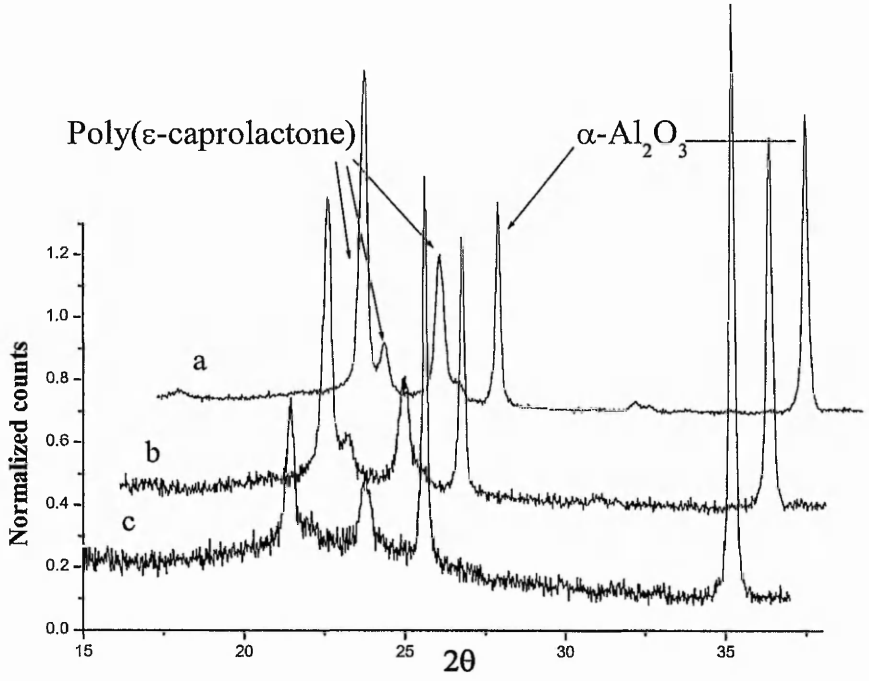

Figure 3.11 : Powder X-ray diffractograms of poly(ε-caprolactone) (a) and α,ω-hydroxyl poly(ε-caprolactone)-silica materials prepared by the sol-gel method with a poly(ε-caprolactone) weight % content of 90 (b) and 70 (c).

The powder XRD data were treated using the Statton's method[14] described in the chapter 2. In Figure 3.12 are plotted the poly(ε-caprolactone) crystallinities measured by powder x-ray diffraction as a function of the poly(ε-caprolactone) weight content in the composite materials.

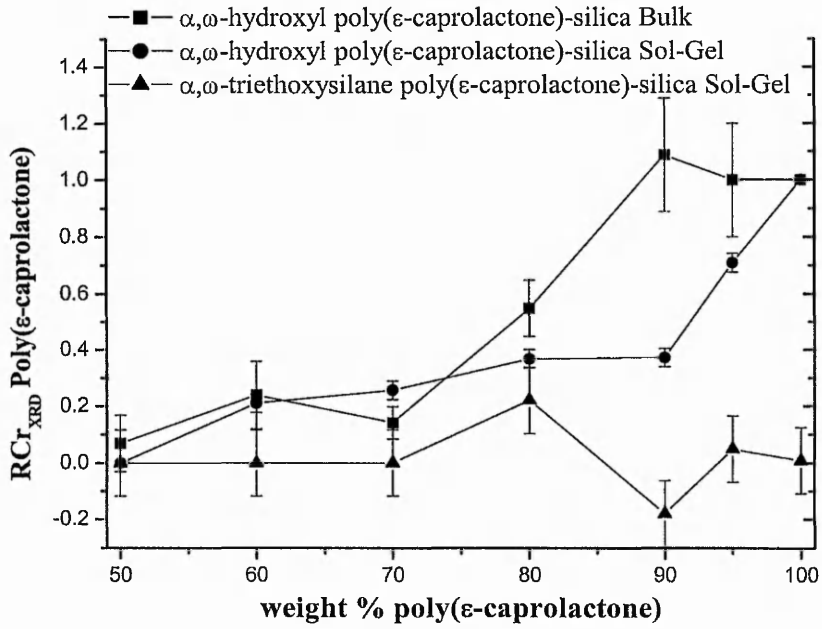

Figure 3.12 : Plots of the poly(ε-caprolactone) crystallinity measured from the X-ray diffraction data (3 repeated measures of RCr_{XRD}) as a function of the poly(ε-caprolactone) weight content in composites.

Figure 3.12 shows that on increase of the silica content (equivalent to the poly(ε-caprolactone) weight content decrease) decreases the polyester crystallinity measured by XRD. This was observed for both bulk and sol-gel methods. The effect of the different reactive groups on poly(ε-caprolactone) had an important effect on the measured value of the RCr_{XRD} crystallinity. By changing the hydroxyl groups to triethoxysilane groups the RCr_{XRD} value went from 1 to 0. It must be strongly emphasised that the RCr_{XRD} is a relative measure of the polyester crystallinity and that a crystallinity value of 1 was given arbitrarily to the α,ω-hydroxyl poly(ε-caprolactone) used in the experiments, and a value 0 was given to a arbitrarily chosen α,ω-hydroxyl poly((-caprolactone)-silica sol-gel material containing 50 % weight of poly(ε-caprolactone). This is why negative values of RCr_{XRD} were found as shown in the figure for the α,ω-triethoxysilane poly(ε-caprolactone)-silica sol-gel materials.

Similarly, the poly(L-lactic acid)-silica sol-gel materials were studied by powder X-ray diffraction analysis. Figure 3.13 shows the powder X-ray diffractograms of α,ω-hydroxyl poly(L-lactic acid) and the α,ω-hydroxyl poly(L-lactic acid)-silica sol-gel materials with different polymer weight content.

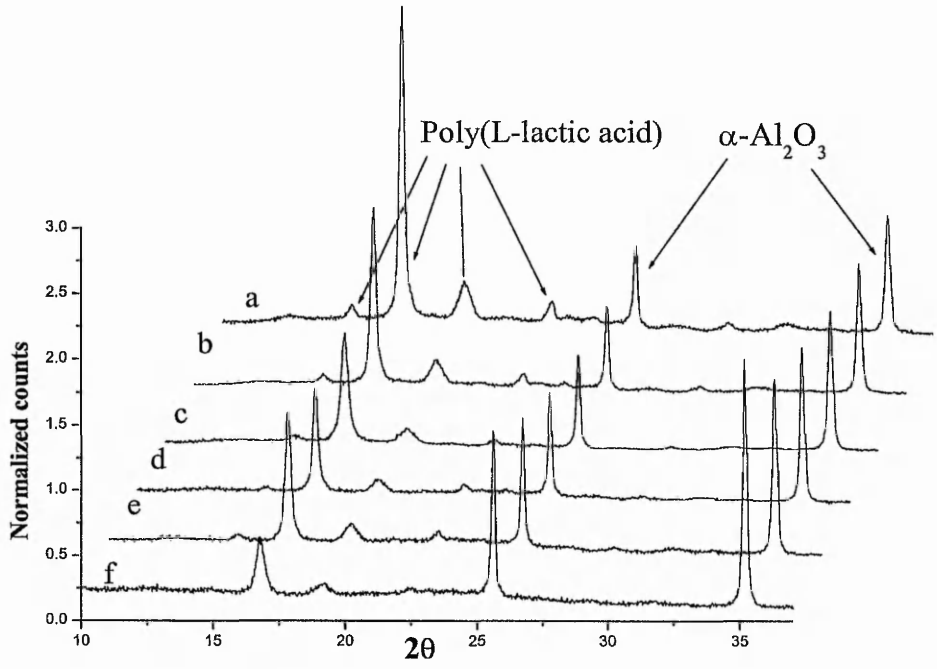

Figure 3.13 : Powder X-ray diffractograms of α,ω-hydroxyl poly(L-lactic acid) (a) and α,ω-hydroxyl poly(L-lactic acid)-silica materials prepared by the sol-gel method with a poly(L-lactic acid) weight % content of 95 (b), 90 (c), 80 (d), 70 (e) and 50 (f).

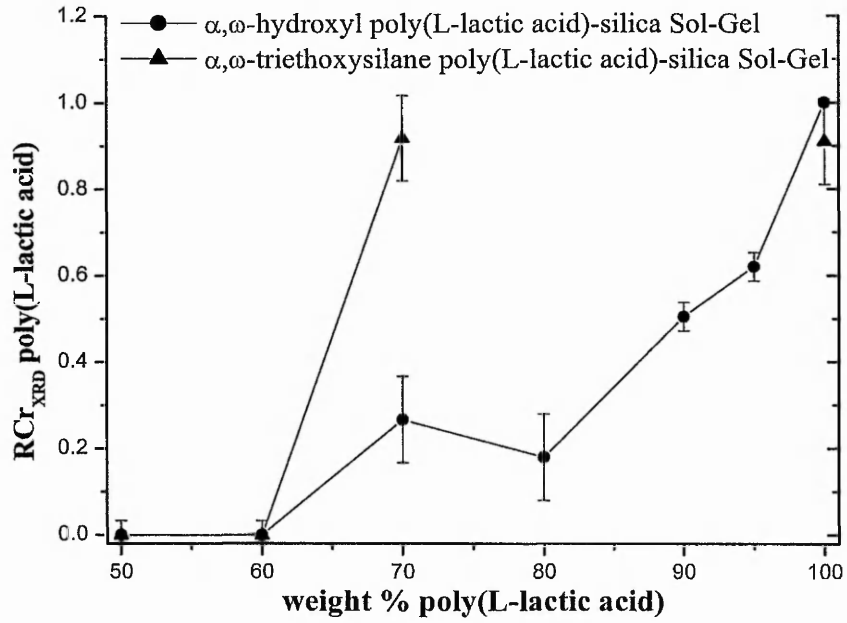

Figure 3.14 : Plots of the hydroxyl and triethoxysilane terminated poly(L-lactic acid) crystallinity measured from the powder X-ray diffraction data (RCr_{XRD}) as a function of the poly(L-lactic acid) weight content in the composites.

As observed for the poly(ε-caprolactone)-silica materials, the increase of silica or decrease of polyester weight content in the composites decreased the RCr_{XRD} value, Figure 3.14. Again the addition of more reactive end-group on the poly(L-lactic acid) strongly influenced the RCr_{XRD} value and therefore the co-continuity of the organic and inorganic phases as already observed for the poly(ε-caprolactone), Figures 3.12 and 3.14.

3.2.3. Differential Thermal Scanning (DSC), Thermo-Gravimetric (TGA) Analysis and Soxhlet Experiments

The weight percent of crystalline poly(ε-caprolactone) (Cr_{DSC}) in the hybrid system was calculated using melting enthalpy data (ΔH_f) as described in the methods section. Figures 3.15 and 3.16 contain the α,ω-hydroxyl poly(ε-caprolactone) crystallinity measured by DSC (Cr_{DSC}) and the melting temperature (T_m) as a function of the α,ω-hydroxyl poly(ε-caprolactone) weight percent content for the bulk and sol-gel methods.

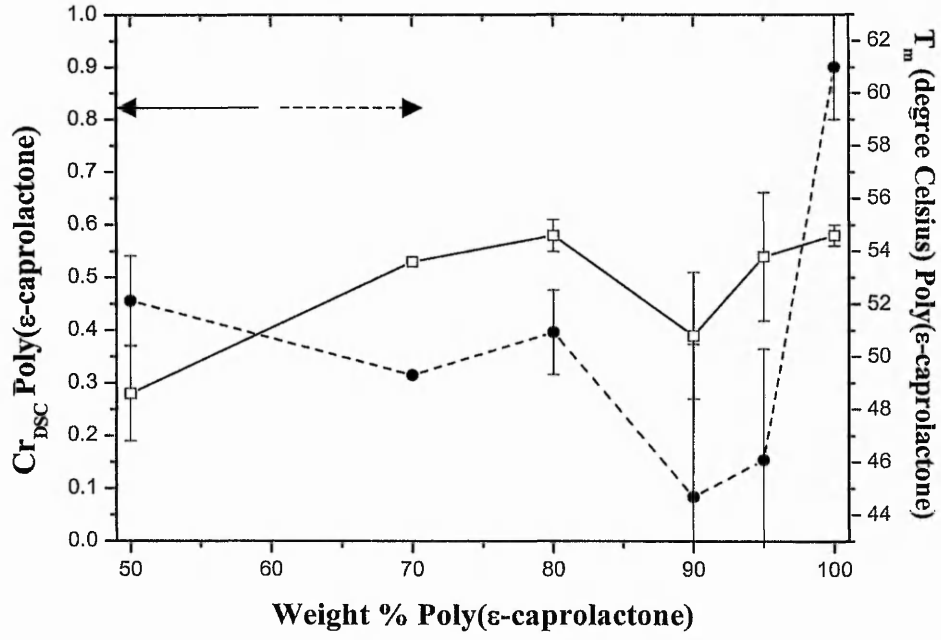

Figure 3.15: Plots of the crystallinity of α,ω-hydroxyl poly(ε-caprolactone) (Cr_{DSC}) in composite bulk materials and melting temperature (T_m) measured by DSC as a function of the poly(ε-caprolactone) weight content percent.

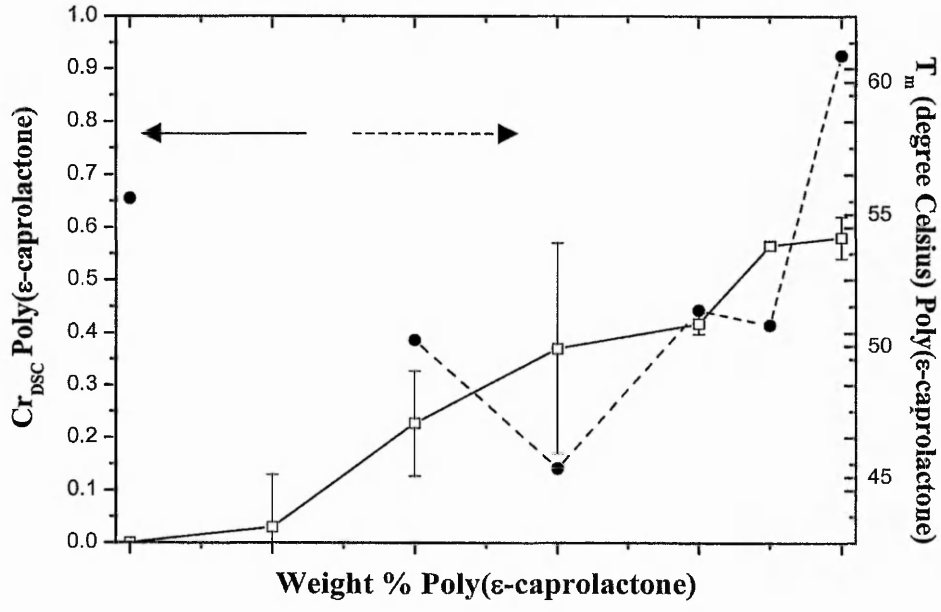

Figure 3.16 : Plots of the α,ω-hydroxyl poly(ε-caprolactone) crystallinity (line) measured by DSC and T_m (dotted line) as a function of the poly(ε-caprolactone) weight content percent, in composite sol-gel materials.

Figures 3.15 and 3.16 showed that decreasing the amount of α,ω-hydroxyl poly(ε-caprolactone) in the composite materials (equivalent to the increase of silica) decreased the α,ω-hydroxyl poly(ε-caprolactone) crystallinity measured by DSC (Cr_{DSC}) for both the bulk and the sol-gel process. The sol-gel process had a stronger influence in decreasing the poly(ε-caprolactone) Cr_{DSC} than the bulk process. The decrease of melting temperatures as a function of the polyester weight content plotted in Figures 3.15 and 3.16, indicated the confinement of the poly(ε-caprolactone) within the composites as proposed by S. Jiang and co-workers[1]. They also reported that the degree of crystallinity (Cr_{DSC}) of α,ω-hydroxyl poly(ε-caprolactone) in hybrid silica sol-gel decreased with the decrease of the polymer content[1] as observed here for the bulk and sol-gel composites prepared. However, they stated that the polyester was completely amorphous only when its content in the hybrids was less than 40 %. In our study, at 60% weight content of α,ω-hydroxyl poly(ε-caprolactone) in the sol-gel composite, the Cr_{DSC} value was already nearly zero. The difference of α,ω-hydroxyl poly(ε-caprolactone) average molecular number (M_n) used to prepare the hybrids; Mn equal to 11,300 g/mol for their study and in our study M_n equal to 2,000 g/mol was a possible reason for the discrepancy between the Cr_{DSC} values. The structural effect resulting from the variation of the polymer molecular weight in a hybrid silica sol-gel has been reported[10]. Low number average molecular weight polymers favour the incorporation of the polymer in the silica phase by increasing the number of reactive end-groups per weight of polymer with higher confinement of the poly(ε-caprolactone) in the inorganic phase giving rise to a lower Cr_{DSC}. These results were correlated with the effect of the addition of more reactive end-groups, triethoxysilane, on the poly(ε-caprolactone) and are reported Figure 3.17.

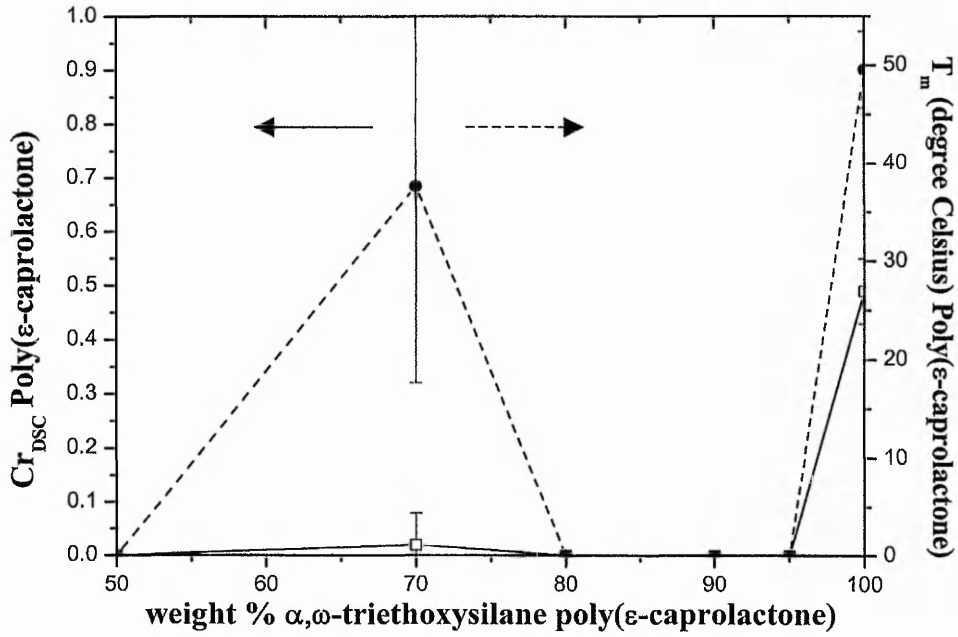

Figure 3.17: Plots of triethoxysilane terminated poly(ε-caprolactone) crystallinity (line) measured by DSC and T_m (dotted line) as a function of the poly(ε-caprolactone) weight percent in composite sol-gel materials.

The effect of changing the reactivity of the poly(ε-caprolactone) end–groups was drastic. Triethoxysilane terminated poly(ε-caprolactone) Cr_{DSC} values for silica sol-gel composites was equal to zero upon addition of the silica phase, Figure 3.17. When compared with Figures 3.15 and 3.16, the results of the Cr_{DSC} collected for triethoxysilane terminated poly(ε-caprolactone) indicated that for the incorporation and homogeneity of polymer-silica phases (low Cr_{DSC} value), the reactive end-groups attached to the poly(ε-caprolactone) had a more important effect than the method used to prepare the inorganic-organic composites.

As for the poly(ε-caprolactone)-silica composites, the poly(L-lactic acid)-silica sol-gel materials were analysed using differential scanning calorimetry.

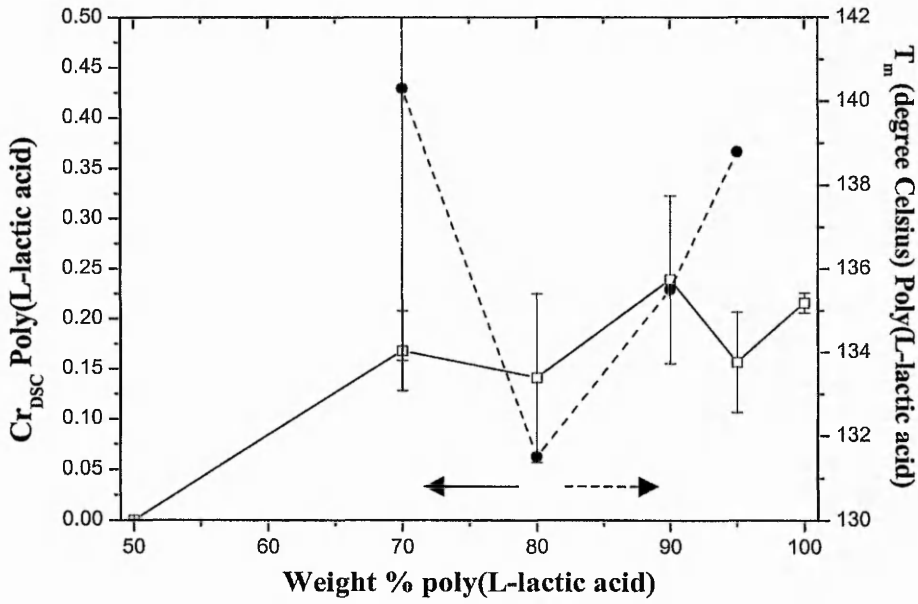

Figure 3.18: Plots of the α,ω-hydroxyl poly(L-lactic acid) crystallinity (line) measured by DSC and T_m (dotted line) as a function of the poly(L-lactic acid) weight per cent in composite sol-gel materials.

The decrease of the α,ω-hydroxyl poly(L-lactic acid) weight content in silica sol-gel composites decreased the Cr_{DSC} values, Figure 3.18. A completely amorphous α,ω-hydroxyl poly(L-lactic acid) was obtained for a polyester weight content of 50 %. For the triethoxysilane terminated poly(L-lactic acid) and the corresponding sol-gel materials, the DSC measurements did not shown a peak corresponding to a phase transformation from crystalline state to amorphous state. Therefore, the polymer crystallinity (Cr_{DSC}) was equal to zero. The comparison of the Cr_{DSC} data obtained for the poly(ε-caprolactone) and poly(L-lactic acid) silica sol-gel composites showed similar behaviour; an increase of the silica phase, decreased the Cr_{DSC} value of the polyesters, indicating confinement and constriction of the organic phase that increased within the increasing inorganic network[15]. Increase of the reactivity of the end-groups on the linear polyesters decreased the Cr_{DSC} values drastically to the limit that no melting transitions (Cr_{DSC} values equal to 0) were observed by differential scanning

calorimetry upon the addition and reaction of triethoxysilane end-groups within the silica sol-gel composites.

In the following paragraph, the thermogravimetric analysis and some Soxhlet experiments are discussed in parallel to reveal the extent of covalent bonding of the polyesters to the silica phase in the composites. A Soxhlet apparatus was used for the extraction of soluble organic compound from the solid composite into an organic solvent. The Soxhlet experiments were carried as follow. The flask containing the solvent (200 ml toluene) was heated, vapours raised in the larger outside tube, enter the water-cooled condenser and reliquify. When the liquid level in the extractor reaches the top of the bent tube, siphoning action returns the extract-enriched solvent to the flask, the reaction was carried out for 48 hours for each material sample. Figure 3.19 shows the weight loss of some of the composite materials prepared as a function of the temperature. The experimental set up for the TGA analysis has already been reported in the previous chapter.

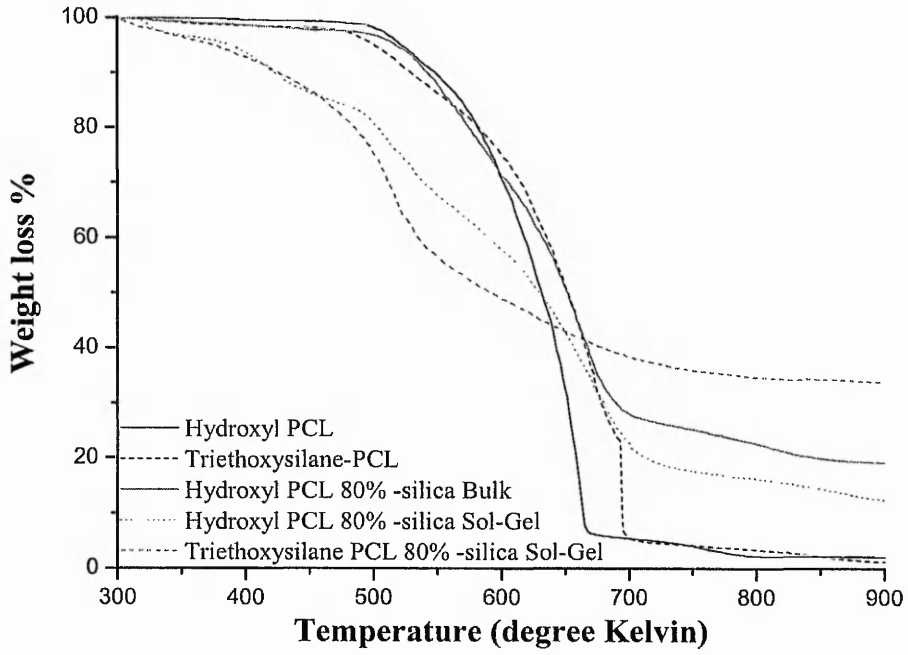

Figure 3.19: Thermogravimetric curves of α,ω-hydroxyl poly(ε-caprolactone), α,ω-triethoxysilane poly(ε-caprolactone), α,ω-hydroxyl and α,ω-triethoxysilane poly(ε-caprolactone)-silica bulk and sol-gel materials containing 80 percent weight of polyester.

Figure 3.19 showed that the degradation profile of the poly(ε-caprolactone) changed thoroughly in the composites. First, the composite prepared by the bulk method had a similar profile to the starting α,ω-hydroxyl poly(ε-caprolactone). The only difference was the shift of the degradation temperature to higher temperature, from 640 to 668 Kelvin. The interaction of the polyester with the silica phase could explain the higher degradation temperature due to the extra energy needed to remove the interaction with the inorganic phase. Instead of the relatively sharp loss of weight observed for the hydroxyl and triethoxysilane terminated poly(ε-caprolactone), the sol-gel composite materials had a more complex degradation profile. For the poly(ε-caprolactone)-silica sol-gel, a first change of slope was observed for both hydroxyl and triethoxysilane terminated poly(ε-caprolactone), from the beginning of the heating to 500 Kelvin. This probably corresponded to the hydrolysis-condensation reaction of non-reacted ethoxysilanes, and loss of ethanol and possible residual solvent. A second change of slope was also observed from 500 to 700 Kelvin probably corresponding to the degradation of the poly(ε-caprolactone). The slopes observed for the degradation of the polyester sol-gel prepared composites were broader and less sharp than for the bulk composite. This may be due to the covalent bonding of the polyesters with the silica (need higher temperature to degrade) and also the more amorphous structure of the polymer in the composites (need lower temperature to degrade).

Table 3.13: α,ω-Hydroxyl poly(ε-caprolactone), triethoxysilane terminated poly(ε-caprolactone) and α,ω-hydroxyl triethoxysilane terminated poly(ε-caprolactone)-silica bulk and sol-gel materials; TGA and Soxhlet experiment results.

Theoretical PCL weight %	**TGA T_d (Kelvin)**	**weight % residue**	**Soxhlet toluene weight % residue**
100	640 ± 12	0.5	2.0
Bulk process			
90	657	9.3	3.4
70	668	21.0	40.0
Sol-Gel process			
90	660	12.5	6.9
70	670	15.3	11.2
50	672	46.7	28.1
Triethoxysilane PCL Sol-Gel			
100	695 ± 30	1.1	12.3
90	520	11.0	60.2
70	622	33.0	41.0

The residue weight % of TGA and Soxhlet experiments are collected in Table 3.13. A higher Soxhlet residue weight % than TGA residue weight % for the same material indicated the incorporation of the poly(ε-caprolactone) within the silica gel. Either, the polyester could be entrapped in the silica network or bond covalently to the inorganic phase. The results, in Table 3.13, showed that the residue weight value of TGA and Soxhlet experiment were close for the α,ω-hydroxyl poly(ε-caprolactone)-silica bulk and sol-gel methods. The cross-bonding and entrapment of poly(ε-caprolactone) were probably minor in the α,ω-hydroxyl poly(ε-caprolactone)-silica bulk and sol-gel materials. For the triethoxysilane terminated poly(ε-caprolactone)-silica sol-gel, the values of the Soxhlet residue weight % were always higher than the TGA residue weight % at all poly(ε-caprolactone) contents. This suggested that covalent bonding via the triethoxysilane end-groups of the polyester between both phases existed and that C-O-Si bonds were more numerous than with the hydroxyl terminated polyester. Mid-IR analysis of the Soxhlet residual material confirmed the presence of vibration signals of the triethoxysilane terminated poly(ε-caprolactone) in the collected material after the Soxhlet experiment, Figure 3.20.

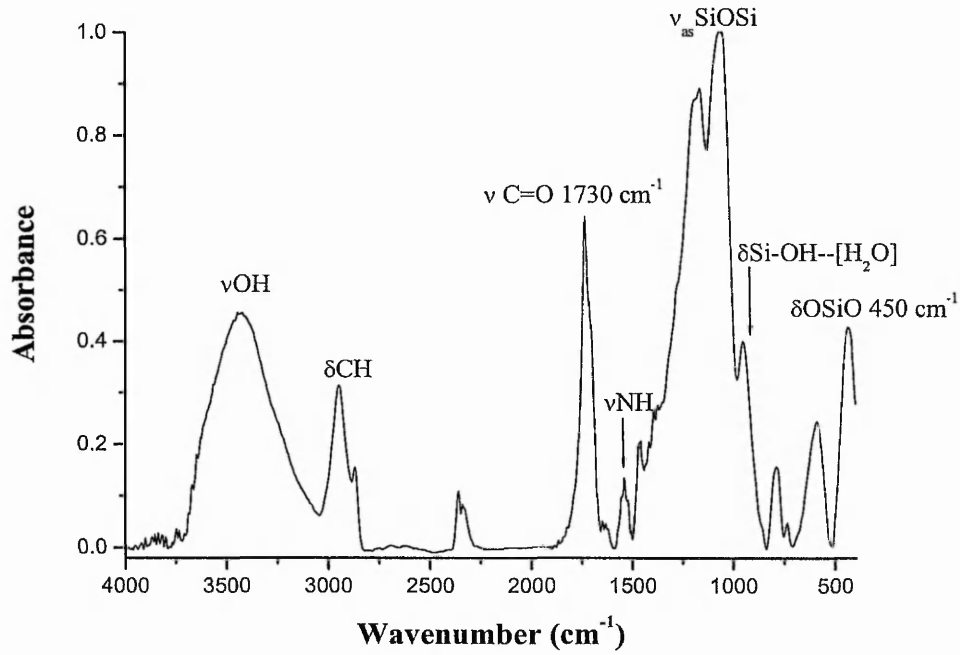

Figure 3.20: Mid-IR spectrum of triethoxysilane terminated poly(ε-caprolactone)-silica sol-gel, insoluble part collected after Soxhlet experiment.

The Mid-IR spectrum, Figure 3.20 showed very strong signals for the carbonyl stretching of poly(ε-caprolactone) at 1730 cm^{-1}, and the urethane band at 1630 cm^{-1}. This suggested that a large amount of triethoxysilane terminated poly(ε-caprolactone) was probably bonded with the silica phase. Interestingly a band at 3750 cm^{-1} attributed to the free OH on silanol groups was newly observed.

Figure 3.21 shows the weight loss % of poly(L-lactic acids) and silica sol-gel composites as a function of the temperature. From the obtained curves, the degradation temperature (maximum of first derivative) and the final weight percent are listed in the Table 3.13.

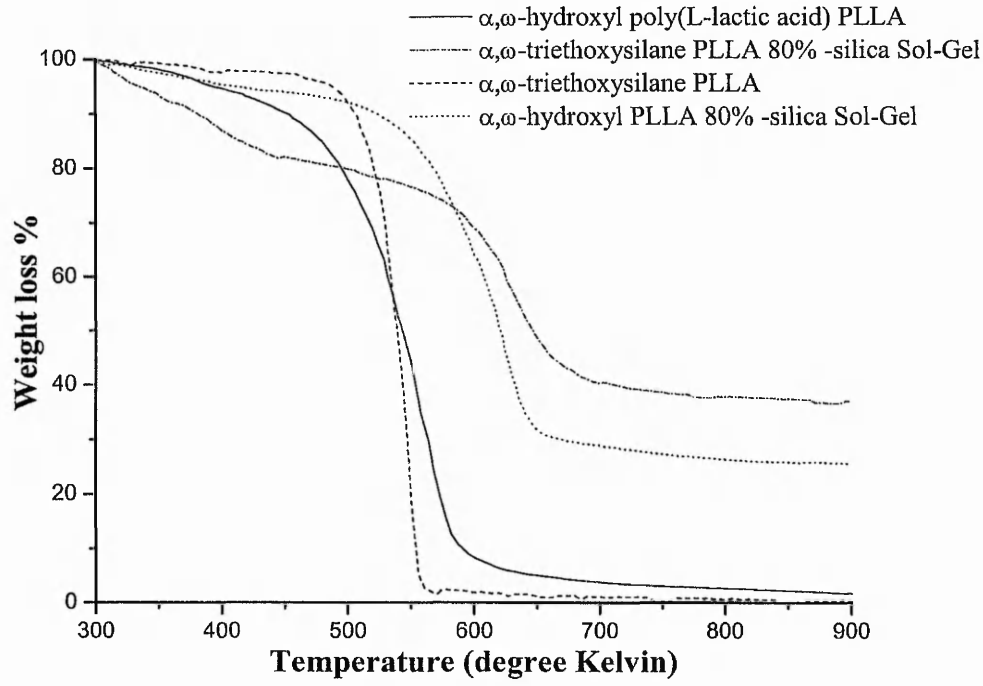

Figure 3.21: TGA curves of α,ω-hydroxyl poly(L-lactic acid), triethoxysilane terminated poly(L-lactic acid), hydroxyl and triethoxysilane terminated poly(L-lactic acid)-silica sol-gel materials with 70 % weight content of polyester.

Figure 3.21 shows that the addition of the silica phase changed the degradation profile of the poly(L-lactic acids). Instead of the relatively sharp loss of weight observed for the poly(L-lactic acids), the composite materials had a more complex degradation profile. A first change of slope was observed for both hydroxyl and triethoxysilane terminated poly(L-lactic acid) from the beginning to 400 Kelvin as observed for the poly(ε-caprolactone)-silica sol-gel, Figure 3.19. The loss of weight was attributable to the incomplete hydrolysis-condensation reaction of ethoxysilane and release of ethanol. The second change of slope occurred respectively at 630 and 625 Kelvin for the hydroxyl and triethoxysilane terminated poly(L-lactic acid) silica sol-gel. Compared to the degradation temperature (T_d) values of the hydroxyl and triethoxysilane terminated poly(L-lactic acids), 570 and 548 Kelvin respectively, the Td value shifted 60 and 77 Kelvin respectively to higher temperature. This was due to the entrapment of the poly(L-lactic acids) in the silica phase. More energy (heat) was needed for the degradation of the poly(L-lactic acids) covalently bonded and confined within the silica

phase. The shift of temperature was more important for the triethoxysilane terminated poly(L-lactic acid) than the hydroxyl terminated poly(L-lactic acid). This effect could have been expected because of the higher reactivity of the triethoxysilane groups and therefore more covalent bonds being formed between the organic and the inorganic phases increased the shift of T_d.

Table 3.14 : α,ω-hydroxyl poly(L-lactic acid), triethoxysilane terminated poly(L-lactic acid) and α,ω-hydroxyl triethoxysilane terminated poly(L-lactic acid)-silica sol-gel materials; TGA and Soxhlet experiment results.

Theoretical PLLA Weight %	**TGA T_d**	**weight % Residue**	**Soxhlet Toluene weight % residue**
100	570 ±10	0.0	1.0
90	625	8.3	10.0
70	630	19.0	36.1
50	665	48.0	46.0
Triethoxysilane PLLA			
100	548 ±4	2.1	-
90	540	6.6	68.27
70	625	26.0	48.0
50	631	41	59.0

In accordance with the results obtained for the poly(ε-caprolactone) sol-gel composites, the comparison of the residual weight % of the TGA and Soxhlet experiment, Table 3.14, shows better bonding of the triethoxysilane terminated poly(L-lactic acid) with the silica phase than that shown for the hydroxyl terminated poly(L-lactic acid) with the silica. The insoluble samples collected after the Soxhlet experiment were analysed by FTIR, Figure 3.22.

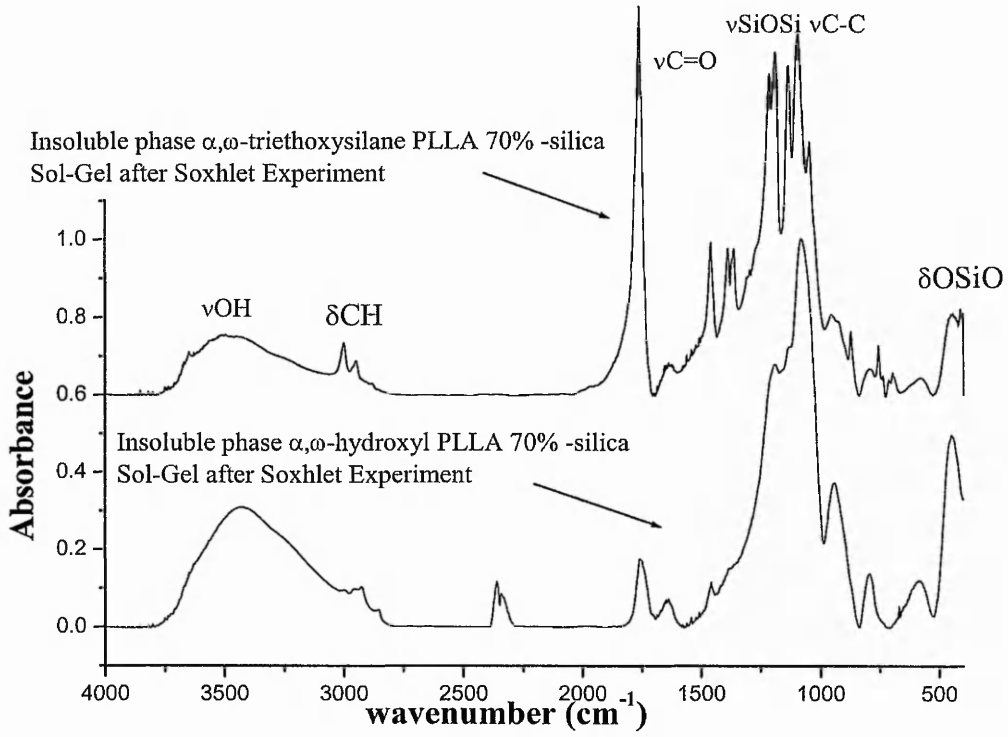

Figure 3.22 : Mid-IR spectrum of hydroxyl, and triethoxysilane terminated poly(L-lactic acid)-silica sol-gel insoluble part collected after the Soxhlet experiment.

Figure 3.22 shows that the carbonyl stretching vibration intensity for the triethoxysilane terminated poly(L-lactic)-silica sol-gel is more intense and therefore covalently bonded and/or entrapped in the silica phase than for the spectrum obtained from the hydroxyl terminated poly(L-lactic acid) sample.

3.2.4. Electron Microscopy

The transmission electron micrograph of poly(α-hydroxyacid)-silica materials are shown below. The silica is seen in black and the polyesters in white. It must be emphazised that the polyesters under the electron beam tend to melt. Therefore, for high polyester content in the composites obtaining a good quality photographs was rather difficult even for materials embedded in an epoxy resin.

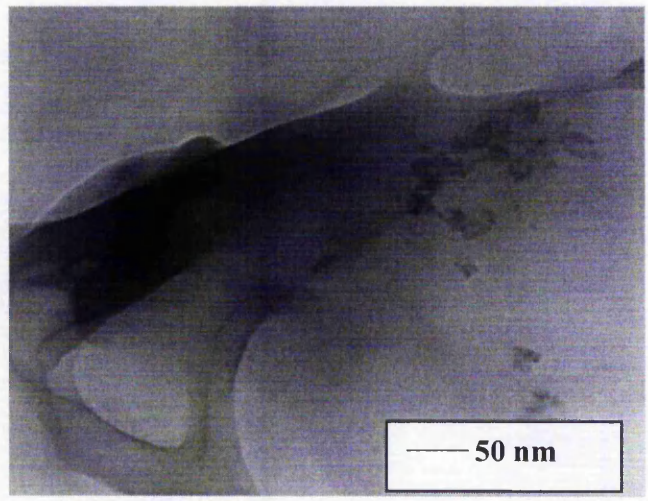

Figure 3.23: TEM micrograph of α,ω-hydroxyl poly(ε-caprolactone)-silica sol-gel materials with 95% weight content of polyester.

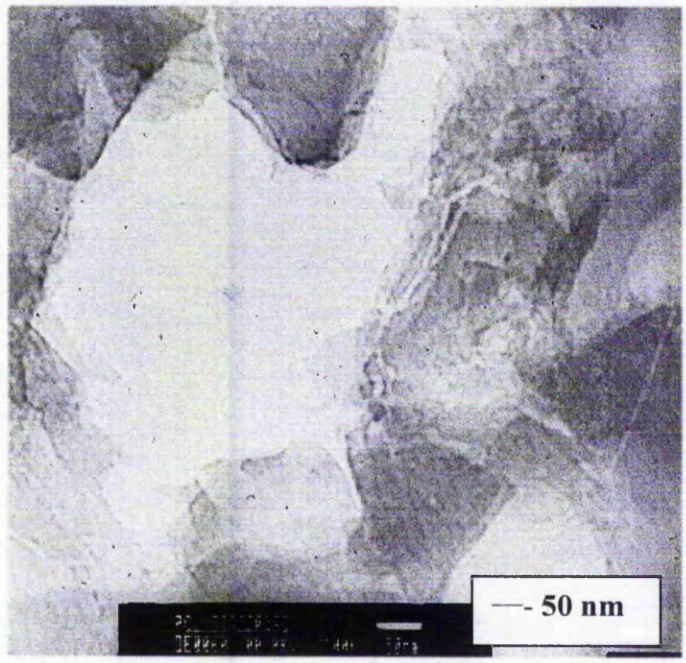

Figure 3.24: TEM micrograph of α,ω-hydroxyl poly(ε-caprolactone)-silica sol-gel materials with 80 % weight content of polyester.

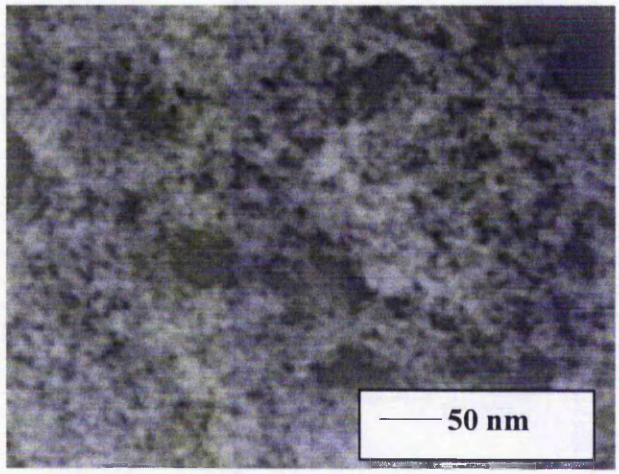

Figure 3.25 : TEM micrograph of α,ω-hydroxyl poly(ε-caprolactone)-silica sol-gel materials with 70% weight content of polyester.

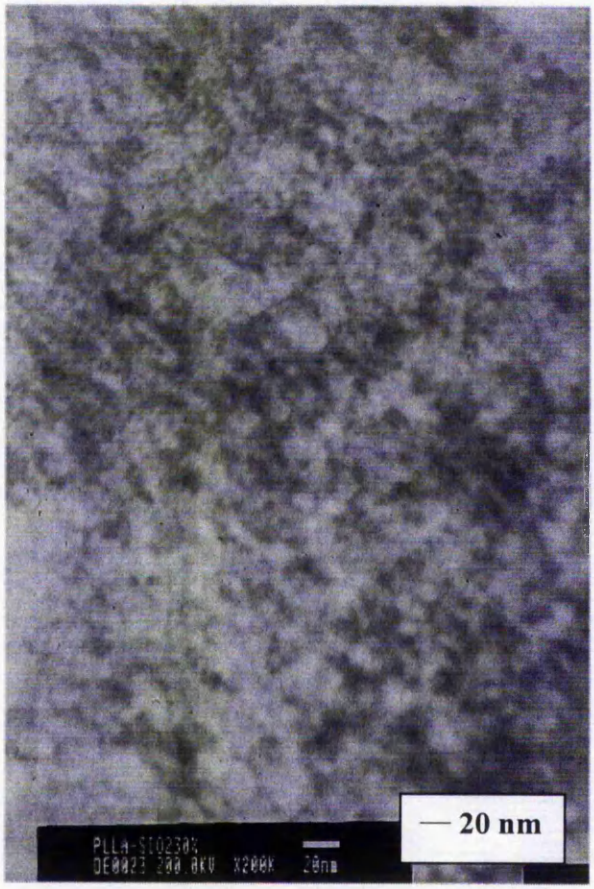

Figure 3.26 : TEM micrograph of α,ω-hydroxyl poly(L-lactic acid)-silica sol-gel materials with 70 % weight content of polyester.

The electron microscopy micrographs of the α,ω-hydroxyl poly(ε-caprolactone) 95 % sol-gel composite, Figures 3.23 showed the presence of non agglomerated, rather dispersed silica particles through the polyester matrix. The approximate diameters of the particles varied from a few nanometers to 20 nanometers in size.

Figures 3.26 and 3.27 show characteristic structural features suggesting some co-continuity in the phase structure for the materials[7] with poly(ε-caprolactone) and poly(L-lactic acid) content of 70 % (silica; black, poly(α-hydroxyacids); white). The TEM observations were in agreement with the formation of a co-continuous interpenetrating network of the poly(α-hydroxyacids) and the silica phases for the composition with 70 % weight content of poly(α-hydroxyacid). The average distances between the constitutive components were not calculated here because of the poor micrograph quality. However, observations indicated that the average distance was below 10 nanometers in accordance with the results reported by D. Tian and co-workers[7]. Some visual observations confirmed the preparation of true ceramers for sol-gel composites with 70% and 60% weight content of polyester. The phase separation existed on a scale sufficiently smaller than the wavelenght of light that no scattering occured within the composite and transparent materials were obtained, Figure 3.27 (b).

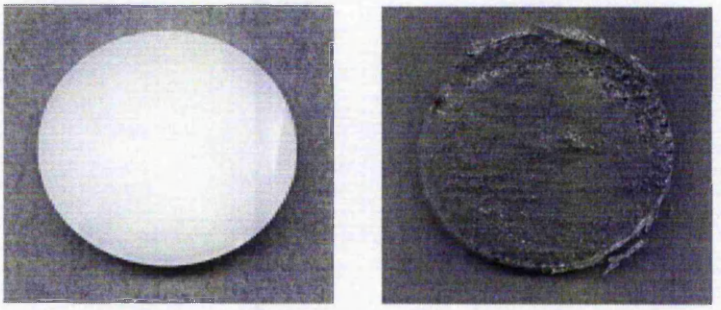

a) b)

Figure 3.27 : Photographs of α,ω-hydroxyl poly(ε-caprolactone)-silica a) bulk and b) sol-gel materials, 70 % weight content polyester.

It has not been possible to correlate the structure of the silica particles observed by TEM with specific variations in the preparation of the composites. The reason is that the poly(α-hydroxyacid)-silica composites were not stable under the electron beam and the materials melted upon observation even at low energy (100 keV instead of 200 keV). Consequently, The structure and morphology of the composites observed under the transmission electron microscope could be due to preparation and observation artefacts and the quality of the micrographs obtained was poor. Embedding the samples in an epoxy resin did not facilitate the observation of the composites and it seems probable that some of the composites have reacted with the resin during sample preparation. A micrograph, Figure 3.24 is presented as an example of the usual poor quality of micrograph obtained.

3.3. Conclusion

The materials studied can be described, when containing a high silica content, as co-continuous organic and inorganic structures[15], and for low silica content, as a dispersed inorganic phases in an organic polymer. A measure of the crystallinity of the organic phase and its variation with synthesis variables was a good indicator of the incorporation of poly(α-hydroxyacids) into the silica network generated by the sol-gel process. The higher the extent of order of the poly(α-hydroxyacid) phase (high crystallinity), the lower the interaction of the silica phase with the organic polymer. The lower the crystallinity of the poly(α-hydroxyacids) phase, the stronger the interaction between the two phases suggesting a more closed structure for the composites. The results obtained for the two statistical studies were in accordance with previous studies[1] and showed that increasing the TEOS/PCL and TEOS/PLLA molar ratios increases the incorporation of poly(α-hydroxyacid) within the silica network.

The statistical model applied to the XRD and DSC data showed that incorporation of poly(ε-caprolactone) within the silica network increased as the HCl/TEOS molar ratio was increased. D. Tian and co-workers noticed identical behavior when analysing similar hybrid materials by dynamic mechanical methods[5]. Their explanation for this behaviour was that the catalyst content increased the overall

rate of hydrolysis-condensation of tetraethyl orthosilicate. Because they only studied one variable at a time they could not determine which reaction (hydrolysis or condensation) of the sol-gel silanol formation mechanism was important. In the present study within the limits defined for the statistical model at the 0.05 α-level of confidence, the interaction between HCl/TEOS and H_2O/TEOS molar ratios had no effect on the Cr_{DSC} (no interaction effect between the molar ratios of HCl/TEOS and H_2O/TEOS were found using the 2^5 central factorial design at 0.05 α-level ($p=0.086>0.05$). Additionally, the model applied to the RCr_{XRD} data also showed that at 0.05 level of confidence there was no interaction effect between the HCl/TEOS and H_2O/TEOS molar ratio ($p=0.724>0.05$). The significance of this was that the increase in catalyst content had a more important effect on the condensation rate of TEOS in the hybrid sol-gel rather than on the hydrolysis rate of TEOS. This was in accordance with the idea of the development of co-continuous phases with confined organic polymers within inorganic phases. Hydrogen bonding between PCL and silica has previously been thought to have a retarding effect on their phase separation and thus on the aggregation of the inorganic constitutive component[13].

The similar statistical study carried out on the new poly(L-lactic acid)-silica sol-gel composite gave different results. Effects of the toluene/PLLA molar ratio and the two-way interactions TEOS/PLLA*H_2O/TEOS and toluene/PLLA*HCl/TEOS molar ratios on RCr_{XRD} and Cr_{DSC} values were observed. A much stronger effect was observed for the solvent compared to the poly(ε-caprolactone)-silica sol-gel study. The amount of toluene (toluene/PLLA molar ratio) affected the solubility of the poly(L-lactic acid) in the reaction mixture and therefore its crystallinity. From the interaction effect observed, the strength of an acid and the rate of the TEOS hydrolysis-condensation reactions were also influenced by the solvents used[9].

The results of these two studies showed that even if catalyst (HCl/TEOS molar ratio) effect exists during the formation of the sol-gel, the structure or order of the poly(α-hydroxyacids) in silica composite materials was mostly dictated by the physical constraints of putting the organic polymer into the open silica network.

Following the statistical studies, the effect and comparison of the preparation methods and reactive end-groups on poly(α-hydroxyacid)-silica composite structures was studied. The homogeneity or the incorporation of the poly(ε-caprolactone) within

the silica phase was higher using the sol-gel method than the bulk method. In fact, the FTIR, the XRD and DSC analysis showed that a decrease of the poly(ε-caprolactone) order (crystallinity) at constant polymer weight content was more marked when the composite was synthesised using the sol-gel method than when using the bulk method. The increase of reactivity of the end-groups on the linear poly(α-hydroxyacid) was obtained by substituting the hydroxyl by triethoxysilane groups, over a large range of polymer weight content, the lower crystallinity of the triethoxysilane terminated poly(α-hydroxyacid) in composites, compared to the hydroxyl terminated poly(α-hydroxyacids), showed that the incorporation of the poly(ε-caprolactone) and poly(L-lactic acid) was higher with the triethoxysilane end-groups than with the hydroxyl end-groups. The TGA and Soxhlet experiments confirmed that the better incorporation was due to the presence of more covalent bonding between the silica and the organic polymer phase.

To conclude, the structural studies carried out show that the degree of crystallinity provides an indication of the confinement of the polyester in a composite material and information on the formation of homogeneous composites. The crystallinity is a fundamental measurement from which the physical properties of the material can be predicted. The incorporation of the poly(α-hydroxyacid) in an inorganic matrix of silica modify their chemical and physical properties and could therefore lead to useful modifications of its biodegradability and possibly its biocompatibility[16]. Furthermore, a recent publication has described the apatite-forming ability of a poly(ε-caprolactone)-silica hybrid material[17]. An understanding of the degree of poly(ε-caprolactone) crystallinity is important since crystallinity affects such physical properties as storage modulus, permeability, density, and melting point, all factors that affect the polymer biodegradation and bioactivity properties.

3. 4. References

[1] S. Jiang, X. Ji, L. An, B. Jiang (2001), "Crystallization behavior of PCL in hybrid confined environment.", *Polymer*, 42, 3901-3907.

[2] R. Christensen (1996), "Analysis of variance design & regression. Applied statistical method.", ed. R. Christensen (Chapman and Hall).

[3] D. Tian, Ph. Dubois, R. Jerome (1997), "Biodegradable and biocompatible inorganic-organic hybrid materials. I. Synthesis and characterization.", *Journal of Polymer Science. Part A: Polymer Chemistry*, 35, 2295-2309.

[4] D. Tian, Ph. Dubois, R. Jerome (1996), "A new poly(ε-caprolactone) containing hybrid creamer prepared by the sol-gel process.", *Polymer*, 37(17), 3983-3987.

[5] D. Tian, S. Blacher, R. Jerome (1999), "Biodegradable and biocompatible inorganic-organic hybrid materials; 4. Effect of acid content and water content on the incorporation of aliphatic polyester into silica sol-gel process.", *Polymer*, 40, 951-957.

[6] S. Aubonnet (1999), "Thesis: Structural and preparative studies of doped silica glasses.", (Nottingham Trent University).

[7] D. Tian, S. Blacher, Ph. Dubois, R. Jerome (1998), "Biodegradable and biocompatible inorganic-organic hybrid materials. 2. Dynamic mechanical properties, structure and morphology.", *Polymer*, 39(4), 855-864.

[8] C. J. Brinker (1990), "Sol-Gel Science: the physics and chemistry of sol-gel processing.", Eds. C. J. Brinker, G. W. Scherer, (Academic press).

[9] C. Reichardt (1988), "Solvents and solvent effects in organic chemistry. 2nd edition.", Ed. H. F. Ebel (VCH, Weinheim).

[10] D. Tian, Ph. Dubois, R. Jerome (1997), "Biodegradable and biocompatible inorganic-organic hybrid materials. I. Synthesis and characterization.", *Journal of Polymer Science. Part A: Polymer Chemistry*, 35, 2295-2309.

[11] M. M. Coleman, J. F. Graf, P.C. Painter (1991), "Specific interactions and the miscibility of polymer blends.", Eds. M. M. Coleman, J. F. Graf, P.C. Painter, (Technomic, Lancaster).

[12] S. W. Kuo, C. F. Huang, F. C. Chang (2001), "Study of hydrogen-bonding strength in poly(ε-caprolactone) blends by DSC and FTIR.", *Journal of Polymer Science: Part B: Polymer Physics,* 39, 1348-1359.

[13] D. Tian, S. Blacher, Ph. Dubois, R. Jerome (1998), "Biodegradable and biocompatible inorganic-organic hybrid materials. 2. Dynamic mechanical properties, structure and morphology.", *Polymer*, 39(4), 855-864.

[14] W. O. Statton (1963), "An X-ray crystallinity index method with application to poly(ethylene terephthalate).", *Journal of Applied Polymer Science*, 7, 803-815.

[15] M. R. Landry, B. K. Coltran, C. J. T. Landry, J. M. O'Reilly (1995), "Structural models for homogeneous organic-inorganic hybrid materials. Simulations of small-angle X-ray scattering profiles.", *Journal of Polymer Science: Part B: Polymer Physics*, 33(4), 637-655.

[16] S. Ramakrishna, J. Mayer, E. Wintermantel, K. W. Leong (2001), "Biomedical applications of polymer-composite materials: a review.", *Composites Science and Technology*, 61, 1189-1224.

[17] S. H. Rhee, H. M. Kim (2002), "Preparation of a bioactive polycaprolactone/silica nanocomposite.", *Key Engineering Materials,* 218-220, 453-456.

The studies presented in this chapter consider the apatite-forming ability of the poly(α-hydroxyacid)-silica composites prepared. First, selected material compositions from both statistical design experiments were tested for their apatite-forming ability *in vitro*, using a static biomimetic process. Secondly, the effect on the *in vitro* osteoconductivity of, (a) the bulk and sol-gel preparation methods, (b) the nature of the polyester used either poly(ε-caprolactone) or poly(L-lactic acid), (c) the polyester end-groups reactivity (hydroxyl and triethoxysilane), were studied. Three *in vitro* osteoconductivity tests (dynamic biomimetic process (DBP), static biomimetic process (SBP), alternate soaking process (ASP)) have been compared and the advantages and drawbacks of each discussed. Finally, the relationship between composite structure and its *in vitro* apatite-forming ability is discussed.

4.1. *In vitro* Biocompatibility

The subject of this work did not include the study of the interaction of the prepared composite materials with biological materials. R. Jerome and co-workers[1] have reported that preliminary *in vitro* cell cultures exhibited favourable behaviour. Fibroblasts attached and spread on the surface of the α,ω-hydroxyl poly(ε-caprolactone)-silica hybrids with a polymer weight content of 50, 30 and 15 percent. It has been thought that *in vitro* biocompatibility tests; cytotoxicity and viability of osteoblasts on the surface of the materials prepared were all necessary before looking at the potential bioactivity properties. Thus *in vitro* cytotoxicity of the silica-poly(α-hydroxyacids) composites was assessed by seeding discs of the materials with human cranio-facial cells (CFC) passage 9 and studying the cell viability with a fluorescent assay kit. Before seeding with the cells, the disks were washed with ethanol and sterile PBS. The methods are not reported here, as the experiments were performed by Dr. D. Heath at Smith & Nephew Research Group Centre, York.

The cells on the surface of the materials were observed using a confocal microscope. The live cells are green, the dead cells red. Thermanox (a commercial polymer used as cell culture scaffold) and α,ω-hydroxyl poly(ε-caprolactone) were used as positive references. The confocal microscope pictures, Figure 4.1, were representative of the *in vitro* toxicity/viability tests carried out. It was observed that osteoblasts were numerous on many of the materials and that they spread which was a

sign of good attachment on the surface of the composites. The results were in accordance the literature data[1].

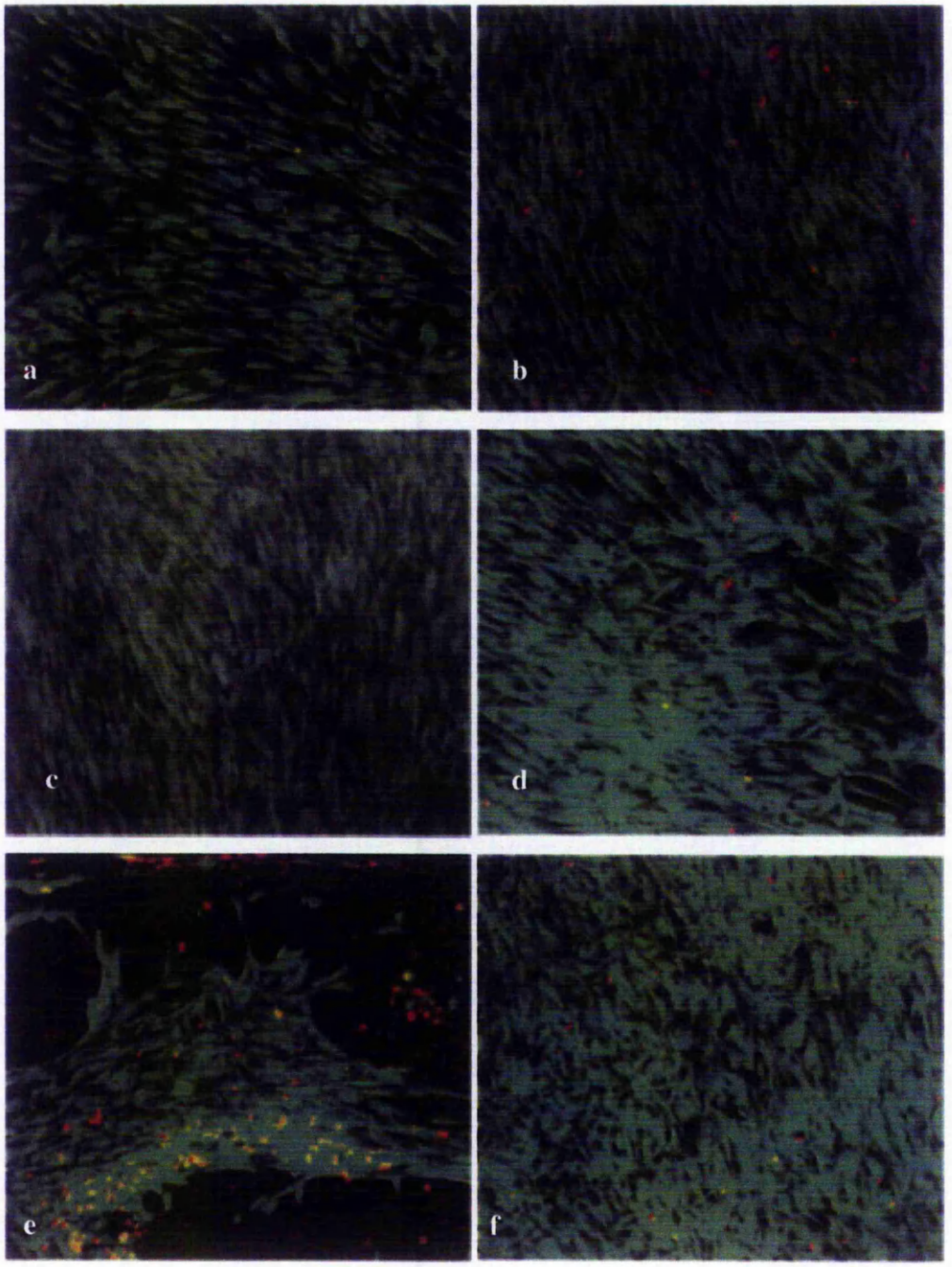

Figure 4.1 : Confocal microscope photos of the *in vitro* cytotoxicity/viability tests on thermanox (a), α,ω-hydroxyl poly(ε-caprolactone) (b), α,ω-hydroxyl poly(ε-caprolactone)-silica sol-gel 95 % weight polymer (c), α,ω-hydroxyl poly(ε-caprolactone)-silica sol-gel 80 % weight polymer (d), α,ω-hydroxyl poly(L-lactic acid)-silica sol-gel 95 % weight polymer (e), α,ω-hydroxyl poly(L-lactic acid)-silica sol-gel 80 % weight polymer (f).

4.2. *In vitro* Apatite-Forming Ability of α,ω-Hydroxyl Poly(α-hydroxyacid)-Silica Sol-Gel Statistical Design Experiments

4.2.1. α,ω-Hydroxyl Poly(ε-caprolactone)-Silica Sol-Gel Statistical Experiments

Only selected compositions used for the statistical experiments with α,ω-hydroxyl poly(ε-caprolactone)-silica sol-gel materials were tested for their *in vitro* apatite-forming ability. The selection of the materials was done bearing in mind the results of the statistical study (Chapter 3). The THF/TEOS, EtOH/TEOS and H_2O/TEOS molar ratios were kept constant at, respectively, 8, 8 and 8 because their variation did not modify significantly the α,ω-hydroxyl poly(ε-caprolactone) crystallinity and therefore the confinement of the polyester in the silica composites. A centre point was also used in the static biomimetic process. Table 4.1 lists the samples used together with the values of the molar ratios of TEOS/PCL and HCl/TEOS.

Table 4.1: TEOS/PCL, HCl/TEOS, H_2O/TEOS molar ratios of materials tested in SBP, Ca/P molar ratio calculated from EDX analysis (mean of 5 measures) on materials soaked for 15 days and values of the poly(ε-caprolactone) crystallinity measured by XRD and DSC.

Sample	Std Oder	TEOS/ PCL	HCl/ TEOS	Ca/P SEM	Ca/P EDX	Crystallinity XRD	Crystallinity DSC
A	**32**	19.35	0.1	yes	2.17 ±0.60	0.014	0.000
B	**16**	19.35	0.025	traces	1.76 ±1.00	0.358	0.438
C	**31**	3.226	0.1	no	-	0.309	0.502
D	**15**	3.226	0.025	no	-	0.533	0.559
E	**36**	11.288	0.0625	no	-	0.374	0.180

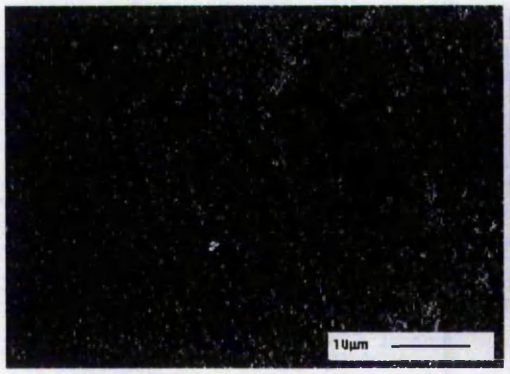

A

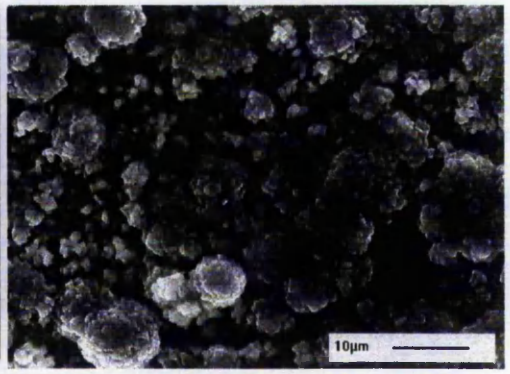

A-15days in SBF

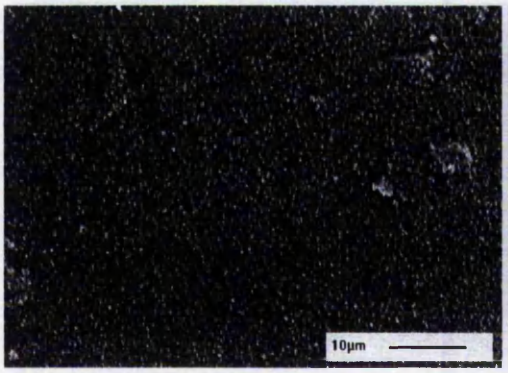

B

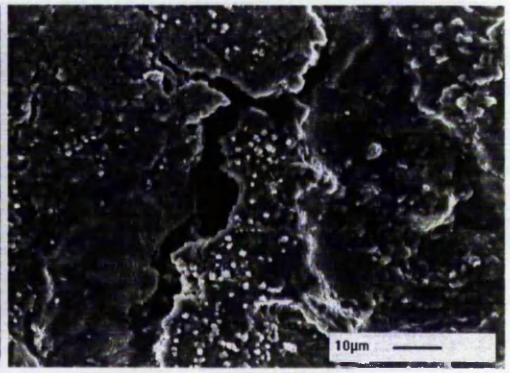

B-15days in SBF

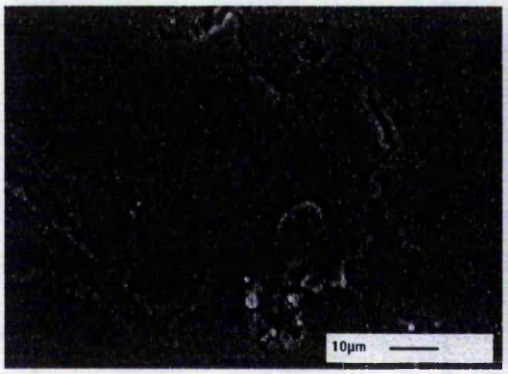

C

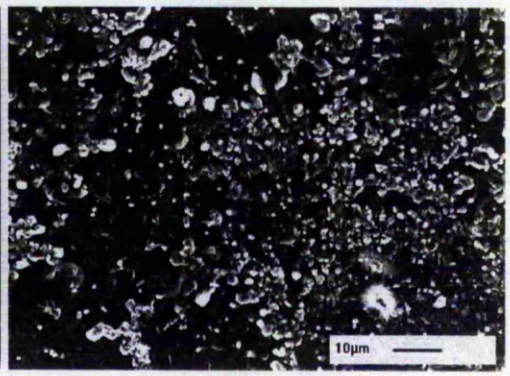

C-15days SBF

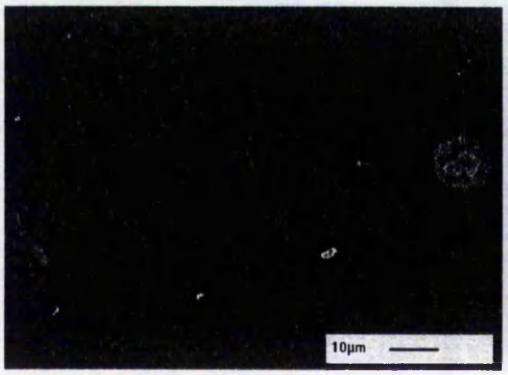

D

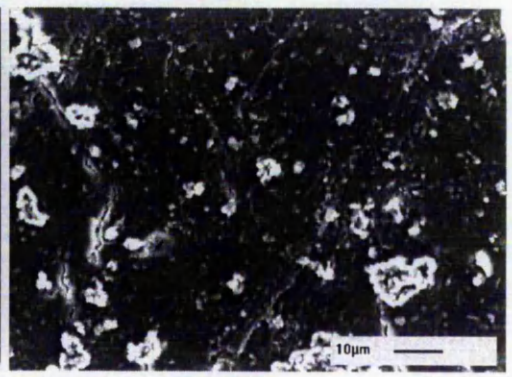

D-15days SBF

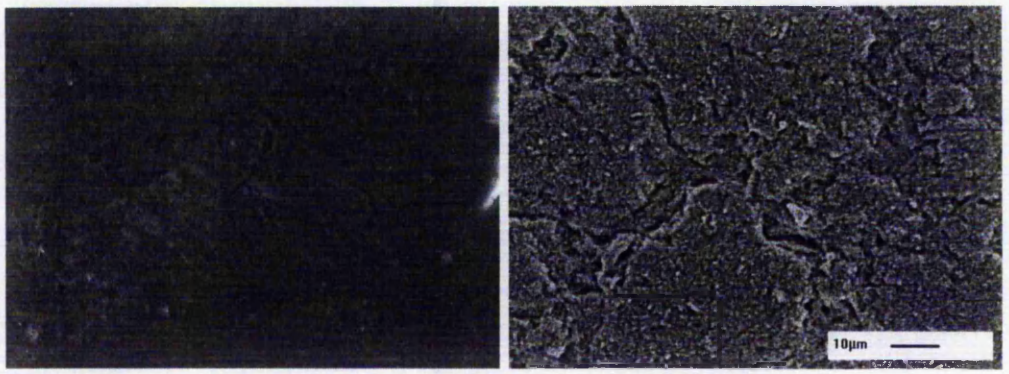

E E-15days SBF

Figure 4.2 : SEM micrographs of the α,ω-hydroxyl poly(ε-caprolactone)-silica sol-gel materials in SBF solution before and after 15 days in SBF for samples A, B, C, D and E (Refer to Table 4.1 for the composition of material samples A to E). For example, the micrograph A shows the surface of the α,ω-hydroxyl poly(ε-caprolactone)-silica sol-gel disk, before, it was tested for its apatite-forming ability. The micrograph A-15days SBF shows the surface of the same disk, after it was tested by soaking in a simulated body fluid (SBF) for 15 days at 37 °C.

The SEM micrographs, Figure 4.2 and EDX microanalysis data, Table 4.1 show that the precipitation of calcium phosphate materials occurred on the surface of α,ω-hydroxyl poly(ε-caprolactone)-silica sol-gel composite materials with a TEOS/PCL molar ratio of 19.35 (samples A and B), and that calcium phosphate precipitate was not observed on samples C, D and E with lower TEOS/PCL molar ratio (3.226 and 11.288). The precipitation of calcium phosphate material was much more significant on the sample with the HCl/TEOS molar ratio equal to 0.1 (sample A) than for the sample with HCl/TEOS molar ratio of 0.025 (sample B). It must be noticed as well that the samples A and B had a degraded aspect after 15 days in simulated body fluid and that the degradation was particularly important for the sample B. EDX and SEM analysis showed the presence of chloride, most likely calcium chloride, in high concentration on the materials, especially for samples C and D. The washing in deionised water of the materials was probably too short to remove all soluble salts and this may be the reason for the large variation of the calcium to phosphorus ratios measured by EDX analysis, Table 4.1. However, the calcium to phosphorus ratio calculated from microanalysis was equal to 2.17 ± 0.60 and 1.76 ± 1.00 for the samples A and B, close to the ratio of hydroxyapatite materials 1.67[2].

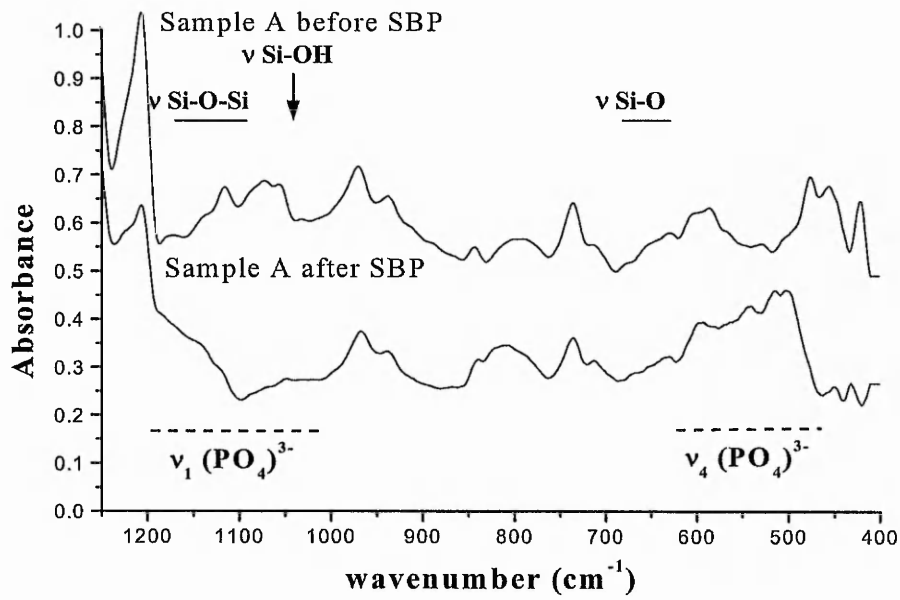

Figure 4.3 : DRIFT spectra of sample A before and after *in vitro* apatite–forming ability test (SBP) from 1250 cm^{-1} to 400 cm^{-1}.

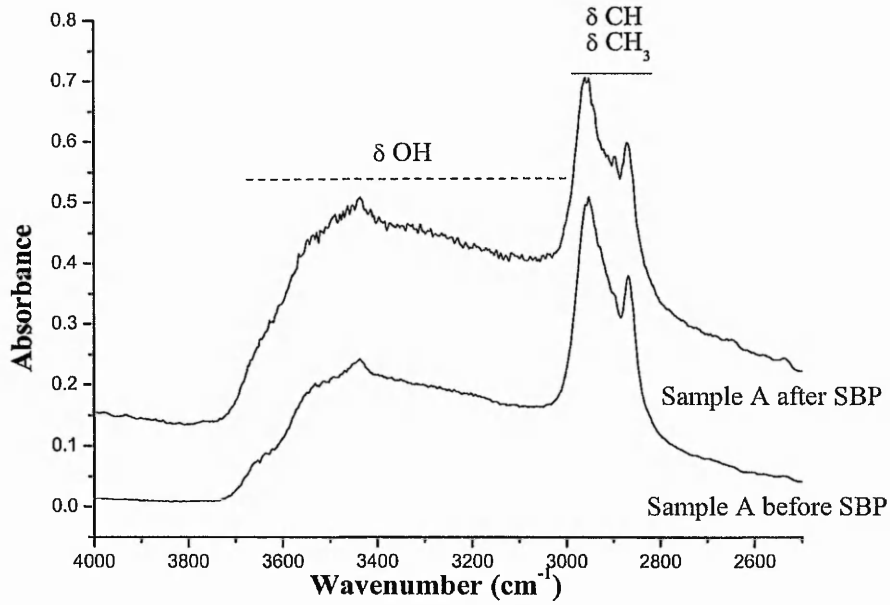

Figure 4.4 : DRIFT spectra of sample A before and after *in vitro* apatite–forming ability test (SBP) from 4000 cm^{-1} to 2550 cm^{-1}.

Figure 4.3 shows an expansion of the DRIFT spectra between 1250 cm^{-1} to 400 cm^{-1} of sample A before and after the *in vitro* apatite-forming ability test. By comparing the spectrum of sample A, new broad signals appeared at 500 cm^{-1}, 550 cm^{-1} and 600 cm^{-1}. These peaks were related to the asymmetric bending of phosphate (ν_4 PO_4^{3-}) in calcium phosphate materials[3], Table 4.3. The frequency region around 1200 cm^{-1} to 1000 cm^{-1} was also to be modified by the SBP test. The peaks attributed to Si-O-Si stretching[4] at 1100-1000 cm^{-1} had disappeared and two broad shoulders appeared around 1150 cm^{-1} and 1050 cm^{-1}. These new signals were possibly attributed to the asymmetric stretching of phosphate in calcium phosphate materials (ν_3 PO_4^{3-}). At 980 cm^{-1} in the sample A spectra a broad large peak attributed to the stretching vibration of silanol at the surface of the sol-gel (ν Si-OH) was observed[4, 5]. The shift of the band at 830 cm^{-1} after the SBP treatment was attributed to the vibrational asymmetric bending of carbonate (ν_2 CO_3^{2-}) which gives a signal at around 870 cm^{-1}. The corresponding asymmetric stretching (ν_3 CO_3^{2-}) bands positioned at around 1455 cm^{-1} and 1425 cm^{-1} were not observed because of the overlap with the strong signals of the polyester.

Finally, in the spectrum of the sample A after SBP treatment, Figure 4.3, the observation of a very weak shoulder at 960 cm^{-1} may indicate the formation of hydroxyapatite material which presents a very specific IR band at around 960 cm^{-1} due to the phosphate symmetric stretch (ν_1 PO_4^{3-})[6].

The region of the hydroxyl stretching vibration at 3800 cm^{-1} to 3200 cm^{-1}, Figure 4.4 presented several overlapped peaks; a broad band centred at 3550 cm^{-1} and two weak sharp signals at 3440 cm^{-1} attributed to hydroxyl groups on the poly(ε-caprolactone) and water absorbed[7]. A weak band at 3770 cm^{-1} was also observed for the poly(ε-caprolactone) studied that has not been reported by others. The poly(ε-caprolactone)-silica materials DRIFT spectra showed an additional shoulder at around 3600 cm^{-1} that was attributed to the hydrogen bonded silanols[4]. Because of the broadness of the silanol hydroxyl stretching band, the hydroxyl stretching band in hydroxyapatite which appears at 3571 cm^{-1} was not observed on the surface of sample A.

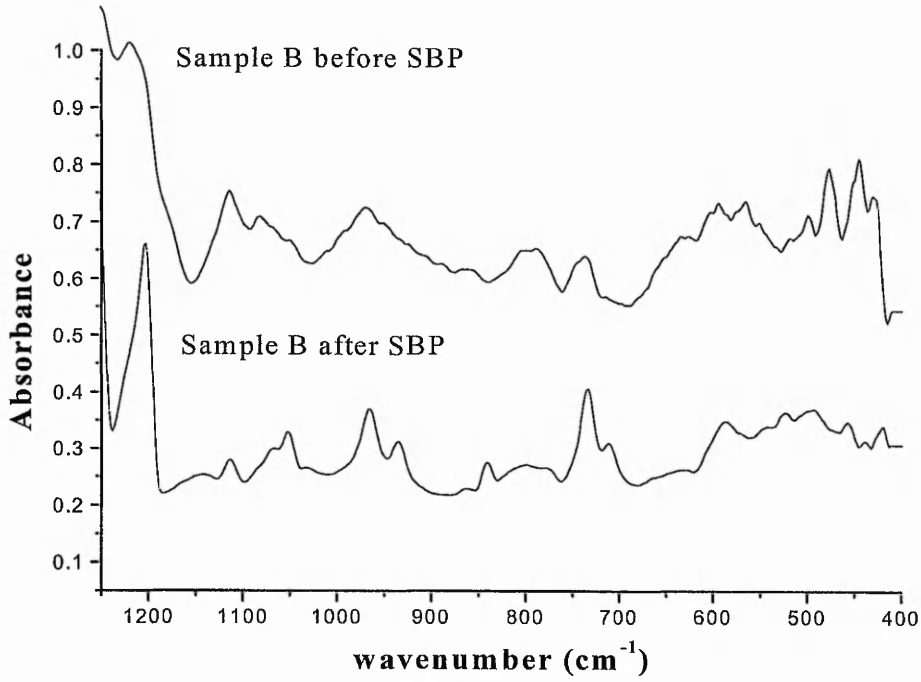

Figure 4.5 : DRIFT spectra of samples B before and after SBP test.

The DRIFT spectra of the sample B, Figure 4.5 did not show clearly that hydroxyapatite precipitated on the prepared composites However the weak broad signals at 1100 cm^{-1} to 1000 cm^{-1} and 500 cm^{-1} attributed to phosphate stretching vibrations suggested the presence of calcium phosphate materials on the surface of the composites but in a smaller quantity than for sample A. Finally the DRIFT spectra of the samples C, D and E did not present any additional peaks after the *in vitro* apatite forming-ability tests as shown for the sample D, Figure 4.6.

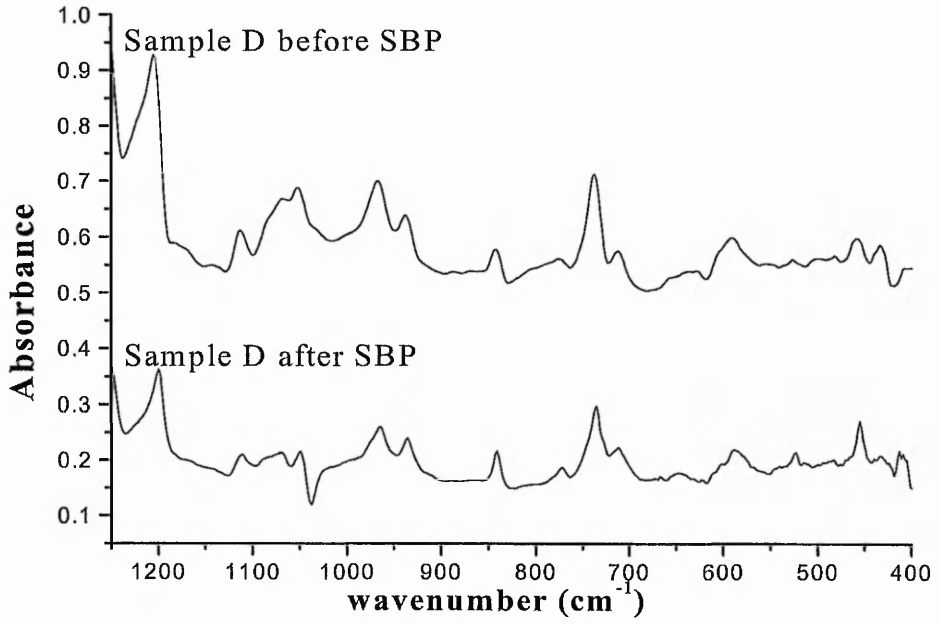

Figure 4.6 : DRIFT spectra of samples D before and after (SBP test).

It must be noticed that for the sample D, the DRIFT spectra, Figure 4.6 indicated that the release of silica in simulated body fluid during the static biomimetic process was probably important because the vibrational band of silanol groups at the surface of the silica sol-gel[4] at 780 cm^{-1} decreased as well as the vibrational Si-O-Si stretching broad band at 1050 cm^{-1}.

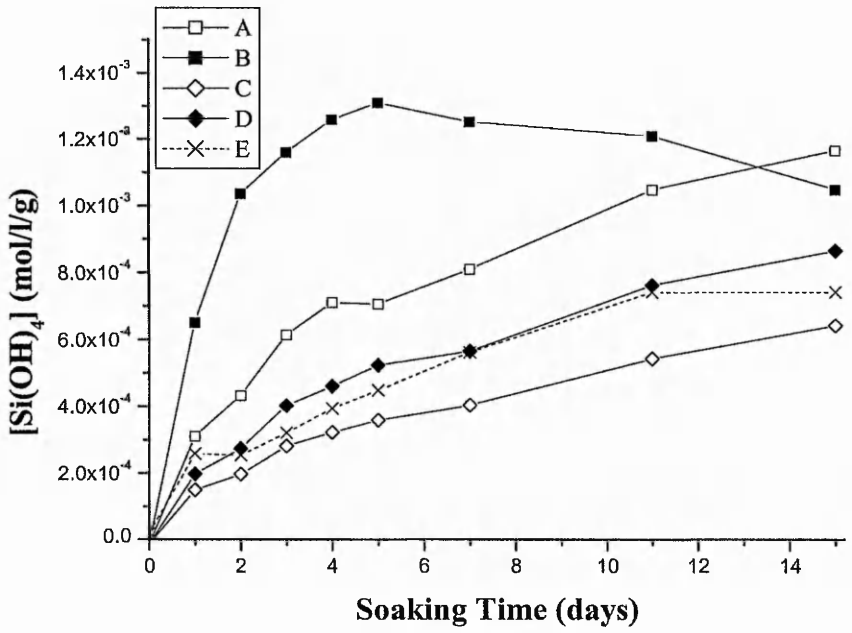

Figure 4.7 : Plot of the concentration of the silicic acid released from the α,ω-hydroxyl poly(ε-caprolactone)-silica sol-gel materials in SBF solution as a function of the soaking time (days), A; , B; , C; ◊, D; , E × (Refer to Table 4.1 for the composition of samples A to E).

In figure 4.7, the release of silicic acid in the SBF is plotted as a function of the soaking time for the five samples. Samples C and D with a TEOS/PCL molar ratio of 3.226 showed a slower release of silicic acid than samples A and B with TEOS/PCL molar ratio of 19.35. The composite materials (samples A and C) with HCl/TEOS molar ratio equal to 0.1 had a slower silicic acid release than the composites (samples B and D) with an HCl/TEOS molar ratio 0.025, respectively in relation to the value of the TEOS/PCL molar ratio. The centre point E (TEOS/PCL, HCl/TEOS molar ratios equal to 11.288 and 0.0625) has a faster release of silicic acid than sample C with TEOS/PCL, HCl/TEOS molar ratios of 3.226, 0.1 respectively and a release similar to sample D with TEOS/PCL, HCl/TEOS molar ratios equal to 3.226 and 0.025.

The results above showed that a minimum amount of silica in the sample was necessary to observe *in vitro* apatite-forming ability on the surface of the α,ω-hydroxyl poly(ε-caprolactone)-silica sol-gel composites. Below a TEOS/PCL molar ratio of

19.35, equivalent to 70 % weight content poly(ε-caprolactone) or 30 % weight of silica, calcium phosphate material did not precipitate on the materials under the condition of the test. For the composites with a TEOS/PCL molar ratio equal to 19.35, it was observed that calcium phosphate materials precipitated on their surface but in larger quantity on the composite prepared with HCl/TEOS molar ratio equal to 0.1 (sample A) than on the composite with HCl/TEOS molar ratio equal to 0.025 (sample B) as shown by SEM and DRIFT analyses. The precipitation of calcium phosphate material observed on the α,ω-hydroxyl poly(ε-caprolactone)-silica sol-gel composites with 70 % weight content polyester were similar to the apatite-forming ability of triethoxysilane terminated poly(ε-caprolactone)-silica sol-gel composite with 60 % weight of polyester immersed in a simulated body fluid for 7 days at 36.5 °C as reported by S. H. Ree and H. M. Kim[8]. Also, our study provided the following new results. For composites with TEOS/PCL molar ratio equal to 3.226 and 11.288, corresponding to 95 and 82.5 percent weight of poly(ε-caprolactone), calcium phosphate precipitation on the surface of the poly(ε-caprolactone)-silica sol-gel after 15 days of soaking in simulated body fluid at 37°C was not observed. Another interesting observation was that the content of the hydrochloric acid catalyst used to make the sol-gel affected the quantity of calcium phosphate precipitate on the surface of the composite. In comparison, in previous studies, the apatite-forming ability of poly(dimethylsiloxane)-silica sol-gel composite containing calcium with a silica charge of 40 % in SBF was observed after 3 days using an identical sol-gel method[9]. The authors observed that increasing the amount of hydrochloric acid in the sol-gel preparation enhanced the apatite formation as observed for the sample A. Their explanation for this behaviour was a higher release of calcium ion from the PDMS-SiO_2-CaO hybrid sol-gel due to better incorporation of calcium in the silica phase. For the present study, the release of calcium ions from the composite was obviously not a possible reason. Other workers also suggested that the increase of catalyst concentration also increased the porosity and pore size[10] and modified the rate of hydrolysis and condensation of the silicon alkoxide[11] and consequently the number of silanols in the silica gel. Therefore, the pore size of the composite materials may have played a role in the apatite-forming ability[12] of the α,ω-hydroxyl poly(ε-caprolactone)-silica sol-gel composites. Finally, the release of the silicic acid measured for the

samples in the simulated body fluid during the SBF indicated that its involvement in the mechanism of calcium phosphate precipitation was unlikely as although J. J. M. Damen and J. M. Ten Cate had reported that silicic acid stimulated the precipitation of hydroxyapatite at concentrations as low as 0.05 mmol/l[13]. The results presented in Figure 4.6, show that at the end of the SBP test, the silicic acid concentrations were equal to 1.15 and 1.00 mmol/l for samples A and B, and respectively 0.57, 0.65 and 0.70 mmol/l for samples C, D and E, with only sample A precipitating a significant amount calcium phosphate material.

4.2.2. α,ω-Hydroxyl Poly(L-lactic acid)-Silica Sol-Gel Statistical Experiments

Only selected compositions of the α,ω-hydroxyl poly(L-lactic acid)-silica sol-gel materials were submitted to *in vitro* apatite-forming ability tests (SBP). The toluene/PLLA molar ratio was kept constant at 300. In Table 4.2, the samples subjected to static biomimetic process and the values of the TEOS/PLLA, EtOH/TEOS, H_2O/TEOS and HCl/TEOS molar ratios are listed. Because the statistical matrix used was fractional, experiments with only one variation at a time, with high and low limits were not run. Consequently, for the composition of the materials submitted for the *in vitro* apatite-forming ability, there were always two modified variables. The EtOH/TEOS molar ratio, which had no effect on the crystallinity of the poly(L-lactic acid) in the silica sol-gel as found by the statistical study, was always selected and the second variable was either the TEOS/PLLA, H_2O/TEOS or HCl/TEOS molar ratios. A centre point was also subject to the static biomimetic process.

Table 4.2: TEOS/PLLA, EtOH/TEOS, H_2O/TEOS and HCl/TEOS molar ratios of materials tested in SBP, Ca/P ratio calculated from EDX analysis on materials soaked for 15 days and values of the poly(ε-caprolactone) crystallinity measured by XRD and DSC.

Sample	Std Order	TEOS/ PLLA	EtOH/ TEOS	H_2O/ TEOS	HCl/ TEOS	Ca/P SEM-EDX	Cr Exp. XRD	DSC
F	**16**	19.35	8	8	0.1	traces	0.674	0.212
G	**14**	19.35	4	8	0.025	no	0.000	0.000
H	**6**	19.35	4	4	0.1	no	0.490	0.286
I	**8**	19.35	8	4	0.025	no	0.813	1.000
J	**13**	3.226	4	8	0.1	no	0.946	0.587
K	**17**	11.288	6	6	0.0625	traces	0.493	0.488

The α,ω-hydroxyl poly(L-lactic acid)-silica sol-gel composites were subjected to the *in vitro* apatite-forming ability test and analysed by SEM and DRIFT analysis. The concentration of silicic acid in the simulated body fluid was measured during the experiment.

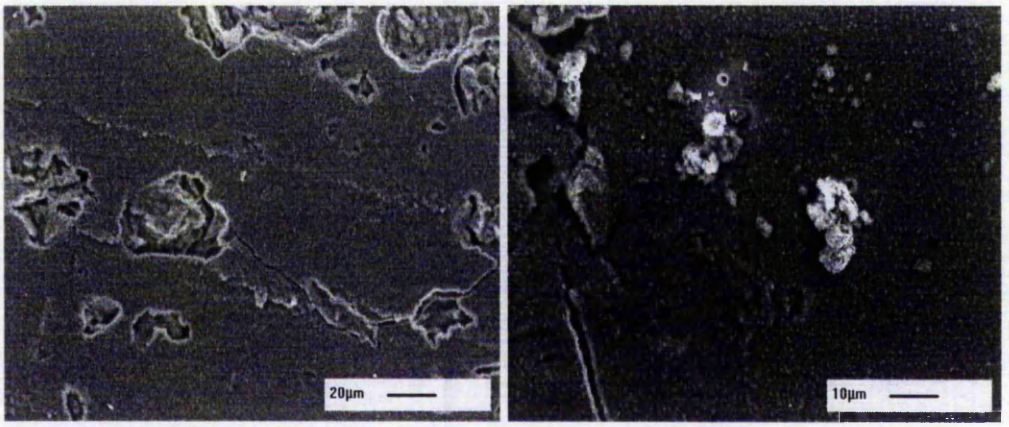

F after 15 days of soaking in simulated body fluid following the SBP treatment

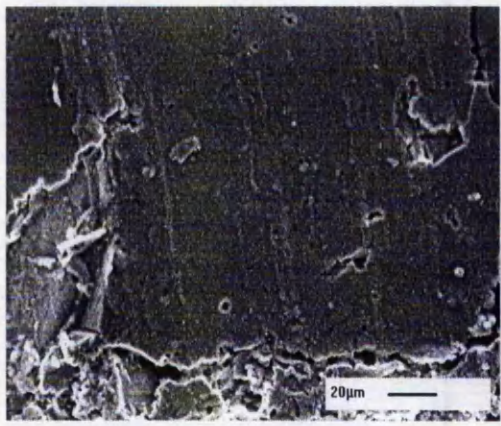

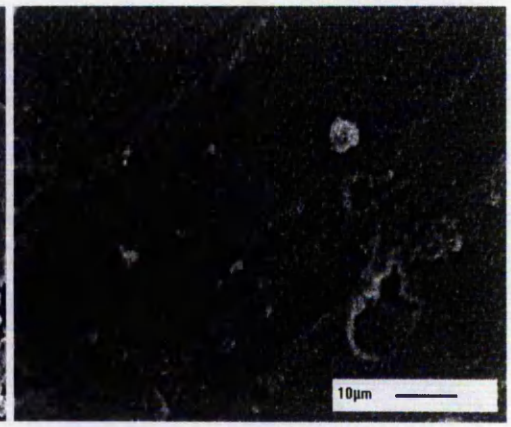

G after 15 days of soaking in simulated body fluid following the SBP treatment

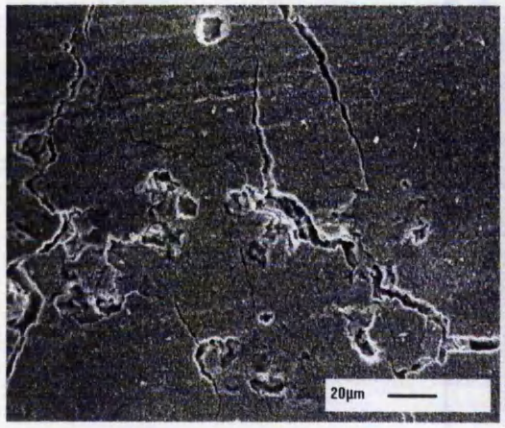

H after 15 days SBP treatment

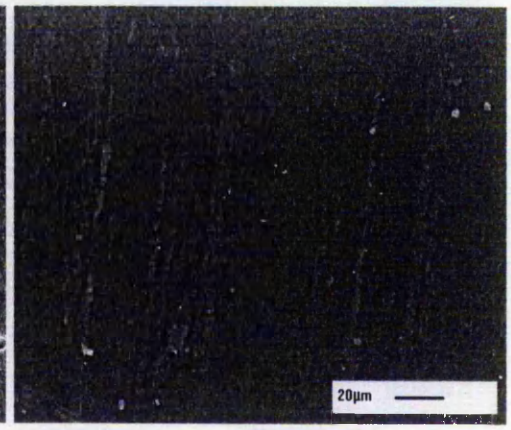

I after 15 days SBP treatment

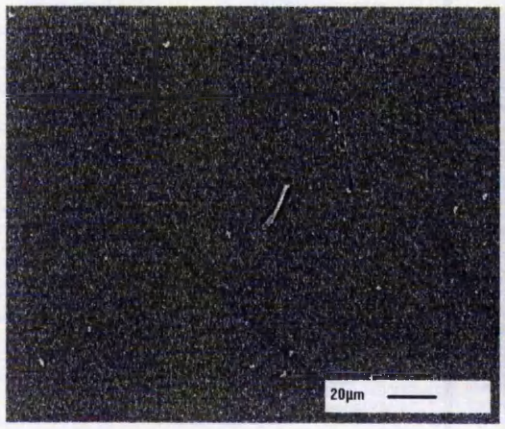

J after 15 days of SBP treatment

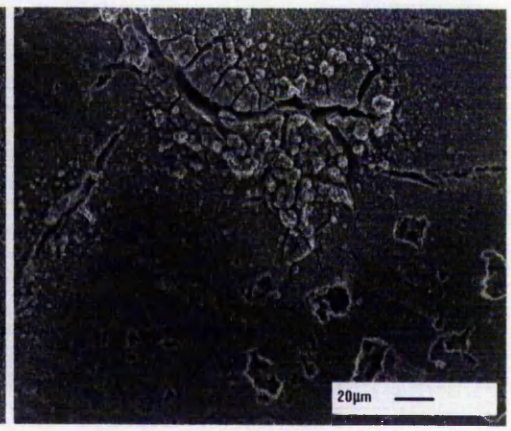

K after 15 days of SBP treatment

Figure 4.8 : SEM photos of the α,ω-hydroxyl poly(L-lactic acid)-silica sol-gel materials after 15 days in static biomimetic process for samples F, G, H, I, J and K (refer to Table 4.2 for the composition of samples F to K).

The SEM analysis of the α,ω-hydroxyl poly(L-lactic acid)-silica sol-gel composite, Figure 4.8, showed little or no precipitation of calcium phosphate materials on the surface of all the samples studied. Only a few rounded precipitate particles of few micrometers were observed on the surface of the sample F, G and K.

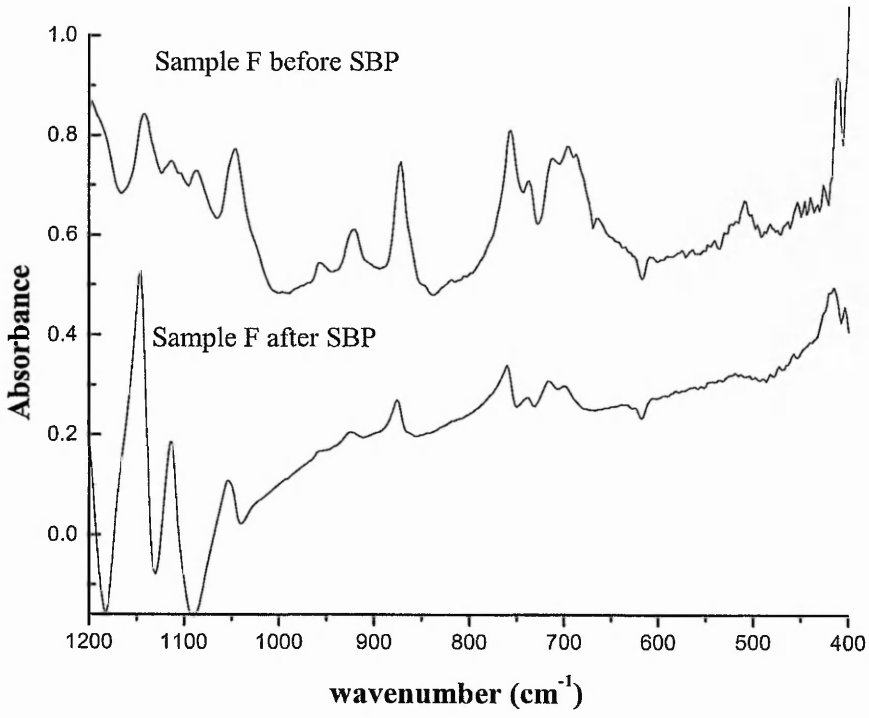

Figure 4.9 : DRIFT spectra of samples F before and after *in vitro* apatite–forming ability test (SBP).

The DRIFT analysis confirmed the microscopy analysis, Figure 4.9. The characteristic vibration bands for the calcium phosphate materials; ν_3 PO_4^{3-} 1190-976 cm^{-1}, ν_4 PO_4^{3-} 660-520 cm^{-1} were not observed in the sample F and on the other composites (results not presented). Figure 4.10 showed the concentration of silicic acid in the simulated body fluid during the *in vitro* apatite-forming ability tests (SBP) for the samples studied.

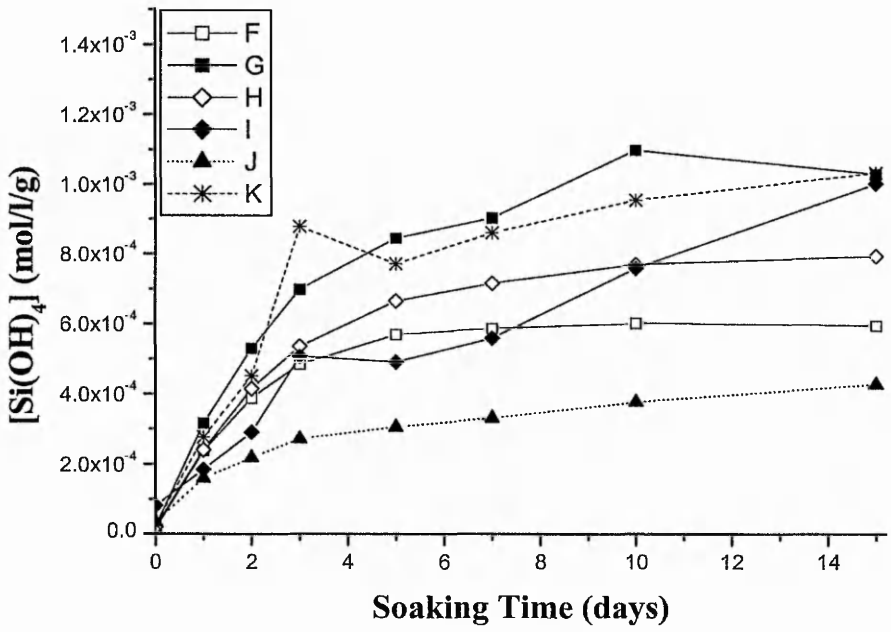

Figure 4.10 : Plot of the concentration of silicic acid released from the α,ω-hydroxyl poly(L-lactic acid)-silica sol-gel materials in SBF solution as a function of the soaking time (days), F; , G; , H; ◊, I; , J; and K; * (refer to Table 4.2 for the composition of the samples F to K).

Figure 4.10 shows the release of silicic acid in simulated body fluid from the α,ω-hydroxyl poly(L-lactic acid)-silica sol-gel studied, samples F to K, as a function of the soaking time in simulated body fluid similarly to the α,ω-hydroxyl poly(ε-caprolactone)-silica sol-gels study, Figure 4.7. Interestingly, as for the α,ω-hydroxyl poly(ε-caprolactone)-silica sol-gels, the α,ω-hydroxyl poly(L-lactic acid)-silica sol-gel, sample F, with a HCl/TEOS molar ratio of 0.1 had a slower release of silicic acid than the sample G with a HCl/TEOS molar ratio of 0.025. It was is accordance with the observation for the poly(ε-caprolactone) composites, samples A and B that increasing the catalyst content increased the formation of the silica gel and slowed down the release of silicic acid. The Figure 4.10 showed that increasing the H_2O/TEOS molar ratio from 4 to 8, decreased the silicic acid released, samples F and H. This was in agreement with the idea of a better formed silica gel degraded more slowly than poorly formed silica gel. The silicic acid concentrations at the end of the SBP treatment were

respectively 0.58, 1.0, 0.77, 0.95, 0.33 and 1.0 mM per litre of simulated body fluid and per gram of material for samples F, G, H, I, J and K.

The results above established that the α,ω-hydroxyl poly(L-lactic acid)-silica sol-gel composites prepared did not form apatite on their surface after 15 days of soaking in simulated body fluid. The small amount of calcium phosphate precipitate observed at some of the compositions may indicate that *in vitro* apatite-forming ability existed but that the soaking time was not long enough to form a full layer of calcium phosphate materials.

4.2.3. Discussion

Compared to the α,ω-hydroxyl poly(ε-caprolactone)-silica sol-gel materials studied, the α,ω-hydroxyl poly(L-lactic acid)-silica sol-gels with identical amount of silica did not exhibit apatite-forming ability under the same experimental conditions. The reasons for such a difference are not straightforward. The kinetics of *in vitro* apatite deposition on bioactive materials such as silica gel is dependent on the inorganic ion composition of simulated body fluid[14]. The simulated body fluid used was prepared following the Kokubo recipe[15] because of the reported better reproducibility of the *in vivo* behaviour of the materials in *in vitro* experiments and to avoid the possible effect of the SBF preparation, the same batch of simulated body fluid was used for both polyester-silica sol-gel composites. Therefore, the type of polyester (poly(ε-caprolactone) and poly(L-lactic acid)) and the structure of the composites were probably the cause for the variation of *in vitro* apatite forming ability.

The comparison of the silicic acid released, Figures 4.7 and 4.10, showed that quantitatively the diffusion of silicic acid from the composites were comparable after 15 days in the simulated body. This was a strong indication that the build up of silicic acid concentration in simulated body fluid did not have a major influence on the calcium phosphate precipitation on the surface of the composites in the SBP tests. It is important to notice that the molybdenum blue assay measured only the concentration of silicic acid and small silica oligomeric species (dimers and trimers) released in simulated body fluid. Higher silica oligomers were not measured. Or it is very likely that such species are also involved in the formation of a silica gel layer necessary for the nucleation and growth of apatite layer[16]. The measure of the total concentration of silica

species released in simulated body fluid by inductively coupled plasma (ICP) analysis may allow an improvement in the understanding of the mechanisms of the *in vitro* apatite-forming ability of the poly(α-hydroxyacid)-silica sol-gels.

Table 4.3 : Position of bands (cm^{-1}) of the deconvoluted spectra of apatitic and non-apatitic calcium phosphates in the ν_4, ν_3 and ν_1 PO_4^{3-} domain [3, 6].

Brushite DCPD	**OCP**	**β TCP**	**Whitlockite**	**OH apatite**	**CO_3 apatite**
	1190	1174			
	1150	1144	1150		
1133	1138		1138		
1124	1126	1126			
	1108				
		1100			1104
1079	1076	1081	1094	1089	1091
		1071	1078		1072
1058	1055	1057	1060	1063	1059
	1038	1042		1044	1044
			1034	1034	
	1022	1024	1018	1026	1023
1004	1003	997	990		1006
987	962	970	958	964	962
	610.4(w)	612.1(s)	614(sh)		
	600.0(s)	605.3(s)	604.6(s)	601.7(s)	603.1(s)
585.7(w)	591.7(w)	589.4(s)	593.2(m)		
575.5(s)	577.1(m)	578.1(m)			
		570.3(m)	572.6(s)	574.7(m)	
	559.5(s)	556.6(s)	555.8(s)	567.2(sh)	564.6(s)
540(sh)	552(sh)	543.8(s)	543.2(sh)		
527(sh)					
522.5(s)	526(b, w)				

b=broad, sh=shoulder, s= strong, m=medium, w=w

4.3. Comparative Study of the Formation of Hydroxyapatite in Simulated Body Fluid Under a Static System, a Dynamic System and a New Alternate Soaking System

In vitro apatite-forming ability or osteoconductivity tests have been developed in order to provide rapid and cost effective information on the bioactivity of potential materials for biomedical applications. This has been possible because the formation of an apatite-like layer occurs not only inside the body but also *in vitro* when bioactive materials are soaked in an acellular simulated body fluid[17, 18]. Numerous studies of *in vitro* bioactivity property have been carried out on bioactive glasses[19, 20], ceramics[21, 22] and silica sol-gel[23, 24] materials. These studies have revealed that the static immersion of a silica sol-gel in a simulated body fluid leads to the formation of an hydroxyapatite layer[25] and that the release of silicic acid from the silica sol-gel promoted apatite-forming ability[26]. In order to avoid the additional effect of build up of released silicic acid and ions from bioactive materials in simulated body fluids several solutions have been proposed; a periodical change of simulated body fluid[27], the use of buffers[28] and the circulation of the simulated body fluid[29]. The last solution mimics more accurately the *in vivo* conditions. In fact, the blood plasma is circulating throughout the human body and it has been reported that the flow of human blood plasma may have an effect on the formation of hydroxyapatite[30]. Comparative studies of the formation of hydroxyapatite on α-$CaSiO_3$ ceramics[31] and SiO_2-CaO-P_2O_5 sol-gel glasses[32] in simulated body fluid under static and dynamic processes have been reported recently.

To date, only the *in vitro* apatite-forming ability of a poly(ε-caprolactone)-silica sol-gel composite with 60 % weight content of poly(ε-caprolactone), using a static process, has been reported[33]. Therefore, the effects of the *in vitro* apatite-forming ability using static and dynamic tests on the formation of hydroxyapatite on α,ω hydroxyl poly(ε-caprolactone)-silica sol-gel composites with 70 % weight content of polyester have been studied in this section of the work and discussed. An alternate soaking process was also developed as described in the methods chapter. This method allowed the precipitation of apatite materials on silica gel[34] and poly(vinyl alcohol)[35] in a remarkably short time, moreover it allowed the quantification of the rate of calcium phosphate deposition on the material surfaces.

4.3.1. Results of the *in vitro* apatite-forming ability tests

Figures 4.11 , 4.12 show respectively the SEM photos, the DRIFT spectra of the surface of a α,ω-hydroxyl poly(ε-caprolactone)-silica sol-gel composite with 70% weight content of polyester, the concentration of silicic acid released in simulated body fluid (SBF), and the pH of the SBF as a function of the soaking time for the static biomimetic process (see chapter 2 for methods).

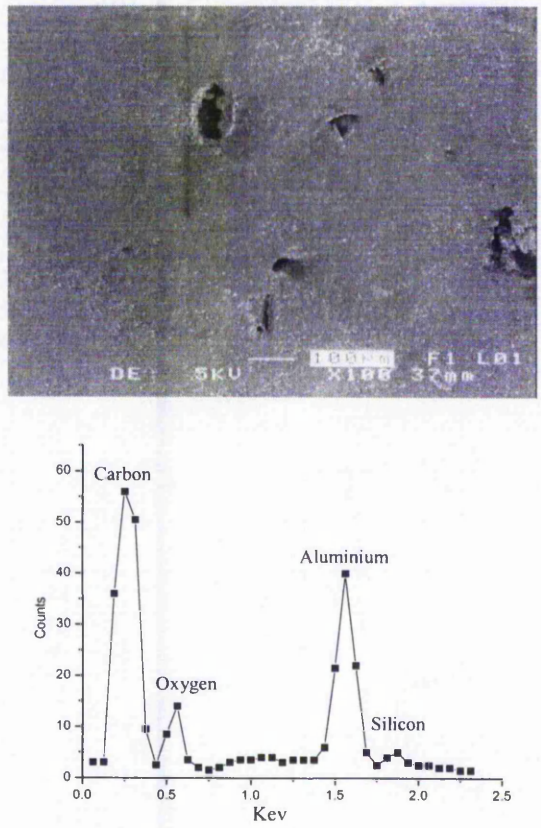

Figure 4.11 : SEM micrograph and EDXA analysis of the α,ω hydroxyl poly(ε-caprolactone)-silica sol-gel 70 % weight content polyester before soaking in simulated body fluid, static biomimetic process.

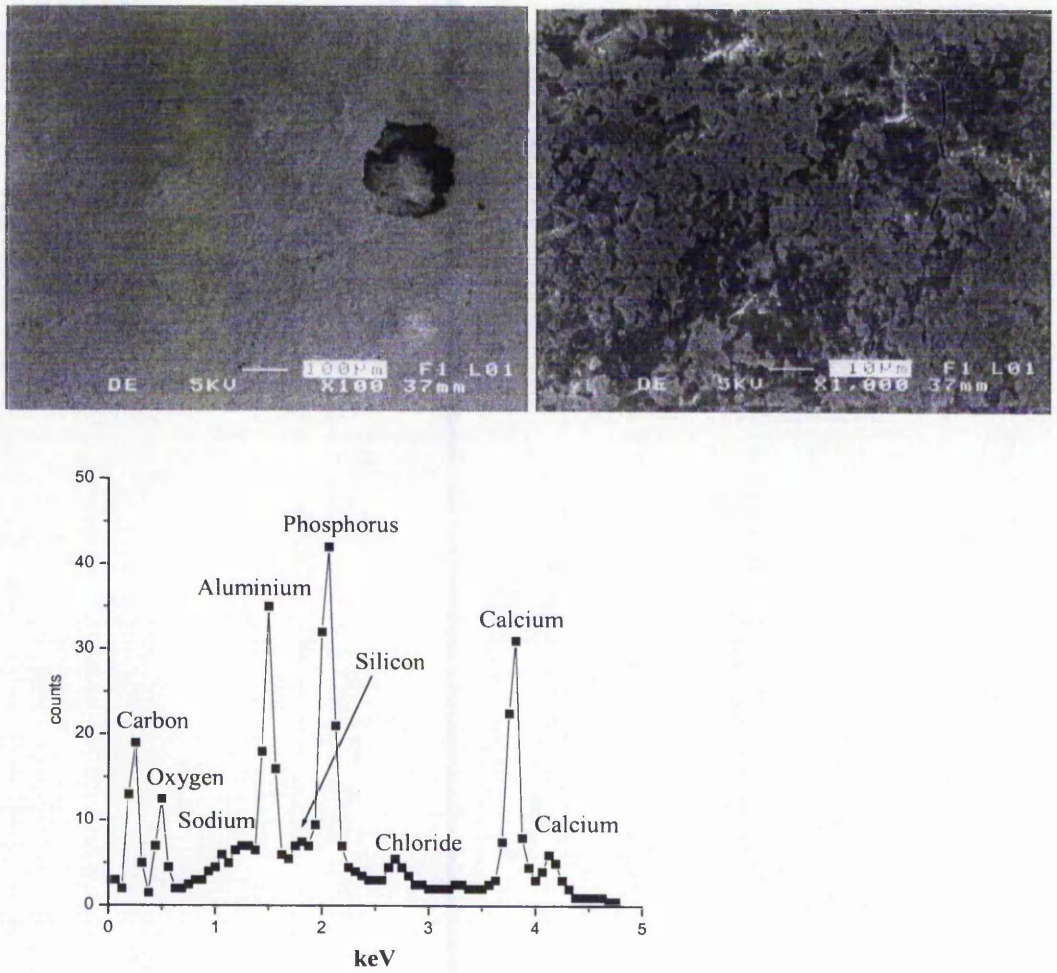

Figure 4. 12 : SEM micrographs and EDXA analysis of the α,ω hydroxyl poly(ε-caprolactone)-silica sol-gel 70 % weight content polyester after 15 days of soaking in SBF (SBP).

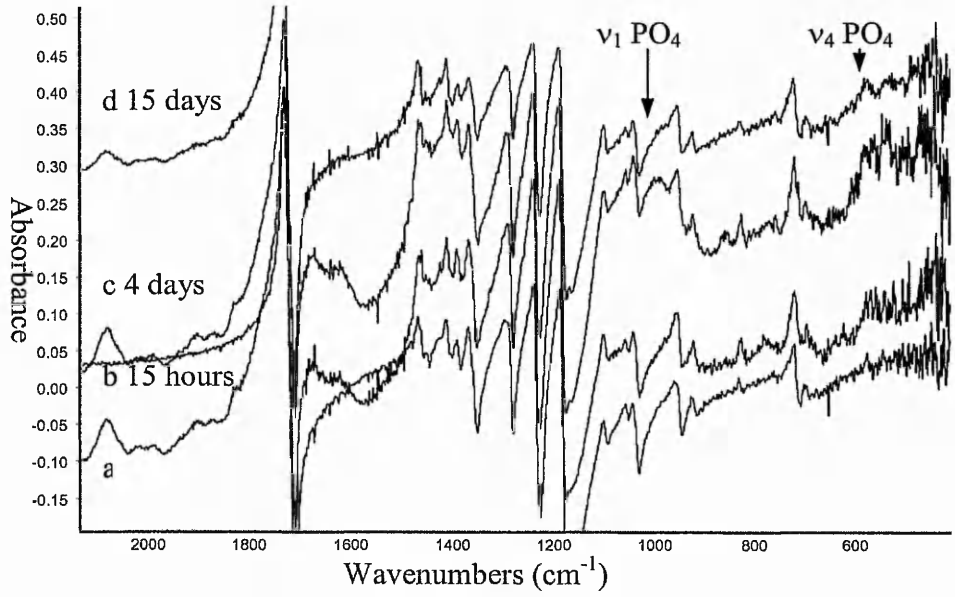

Figure 4.13 : DRIFT spectrum a) α,ω hydroxyl poly(ε-caprolactone), b), c) and d) α,ω hydroxyl poly(ε-caprolactone)-silica sol-gel composite 70 percent weight polyester after respectively 15 hours, 4 days and 15 days in a static biomimetic process.

The SEM photography, Figure 4.12 showed that the precipitation of calcium phosphate materials occurred on the surface of the α,ω-hydroxyl poly(ε-caprolactone)-silica sol-gel composite material with 70 percent weight content of polyester. The EDXA microanalysis Figure 4.12, gave a calcium to phosphorus molar ratio equal to 1.3 ± 0.1 close to hydroxyapatite Ca/P molar ratio, Table 4.4 below.

Table 4.4 : Theoretical calcium to phosphorus molar ratio (Ca/P) for some calcium phosphate compounds[36].

Ca/P ratio	compound		Formula
0.5	Monocalcium phosphate monohydrate	(MCPM)	$Ca(H_2PO_4)_2.H_2O$
0.5	Monocalcium phosphate anhydrous	(MCPA)	$Ca(H_2PO_4)_2$
1	Dicalcium phosphate dihydrate	(DCPD)	$CaHPO_4.2H_2O$
1	Dicalcium phosphate	(DCP)	$CaHPO_4$
1.33	Octacalcium phosphate	(OCP)	$Ca_8H_2(PO_4)_6.5H_2O$
1.5	β-Tricalcium phosphate	(β-TCP)	β-$Ca_3(PO_4)_2$
1.5	α-Tricalcium phosphate	(α-TCP)	α-$Ca_3(PO_4)_2$
1.0-1.5	Amorphous calcium phosphate	(ACP)	$Ca_{9-x}H_{2x}(PO_4)_6.nH_2O$
1.4-1.6	Calcium-deficient hydroxyapatite	(CDHA)	$Ca_{10-x}H_x(PO_4)_6.(OH)_{2-x}$
1.67	Hydroxyapatite	(HAP)	$Ca_5(PO_4)_3(OH)$
2.0	Tetracalcium phosphate	(TTCP)	$Ca_4(PO_4)_2O$

The DRIFT spectrum of the composite, Figure 4.13, had new vibration bands appearing after 4 days of soaking in a simulated body fluid. From 650 cm^{-1} to 500 cm^{-1} the signals were attributed to ν_4 PO_4^{3-} and from 1050 cm^{-1} to 950 cm^{-1} to ν_1 PO_4^{3-}. This confirmed the precipitation of calcium phosphate materials observed by SEM and the broadness of the signals probably indicated the relatively amorphous state of the forming apatite layer.

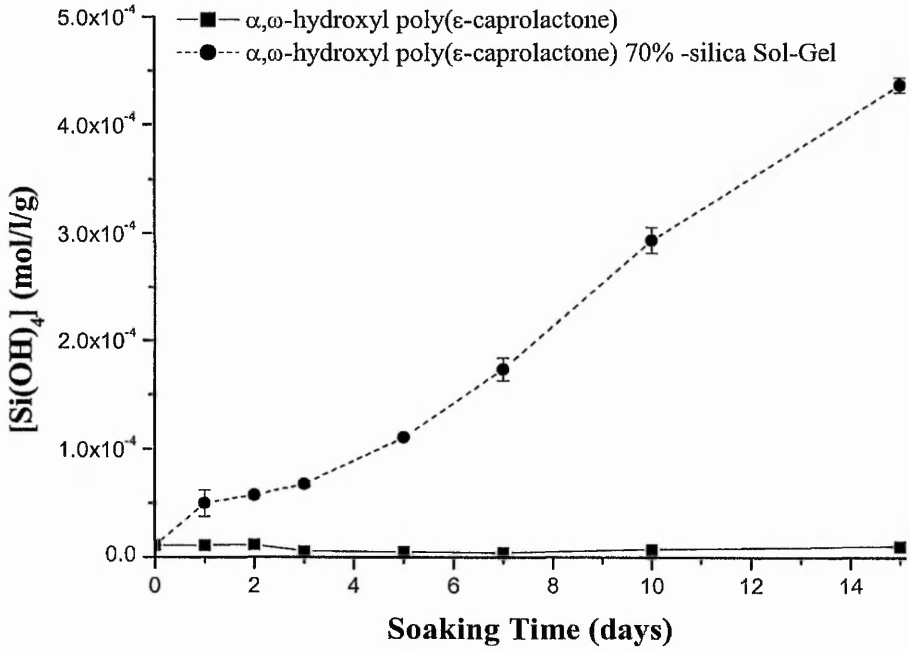

Figure 4.14 : Plot of the concentration of silicic acid release in simulated body fluid as a function of soaking time in the static biomimetic process.

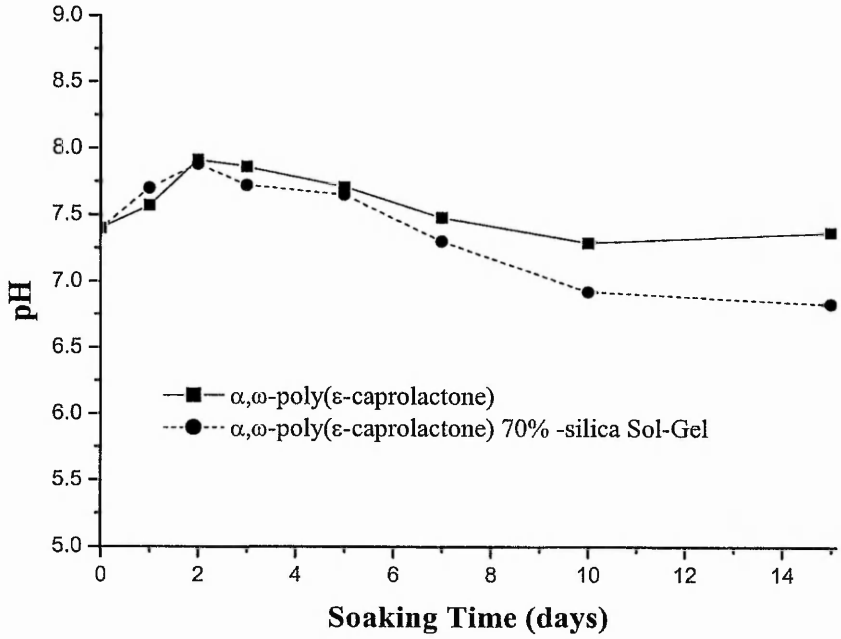

Figure 4.15 : Plot of the pH of the simulated body fluid as a function of the soaking time in the static biomimetic process.

During the static biomimetic process, pH measurement and sampling were carried out to measure the pH and the concentration of silicic acid released in the simulated body fluid. Figure 4.14 shows clearly the release of silicic acid in SBF as a function of the soaking time, indicating the rapid degradation of the silica gel in the composite and diffusion of silicic acid to the solution medium. The SBF pH during the static process for the α,ω-hydroxyl poly(ε-caprolactone) and the α,ω-hydroxyl poly(ε-caprolactone)-silica sol-gel composite with 70 percent weight content of polyester are presented in Figure 4.15. They were very similar. A slight increase of pH was observed for both *in vitro* tests during the two first days up to 7.9, then a slower decrease to the end of the tests. Also, the final pH for the sol-gel composite was equal to 6.90 and for the polyester reference material 7.45. The lower pH observed for the sol-gel composite could be due to the build up of the silicic acid in the simulated body fluid solution even if the medium was buffered.

Figures 4.16, 4.17 show respectively the SEM photos, the DRIFT spectra of α,ω hydroxyl poly(ε-caprolactone)-silica sol-gel 70 percent weight content polyester tested using the dynamic biomimetic process (DBP) described in the methods chapter (2).

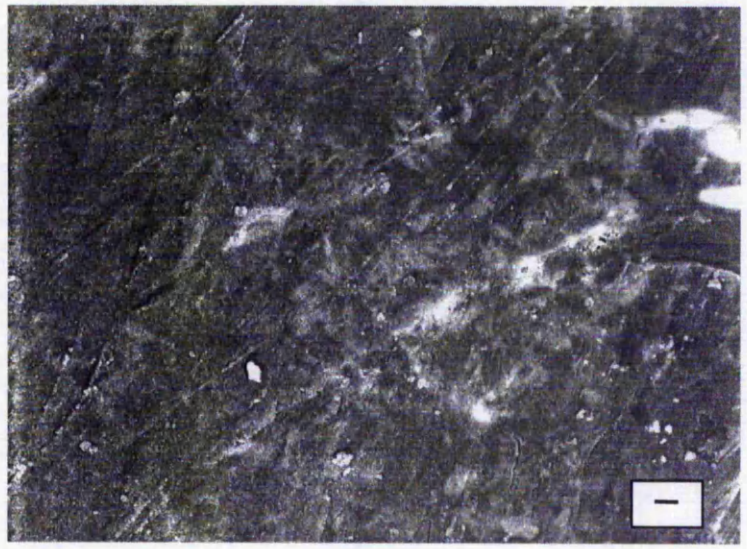

Figure 4. 16: SEM micrograph of the α,ω-hydroxyl poly(ε-caprolactone) 70 %-silica sol-gel composite before DBP test (Bar scale equal to 10 μm).

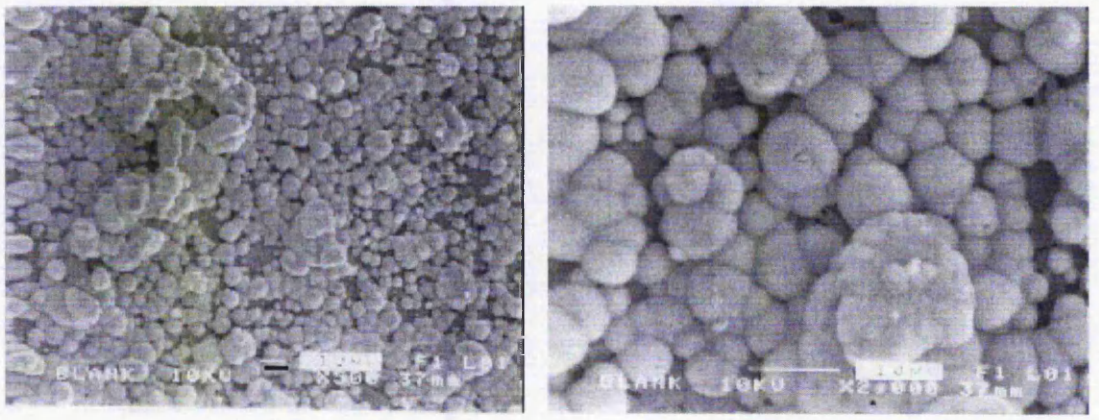

Figure 4. 17: SEM micrographs of the α,ω-hydroxyl poly(ε-caprolactone) 70 %-silica sol-gel composite after 15 days of DBP test. (Bar scale 10 μm)

The SEM micrographs, Figures 4.16 and 4.17 showed precipitate on the surface of the composites after 15 days of soaking in simulated body fluid during the dynamic biomimetic process. EDXA analysis detected a calcium to phosphorus molar ratio equal to 1.60 ± 0.12, indicating the probable formation of a hydroxyapatite (Table 4.4) rich layer on the surface of the polyester-silica sol-gel composite.

For comparison, the alternate soaking process was also carried out on α,ω-hydroxyl poly(ε-caprolactone) 70%-silica sol-gel composite. Figures 4.18 and 4.19 showed respectively the SEM and TEM micrographs of the material surfaces and the amount of calcium precipitate on the α,ω-hydroxyl poly(ε-caprolactone)-silica sol-gel 70 percent weight content polyester tested using the alternate soaking process (ASP) described in the chapter 2.

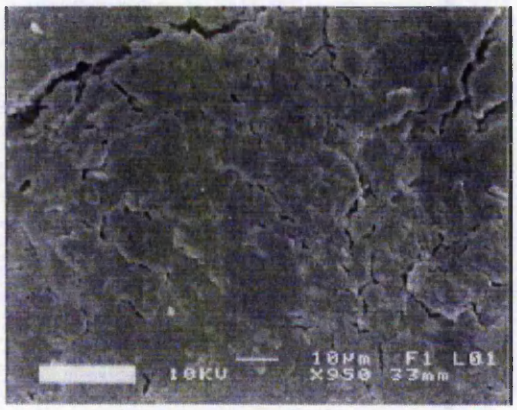

a) PCL 70%-Silica Sol-Gel

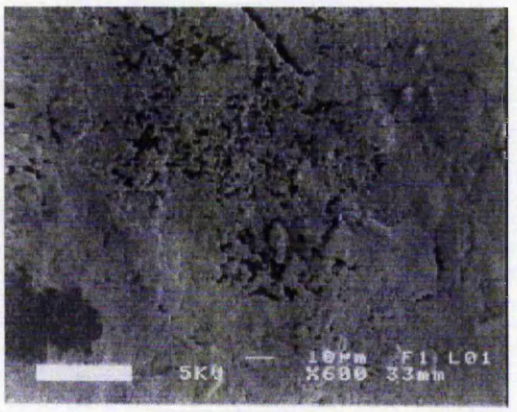

b)PCL 70%-silica S-G after 20ASP cycles

Figure 4.18 : SEM micrographs of α,ω-hydroxyl poly(ε-caprolactone) 70 %-silica sol-gel composite a) 0 cycle and b) 20 cycles of the alternate soaking process (ASP) (Bar scale 10 µm).

The SEM photography, Figure 4.18 show the formation of a calcium phosphate precipitate on the surface of the composite after 20 cycles which covered nearly all the surface of the material. The precipitate was collected by scratching the surface and analysed by transmission electron microscopy.

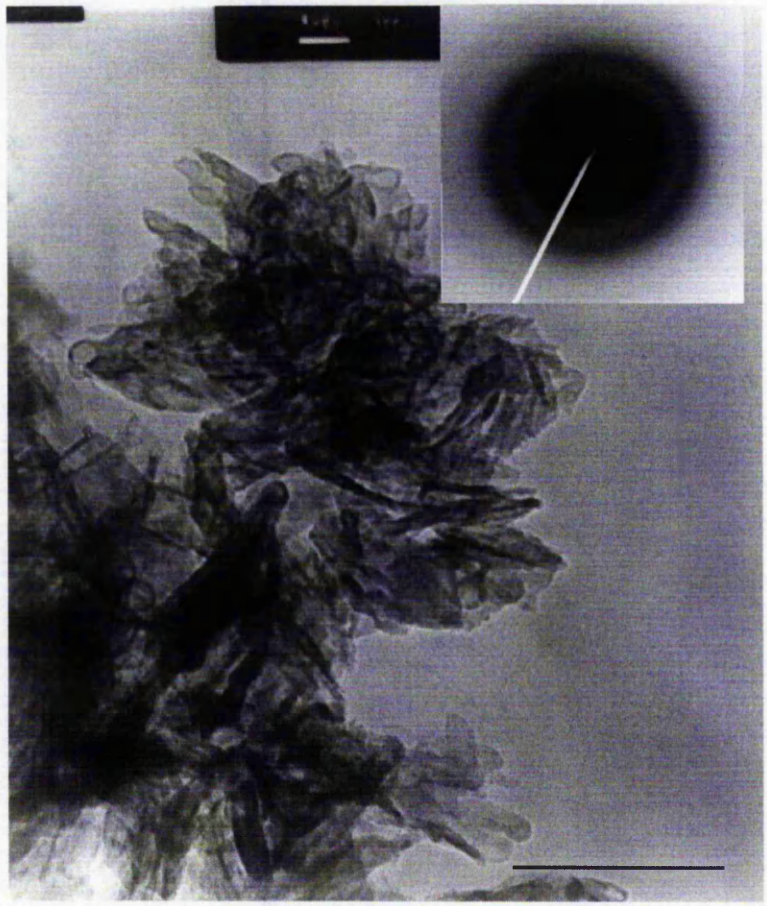

Figure 4.19 : TEM and electron diffraction photography of calcium phosphate material precipitated on the surface of α,ω-hydroxyl poly(ε-caprolactone) 70 % -silica sol-gel composite by the ASP method (Bar scale 500 nm) with inset electron diffraction pattern.

The TEM photography, Figure 4.19, showed that the precipitate was in the form of aggregates of flake-like crystals with length approximately 500 nm. Table 4.5 shows the d-spacing calculated from the electron diffraction pattern and their possible assignment based on expected d spacing for hydroxyapatite and octacalcium phosphate crystal from the joint committee on powder diffraction standards (JCPDS) files.

Table 4.5 : d-spacings ( ) calculated from electron diffraction data of calcium phosphate precipitates, for example Figure 4.18, and the d-spacings for HAP (JCPDS 9-432) and OCP (JCPDS 26-1056).

d-spacing ( ), ± StDev	**HAP (JCPDS 9-432)**	**OCP (JCPDS 26-1056)**
3.521, ± 0.13	3.51	
		3.49(s)
	3.44(s)	3.31
		3.21
	3.17	
	3.08	3.11
		2.87
2.856, ± 0.10	2.81(s)	2.83(s)
	2.78(s)	2.74
	2.63(s)	
	2.29	2.56
		2.27
2.307, ± 0.08	2.26(s)	2.26
		2.16
		1.99
1.904, ± 0.07	1.87	
	1.75	
		1.74

The electron diffraction ring patterns obtained for the flakes were diffuse indicating a low crystallinity. However, the d-spacings obtained were attributable to an apatitic material.

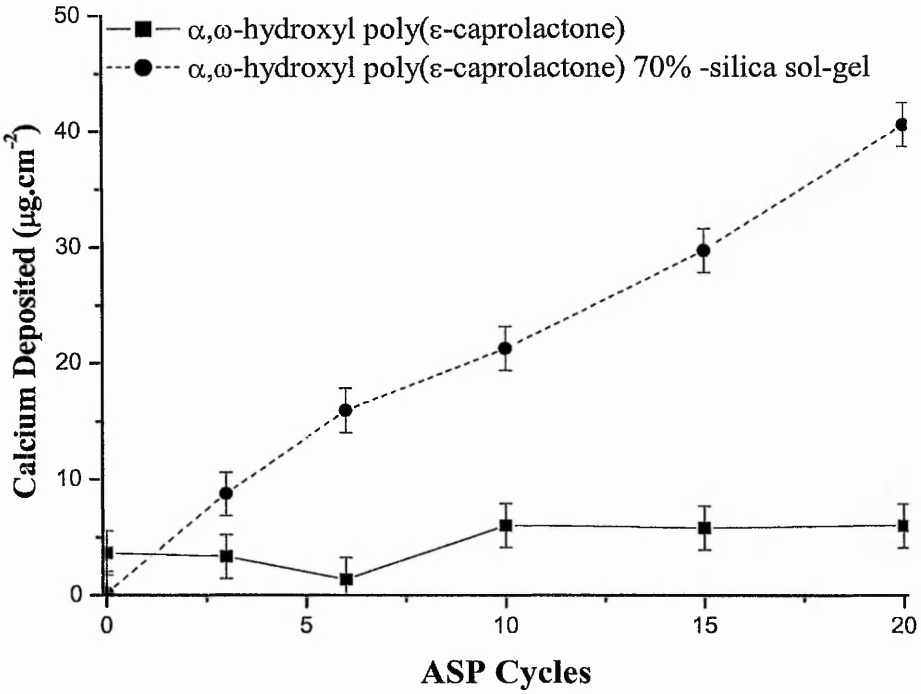

Figure 4.20 : Plot of the oncentration of calcium precipitate on α,ω-hydroxyl poly(ε-caprolactone) and α,ω-hydroxyl poly(ε-caprolactone) 70 %-silica sol-gel composite as a function of the ASP cycles.

Figure 4.20 indicates clearly that the amount of calcium deposited increased on the sol-gel composite with the increase of ASP cycles but did not vary significantly on the surface of the α,ω-hydroxyl poly(ε-caprolactone). For the α,ω-hydroxyl poly(ε-caprolactone) sample, the number of ASP cycles was increased up to 60 and even then no calcium phosphate material precipitated on its surface ([Ca] PCL 60 ASP cycles equal to 41 $\mu g.cm^{-2}$). It was noted that even if there was no precipitation of calcium phosphate material on the surface of the poly(ε-caprolactone), calcium measured by the colorimetric assay was found on the soaked polyester samples at an average value of 5 $\mu g.cm^{-2}$. This was due to traces of the alternate soaking solution on the surface and in the porosity of the polyester sample. Therefore, any significant calcium phosphate material deposition on a bioactive material surface should show a value of calcium as measured by the calcium assay superior to 5 $\mu g.cm^{-2}$.

4.3.2. Discussion

The static and the dynamic biomimetic processes results were concordant and both showed that the α,ω-hydroxyl poly(ε-caprolactone)-silica sol-gel with 70 % weight content of polyester developed an apatite rich layer on its surface confirming the finding of S. H. Rhee and H. M. Kim[33]. Therefore, both methods were adequate even if the continuous exchange of simulated body fluid leads to a better simulation of the *in vivo* conditions in the dynamic biomimetic process[37]. Table 4.6 lists important experimental parameters for the *in vitro* tests carried out in this study and two published studies on other materials containing silica[31, 32]. It should be noted that the two materials, SiO_2-CaO-P_2O_5 glass[32] and the α-$CaSiO_3$ ceramics[31] contains both calcium and silicon whereas the poly(ε-caprolactone)-silica sol-gel samples contains silicon only. The concentration of calcium in the simulated body fluid was reported because it is known that an excess of calcium ions in SBF increases the rate of formation of the apatite layer[38]. The variation of other ions could also lead to variation of precipitation rate[39] but in these three studies, their concentrations were identical as noted in the chapter 2. The pH of the simulated body fluid adjusted by hydrochloric acid and tris(hydroxymethyl)aminoethane (Trizma base®-Sigma) was a second important factor which could affect the kinetics of precipitation and the morphology of the apatite formed[40]. For the static biomimetic process, the following factors were reported because they could affect either the kinetics and the morphology of the precipitated apatite; the solid/liquid ratio (S/L), the soaking time and the temperature. For the dynamic biomimetic process, the flow rate, soaking time and temperature were also listed. Finally, a succinct description of the apatite morphology precipitated on the bioactive materials was reported for each study.

Table 4.6 : Important experimental parameters for the static and dynamic biomimetic processes used and reported by two others publications.

***In vitro* apatite-formation ability comparison studies**			
Authors	This work	M. Vallet-Regi & al.[32]	S. Hayashi & al.[31]
Material	PCL-SiO_2	SiO_2-CaO-P_2O_5 glass	α-$CaSiO_3$ ceramic
[Ca] in SBF	1.5 mM/l	1.0 mM/l	1.0 mM/l
pH	7.4	7.4	7.25
Static System			
S/L ratio	1 g/ 150ml	0.5 g/?	1 g/ 850ml
Time	15 days	7 days	30 days
Temperature	37 °C	37 °C	36.5 °C
Morphology precipitate	flakes poorly defined	HAP spheres 1μm of needle like aggregates	Ball like particles HAP 10-25 μm
Dynamic System			
Flow rate	300 ml/day	1440 ml/day	40 ml/day 241,920 ml/day
Time	15 days	7 days	30 days
Temperature	37 °C	37 °C	38 °C
Morphology precipitate	HAP spheres 1 to 10 μm of needle like aggregates	idem static	layer HAP for the slow flow rate 1 to 10 μm spheres for fast flow rate

From the Table 4.6, it was obvious that comparison of the deposition rate and the morphology of the hydroxyapatite on the surface of the bioactive materials between the three studies, was not possible because important parameters such as the SBF composition, pH, S/L ratio and the flow rate varied from one study to the other. It is not surprising that the two previously reported studies gave to some extent contradictory results. M. Vallet-Regi and co-worker[32] found that the rate of apatite formation was

faster using a dynamic biomimetic process than a static process. S. Hayashi & al.[31] found the opposite in their study.

The α,ω-hydroxyl poly(ε-caprolactone)-silica sol-gel with 70 % weight content of poly(ε-caprolactone) was found to have precipitated calcium phosphate material on its surface after 4 days in the static biomimetic process as shown by DRIFTs analysis (Figure 4.13). An apatite-layer was observed on the same material after 15 days in the dynamic biomimetic process. This was in accordance with the study of S. Hayashi & al.[31]. The morphology of the apatite material formed on the surface of the polyester-silica composite studied was similar; sphere-like particles from 1 to 25 μm in diameter, formed of needle or flake-like crystals was observed. However, it seems to be rather difficult to draw a conclusion about the *in vitro* bioactivity efficiency of one material compared to another as, to date, a general *in vitro* apatite-forming ability method has not been defined. The choice of a static or a dynamic biomimetic process is not an issue. They can both be used to demonstrate the *in vitro* apatite-forming ability of a bioactive material. The dynamic biomimetic process mimics probably more closely the conditions of an *in vivo* study but for the study of several materials and compositions, it could be a very long process or parallel equipment would be necessary to decrease the time scale of such a study.

Consequently, the development of the alternate soaking process was carried out to provide complementary quantitative information to the other processes. This method is a relatively rapid process (alternate soaking 60 minutes + calcium deposition measure 60 minutes) and as shown by the ASP results, calcium phosphate precipitation occurred preferentially on the *in vitro* bioactive α,ω-hydroxyl poly(ε-caprolactone)-silica sol-gel composite material. Non-bioactive α,ω-hydroxyl poly(ε-caprolactone) and quartz samples did not precipitate calcium phosphate material on their surface after 20 cycles and 60 cycles (results not shown). This process provides a rapid and easy method to test and quantify the *in vitro* apatite-forming ability of a large number of materials.

4.4. Effect and Comparison of the Reactive End-Groups on the Poly(α-hydroxyacid)-Silica Composites *In Vitro* Apatite-Forming Ability

4.4.1. Results of the *In Vitro* Apatite-Forming Ability Tests

The static biomimetic process and the alternate soaking process were carried out on α,ω-hydroxyl poly(ε-caprolactone)-silica sol-gel composites with different weight content of poly(ε-caprolactone). Figures 4.21 and 4.22 show the SEM images of α,ω-hydroxyl poly(ε-caprolactone)-silica sol-gel composites with 90 and 70 percent weight poly(ε-caprolactone) after 15 days of soaking in simulated body fluid. The calcium deposited on the surface of the materials is reported as a function of the number of ASP cycles, Figure 4.23.

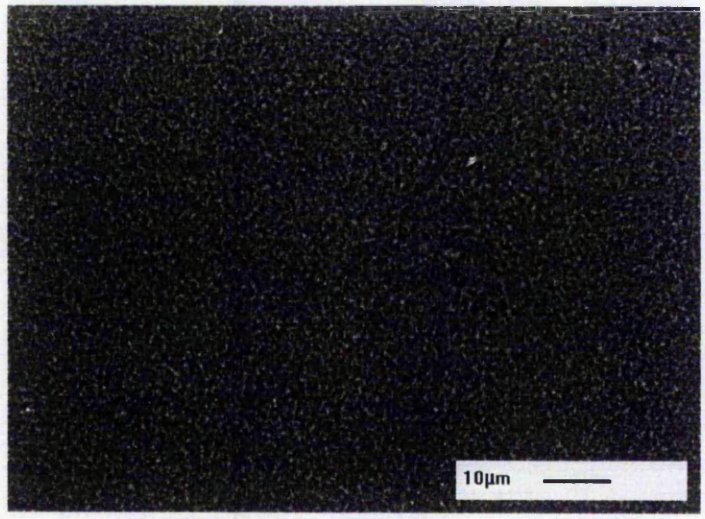

Figure 4.21 : SEM photography of the α,ω-hydroxyl poly(ε-caprolactone) 90 %-silica sol-gel after 15 days in static biomimetic process.

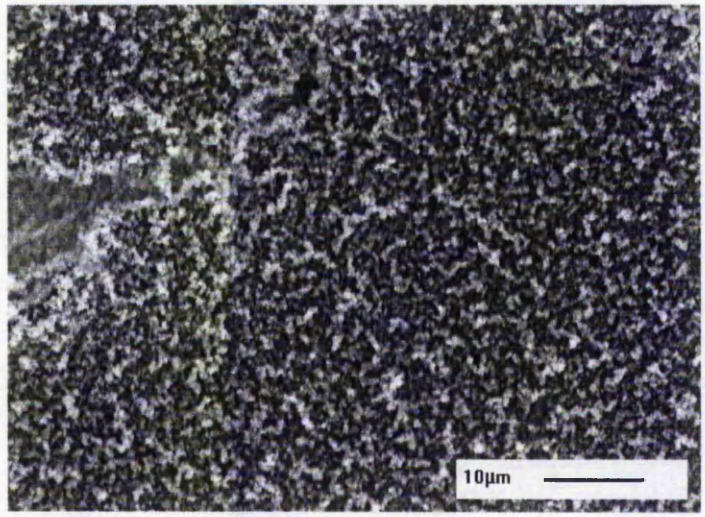

Figure 4.22 : SEM photography of α,ω-hydroxyl poly(ε-caprolactone) 70 %-silica sol-gel after 15 days in static biomimetic process (repeated experiment from Figure 4.11).

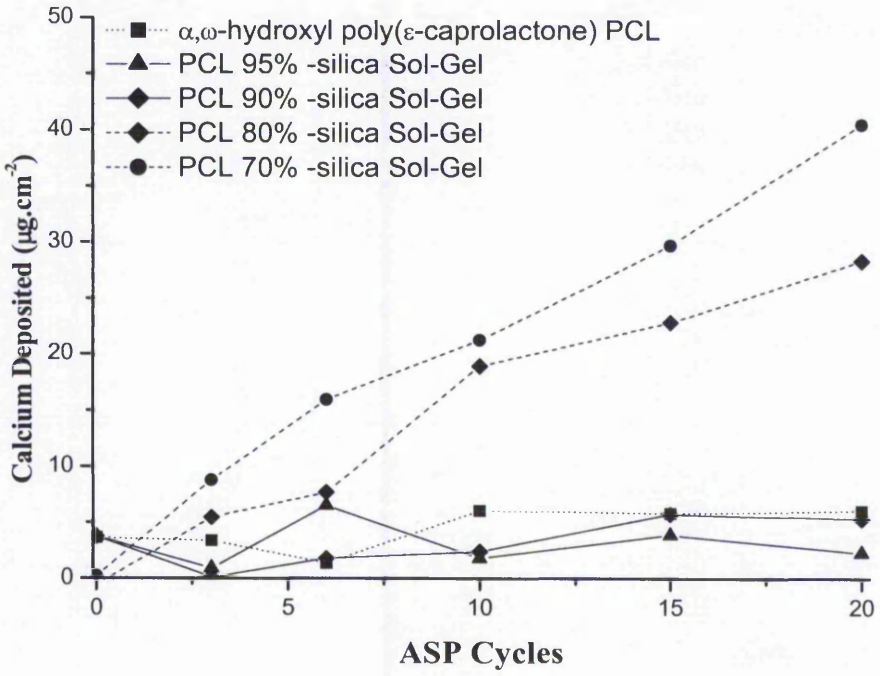

Figure 4.23 : Plot of the calcium deposit as a function of the ASP cycles for α,ω-hydroxyl poly(ε-caprolactone) and the α,ω-hydroxyl poly(ε-caprolactone)-silica sol-gel with 95, 90, 80 and 70 percent weight content of poly(ε-caprolactone).

The results obtained from the alternate soaking process, Figure 4.21 indicated that α,ω-hydroxyl poly(ε-caprolactone)-silica sol-gels with 90 and 95 percent weight content of poly(ε-caprolactone) did not significantly precipitate calcium phosphate material on their surfaces as the levels of calcium deposit measured by the calcium assay were not significantly different to those for the pure poly(ε-caprolactone). For composites with lower polyester content, the ASP results, Figure 4.23 showed that calcium materials precipitated on the composites and that increasing the number of ASP cycles increased linearly the amount of calcium deposited. This result was confirmed by the static biomimetic process as shown Figure 4.22. The calcium to phosphorus ratio measured by EDXA on the α,ω-hydroxyl poly(ε-caprolactone)-silica sol-gel 70 % weight content of polyester was equal to 1.5 ± 0.10, close to apatite as already reported before (Table 4.4).

In a similar fashion, α,ω-triethoxysilane poly(ε-caprolactone)-silica sol-gels with 90 and 70 percent weight content of polyester were subject to SBP and ASP tests and the results obtained compared to these obtained for the equivalent hydroxyl terminated poly(ε-caprolactone)-silica sol-gel composites.

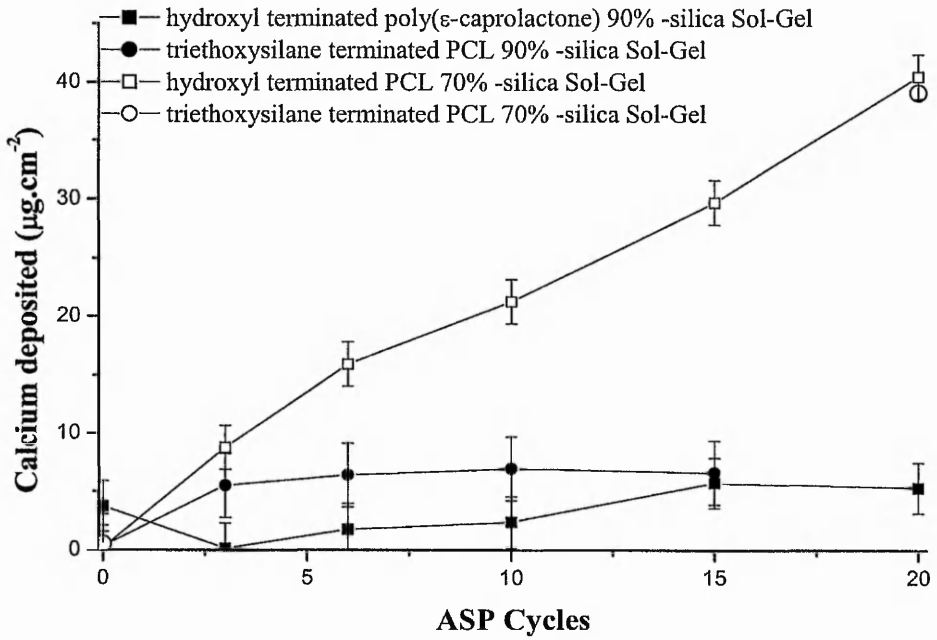

Figure 4.24 : Plot of the calcium deposit as a function of the number of ASP cycles for the hydroxyl and the triethoxysilane terminated poly(ε-caprolactone)-silica sol-gels with 90 and 70 percent weight content of poly(ε-caprolactone) respectively.

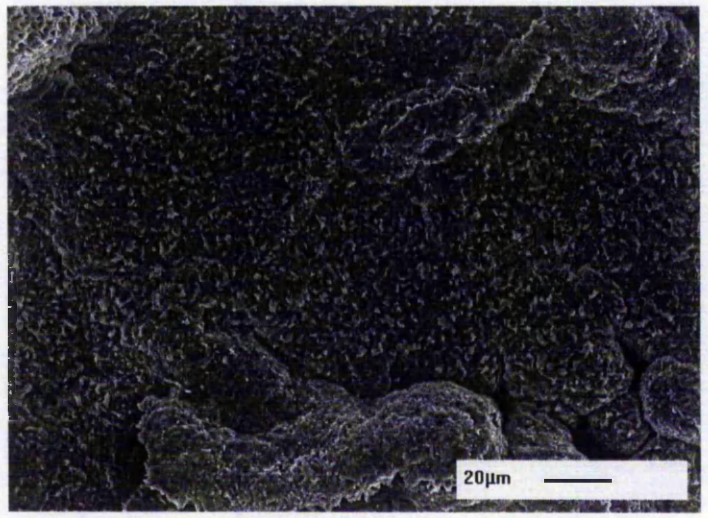

Figure 4.25 : SEM photography of the triethoxysilane terminated poly(ε-caprolactone) 90 %-silica sol-gel after 15 days in static biomimetic process.

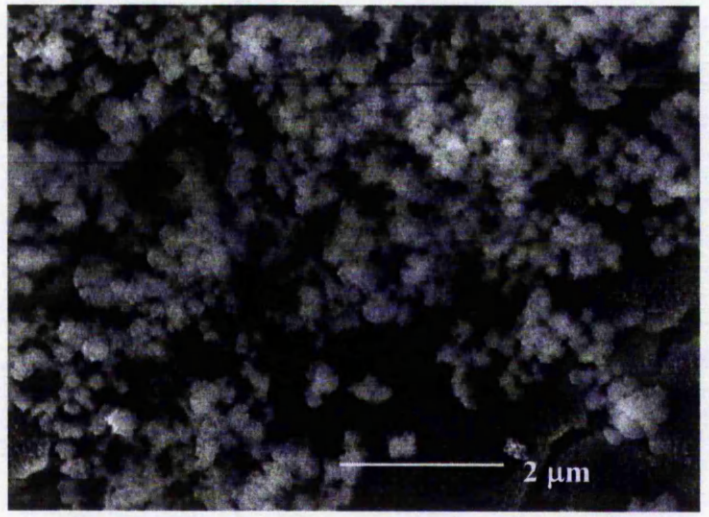

Figure 4.26 : SEM photography of the triethoxysilane terminated poly(ε-caprolactone) 70 %-silica sol-gel after 15 days in static biomimetic process.

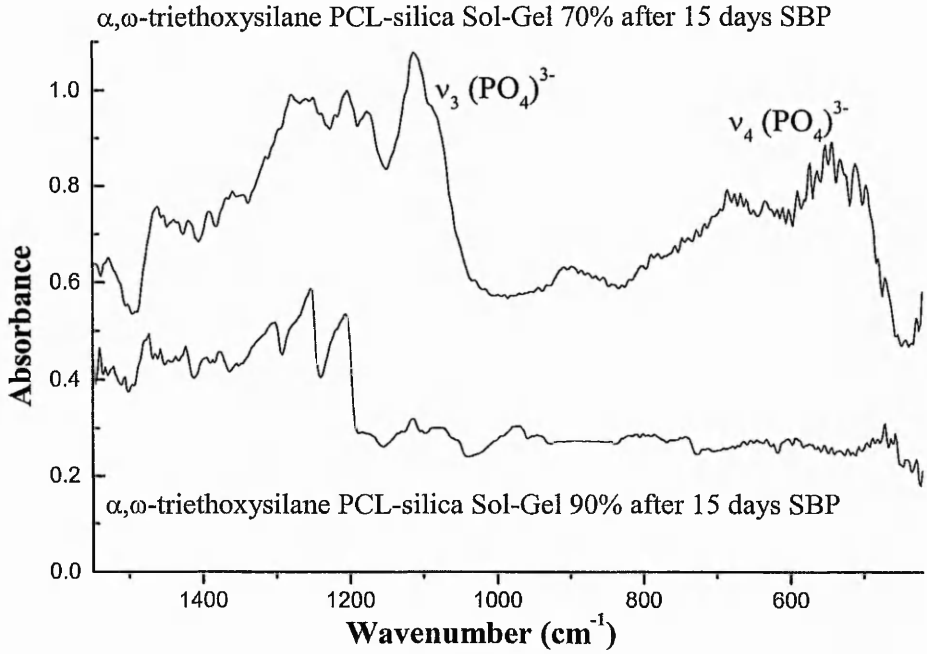

Figure 4.27 : DRIFT spectrum of α,ω-triethoxysilane poly(ε-caprolactone)-silica sol-gels with 70 and 90 percent weight content of poly(ε-caprolactone) after 15 days of soaking in SBF in the static biomimetic process.

Again, the ASP and the SBP *in vitro* apatite-forming ability tests carried out on α,ω-triethoxysilane poly(ε-caprolactone)-silica sol-gel gave concordant results. With 90% weight content of poly(ε-caprolactone), composites with triethoxysilane end-groups, similarly to the hydroxyl terminated poly(ε-caprolactone), did not form calcium phosphate material on its surface, Figures 4.25 and 4.26 . Figure 4.26 showed that the *in vitro* apatite-forming ability test (SBP) was positive when the weight content of triethoxysilane terminated poly(ε-caprolactone) was equal to 70 percent in the composite as found for the hydroxyl terminated equivalent polyester composite. The calcium to phosphorus ratio calculated from the EDXA analysis was equal to 1.77 ± 0.31, close to that expected for hydroxyapatite (Table 4.4). DRIFTs analysis, Figure 4.27 showed the presence of bands; between 650 cm^{-1} to 500 cm^{-1} and a broad band at around 1090cm^{-1} attributable respectively to the ν_4 and ν_3 vibrations of PO_4^{3-} indicating the probable formation of apatite material layer. The *in vitro* apatite forming ability tests

carried out on the hydroxyl and triethoxysilane terminated poly(ε-caprolactone)-silica sol-gels seem to indicate that the reactivity of the end-groups on the linear poly(ε-caprolactone) was not detrimental to the *in vitro* bioactivity property of the composites.

As for the poly(ε-caprolactone)-silica sol-gel composites, the *in vitro* bioactivity of hydroxyl and triethoxysilane terminated poly(L-lactic acid)-silica sol-gel materials was studied.

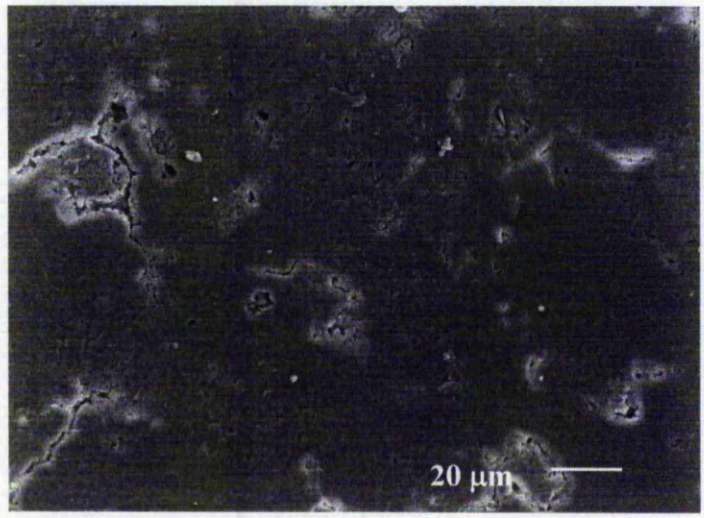

Figure 4.28 : SEM photography of α,ω-hydroxyl poly(L-lactic acid) 70 % -silica sol-gel weight content poly(L-lactic acid) after 15 days in the dynamic biomimetic process.

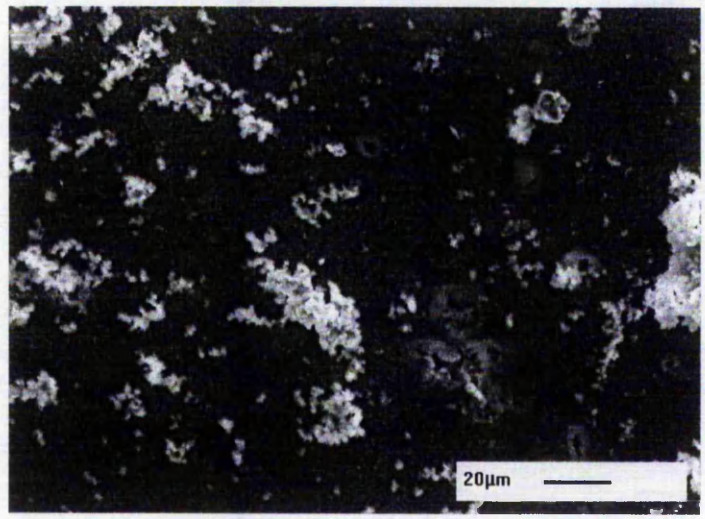

Figure 4.29 : SEM photography of α,ω-hydroxyl poly(L-lactic acid) 70 % -silica sol-gel weight content poly(L-lactic acid) after 15 days in the static biomimetic process.

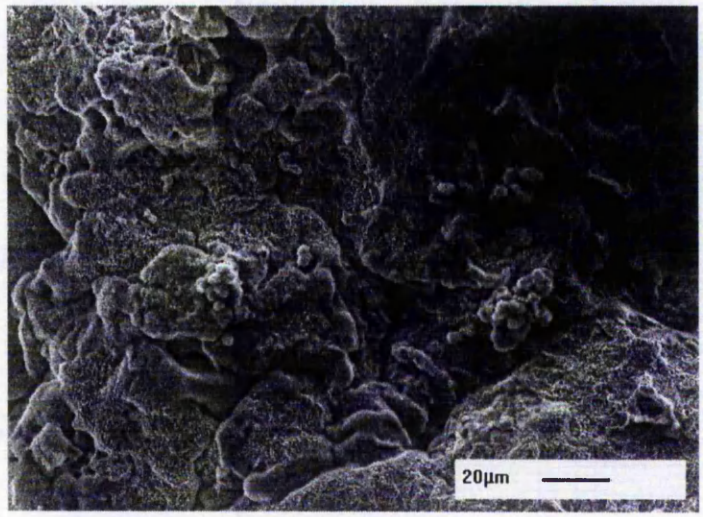

Figure 4.30 : SEM photography of α,ω-triethoxysilane poly(L-lactic acid) 70 %-silica sol-gel after 15 days in the static biomimetic process.

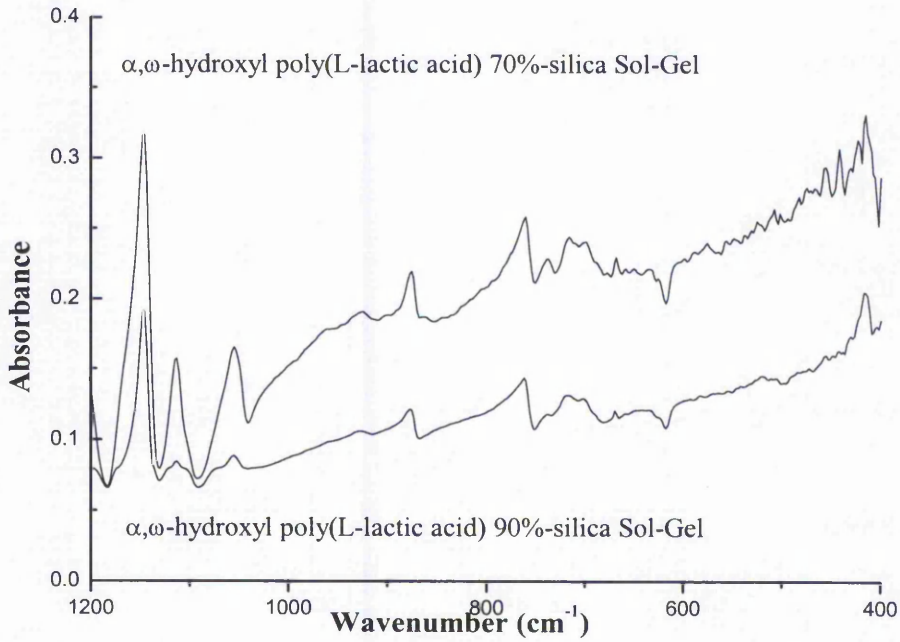

Figure 4.31 : DRIFT spectra of α,ω-hydroxyl poly(L-lactic acid)-silica sol-gel composites with 70 and 90 percent weight content of poly(L-lactic acid) after 15 days in the static biomimetic process.

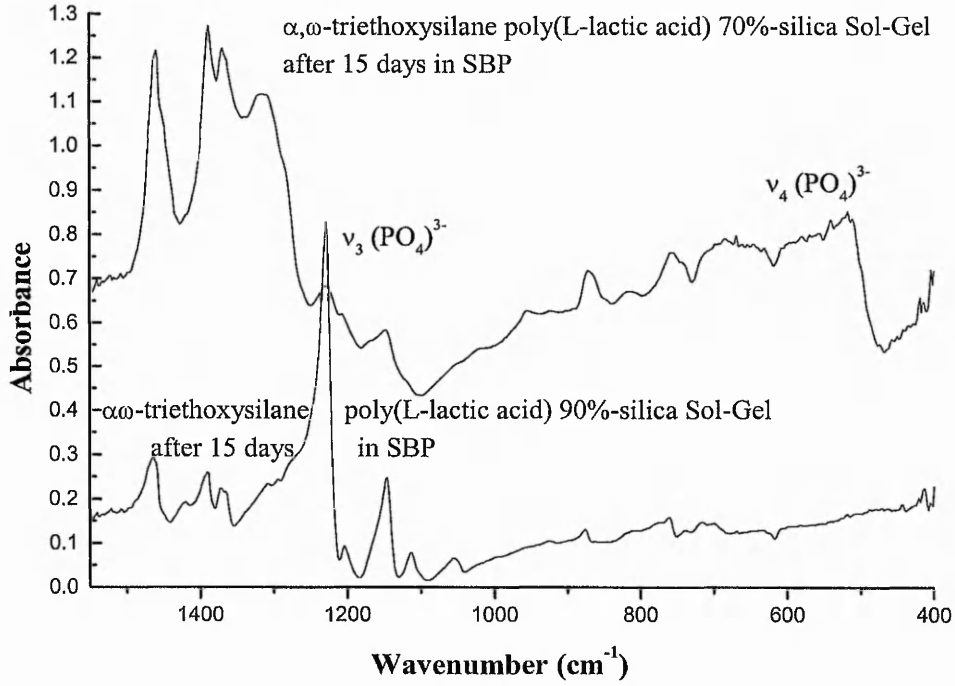

Figure 4.32 : DRIFT spectra of triethoxysilane terminated poly(L-lactic acid)-silica sol-gel composites with 70 and 90 percent weight content of poly(L-lactic acid) after 15 days in SBF following the static biomimetic process.

α,ω-Hydroxyl and α,ω-triethoxysilane poly(L-lactic acid)-silica sol-gel 90 % and 70 % composites were tested for their *in vitro* apatite-forming ability by the static and the dynamic biomimetic process. The results for the dynamic test were negative as no calcium phosphate material was precipitated on the surface of the composite after 15 days of soaking in simulated body fluid for both compositions 90 % and 70 % and both poly(L-lactic acid) with hydroxyl and triethoxysilane end-groups. As an example of a negative DBP test, Figure 4.28 shows the SEM micrograph of α,ω-hydroxyl poly(L-lactic acid)-silica sol-gel 70% soaked in dynamic biomimetic process for 15 days. However, in the static biomimetic process, calcium phosphate materials were observed on the α,ω-hydroxyl and α,ω-triethoxysilane poly(L-lactic acid) 70 % -silica sol-gels

surface (Figures 4.29 and 4.30) but in small quantity compared to the α,ω-hydroxyl poly(ε-caprolactone) 70% -silica sol-gel composite. The calcium to phosphorus molar ratio calculated from the EDXA analysis was equal to 2.12 ± 0.52 for the hydroxyl terminated poly(L-lactic acid) 70%-silica sol-gel. The observed precipitates did not cover homogeneously the surface of the poly(L-lactic acid)-silica sol-gel samples but had a rather erratic distribution. The DRIFT spectrum, Figure 4.31, collected for α,ω-hydroxyl poly(L-lactic acid) 70% and 90%-silica sol-gel composites did not show the vibrational bands observed for calcium phosphate materials for both composition. It was probable that the calcium phosphate precipitate was not sufficient to be observed by DRIFT analysis. This indicated also that the calcium phosphate materials precipitated was probably very amorphous on the surface of the α,ω-hydroxyl poly(L-lactic acid) 70 %-silica sol-gel. For the α,ω-triethoxysilane poly(L-lactic acid) 70 % -silica sol-gel composite after 15 days in the static biomimetic process, presented in Figure 4.32 with the α,ω-triethoxysilane poly(L-lactic acid) 90 %-silica sol-gel; the following ν_4 and ν_3 vibrational bands of PO_4^{3-} were observed by DRIFT analysis respectively between 650 cm^{-1} to 500 cm^{-1} and 1150 cm^{-1}.

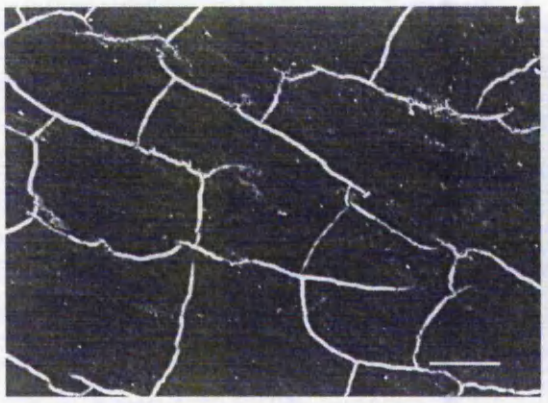

a) α,ω hydroxyl PLLA, 0 ASP cycles

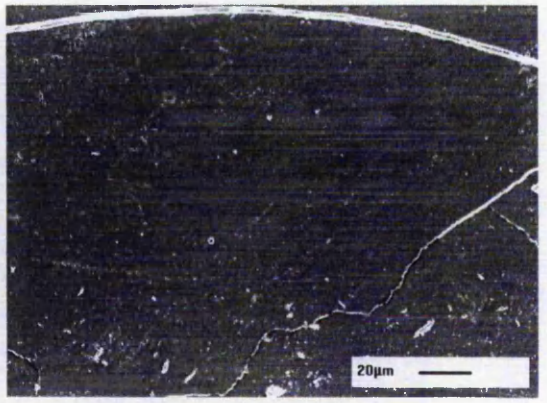

b) α,ω hydroxyl PLLA 20 ASP cycles

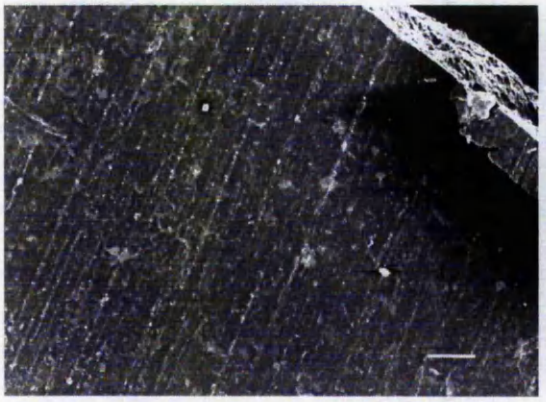

c) α,ω hydroxyl PLLA 90%-silica 0 ASP cycle

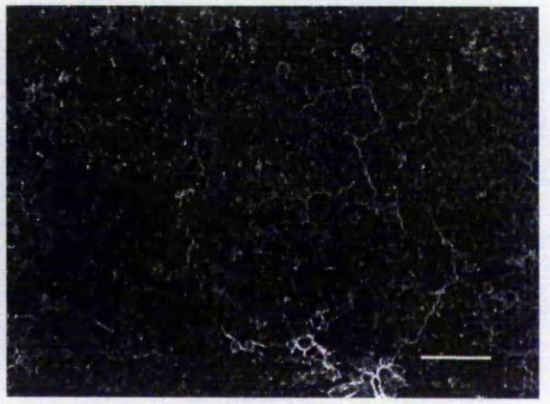

d) α,ω hydroxyl PLLA 90%-silica 20 ASP cycles

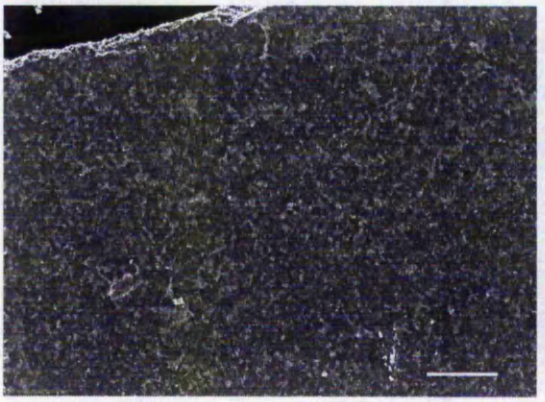

e) α,ω hydroxyl PLLA 70%-silica 0 ASP cycle

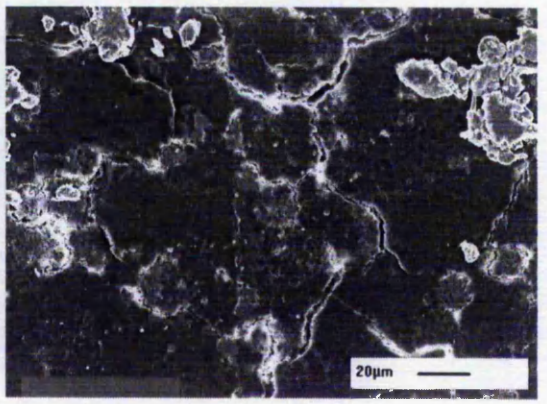

f) α,ω hydroxyl PLLA 70%-silica 20 ASP cycles

Figure 4.33 : SEM photos of α,ω-hydroxyl poly(L-lactic acid) (PLLA) a) 0 and b) 20 ASP cycles and α,ω-hydroxyl poly(L-lactic acid)-silica sol-gels with 90 % and 70 % weight content poly(L-lactic acid) c), e) 0 and d), f) 20 ASP cycles (bar scale equal to 20 µm).

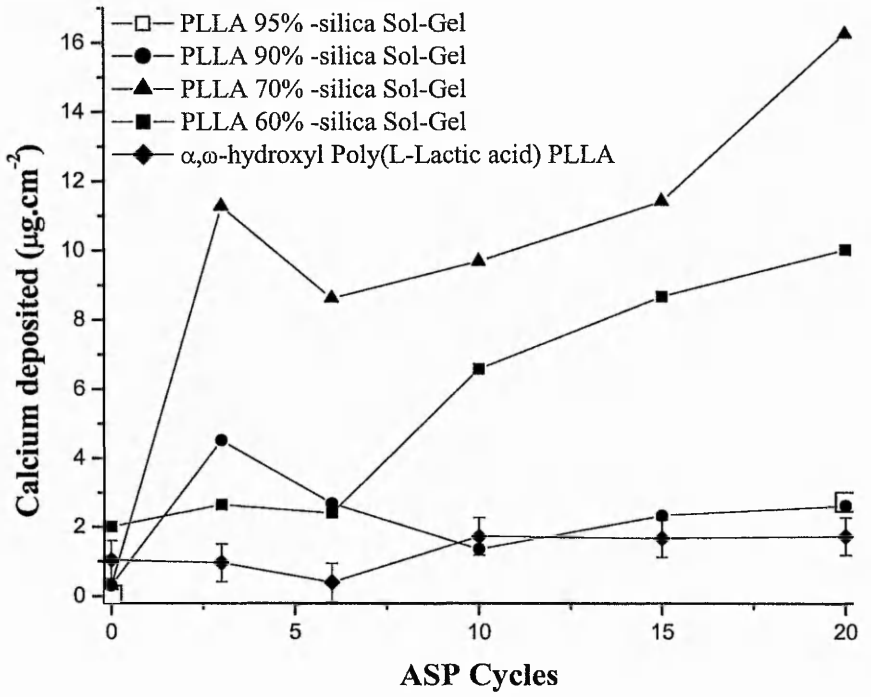

Figure 4.34 : Plot of the calcium deposit as a function of the ASP cycles for α,ω-hydroxyl poly(L-lactic acid) and α,ω-hydroxyl poly(L-lactic acid)-silica sol-gels with 95, 90, 70 and 60 percent weight content of poly(L-lactic acid).

Both the alternate soaking process (Figure 4.34) and the static biomimetic process (Figures 4.28 and 4.29) showed the poor *in vitro* apatite-forming ability of the α,ω-hydroxyl poly(L-lactic acid)-silica sol-gels. Only poly(L-lactic acid)-silica sol-gels with 70 % weight content of poly(L-lactic acid) precipitated any calcium phosphate material on its surface during the chosen reaction conditions as shown by the calcium deposited plot as a function of ASP cycles, Figure 4.34.

Interestingly, the calcium phosphate deposition rate on the surface of α,ω-hydroxyl poly(ε-caprolactone)-silica sol-gels and α,ω-hydroxyl poly(L-lactic acid)-silica sol-gel can be compared from the calcium deposited after a set number of ASP cycles. In Figure 4.35 is plotted the calcium deposited on α,ω-hydroxyl poly(ε-caprolactone) and α,ω-hydroxyl poly(L-lactic acid)-silica composites with 95 % and 70% weight content of polyester as a function of the number of alternate soaking process cycles.

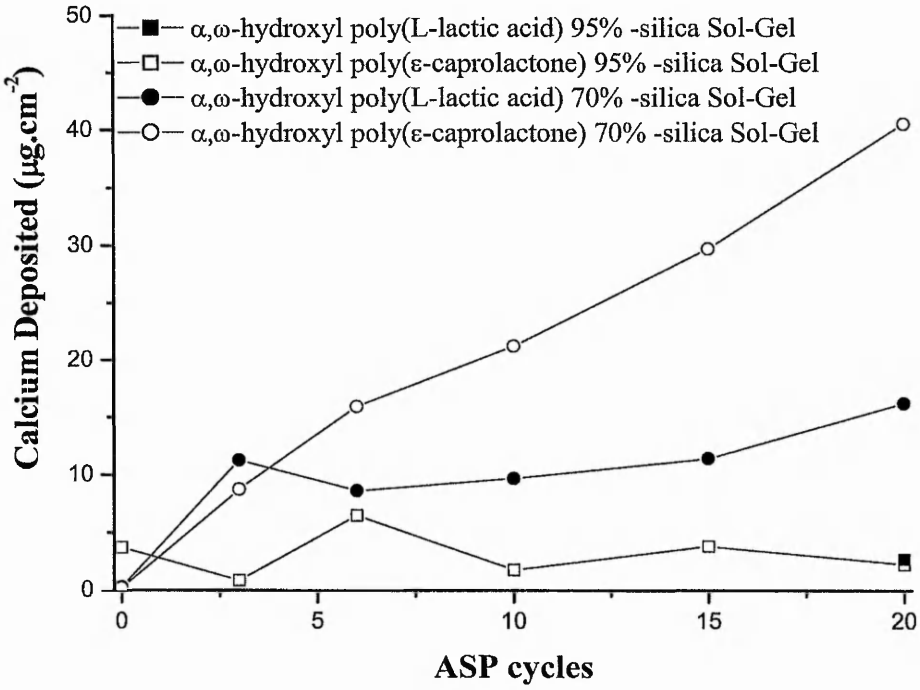

Figure 4.35 : Plot of the calcium deposit as a function of the ASP cycles for α,ω-hydroxyl poly(L-lactic acid) and α,ω-hydroxyl poly(ε-caprolactone)-silica sol-gels with 95 and 70 percent weight content of polyester.

Figure 4.35 shows that the calcium deposition of the α,ω-hydroxyl poly(ε-caprolactone)-silica sol-gel with 70% weight content poly(ε-caprolactone) was faster than on the α,ω-hydroxyl poly(L-lactic acid)-silica sol-gel 70 % weight content of poly(L-lactic acid). The ASP tests confirmed unequivocally what was observed by the *in vitro* biomimetic processes. Poly(L-lactic)-silica sol-gel composites do form apatite on their surfaces but at a slower rate than the poly(ε-caprolactone)-silica sol-gel composites with 70% polyester content.

4.4.2. Discussion

Hydroxyl and triethoxysilane terminated poly(ε-caprolactone) 70 %-silica sol-gels were introduced in a static biomimetic process and an alternate soaking process. The results showed that both materials precipitate hydroxyapatite type materials on their surface in similar conditions. The amount of calcium deposited after 20 cycles of the

alternate soaking process were close for the hydroxyl and triethoxysilane terminated poly(ε-caprolactone) 70 %-silica sol-gels studied. It can be then concluded that a higher reactivity of end-groups on the polyester and consequently a better bonding of the organic and inorganic phases was not detrimental to the *in vitro* apatite-forming ability of the sol-gel composites.

Concentration of silicic acid released from the poly(L-lactic acid) 70 % -silica sol-gel was lower than the concentration of silicic acid released from a poly(ε-caprolactone) 70 % -silica sol-gel. This seems to indicate that the nature of the poly(α-hydroxyacid) influenced the release of silicic acid either indirectly as the sol-gel reaction and therefore the composition of silica species presents in composite was influenced by the polymer and therefore dissolution and diffusion of the silica phases are different or directly by the possible difference of interactions between the silica phase and the poly(ε-caprolactone) and poly(L-lactic acid). A consequence of these variations may be observed by the slower rate of apatite formation on poly(L-lactic acid) 70 %-silica sol-gel compared to the poly(ε-caprolactone) 70 %-silica sol-gel.

4.5. Conclusion

The study of the *in vitro* apatite forming ability of the poly(α-hydroxyacid)-silica sol-gel composites showed that hydroxyl and triethoxysilane terminated poly(ε-caprolactone)-silica sol-gels and poly(L-lactic acid)-silica sol-gels could form an apatite layer on their surface after soaking in a simulated body fluid for 15 days at 37 °C. The apatite deposition was dependent on the amount of silica in the composites. Thirty percent by weight of the total composite weight was the minimum amount of silica where the formation of hydroxyapatite was observed in the conditions of the bioactivity tests.

Na_2O-CaO-P_2O_5-SiO_2 glasses where the amount of silica is between 53 and 60 percent of the total weight can bond to bone and are called bioactive glasses[41]. The *in vitro* and *in vivo* apatite-forming ability or osteoconductivity mechanisms of the

bioactive silica containing glass-ceramics have been extensively discussed by L. L. Hench[42] and T. Kokubo[21]. Bioactive glasses and silica sol-gels develop a calcium phosphate-rich layer after exposure *in vivo* or to simulated body fluids.

Soluble silicon has been suggested to be involved in the nucleation of calcium phosphate. J. J. M. Damen and J. M. Ten Cate[13] studied the effect of silicic acid on calcium phosphate precipitation. Silicic acid stimulated the precipitation of hydroxyapatite. The active compounds appeared to be polymerised silicic acid and even larger silica particles. This seems to imply that soluble silica act as heterogeneous nucleation substrates and provides favourable sites for the nucleation of apatite. A. Caballero[43] also suggested that orthosilicic acid could induce heterogeneous calcium phosphate precipitation from a supersaturated solution.

The measures of silicic acid concentration released in simulated body fluid by the poly(ε-caporlactone)-silica and poly(L-lactic acid)-silica sol-gels during the static biomimetic tests indicated that the composites with increasing amount of silica have increasing release of silicic acid. Therefore, silicic acid in the simulated body fluid probably influenced the rate of calcium phosphate precipitation. The *in vitro* dynamic biomimetic process showed that the apatite-forming ability of the composites was conserved even if the rate of apatite formation was decreased. This indicated that the build up of silicic acid concentration in the static biomimetic process was not vital for the observation of the *in vitro* bioactivity behaviour. However, most of the recent studies reported are agreed that a silica-gel layer is necessary in establishing a calcium phosphate layer[44]. It is then possible that the rapid release of silica species speeds up the formation of this silica sol-gel layer[45], the silanol groups on the surface of silica gel acting as nucleation sites for apatite. Several apatite nucleation mechanisms have been proposed involving; the silanol groups at the surface acting as nucleation sites for apatite crystals[46], and small siloxane rings lowering the enthalpy of calcium phosphate nucleation and facilitating precipitation. To date, little experimental evidence supports one or other of the hypotheses. However, recent molecular orbital modelling has indicated that partially deprotonated 3-ring [$(Si_3O_6H_6)$] could be an active site for the nucleation of calcium phosphate[47].

It has also been reported that the textural features of bioactive materials affect the nucleation of calcium phosphate (i.e. pore size, surface characteristics)[48]. The surface of silica and bioglass® ceramics has been considered as critical for the precipitation of calcium phosphate. It is well known that dense silica glasses and quartz will not induce the precipitation of hydroxyapatite in simulated body fluid[23] while a silica gel will do. T. Kokubo[49] and L. L. Hench[41] investigated the porosity effect on the precipitation of calcium phosphate. The porosity of a silica gel was changed by heat treatment, and the ability to form calcium phosphate precipitates in SBF solution investigated by the authors[42]. The induction time for apatite nucleation on the gel silica decreased as pore size and pore volume increased. The pores were thought to be the sites for the nucleation of apatite through the establishment of an electrical double layer with high ionic concentration. Porous gel-glasses with pores <2 nm were found to be less effective due to the restricted diffusion of Ca and P ions[16].

Otherwise, the study of the *in vitro* apatite-forming ability of poly(ε-caprolactone)-silica sol-gel composites prepared with different amounts of the hydrolysis-condensation reactions catalyst (hydrochloric acid) pointed to the possible dependence of the apatite formation rate on the hydrochloric acid content in composites. Thus indicating a probable effect of the structure properties and consequently the topography and the surface chemistry on the *in vitro* apatite forming ability of the composites. The different apatite-forming ability of the poly(ε-caprolactone) and poly(L-lactic acid)-silica sol-gel composite materials reported in this chapter, indicated also a possible structural and chemical effect on the apatite forming ability of the composites. Interestingly, the modification of the reactive end-groups on the poly(α-hydroxyacid)-silica sol-gel composites did not impede the *in vitro* apatite-forming ability of the materials which again suggested that the *in vitro* apatite-forming ability of the materials are not only dependent on the fast release of silicic acid but probably the overall structure of the composites which govern the chemistry and topography of the materials surfaces. Finally, for a full understanding of the *in vitro* bioactive property of the poly(α-hydroxyacid)-silica composites, future studies will have to take account of the biodegradation behaviour of these composites as the erosion of the surface, the diffusion of silica species and oligomeric lactic acid species may all affect the apatite-forming ability of these materials.

4.6. References

[1] D. Tian, P. Dubois, C. Grandfils, R. Jerome, P. Viville, R. Lazzaroni, J. L. Bredas, P. Leprince (1997), "A novel biodegradable and biocompatible creamer prepared by the sol-gel process.", *Chemistry of Materials*, 9(4), 871-874.

[2] M. Vallet-Regi (2001), "Ceramics for medical applications.", *Journal of the Chemical Society, Dalton Transactions*, 2, 97-108.

[3] C. Rey, M. Shimizu, B. Collins, M. J. Glimcher (1990), "Resolution-enhanced fourier transform infrared spectroscopy study of the environment of phosphate ion in the early deposits of a solid phase of calcium phosphate in bone and enamel and their evolution with age: 1. Investigation in the ν_4 PO_4 domain." *Calcified Tissue International*, 46, 384-394.

[4] A. Burneau, J. P. Gallas (1998), "The surface properties of silicas." ed. A. P. Legrand (Wiley and Sons, Chichester), 191-196.

[5] R. L. Orefice, L. L. Hench, A. B. Brennan (2000), "*In vitro* bioactivity of polymer matrices reinforced with a bioactive glass phase." *Journal of Brazilian Chemistry Society*, 11(1), 78-85.

[6] C. Rey, M. Shimizu, B. Collins, M. J. Glimcher (1991), "Resolution-enhanced fourier transform infrared spectroscopy study of the environment of phosphate ion in the early deposits of a solid phase of calcium phosphate in bone and enamel and their evolution with age: 2. Investigation in the ν_3 PO_4 domain." *Calcified Tissue International*, 49, 383-388.

[7] S. W. Kuo, C. F. Huang, F. C. Chang (2001), "Study of hydrogen-bonding strength in poly(ε-caprolactone) blends by DSC and FTIR.", *Journal of Polymer Science. Part B. Polymer Physics,* 39, 1348-1359.

[8] S. H. Rhee, H. M. Kim (2002), "Preparation of a bioactive polycaprolactone/silica nanocomposite.", *Key Engineering Materials*, 218-220, 453-456.

[9] K Tsuru, Y. Aburatani, T. Yabuta, S. Hayakawa, C. Ohtusuki, A. Osaka (2001), "Synthesis and In vitro behavior of organically modified silicate containing Ca ions.", *Journal of Sol-Gel Science and Technology*, 89-96.

[10] J. D. Mackenzie, Y. J. Chung, Y. Hu (1992), "Rubbery ormosils and their applications.", *Journal of Sol-Gel Science and Technology*, 147, 271-279.

[11] R. K. Iler (1979), "Chemistry of Silica: Solubility, Polymerization, Colloid and Surface Properties and Biochemistry", Eds. R. K. Iler, R. K. Aler (John Wiley and Sons).

[12] M. M. Pereira, L. L. Hench (1996), "Mechanisms of hydroxyapatite formation on porous gel-silica substrates.", *Journal of Sol-Gel Science and Technology,* 7, 59-68.

[13] J. J. M. Damen, J. M. Ten Cate (1989), "The effect of silicic acid on calcium phosphate precipitation.", *Journal of Dental Research*, 68(9), 1355-1359.

[14] K. Tsuru, M. Kubo, S. Hayakawa, C. Ohtsuki, A. Osaka (2001), "Kinetics of apatite deposition of silica gel dependent on the inorganic ion composition of simulated body fluids.", *Journal of the Ceramic Society of Japan*, 109(5), 412-418.

[15] T. Kokubo, H. Kushitani, S. Sakka, T. Kitsugi, T. Yamamuro (1990), "Solution able to reproduce in vivo surface-structure changes in bioactive glass-ceramic A-W3.", *Journal of Biomedical Materials Research*, 24(6), 721-734.

[16] M. M. Pereira, L. L. Hench (1996), "Mechanisms of hydroxyapatite formation on porous gel-silica substrates.", *Journal of Sol-Gel Science and Technology*, 7, 59-68.

[17] L. L. Hench (1991), "Bioceramics- From concept to clinic.", *Journal of the American Ceramic Society,* 74(7), 1487-1510.

[18] T. Kokubo (1997), "Novel Bioactive Materials.", *Anales de Quimica*, 93(1), S49-S55.

[19] P. Saravanapavan, L. L. Hench (2001), "Bioactive Sol-Gel glasses in the CaO-SiO_2 System.", *Key Engineering Materials*, 192-195, 609-612.

[20] A. J. Salinas, M. Vallet-Regi, I. Izquierdo-Barba (2001), "Biomimetic apatite deposition on calcium silicate gel glasses.", *Journal of Sol-Gel Science and Technology*, 21, 13-25.

[21] T. Kokubo (1990), "Surface chemistry of bioactive glass-ceramics.", *Journal of Non-Crystalline solids*, 120, 138-151.

[22] T. Kokubo (1998), "Apatite formation on surfaces of ceramics, metals and polymers in body environment.", *Acta Materials*, 46(7), 2519-2527.

[23] P. Li, C. Ohtsuki, T. Kokubo, K. Nakanishi, N. Soga, T. Nakamura, T. Yamamuro (1992), "Apatite formation induced by silica gel in a simulated body fluid.", *Journal of the American Ceramic Society*, 75(8), 2094-2097.

[24] P. Li, K. Nakanishi, T. Kokubo, K. De Groot (1993), "Induction and morphology of hydroxyapatite, precipitated from metastable simulated body fluids on sol-gel prepared silica.", *Biomaterials*, 14(13), 963-968.

[25] T. Kokubo (1992), "Bioactivity of glasses and glass ceramics. Bone Bonding.", eds. Ducheyne, Kokubo & Van Blitterswijk, (Reed Healthcare communications) 31-46.

[26] S. B. Cho, F. Miyaji, T. Kokubo, K. Nakanishi, N. Soga, T. Nakamura (1996), "Apatite-forming ability of silicate ion dissolved from silica gels.", *Journal of Biomedical Materials Research*, 32, 375-381.

[27] S. Falaize, S. Radin, P. Ducheyne (1999), "In vitro behaviour of silica-based xerogels intended as controlled release carriers.", *Journal of American Ceramic Society*, 82, 969-976.

[28] J. Hlavac, D. Rohanova, A. Helebrant (1994), "The effect of tris-buffer on the leaching behaviour of bioactive glass-ceramics.", *Ceram-Silikaty*, 38, 119-122.

[29] I. Izquierdo-barba, A. J. Salinas, M. Vallet-Regi (2000), "Effect of continuous solution exchange on in vitro reactivity of a CaO-SiO_2 sol-gel glass.", *Journal of Biomedical Materials Research*, 51, 191-199.

[30] B. D. Ratner, A. S. Hoffman, F. J. Schoen, J. F. Lemons (1996), "Biomaterials science: an introduction to materials in medicine.", (Academic press, San Francisco) 233-234.

[31] P. Siriphannon, Y. Kameshima, A. Yasumori, K. Okada, S. Hayashi (2002), "Comparative study of the formation of hydroxyapatite in simulated body fluid under static and flowing systems.", *Journal of Biomedical Materials Research*, 60, 175-185.

[32] A. Ramila, M. Vallet-Regi (2001), "Static and Dynamic in vitro study of a sol-gel glass bioactivity.", *Biomaterials*, 22, 2301-2306.

[33] S. H. Rhee, H. M. Kim (2002), "Preparation of a bioactive polycaprolactone/silica nanocomposite.", *Key Engineering Materials*, 218-220, 453-456.

[34] K. Suzuki, T. Yumura, M. Mizuguchi, T. Taguchi, K. Sato, J. Tanaka, M. Akashi (2001), "Apatite-silica gel composite materials prepared by a new alternate soaking process.", *Journal of Sol-Gel Science and Technology*, 21, 55-63.

[35] T. Taguchi, A. Kishida, M. Akashi (1998), "Hydroxyapatite formation on/in poly(vinyl alcohol) hydrogel matrices using a novel alternate soaking process.", *Chemistry Letters*, 8, 711-712.

[36] E. Fernandez, F. J. Gil, M. P. Ginebra, F. C. M. Driessens, J. A. Planell, S. M. Best (1999), *Journal of Materials Science: Materials in Medicine*, 10, 177-183.

[37] M. Vallet-Regi (2001), "Ceramics for medical applications.", *Journal of chemical Society. Dalton Transaction*, 97-108.

[38] S. B. Cho, F. Miyaji, T. Kokubo, K. Nakanishi, N. Soga, T. Nakamura (1996), "Apatite formation on various silica gels in a simulated body fluid containing excessive calcium ion.", *Journal of the Ceramic Society of Japan*, 104(5), 399-404.

[39] K. Tsuru, M. Kubo, S. Hayakawa, C. Ohtsuki, A. Osaka (2001), "Kinetics of apatite deposition of silica gel dependent on the inorganic ion composition of simulated body fluids.", *Journal of the Ceramic Society of Japan*, 109(5), 412-418.

[40] P. Li, K. Nakanishi, T. Kokubo, K. De Groot (1993), "Induction and morphology of hydroxyapatite, precipitated from metastable simulated body fluids on sol-gel prepared silica.", *Biomaterials*, 14(13), 963-968.

[41] I. Rehman, L. L. Hench, W. Bonfield, R. Smith (1994), "Analysis of surface layers on bioactive glasses.", *Biomaterials*, 15(10), 865-870.

[42] M. M. Pereira, A. E. Clark, L. L. Hench (1995), "Effect of texture on the rate of hydroxyapatite formation on gel-silica surfaces.", *Journal of American Ceramics Society*, 78(9), 2463-2468.

[43] A. M. Caballero-Alias (1999), "The role of silica in mineralising tissues.", (Nottingham Trent University).

[44] M. Neo, S. Kotani, T. Nakamura, T. Yamamuro, T. Kokubo, C. Ohtsuki, T. Kokubo, Y. Bando (1992), "A comparative study of ultrastructures of the interfaces between 4 kinds of surface active ceramic and bone.", *Journal of Biomedical Materials Research*, 26(11), 1419-1432.

[45] J. M. Oliveira, R. N. Correia, M. H. Fernández (2002), "Effects of Si speciation on the in vitro bioactivity of glasses.", *Biomaterials*, 23, 371-379.

[46] K. H. Karlsson, K. Froberg, T. Ringbom (1989), "A structural approach to bone adhering of bioactive glasses.", *Journal of non-Crystalline Solids*, 112, 69-72.

[47] N. Sahai, J. A. Tossell (2000), "Molecular orbital study of apatite ($Ca_5(PO_4)_3OH$) nucleation at silica bioceramic surfaces.", *Journal of Physic Chemistry*, B104, 4322-4341.

[48] L. L. Hench, J. K. West (1994), "Inorganic pathways for biosynthesis. A molecular orbital modelling approach.", *Journal of Vacuum Science Technology. A,* 12(5), 2962-2965.

[49] S. Cho, K. Nakanishi, T. Kokubo, N. Soga, C. Ohtuki, T. Nakamura, T. Kitsugi, T. Yamamuro (1995), "Dependence of apatite formation on silica gel on its structure. Effect of heat treatment.", *Journal of the American Ceramic Society,* 78(7), 1769-1774.

The objective of this chapter was to investigate a novel route to poly(α-hydroxyacid)-silica composites. The possibility of forming a hybrid system with strong covalent bonds between the organic polymer and the silica phase was appealing because, as it has been shown in chapter 4, the use of more reactive end-groups such as triethoxysilane on the poly(α-hydroxyacids) of the studied sol-gels did not impede the *in vitro* apatite forming ability of the materials. Additionally, the mechanical properties of a composite are strongly dependent on the good bonding at the interface of the mixed phases. The following chapter presents the study of the hydrolysis-condensation of silicon alkoxides and the cross-linking with α,ω-hydroxyl poly(ε-caprolactone) using an organotin catalyst to produce novel polymeric materials

5.1. Organotin Catalyst- Tin(II) 2-ethylhexanoate

5.1.1. Ring-Opening Polymerisation of Lactone

An effective preparative route to a variety of useful poly(α-hydroxyacids) is the metal-mediated ring-opening polymerisation of cyclic esters. The poly(α-hydroxyacids) can be prepared by the polycondensation of hydroxycarboxylic acids but the synthesis leads to low molecular weight polymers and specific end groups are difficult to obtain[1]. The ring-opening polymerisation of lactones can enable control of polymer molecular weight and backbone stereochemistry and can yield macromolecules with narrow molecular weight distributions[2]. Efforts toward this goal have been extensive for polylactic acid and poly(ε-caprolactone). B. J. O'Keefe and co-workers[3] and A. C. Albertsson[1] have reviewed the recent advances in the field of lactone catalytic ring-opening polymerisation. The most frequently used catalyst for the ring opening polymerisation of lactide and ε-caprolactone is tin(II) 2-ethylhexanoate[4, 5, 6]. It has been approved as a food additive by the American Food and Drug Administration (FDA). The mechanism of cyclic ester (lactide and ε-caprolactone) polymerisation initiated with tin(II) 2-ethylhexanoate in the presence of an alcohol or water has been thoroughly discussed but it is only recently that it has been elucidated[7, 8].

Figure 5.1 shows the general scheme of the polymerisation mechanism of a cyclic ester (Est) in the presence of a tin catalyst ($Sn(Oct)_2$) and a co-initiator (alcohol: ROH).

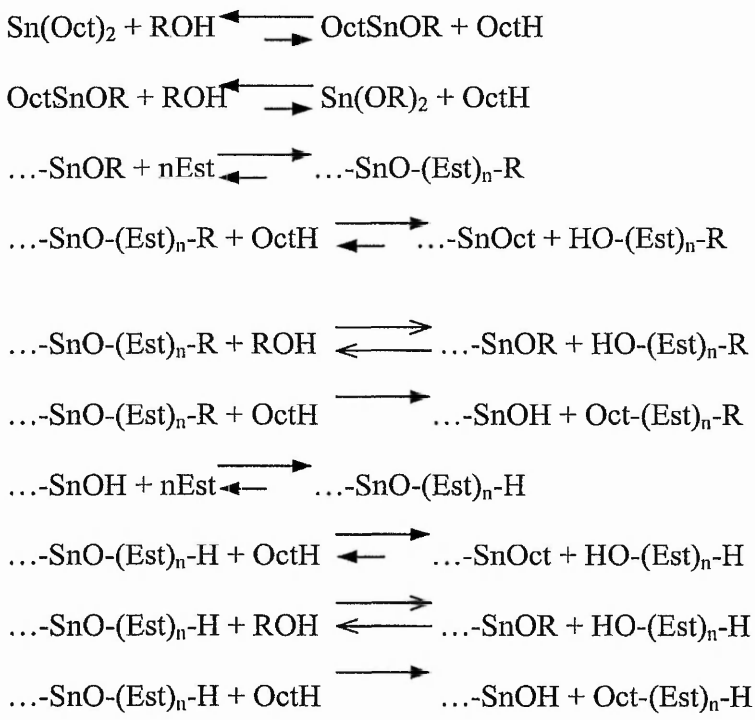

Figure 5.1 : Scheme of the ring-opening polymerisation mechanism cyclic ester catalysed by tin(II) 2-ethylhexanoate in presence of an alcohol[16].

The tin(II) 2-ethylhexanoate does not play an active role in the polymerisation since the polyester molecular weight does not depend on the monomer/catalyst molar ratio[7]. The formation of an active tin(II) alkoxide or hydroxide is necessary in order to initiate the polymerisation[8]. It has been shown that the tin catalyst and the alcohol yield a complex system of reactions, Figure 5.1, with a rapid equilibration involving the liberation of octanoic acid followed by a slower tin catalyst esterification of alcohol and octanoic acid. The liberated water yields tin hydroxide groups that at high concentration and temperature undergo condensation reaction yielding stannoxanes. However, this reaction is modified by alcohols capable of forming chelate-type Sn complexes such as OctSn-OR and RO-Sn-OR, especially at temperatures below 100°C. The polymerisation is said to proceed by a simple monomer coordination-insertion mechanism into the

reversible –Sn-OR bond, where ROH is either the co-initiator (alcohol, hydroxy acid, or water) or a macromolecule containing an hydroxyl end group. Therefore the monomer/co-initiator (alcohol) ratio controls the molecular weights. It has been reported that the tin(II) 2-ethylhexanoate to alcohol (catalyst/co-initiator) ratio allows the preparation of polyesters with molar mass up to 10^6 but that practically it can be adjusted by the lactone/ROH molar ratio only in the range from 10^2 to10^4. For higher molecular weight it must be done by a trial and error procedure[9].

Probable reasons are the impurities present in the reactants. It must be noted that Kricheldorf and co-workers[10] have proposed a slightly different reaction pathway where the co-initiating alcohol and the monomer are both coordinated to the tin catalyst complex during chain propagation, Figure 5.2.

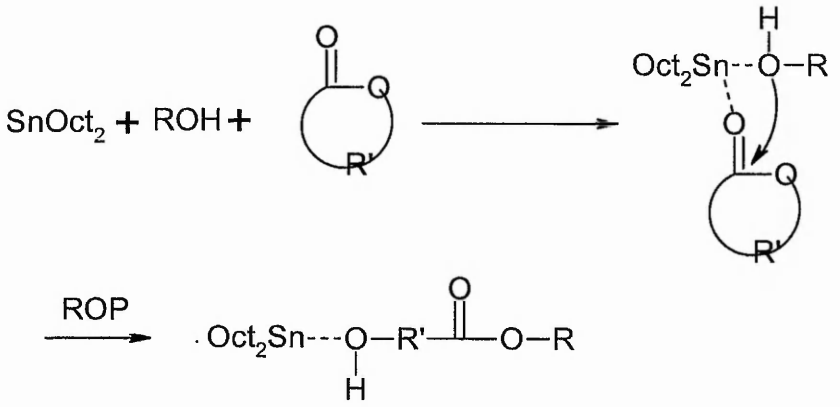

Figure 5.2 : Scheme of Kricheldorf and co-workers[10] mechanism proposed for ring-opening polymerisation with tin(II) 2-ethylhexanoate ($SnOct_2$) as catalyst and an alcohol (ROH) as co-initiator.

The structure of the polyesters depends on the alcohols used as co-initiators. Mono and di-functional alcohols yield linear polymers, while alcohols with hydroxyl functionality higher than two give star shaped polymers[11, 12]. The initiation of lactone polymerisation with mono- and poly-functional alcohols increases the rate of the polymerisation reaction and high molecular weight polyesters can be obtained. Because the ratio lactone to co-initiator molar ratio controls the final molecular weight of the polyester, only a small amount of co-initiator is needed for high molecular weight

polymers. It has been shown that increasing the number of hydroxyl groups on the co-initiator increases the conversion rate of lactone ring-opening polymerisation with identical lactone to co-initiator molar ratio[12]. The fastest polymerisation with the co-initiator having an higher number of hydroxyl groups is explained by the larger number of growing chains. It has also been reported that high molecular weight can be obtained using poly-functional alcohols[13]. This has been explained by the fastest polymerisation and therefore less time for transesterification and degradation reactions during the molecular weight build up[12]. It has been observed that after passing through a maximum molecular weight, the molecular weight of poly(lactic acid) in the ring opening polymerisation catalysed by the tin(II) 2-ethylhexanoate decreases. H. Korhonen and co-workers[12] reported that there was little variation on the weight average molecular weight but a decrease in number average molecular weight for high hydroxyl functional co-initiators and therefore an increase of polydispersity or molecular weight distribution. The decrease of polylactic acid molecular weight was supposing caused by random breakages in the polymer chains by traces of lactic acid and other impurities. Intermolecular transesterification by hydroxyl end groups, and hydroxyl groups with different reactivity are other possible causes for the higher polydispersity of the obtained polyesters[14].

The knowledge gained on the mechanisms of ring opening polymerisation of lactones has been exploited to synthesise linear and star shaped polyester block co-polymers[11]. The synthesis consists of the ring-opening polymerisation of a lactone in the presence of a polymer with hydroxyl functional groups. Poly(lactic acid)-polyglycerine[12], poly(lactic acid) and poly(ε-caprolactone) co-poly(ethylene oxide)[15, 16, 17], poly(lactic co-glycolic acid) grafted poly(vinyl alcohol)[18], poly(ε-caprolactone co-perfluoropolyether)[19], poly(D,L-lactic acid) grafted gelatine[20], poly(ε-caprolactone) grafted dextran[21] poly(lactide), poly(ε-caprolactone) block poly(glycolide-lactide)[22, 23] are some the block copolymer preparations reported. Those block co-polymers were completely organic materials, nevertheless H. R. Kricheldorf and D. Langanke have described the preparation of triblock copolymers derived from ε-caprolactone and L-lactide and a central inorganic polysiloxane block[24]. The synthesis consisted in the condensation of a oligosiloxane diol with $Bu_2Sn(OMe)_2$ and formation of a macrocyclic

siloxane containing butyl tin, Then, ring-opening polymerisation of ε-caprolactone and L-lactide and formation of block polymers was then carried out in the presence of 2-butyl tin cyclosiloxane as the initiator, Figure 5.3

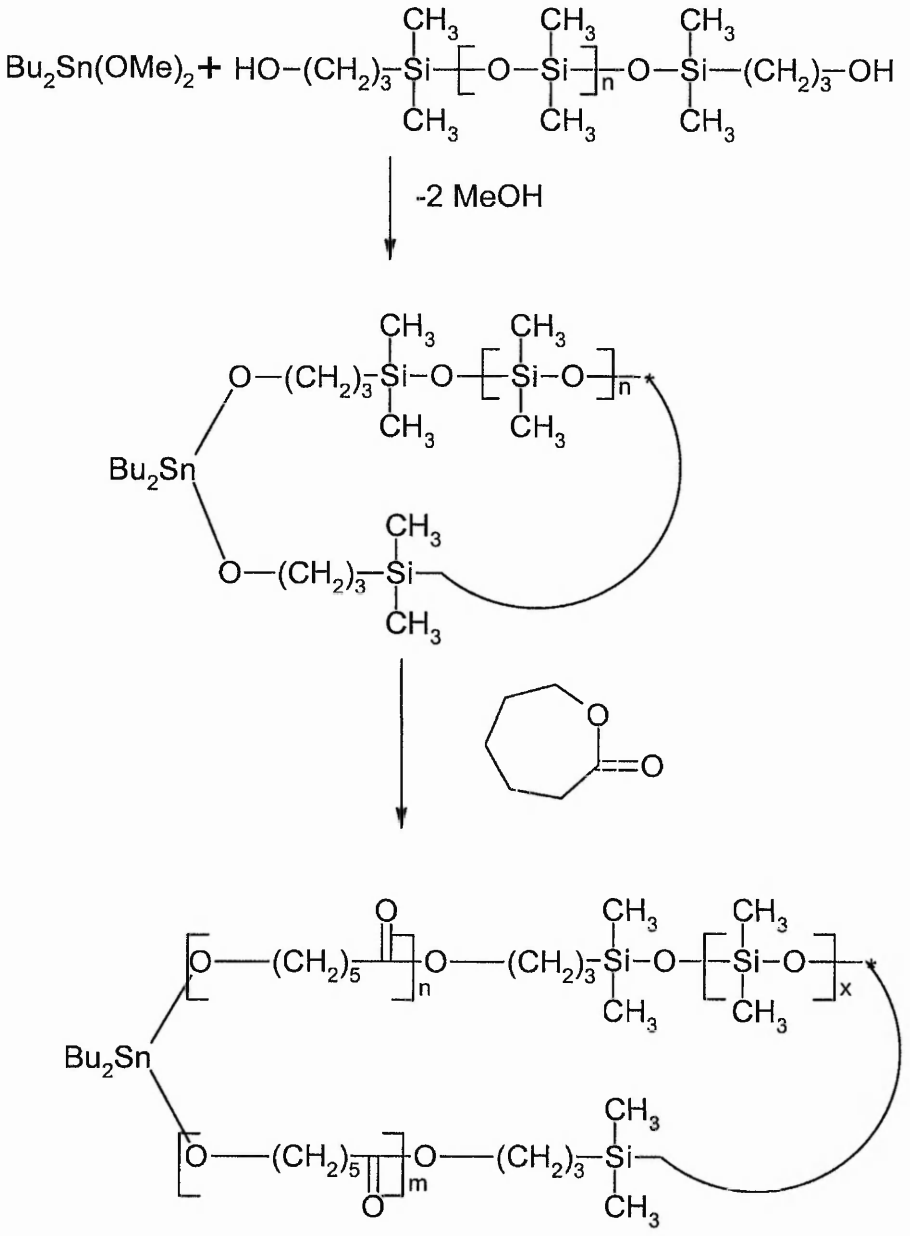

Figure 5.3 : Scheme of poly(ε-caprolactone) block co-polysiloxane synthesis[24].

5.1.2. Condensation alkoxysilane

Organotin compounds such as dialkyltin dicarboxylate have been used as a catalyst for the vulcanization of silicone rubber at room temperature[25]. It has been shown that the hydrolyzed form of the catalyst was the actual active catalyst and traces of water were necessary to carry out the curing of silicone rubbers composed of poly(dimethylsiloxane)-α,ω-diol and a poly-functional alkoxysilane[26] in the presence of organotins. It has been reported that tetraethyl orthosilicate and dialkyltin dicarboxylate formed an organotin silanolate which reacted with the poly(dimethylsiloxane)-α,ω-diol with the formation of a new siloxane linkage and recovery of the catalyst. The alkoxysilane in which part of the alkoxy group was replaced by siloxy groups appeared to be more reactive than the initial alkoxysilane and future cross-linking occurred. At elevated temperatures side reactions such as condensation of silanols with alcohols under the action of organotin compounds become increasingly prominent. The presence of alcohol because of equilibrium reactions can lead to degradation reactions. A recent publication from G. Spinolo and co-workers[27, 28] reported the novel preparation of a tin-doped silica sol-gel using tetraethyl orthosilicate and dibutyltin diacetate. The tin acetate in concentrations ranging from 1 to 4 weight percent reacted with tetraethyl orthosilicate in the presence of ethanol and a deficient amount of water. Gelation occurred after 12 hours at room temperature and a tin-doped silica gel was formed.

Figure 5.4 shows the possible schematic of the hydrolysis-condensation reaction mechanism of tetraalkoxysilane catalysed by the tin(II) 2-ethylhexanoate[25].

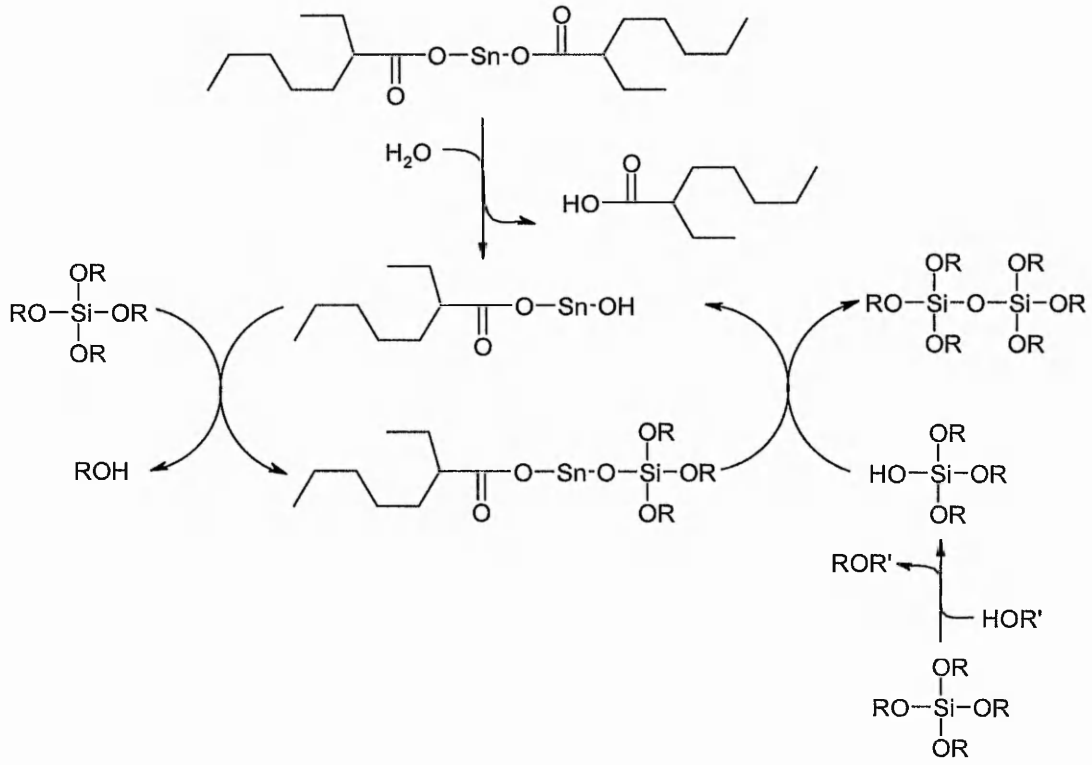

Figure 5.4 : Schematic of the hydrolysis-condensation reactions mechanism of tetraalkoxysilane catalysed by the tin(II) 2-ethylhexanoate (R: ethyl or methyl, R': H, ethyl or methyl)[25].

Therefore, it was thought from the bibliographic search on the organotin catalytic activity that it may be possible to carry out the hydrolysis-condensation reaction of an alkoxysilane and the ring-opening polymerisation of ε-caprolactone using an unique catalyst. B. M. Novak[29] has reviewed several routes to the synthesis of organic-inorganic hybrid materials. One method involves the *in situ* formation of both organic and inorganic polymers[30], but the success depended on the identification of an aqueous polymerisation of organic monomer that can match the hydrolysis condensation of the metal alkoxides. In our system, it is very unlikely that simultaneous silica gel formation and polymerisation of lactone could be carried out as the ring-opening polymerisation of lactone is very sensitive to traces of water which acts as a co-initiator in the ring-opening polymerisation of lactones. However, the incorporation of the α,ω-hydroxyl poly(ε-caprolactone) in the silica was thought to be possible by the reaction of the poly(ε-caprolactone) hydroxyl end-groups with the organotin silanolate specie which undergo silanolysis and yield the hydroxyl tin 2-ethylhexanoate and the

alkoxysilane substituted with a poly(ε-caprolactone) chain (Figure 5.4). Consequently, reaction should lead to a cross-linked material. It also seems that the removing of the ethanol from the reaction mixture by heating and/or vacuum would probably speed up the formation of the organotin silanolate and increase the side reaction of the α,ω-hydroxyl poly(ε-caprolactone) with a silanolate species as previously reported[25].

A general procedure has been developed. α,ω-Hydroxyl poly(ε-caprolactone) was heated, between 60 °C to 100 °C until it melted. The required amount of tetraethyl orthosilicate (TEOS/Polymer molar ratio between 0.1 to 1) was added followed by the addition of the catalyst, tin(II) 2-ethylhexanoate (T22EH/Polymer molar ratio 0.02). The mixture was stirred for 4 to 24 hours, between 60 °C to 100 °C, with or without vacuum (0.2 mbar). Below are presented some of the most relevant experiments carried out.

5.2. Reaction of α,ω-hydroxyl Poly(ε-caprolactone), Tetraethyl Orthosilicic Acid and Tin(II) 2-ethylhexanoate– Effect of Procedure Modifications and Effect of Reaction Conditions

5.2.1. Experiments

The following procedure called (PCL/TEOS(1)), is an example of the synthesis reaction carried out. 1.75×10^{-2} mole of α,ω-hydroxyl poly(ε-caprolactone) (M_n= 2,000 $g.mol^{-1}$) was added to a flask. The polymer was heated at 85 °C. 1.29 10^{-2} mole of tetraethyl orthosilicate was then added to the melted polymer and the mixture was stirred at 85 °C. Then, partial vacuum was applied to the reactor (0.1 torr) and 4.9 10^{-5} mole of tin(II) 2-ethylhexanoate was added via a syringe through a septum. The reaction mixture was heated and stirred at 85 °C under vacuum for 5 hours. The final product, a white solid material was collected and analysed. The product was washed with tetrahydrofuran and an insoluble gel was collected indicating the formation of a cross-linked poly(ε-caprolactone)-silica composite. Table 5.1 lists the synthesis procedures studied for the understanding of the composite preparation.

Table 5.1 : Name and description of experiment procedures.

Name	Experiment Description
PCL	ROP ε-caprolactone catalysed by T22EH (0.02 %) at 100 °C for 24 hours
PCL/TEOS(1)	α,ω-poly(ε-caprolactone) + T22EH (0.02 %) at 85 °C + Addition of TEOS (PCL/TEOS molar ratio equal to 1) at 85 °C for 5 hours with vacuum.
PCL/TEOS(2)	ROP ε-caprolactone catalysed by T22EH (0.02 %) at 100 °C for 20 hours + Addition of TEOS (PCL/TEOS molar ratio equal to 1) at 100 °C for 4 hours without vacuum.
PCL/TEOS/H_2O	ROP ε-caprolactone catalysed by T22EH (0.02 %) at 100 °C for 20 hours + Addition of TEOS (PCL/TEOS molar ratio equal to 1) at 100 °C for 2 hours + H_2O (H_2O/TEOS molar ratio equal to 4) at 100 °C for 2 hours without vacuum
PCL/(TEOS/EtOH /H_2O/HCl)(1)	ROP ε-caprolactone catalysed by T22EH (0.02 %) at 100 °C for 20 hours + Addition of pre-hydrolysed TEOS/EtOH/H_2O/HCl (molar ratio 1/4/4/0.1 for 1 hour at room temperature) at 100 °C for 4 hours without vacuum.
PCL/(TEOS/EtOH /H_2O/HCl)(2)	ROP ε-caprolactone catalysed by T22EH (0.02 %) at 100 °C for 20 hours + Addition of pre-hydrolysed TEOS/EtOH/H_2O/HCl (molar ratio 1/4/4/0.1 for 2 hours at room temperature) at 100 °C for 4 hours without vacuum.

The products synthesised were analysed using several techniques such as FTIR, DSC and TGA analysis. Gel permeation chromatography (GPC) and liquid ^{1}H NMR analysis were used when the materials were soluble or partially soluble. Liquid and solid state ^{29}Si NMR analyses were also obtained for selected materials. The analytical methods were either reported in chapter 2 or are described briefly here.

5.2.2. Results

Figure 5.5 shows the mid-IR spectrum of the α,ω-hydroxyl poly(ε-caprolactone) reactant and the mid-IR spectra of the PCL/TEOS(1) reaction product, the soluble part and insoluble part of the product of the PCL/TEOS(1) reaction.

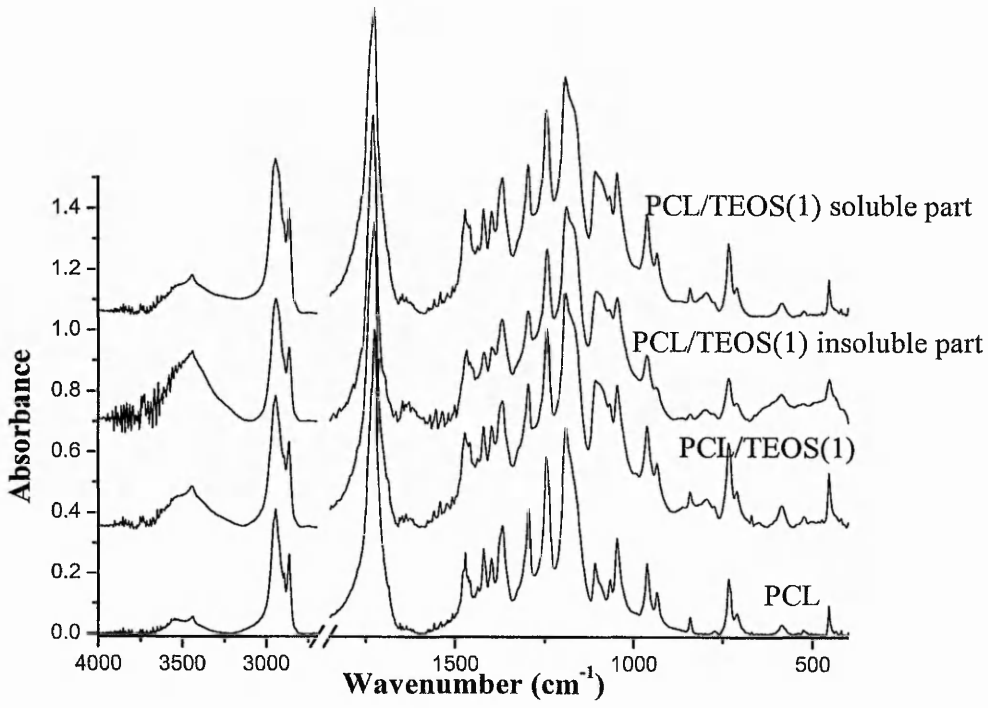

Figure 5.5 : IR spectra from 4000 cm^{-1} to 2700 cm^{-1} and from 1850 cm^{-1} to 400 cm^{-1} of α,ω-hydroxyl poly(ε-caprolactone) (PCL), α,ω-hydroxyl poly(ε-caprolactone)/tetraethyl orthosilicate/tin(II) 2-ethylhexanoate reaction product (PCL/TEOS(1)), PCL/TEOS(1) insoluble part and PCL/TEOS(1) soluble part.

The comparison of the α,ω-hydroxyl poly(ε-caprolactone) mid-IR spectrum with the mid-IR spectrum of the reaction product of PCL/TEOS(1), Figure 5.5, showed the appearance of three broad vibrational bands at 1190 cm^{-1}, 1075 cm^{-1} and 860 cm^{-1}. Characteristic IR vibrational band envelopes for a silica gel appear from 1200 cm^{-1} to 1100 cm^{-1} for the ν_{as} SiOSi, at 1076 cm^{-1}, 820 cm^{-1}, 450 cm^{-1} and 950 cm^{-1} for the ν_{as} SiOSi, ν_s SiOSi, δ OSiO and δ SiOH. It was not clear from the IR spectrum of the prepared material that a silica gel was formed. The δ OSiO and ν_s SiOSi vibrational

bands were not observed but overlapping with the α,ω-hydroxyl poly(ε-caprolactone) bands may have hidden the presence of the silica network signals. The broadening of the band at 450 cm^{-1} in the IR spectrum of the composite insoluble phase was attributed to the δ OSiO vibration signal overlapping. Therefore, a silica gel was probably formed but in small amount as indicated by the weakness of the characteristic IR vibrational bands. A likely contribution to the appearance of the new vibrational bands in the composite mid-IR spectrum could be the SiOC stretching band which is observed usually at 1190 cm^{-1}. As the δ CH vibrational region between 2950 cm^{-1} and 2650 cm^{-1} in the polyester and the composite spectra were identical and as no extra signals were observed, these indicated that a small amount or no ethoxy groups were present in the composite. The ^{1}H NMR spectrum of the soluble phase, Figure 5.6 confirmed that that the residual ethoxy groups were not present in large quantity as triplet signal was observed at 1.25 ppm in $CDCl_3$[31] for the chemical shift of methyl group on ethanol. Therefore, it seems very likely that silicon, oxygen carbon bonds have been formed between the hydroxyl terminated poly(ε-caprolactone) and silica species. The formation of an insoluble gel was a good indication for the presence of covalent bonding between the organic and inorganic phases.

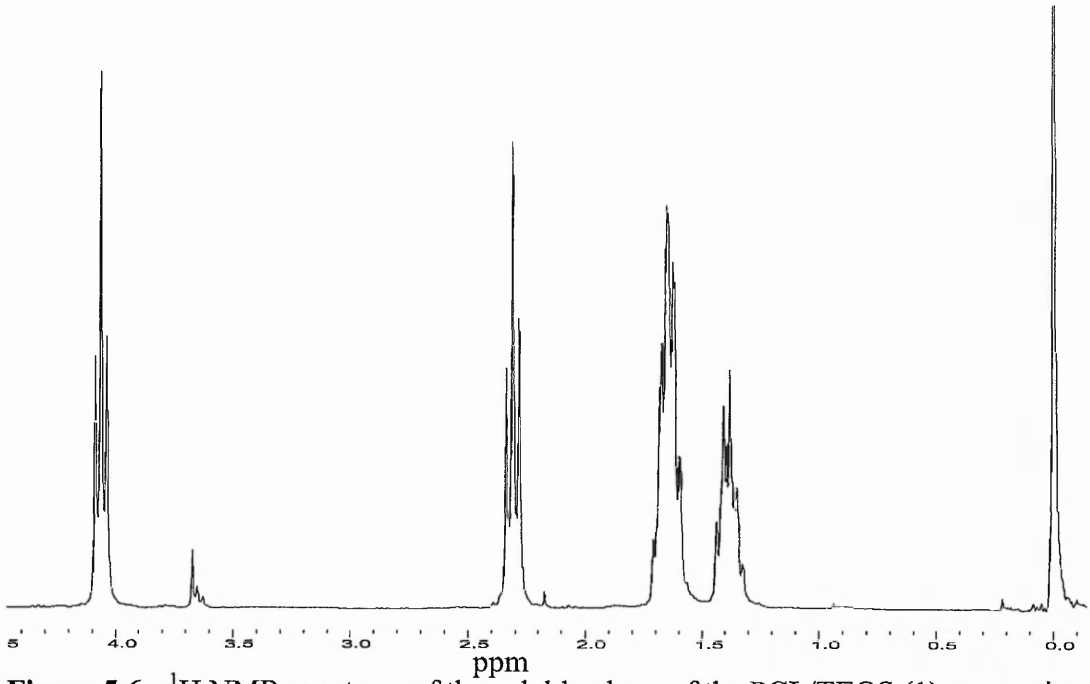

Figure 5.6 : ^{1}H NMR spectrum of the soluble phase of the PCL/TEOS (1) composite.

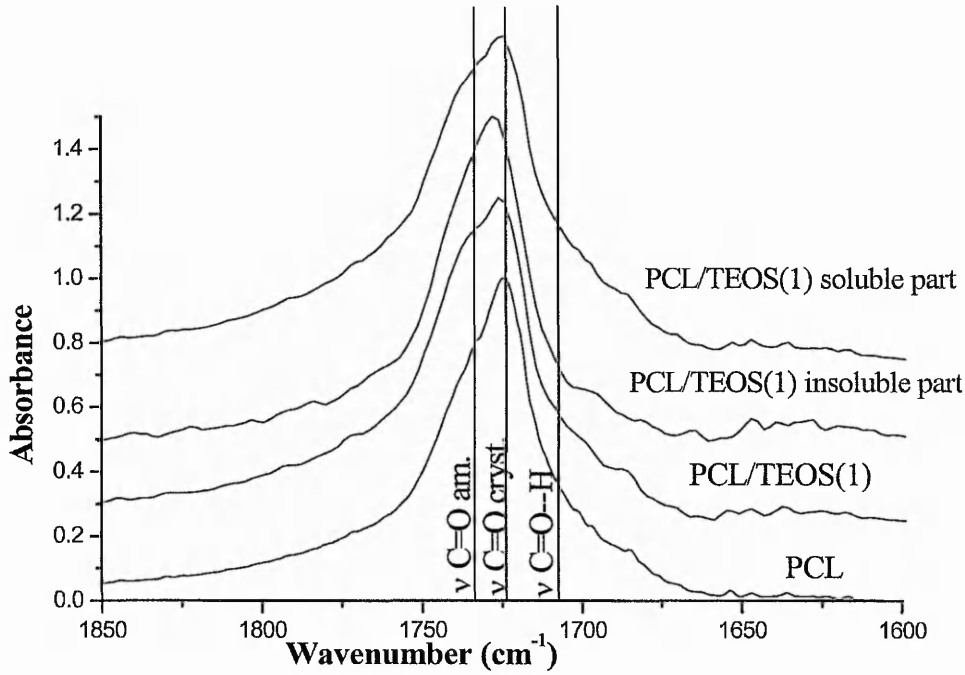

Figure 5.7 : IR spectra carbonyl stretching vibrational region of α,ω-hydroxyl poly(ε-caprolactone) (PCL), α,ω-hydroxyl poly(ε-caprolactone)/tetraethyl orthosilicate/tin(II) 2-ethylhexanoate reaction product (PCL/TEOS(1)), PCL/TEOS(1) insoluble part and PCL/TEOS(1) soluble part.

The carbonyl stretching IR band of the α,ω-hydroxyl poly(ε-caprolactone)/tetraethyl orthosilicate/tin(II) 2-ethylhexanoate reaction product was broader than the band of the α,ω-hydroxyl poly(ε-caprolactone), Figure 5.7. The increase of the ν C=O amorphous signal contribution was important and the broadening of the ν C=O band toward lower wavenumber at around 1700 cm^{-1} indicated the likely contribution of ν C=O hydrogen bonded signal. These observations as discussed in an early chapter, showed the decrease of polymer crystallinity in the composites and the formation of a co-continuous network composite.

The examination of the frequency region at 575 cm^{-1} in the spectrum of the prepared composite, Figure 5.5, did not reveal the presence of a signal characteristic of the ν SiOSn[27]. The small catalytic amount of organotin used could explain why the vibration was not observed, however some of the materials prepared using this preparation method with high catalyst content (around 2 % total weight) showed a slight yellow coloration that could be attributed to Sn-O-Si or/and Sn-O-Sn gel[28].

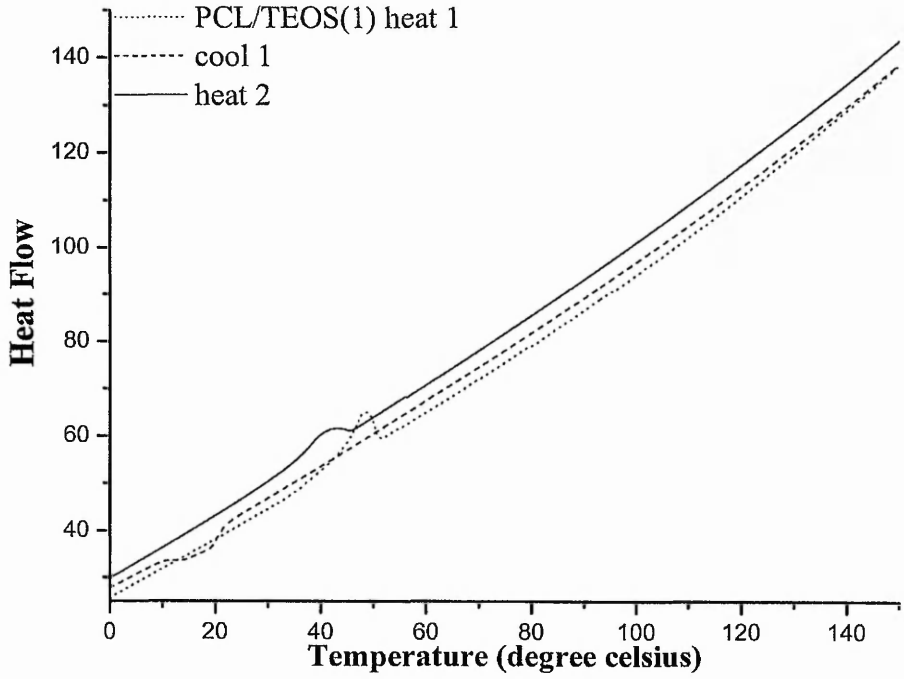

Figure 5.8 : DSC thermogram of the α,ω-hydroxyl poly(ε-caprolactone)/ tetraethyl orthosilicate /tin(II) 2-ethylhexanoate reaction product (PCL/TEOS(1)).

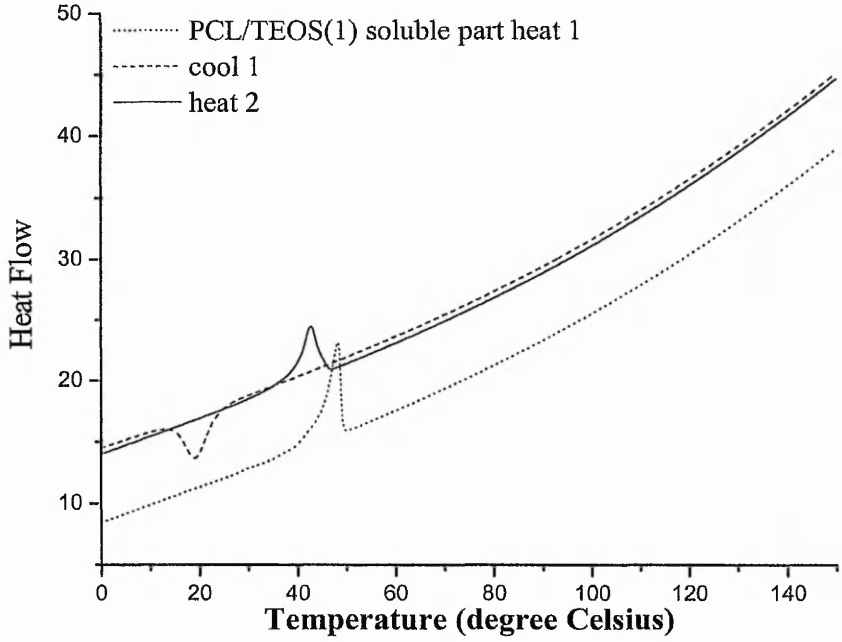

Figure 5.9 : DSC thermogram of the α,ω-hydroxyl poly(ε-caprolactone)/ tetraethyl orthosilicate/ tin(II) 2-ethylhexanoate reaction soluble product (PCL/TEOS(1)).

The differential scanning calorimetrie analysis of the PCL/TEOS(1) materials showed an important shift of the melting temperature toward lower value 40.46 °C and 44.71 °C respectively, Figures 5.8 and 5.9. The ΔH_f calculated were equal to 33.93 J/g and 60.55 J/g. Further more, The TGA analysis of the PCL/TEOS(1) product (data not shown here) gave a residual final weight of silica equal to 5 percent of the total initial weight. The Cr_{DSC} value calculated for the composite was equal to 0.264 (Cr_{DSC} initial polyester equal to 0.580). The polyester crystallinity decreased drastically with the incorporation of silica. The comparison of the composites Cr_{DSC} values with 95 % weight content of poly(ε-caprolactone) prepared by this method (Cr_{DSC} equal to 0.264) and the sol-gel method (Cr_{DSC} value of 0.570) indicated that the synthesis method using the organotin catalyst was more efficient in term of interaction of the organic and inorganic phases (covalent bonds) than the sol-gel method. The final amount of silica was less important than the theoretical amount added (30 % weight content silica). This indicated that a large amount of TEOS was stripped out in the conditions of the reaction (85 °C under vacuum).

A similar experiment was carried out at 40 °C for 24 hours with the use of a co-solvent, tetrahydrofuran, at a concentration equal to 4 times the concentration of poly(ε-caprolactone) used. The mixture was heated at 80 °C under vacuum for 5 hours to remove the solvent. The product was partly solubilised in tetrahydrofuran. The soluble and insoluble part (white particles) were separated, dried and analysed by FTIR analysis (Figure 5.10).

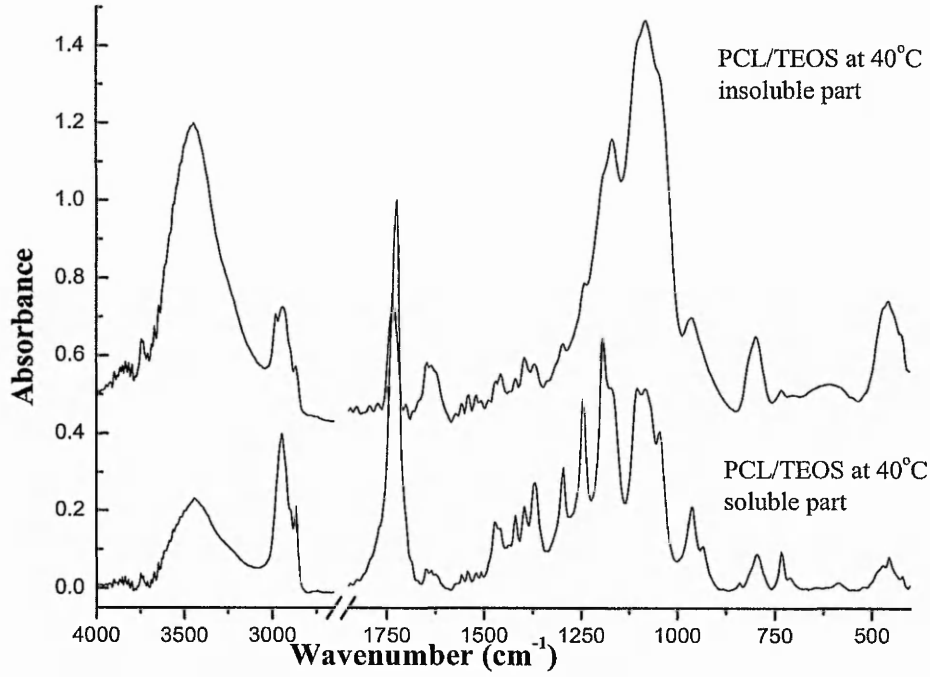

Figure 5.10 : Mid-IR spectra of the soluble and insoluble phases of the PCL/TEOS reaction carried out at 40 °C in tetrahydrofuran.

Figure 5.10 showed that the insoluble part of the material consisted mainly of silica gel. The stretching vibration ν SiOSi at 1200 cm^{-1} and 1075 cm^{-1} were clearly observed as well as the δ OSiO at 450 cm^{-1} and the δ SiOH at 950 cm^{-1}. A narrow signal was observed at 1730 cm^{-1} attributable to the stretching carbonyl groups of the poly(ε-caprolactone). The mid-IR spectrum of the soluble part contained signals attributable mainly to the poly(ε-caprolactone) but also showed the presence of silica vibrational bands at 1200 cm^{-1}, 1100 cm^{-1} and 450 cm^{-1}. The results indicated that at room

temperature the hydrolysis-condensation reaction of tetraethyl orthosilicates was probably predominant as a silica network was formed as shown in Figure 5.10. The cross-linking with the α,ω-hydroxyl poly(ε-caprolactone) did not seem to occur, or only to a small degree, as most of the silica phase of the material was separated from the organic phase by dissolution of the polyester in tetrahydrofuran.

A set of experiments was carried out to determine the effect of the following procedural modifications; the effect of the use of the T22EH catalyst for the ring-opening polymerisation of ε-caprolactone and the hydrolysis-condensation of tetraethyl orthosilicate and cross-linking reactions. Three variant procedures were also carried out. The tetraethyl orthosilicate was added in the PCL reaction (PCL/TEOS(2)) as for the PCL/TEOS(1) reaction. The tetraethyl orthosilicate and water were added sequentially in the ring opening polymerisation of ε-caprolactone (PCL/TEOS/H_2O reaction). A pre-hydrolysed tetraethyl orthosilicate was added in the α,ω-hydroxyl poly(ε-caprolactone) ring-opening reaction catalysed by T22EH (PCL/(TEOS/EtOH/H_2O/HCl) (1) reaction). The reaction descriptions are listed Table 5.1. The aim of the last two procedures was to be able to form a composite with relatively high silica gel content with silanol groups because it was important for the apatite-forming ability of other composite materials investigated (chapter 4).

The following procedure is an example of the PCL/(TEOS/EtOH/H_2O/HCl) (1) reaction. The ring-opening polymerisation of ε-caprolactone ($2.6\ 10^{-2}$ mole) was carried out in the bulk at 100 °C in the presence of $5.3\ x10^{-5}$ mole of T22EH for 20 hours under an atmosphere of nitrogen without co-initiator except for the trace of moisture in the reaction mixture. A pre-hydrolysed silica solution (TEOS ($4.3\ x10^{-3}$ mole) /EtOH/H_2O/HCl molar ratio 1/4/4/0.1 at room temperature for 1 hour) was added to the viscous polymerisation reaction. The mixture was mechanically stirred and heated for 4 hours at 100 °C under a strong nitrogen flow to allow the rapid removal of ethanol. The reactor was equipped with a liquid nitrogen finger trap. The reaction product was characterised by several analysis techniques.

The number average molecular weight and the polydispersity in the 4 experiments were measured by gel permeation chromatography as a function of the reaction time. The results are shown Figures 5.11 and 5.12.

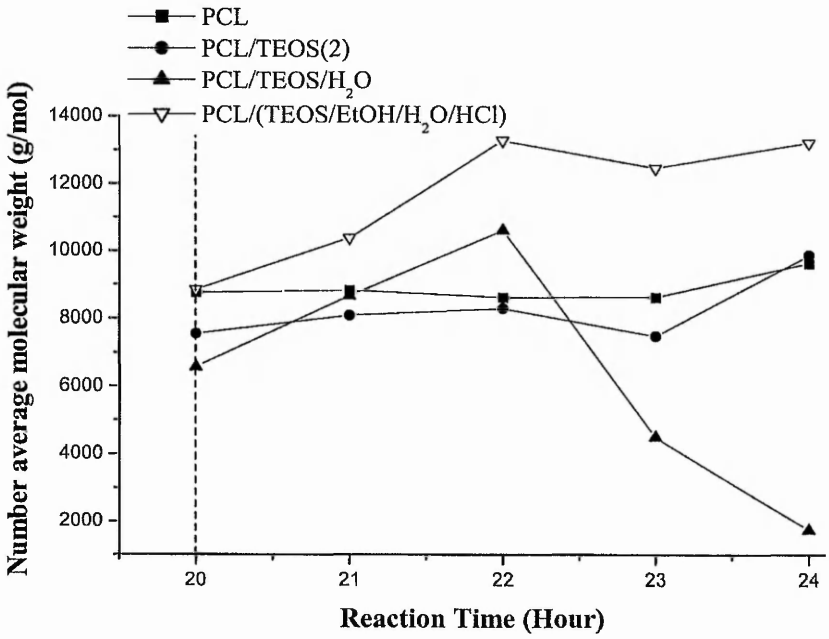

Figure 5.11 : Number average molecular weight of poly(ε-caprolactone) measured by GPC as a function of the reaction time for the PCL, PCL/TEOS(2), PCL/TEOS/H_2O and PCL/(TEOS/EtOH/H_2O/HCl) (1) reactions.

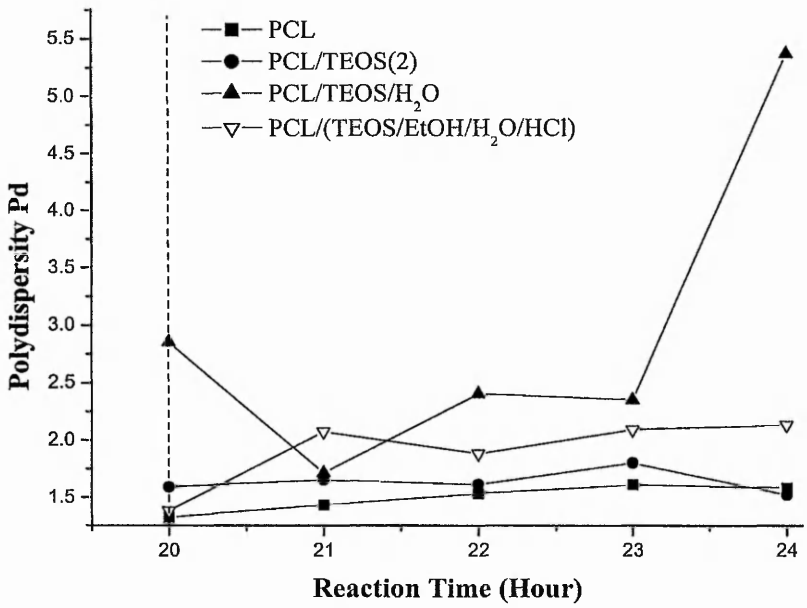

Figure 5.12 : Polydispersity of poly(ε-caprolactone) measured by GPC as a function of the reaction time for the PCL, PCL/TEOS(2), PCL/TEOS/H_2O and PCL/(TEOS/EtOH/H_2O/HCl) (1) reactions.

Figures 5.11 and 5.12 showed for the ring-opening polymerisation of ε-caprolactone (PCL) a slight increase of M_n from 8,751 g/mol after 20 hours of reaction to 9,628 g/mol after 24 hours of reaction. The polydispersity was equal to 1.38 at 20 hours and increased to 1.58 after 24 hours of reaction. The conversion rate of the ε-caprolactone was calculated from the liquid ^1H NMR spectrum of the polyester (spectrum not shown). The value of the conversion rate was 61.10 % after 24 hours indicating the presence of a large amount of un-reacted ε-caprolactone. The results for the PCL/TEOS(2) reaction, M_n, Pd and conversion rate showed that the final lactone conversion was equal to 86.60 %; higher than for the ring-opening polymerisation reaction (PCL). The number average molecular weight and the polydispersity measured were comparable to those of the PCL reaction. The reaction with the sequential addition of TEOS and water (PCL/TEOS/H_2O) had its M_n value increasing slightly upon the addition of TEOS and then an important decrease was observed when water was added. The consumption of lactone was complete after 24 hours of reaction as the final conversion was equal to 99.40 %. The polydispersity increased to 5.36 after the addition of water. The final reaction which consisted of the addition of pre-hydrolysed

TEOS in the ring-opening polymerisation of ε-caprolactone (PCL/(TEOS/EtOH/H_2O/HCl)) (1) showed an increasing poly(ε-caprolactone) M_n value from 8,839 g/mol before the addition of the silica species up to 13,220 g/mol at the end of the experiment. The polydispersity stayed relatively constant at 2.10 ± 0.1.

The results showed that the addition of TEOS did not increase significantly the average molecular number and polydispersity of the prepared material (PCL/TEOS(2)). It was observed that a cross-linked gel material was not formed as observed for PCL/TEOS(1) when tetrahydrofuran was added the product of the PCL/TEOS(2) reaction. A completely soluble material was obtained. The mid-IR analysis was carried out on the material dissolved in tetrahydrofuran, filtered, reprecipitated in cold methanol and finally dried, Figure 5.13.

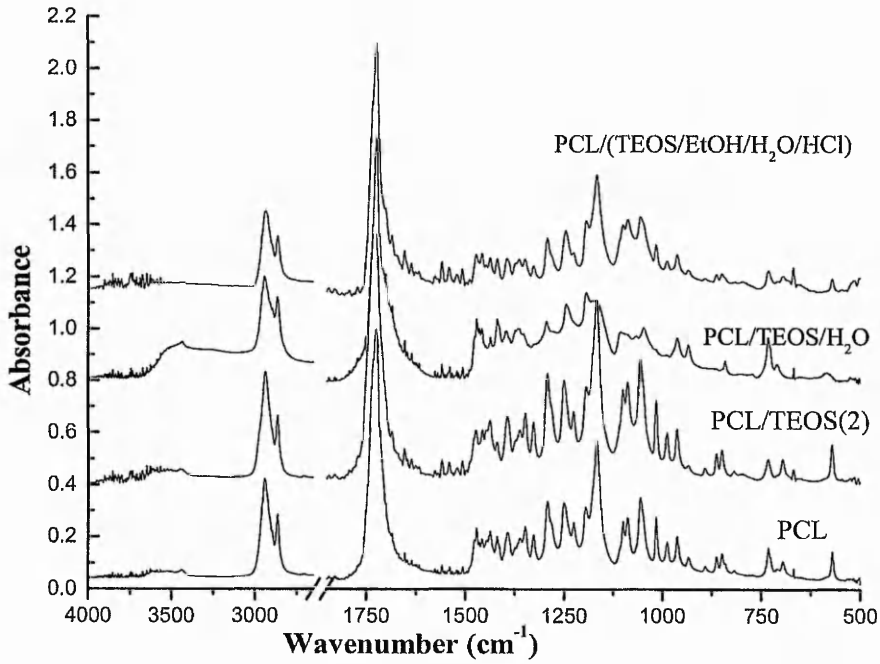

Figure 5.13 : IR spectra from 4000 cm^{-1} to 2650 cm^{-1} and from 1850 cm^{-1} to 500 cm^{-1} of α,ω-hydroxyl poly(ε-caprolactone) (PCL), α,ω-hydroxyl poly(ε-caprolactone)/Tetraethyl orthosilicate/tin(II) 2-ethylhexanoate (PCL/TEOS(2)), PCL/TEOS/H_2O and PCL/(TEOS/EtOH/H_2O/HCl) (1) reaction products.

Table 5.2 : IR assignments of some important vibrational bands of the poly(ε-caprolactone) and silica sol-gel and the frequency of signals observed for the PCL, PCL/TEOS(2), PCL/TEOS/H_2O and PCL/(TEOS/EtOH/H_2O/HCl) (1) reaction products (see Table 5.1 for the description of the reaction procedures).

Assignment	Frequency (cm^{-1})	PCL	PCL/ TEOS(2)	PCL/TEOS /H_2O	PCL/(TEOS/ EtOH/H_2O/HCl)
-OH (H bonded)	3500-3450	3462	3462	3452	-
νC=O	1733-1725	1726	1734	1717	1725
δ(H_2O)	1677	-	-	-	-
νs(Si-O-Si)	1200-1100				
νSiOC	1190			1195-1165(b)	1110(b)
νas(Si-O-Si)	1076(b)			1109(b)	1054(b)
δ(Si-OH)	950				942
δOSiO(LO)	550			590	552
δOSiO(TO)	450				453

(b) broad band

Table 5.2 lists the more interesting IR vibrational bands observed, Figure 5.13, for PCL/TEOS(2) and the other prepared materials. Tetraethyl orthosilicates did not cross-link with the polyester in the conditions of the PCL/TEOS(2) experiment as the vibration bands assign to silica gel and to Si-O-C bonds were not observed. For the sequential addition of TEOS and water in the ring-opening polymerisation of ε-caprolactone reaction (PCL/TEOS/H_2O), the water acted as a co-initiator for the ring-opening polymerisation of the ε-caprolactone. For this reason, the poly(ε-caprolactone) M_n value dropped from 10,600 g/mol to 1,739 g/mol and the polydispersity increased from 2.35 to 5.36. The mid-IR analysis data of the soluble part of the PCL/TEOS/H_2O reaction product showed vibrational bands attributable to a silica network, Table 5.2, indicating that cross-linking reaction occurred in some extent. It must be noticed that the νs Si-OH vibrational band at 950 cm^{-1} was not observed. Finally, for the addition of the pre-hydrolysed TEOS in the ring-opening reaction of ε-caprolactone, the poly(ε-caprolactone) (PCL/(TEOS/EtOH/H_2O/HCl) (1)), the number average molecular weight, M_n increased from 8,839 g/mol to a final M_n value equal to 13,220 g/mol higher than the final M_n 9,628 g/mol of the ring-opening polymerisation (PCL). The polydispersity increased also but in a lesser extent that for the PCL/TEOS/H_2O reaction. The results indicated the probable cross-linking of the poly(ε-caprolactone) with the

silica. This was confirmed by the presence of vibrational bands in the mid-IR spectrum of the soluble part of the material arising for silica-oxygen bonds and moreover a band at 942 cm^{-1} was observed and possibly attributable to silanol groups on the surface of a silica gel. The shift of frequency observed compared to the usually observed δ Si-OH bond at 950 cm^{-1} could be due to hydrogen bonding with the carbonyl groups of the poly(ε-caprolactone).

Liquid ^{29}Si NMR analysis on the materials product was not successful as the concentration of silica in the materials was probably not high enough that it could be observed with the instrument at our disposition and in a reasonable time scale (<48 hours). The insolubility of the materials such as the TEOS/PCL(1) which formed a gel also deterred the use of this analytical technique. However, the liquid ^{29}Si NMR analysis at low temperature of the pre-hydrolysed TEOS allowed the determination of the silica species added to the ε-caprolactone ring-opening polymerisation in the PCL/(TEOS/EtOH/H_2O/HCL) (1) reaction. Figure 5.14 and Table 5.3 give the liquid ^{29}Si NMR results.

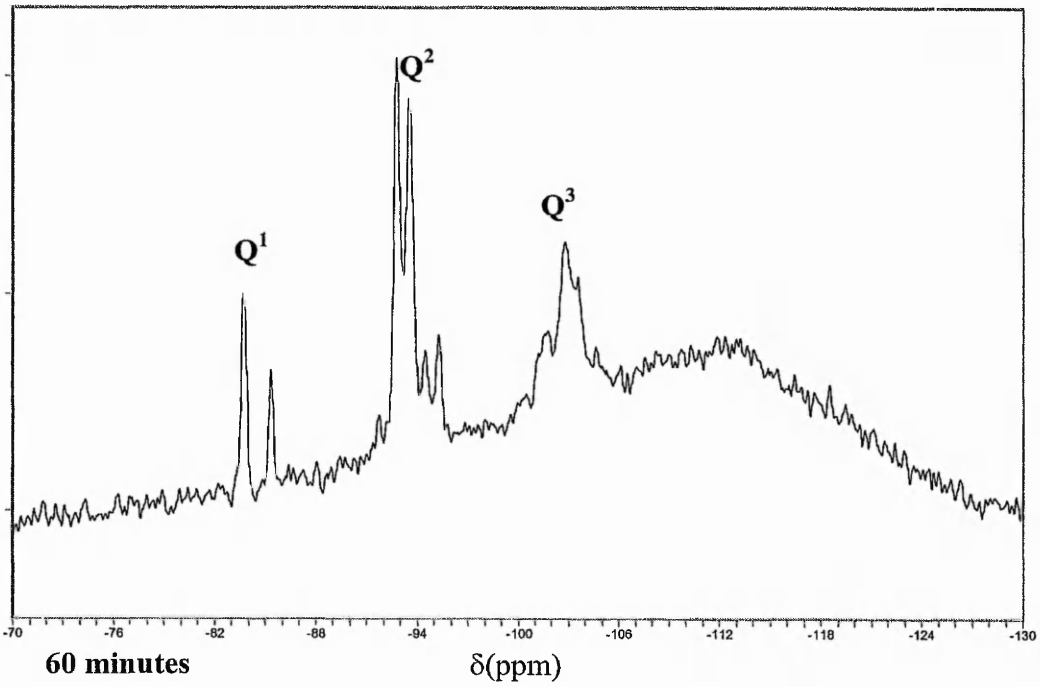

Figure 5.14: Liquid ^{29}Si NMR spectrum of tetraethyl orthosilicate in presence of ethanol, water and hydrochloric acid (molar ratios 1/4/4/0.1) after 60 minutes at room temperature (sample withdrawn was frozen in liquid nitrogen and NMR analysis carried out at - 60 °C to avoid variation of silica species distribution).

Table 5.3: Assignments and chemical shifts of liquid ^{29}Si NMR analysis; from the literature[32] and the hydrolysis-condensation reaction of TEOS at room temperature for 60 minutes and 120 minutes.

Groups	Species	Shift (ppm) literature	60 minutes	120 minutes
	Si$(OH)_4$	-73.87		
	Si$(OC_2H_5)(OH)_3$	-75.37		
Q^0	**Si**$(OC_2H_5)_2(OH)_2$	-77.06		
	Si$(OC_2H_5)_3OH$	-79.10		
TEOS	**Si**$(OC_2H_5)_4$	-81.78	-	-
	Si**O**Si$(OH)_3$	-83.21		
	Si**O**Si$(OH)_3$	-83.42	-83.71	
	Si**O**Si$(OC_2H_5)(OH)_2$	-84.82		
Q^1	Si**O**Si$(OC_2H_5)(OH)_2$	-84.99	-85.36	
	Si**O**Si$(OC_2H_5)_2OH$	-86.31		
	Linear			
	Si**O**Si$(OC_2H_5)_2OH$	-86.83		
	Cyclic			
	$(SiO)_2$**Si**$(OH)_2$ linear	-92.22	-91.74	-91.75
	$(SiO)_2$**Si**$(OH)(OC_2H_5)$	-92.97	-92.76	
	cyclic			
Q^2	$(SiO)_2$**Si**$(OH)(OC_2H_5)$	-93.96	-93.52	-94.03
	Linear		-94.48	
	$(SiO)_2$**Si**$(OC_2H_5)_2$ cyclic	-94.69	-95.31	
	$(SiO)_3$**Si**(OH)	-100.46	-100.49	-97.08
Q^3	$(SiO)_3$**Si**(OC_2H_5)	-101.88	-101.68	-99.18
	$(SiO)_3$**Si**(OH)	-102.05	-102.56	-101.54
			-103.38	
			-104.22	
			-106.12	-106.95
Q^4	$(SiO)_4$**Si**	-110.0		

Where $Q^n = (RO)_{4-n}Si(-OSi\ )_n$ [R = H or C_2H_5]

The silica species added in the ring-opening polymerisation of ε-caprolactone in the second step of the PCL/(TEOS/EtOH/H_2O/HCl) (1) reaction were probably oligomeric silica species. Table 5.3 and Figure 5.14 showed mostly Q^2 and Q^3 silica species with some Q^0 silica species in the hydrolysis-condensation reactions of TEOS after for 60 minute. Q^4 species were not observed as the silica glass NMR tube presented a broad large signal at similar chemical shift, -110 ppm but they were probably present.

Solid state ^{29}Si NMR analysis was carried out on the PCL/(TEOS/EtOH/H_2O/HCl) (1) reaction product. The ^{29}Si analysis was performed on a Brucker DSX400 instrument (79 MHz) with a pulse of 2 microseconds and delay of 5 seconds and 2000 scans.

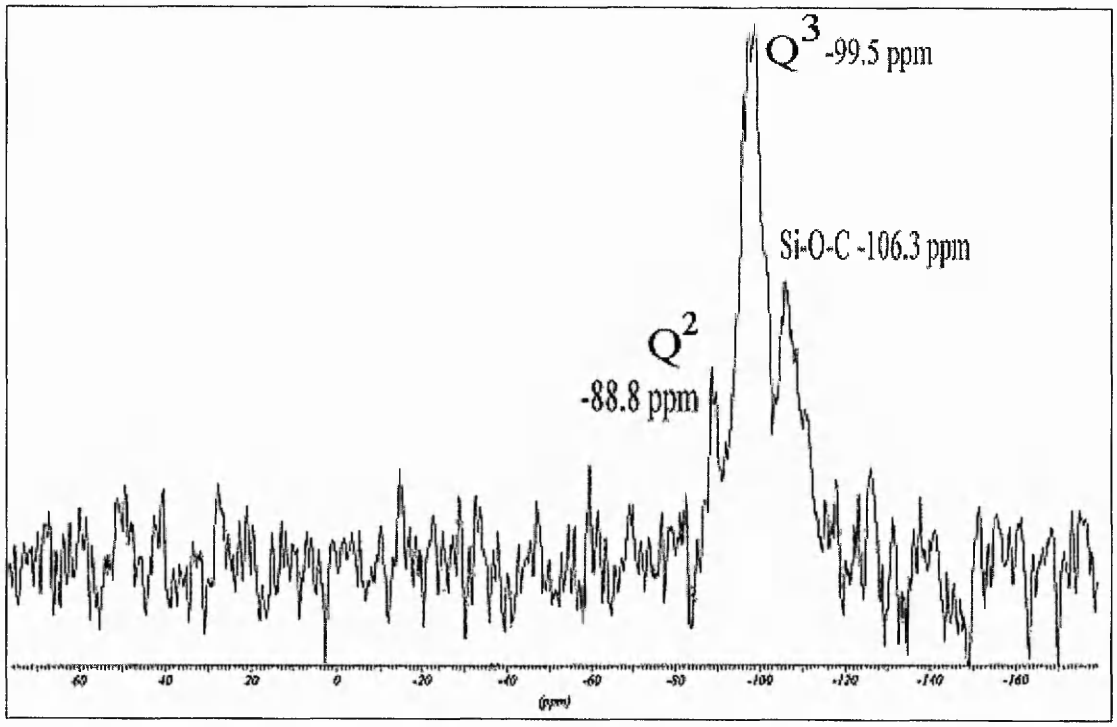

Figure 5.15 : Solid state ^{29}Si NMR spectrum of the PCL/(TEOS/EtOH/H_2O/HCl) (1) reaction product.

The solid state ^{29}Si NMR analysis of the composite prepared by adding pre-hydrolysed tetraethyl orthosilicate in the ring-opening polymerisation of ε-caprolactone, Figure 5.15 confirmed the covalent bonding between the silica and the poly(ε-caprolactone) as a signal at -106.3 ppm attributable to Si-O-C bonds[33] was observed. Other signals in the solid state ^{29}Si NMR spectrum at -88.8 ppm and 99.5 ppm were attributable to Q^2 and Q^3 silicon species. Compared to the silicon species in the pre-hydrolysed TEOS, Table 5.3, it indicated that further hydrolysis-condensation reaction occurred. Q^4 silicon species typical of a silica gel network (-110 ppm) were not detected by the solid state ^{29}Si NMR analysis. The silica phase in the material almost certainly did not form a true silica gel in the PCL/(TEOS/EtOH/H_2O/HCl) (1) reaction composite but more probably a very lose silica network.

The PCL/(TEOS/EtOH/H_2O/HCl) reaction was repeated but the time of hydrolysis and condensation reaction of the tetraethyl orthosilicate was increased to 2 hours; reaction PCL/(TEOS/EtOH/H_2O/HCl) (2). The hydrolysed TEOS was analysed by liquid state ^{29}Si NMR after 120 minutes.

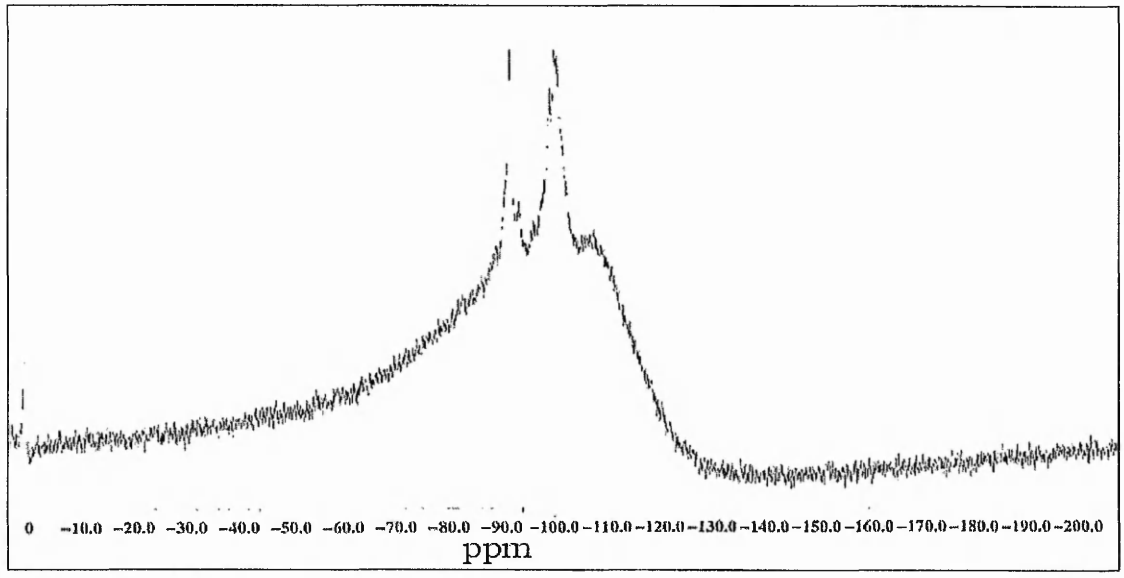

Figure 5.16 : Liquid state ^{29}Si NMR spectrum of tetraethyl orthosilicate in presence of ethanol, water and hydrochloric acid (molar ratios 1/4/4/0.1) after 120 minutes at room

Figure 5.16 showed that the silica species added in the ring-opening polymerisation of ε-caprolactone reaction were Q^2 and Q^3 species with very little probably very little alkoxysilane bonds non-hydrolysed. Compared to the results from the hydrolysis of TEOS for 60 minutes, Table 5.3, the silica species were completely hydrolysed and already starting to condense to form polymeric silica species. The PCL/(TEOS/EtOH/H_2O/HCl) (2) composite was analysed by solid state ^{29}Si NMR analysis, Figure 5.17.

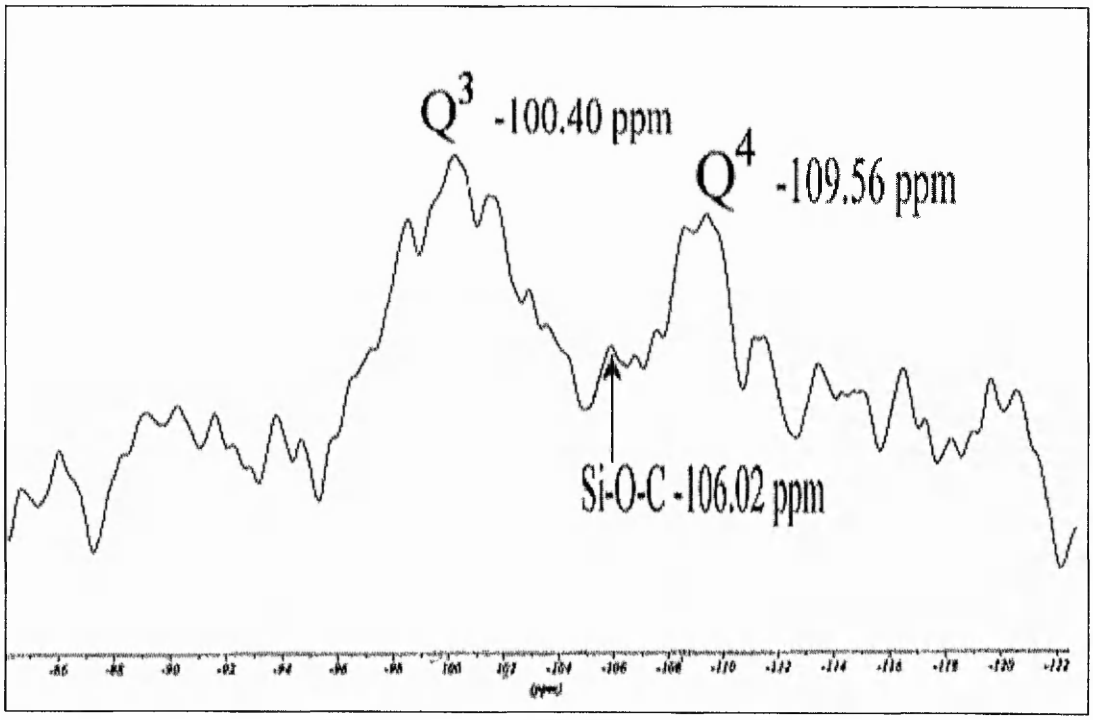

Figure 5. 17 : Solid state ^{29}Si NMR spectrum of the PCL/(TEOS/EtOH/H_2O/HCl) (2) reaction product with pre-hydrolysed reaction time of 120 minutes.

The solid state ^{29}Si NMR spectrum, Figure 5.17 showed signals at -100.40 ppm, -106.02 ppm and -109.56 ppm attributable respectively to Q^3, Si-O-C and Q^4 silicon. Compared to the solid ^{29}Si NMR spectrum of the PCL/(TEOS/EtOH/H_2O/HCl) (1) Figure 5.15, the solid NMR analysis of PCL/(TEOS/EtOH/H_2O/HCl) (2) showed a more condensed silica network. The signal attributable to Si-O-C silicon species was also weaker than for the reaction (1) compared to the intensity of the other silicon

species. Solid state ^{29}Si NMR results obtained from the two PCL/(TEOS/EtOH/H_2O/HCl) reaction (1) and (2) indicated that covalent bonding between the silica species and the polyester occurred in both cases but in a larger extent when less condensation had occurred in the pre-hydrolysed TEOS.

It must be noticed that the composite materials synthesis has not yet been optimised and that one of the important draw backs of the PCL/(TEOS/EtOH/H_2O/HCl) reaction was the addition and homogenization of the pre-hydrolysed TEOS at room temperature in the ring-opening polymerisation of ε-caprolactone at 100 °C. The mixing was not always efficient as a strong mechanical stirring was needed even at a laboratory scale (between 2 g and 5 g). The fast removal of the ethanol was also an important issue in the PCL/(TEOS/EtOH/H_2O/HCl) reaction. Ethanol reacted as a co-initiator for the ring-opening polymerisation of ε-caprolactone as did the water in the PCL/TEOS/H_2O reaction and polymer low average molecular number was obtained by transesterification reaction when it was not rapidly stripped out of the reaction mixture.

5.2.3. Discussion

The synthesis of poly(ε-caprolactone)-silica composites prepared by the cross-linking or curing reaction of alkoxysilanes with hydroxyl terminated poly(ε-caprolactone) polymers catalysed by tin(II) 2-ethylhexanoate was carried out successfully. The presence of covalent bonds between the organic and inorganic phases characteristic of a cross-linked /cured material was possibly indicated by FTIR and solid state ^{29}Si NMR analysis. The formation of a insoluble structure using the procedure PCL/TEOS(1) indicated also the formation of a cross-linked composite material. Transmission electron micrograph image of the PCL/(TEOS/EtOH/H_2O/HCl) (1) Figure 5.18 showed the co-continuous structure of the composite material. The domain size of the organic and inorganic phases was around 10 nanometers.

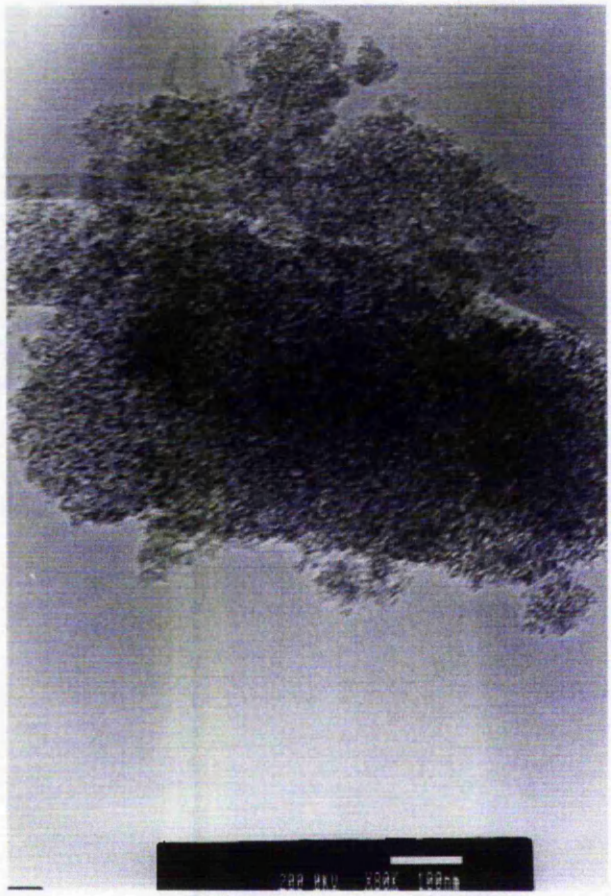

Figure 5.18 : TEM micrograph of the composite PCL/(TEOS/EtOH/H_2O/HCl) (1).

The mechanisms of the reaction were probably complex as the tin(II) 2-ethylhexanoate could act as a cross-linker between the organic and inorganic phases[25] as well as for the hydrolysis-condensation of the alkoxysilanes[28]. The mechanism of hydrolysis-condensation of tetraethyl orthosilicate with dibutyl tin diacetate has been reported[28]. The hydrolysis of the tin diacetate catalyst was proposed as the first reaction step. The hydrolysed dibutyl tin acetate then reacted with a hydrolysed tetraethyl orthosilicate to form an organotin silanolate. Another hydrolysed tetraethyl orthosilicate could condense with the organotin silanolate to yield the condensed silica species and the active organotin. Two hydrolysed tetraethyl orthosilicates could condense without catalyst but the dibutyl tin diacetate acts as a crosslinker between hydrolysed silica species. It is important to note that the gelation time of the tin doped silica gel decreased by increasing the amount of catalyst up to 10 % total weight[27] or by using partially hydrolysed TEOS[28]. In our case, the organotin catalyst used was tin(II) 2-ethylhexanoate. The hydrolysed T22EH is known to be the active form of the catalyst

and as the dibutyl tin diacetate it acts as a cross-linker between hydrolysed silica species[25]. The cross-linking of hydroxyl functional silicone and poly-functional alkoxysilane has been developed and employed in the industrial condensation reaction of vulcanized silicon rubbers[26]. The mechanism is similar to this of the condensation for hydrolysed TEOS. Tetraethyl orthosilicate and dialkyltin dicarboxylate form a organotin silanolate which reacts with the poly(dimethylsiloxane)-α,ω-diol with the formation of a new siloxane linkage and recovery of the catalyst.

In our system, the hydroxyl functional silicone was substituted by an hydroxyl functional poly(ε-caprolactone) in the presence of TEOS, T22EH and water. The condensation reaction of tetraethyl orthosilicates and the cross-linking reaction of the hydrolysed silica species with the hydroxyl functional polyester were competitive. The PCL/TEOS (1) reaction results at high and low temperature confirmed that the kinetics of the cross-linking reaction between the hydrolysed silica species and the hydroxyl functional increased with an increase of temperature[25]. For the reaction carried out with pre-hydrolysed alkoxysilanes PCL/(TEOS/EtOH/H_2O/HCl) (1), (2), the cross-linking between the hydroxyl functional polyester and the silica phase was less important with the increased of hydrolysed silica in the system[27] because the cross-linking reaction of the hydrolysed alkoxysilane became dominant. This was confirmed by solid state ^{29}Si NMR analysis that showed a more intense Si-O-C signal for reaction (1) than reaction (2) where the hydrolysis time was increased. It is also probable that the miscibility of the silica species in the melted polyester decreased with the increase of the silica specie size and therefore the cross-linking reaction was also disadvantaged. Furthermore, in the PCL/TEOS/T22EH (2) procedure, T22EH was used consecutively for the ring-opening polymerisation of ε-caprolactone and the cross-linking reaction with the TEOS. The conversion of the lactone was not complete when tetraethyl orthosilicate was added and it was observed that an adding of tetraethyl orthosilicate a quick consumption of the lactone occurred. It was probable in the condition of the reaction (high temperature), that the insertion of organic and inorganic materials was prevalent. Also, it is most likely that one molecule of lactone reacts more easily with the tin silanolate species than one molecule of hydroxyl functional poly(ε-caprolactone). This explains why little insertion occurred between the organic macromolecule and the silica phase and no

cross-linked composite was obtained. Therefore, it is critical for the cross-linking of the hydroxyl functional polyester with silica species catalysed by T22EH to avoid the presence of ε-caprolactone. This also is in accordance with the fact that removing ethanol during the "curing" or cross-linking phase is important to minimise the possibility of reaction between the alcohol and the tin-silanolate species to yield back the tin catalyst and the alkoxysilane. The PCL/TEOS/H_2O reaction showed that water was also critical. The addition of water decreased drastically the polyester M_n and increased the polydispersity of the final polyester. Water added after the addition of tetraethyl orthosilicate in the ring-opening polymerisation of the ε-caprolactone had an effect. The water speeded up the hydrolysis reaction of TEOS but it also acted as a co-initiator for the polymerisation of lactone. Therefore, the increase of polydispersity of the polyester was probably due to the ring-opening polymerisation of un-reacted ε-caprolactone, the final molecular weight of these last formed polyesters being controlled by the amount of water in the reaction. It is also possible that the poly(ε-caprolactone) transesterification (inter or intramolecular) reaction and degradation could occur at high temperature as reported for the ring-opening polymerisation of lactide[14] which again could be responsible for the decrease of the polyester molecular weight.

5.3. Example of a Poly(ε-caprolactone)-Silica Composite Prepared by PCL/(TMOS/MeOH/H_2O/HCl) Reaction Method, Characterisation and *In vitro* Apatite-Forming Ability.

The *in vitro* apatite-forming ability of a composite prepared by the addition of pre-hydrolysed alkoxysilane in the ring-opening polymerisation of ε-caprolactone was tested. The mechanical properties of the composite were also characterised using differential mechanical thermo analysis. The objectives were to investigate the possibility of preparing a composite material with bioactivity properties and mechanical properties suitable for future biomedical applications.

5.3.1. Composite Preparation and Characterisation

The preparation method used was derived from the preparation of the PCL/(TEOS/EtOH/H_2O/HCl) (1). However instead of tetraethyl orthosilicate, tetramethyl orthosilicate (TMOS) was used because it was thought that the removal of methanol during the reaction would be faster than the removing of ethanol because of its lower boiling point. The preparation procedure was as follows; in dry conditions, 0.306 mole of ε-caprolactone, 1.75 $x10^{-4}$ mole of propanediol and 6.13 $x10^{-4}$ mole of T22EH were added, stirred and heated at 100 °C for 20 hours under nitrogen (conversion rate 99.0 % calculated using ^{1}H NMR spectrum). 5.64 $x10^{-2}$ mole of tetramethyl orthosilicate (TMOS), in presence of methanol (MeOH), water and hydrochloric acid (HCl); molar ratio 1/4/4/0.1 was pre-hydrolysed at room temperature for 15 minutes. The liquid state ^{29}Si NMR spectrum of the pre-hydrolysed TMOS after 15 minutes, Figure 5.19, showed the presence of Q^2 and Q^3 silica species, and Q^1 in very small quantity. The silica species present are close to what could have been obtained for the pre-hydrolysed TEOS after 120 minutes. The higher reactivity of tetramethyl orthosilicate toward hydrolysis-condensation reactions explained why shorter time of hydrolysis was used. The pre-hydrolyzed TMOS was added to the ring opening polymerisation reaction of the ε-caprolactone at 100 °C under a strong nitrogen flow and strong stirring. A cold trap of liquid nitrogen was used to remove and trap the methanol. The reaction was then carried out for a further 4 hours at 100 °C. Half of the product was collected. The other half was heated at 130 °C equipped with a stirrer under an atmosphere of nitrogen and 5.94 $x10^{-4}$ mole of hexamethyldiisocyanate (HMDI) was added via a septum with a syringe and the mixture stirred until it stopped. Then, the solid was heated for 24 hours at 130 °C. 200 ml of toluene was added to the flask. The insoluble gel obtained was collected and washed with cold methanol. The white solid obtained was dried under vacuum for 24 hours. The prepared materials were analysed by TGA, DSC, GPC and ^{1}H NMR analysis.

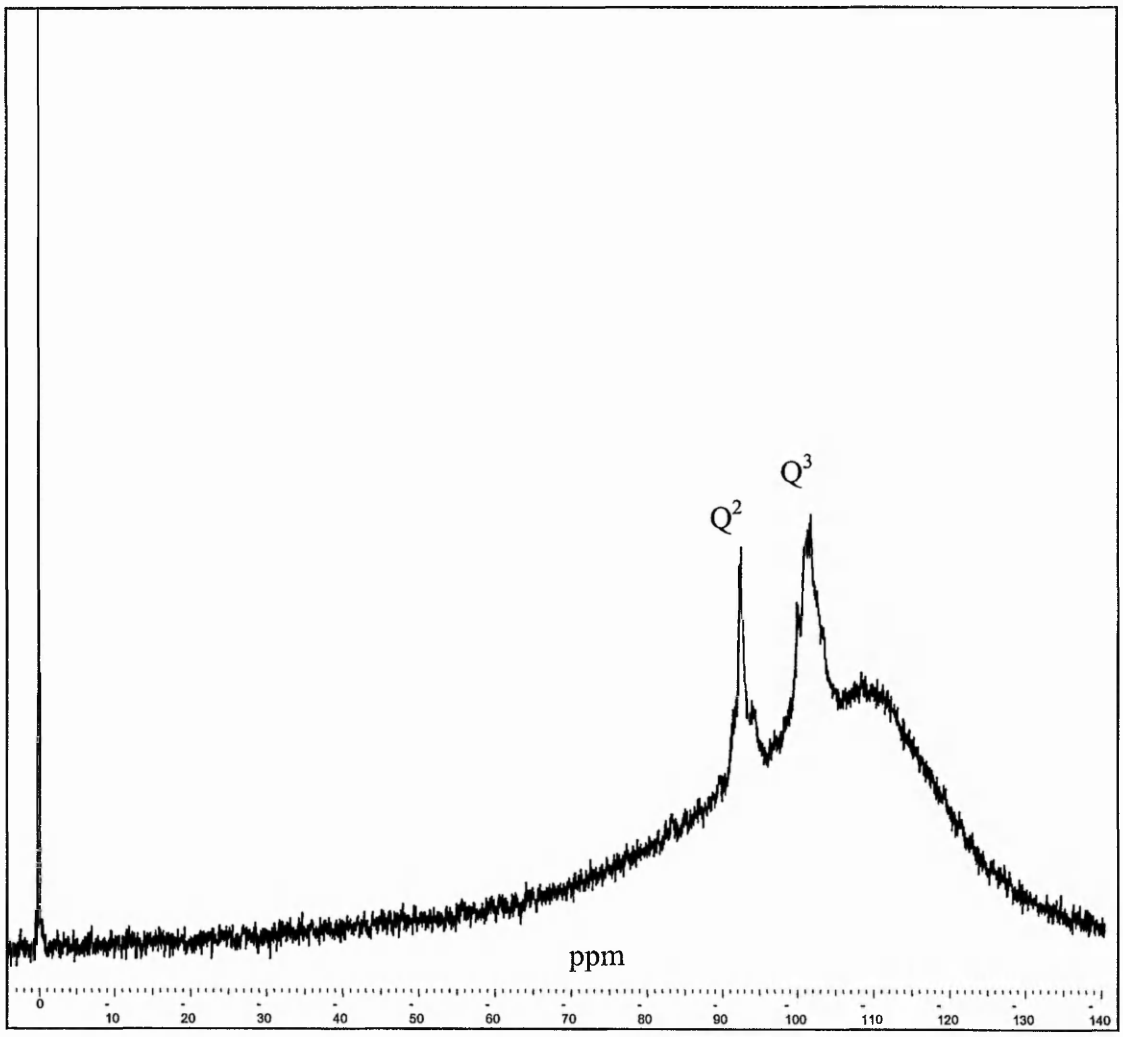

Figure 5.19 : Liquid state ^{29}Si NMR spectrum of tetramethyl orthosilicate in presence of methanol, water and hydrochloric acid (molar ratios 1/4/4/0.1) after 15 minutes at room temperature (sample withdrawn was frozen in liquid nitrogen and NMR analysis carried out at 60 °C to avoid variation of silica species distribution).

Table 5.4 lists the number average molecular weights calculated from GPC and ^{1}H NMR data and the polydispersity of the prepared poly(ε-caprolactone) and the poly(ε-caprolactone)-polysilicic acid composite.

Table 5.4 : M_n and Pd of poly(ε-caprolactone) and the poly(ε-caprolactone)-silica composite.

Sample Name	M_n (g.mol^{-1}) ^{1}H NMR	GPC	Pd
Poly(ε-caprolactone)	48,055	60,000	2.1
Poly(ε-caprolactone)-silica	21,005	8,123	2.77
Poly(ε-caprolactone)-silica + HMDI (Soluble Part)		8,614	

The data presented in Table 5.4, shows that the addition of pre-hydrolysed TMOS in the ring-opening polymerisation of ε-caprolactone decreased the number average molecular weight of the poly(ε-caprolactone) and increased the polydispersity from 2.1 to 2.77. This indicated the possible trans-esterification and backbiting of the polyester chains by the tin catalyst[12]. The thermo-gravimetric analysis results, Figure 5.19 showed that the composite had a organic part which degraded at lower temperature than the poly(ε-caprolactone) initial, confirming the backbiting of the polyester. The soluble part of the HMDI cross-linked poly(ε-caprolactone)-silica composite had a M_n (8,614 g.mol^{-1}) nearly equal to the non cross-linked composite (8,123 g.mol^{-1}) suggesting that a part of the polyester did not react with the hexamethyldiisocyanate. The thermograph of the cross-linked composite, Figure 5.20, shows a thermal degradation profile close to this of the initial high number average molecular weight.

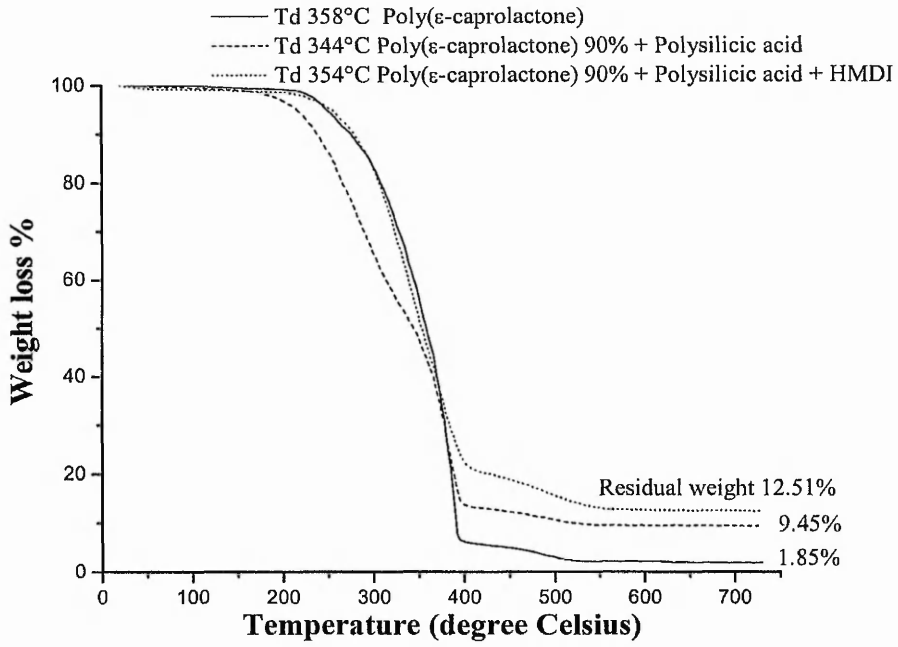

Figure 5. 20 : TGA curves for poly(ε-caprolactone), poly(ε-caprolactone)-polysilicic acid with 90 % weight content poly(ε-caprolactone) and poly(ε-caprolactone)-polysilicic acid 90 % cross-linked with hexamethyldiisocyanate (HMDI).

Table 5.5 lists the melting temperature, the onset, the enthalpy and the crystallinity measured by differential scanning calorimetry.

Table 5.5 : T_m, onset and ΔH_f and crystallinity of the materials from second heating DSC curves.

Sample Name	T_m (°C)	Onset (°C)	ΔH_f (J/g)	Cr
poly(ε-caprolactone)	54.55	51.41	52.25	0.390
poly(ε-caprolactone) 90%-silica	54.06	50.89	53.02	0.430
poly(ε-caprolactone) 90%-silica + HMDI	50.86	45.61	21.42	0.180

ΔH_f^0 = 135.31 J/g for pure 100 % crystalline poly(ε-caprolactone)

The DSC results, Table 5.5 showed that the poly(ε-caprolactone) 90 %- silica composite had a Cr_{DSC} equal to 0.43 higher than the poly(ε-caprolactone) obtained from the ring-opening polymerisation reaction, Cr_{DSC} equal to 0.390, or for the sol-gel

materials studied in chapter 3. An increase of crystallinity measured by DSC denoted an heterogeneous composite. But the M_n measured by GPC (Table 5.4) was 60,000 $g.mol^{-1}$ for the polyester and 8,123 $g.mol^{-1}$ for the composite and it is known that a polymer with smaller chains crystallises more easily than a polymer with longer chains. These explains the apparently contradictory results. Figure 5.21 shows the characteristic DSC curves for the cross-linked composite.

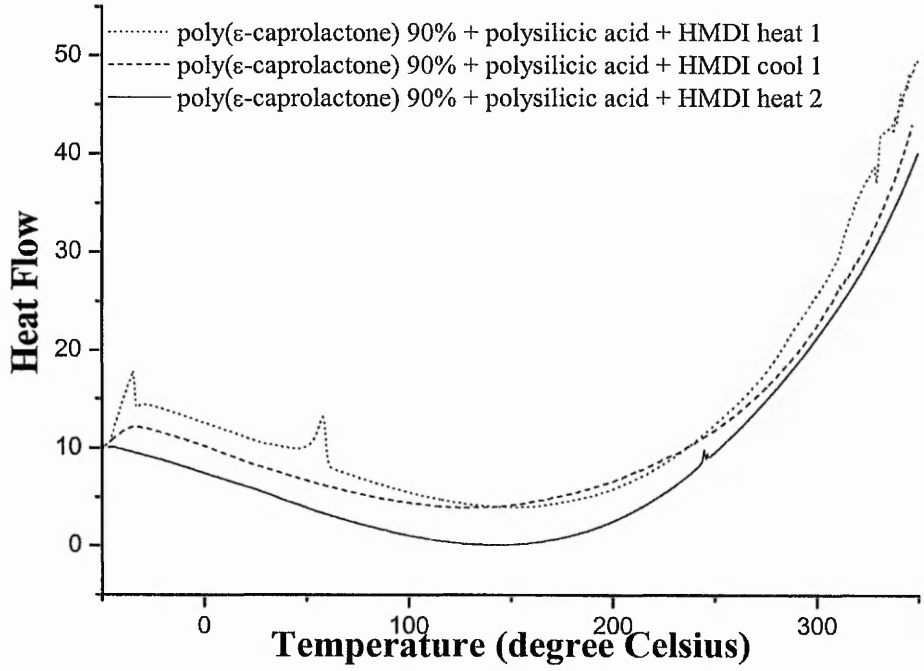

Figure 5.21 : DSC curves of poly(ε-caprolactone) 90 %-silica composite cross-linked with hexamethyldiisocyante (HMDI).

The materials prepared in this section had their mechanical properties characterised using differential mechanical thermal analysis. It must be noted that the tests were carried out by S&N laboratory at York. Samples were pressed as thin (0.8 mm) sheets. The tests were performed on a Rheometrics RSA2 (DMTA) with the specimens in a three-point bending mode. Two tests were performed, ramp load/deformation at room temperature and temperature ramp (5 $°C.min^{-1}$) from room

temperature up to 80 °C, with fixed frequency (10 s^{-1}) and fixed strain (0.05 %). The choice of span depended on the dimensions of the sample supplied. Strength was tested on a small dumbbell specimen, using a Zwick 1435 instrument initially (first sample) with 200 N load cell and later with 5 kN load cell, using cross-hatched metal faced grips at 50 $mm.min^{-1}$ in tension. The results are presented in Table 5.6. The measures were done in triplicate except when the quantity of material was not sufficient, then the individual response was noted

Table 5.6 : Results of mechanical tests.

Sample	**Modulus at 0.25% strain (MPa)**			
Poly(ε-caprolactone)	440-430			
Poly(ε-caprolactone) 90%-silica	480			
Poly(ε-caprolactone) 90%-silica + HMDI	610			
	Dynamic modulus 40°C (MPa)		**tan(delta) at 40°C**	**Temperature of modulus drop**
	E'	**E''**		
Poly(ε-caprolactone)	900	20	0.02	52
Poly(ε-caprolactone) 90%-silica	400	20	0.05	52
Poly(ε-caprolactone) 90%-silica + HMDI	500	20	0.04	60
	Strength (at max. load) (MPa) [Standard deviation]		**Strain at break (%)**	
Poly(ε-caprolactone)	17, 19		200, 500	
Poly(ε-caprolactone) 90%-silica	8.1 [1]		3.4 [0.5]	
Poly(ε-caprolactone) 90%-silica + HMDI	11 [1]		16 [5]	

The results, Table 5.6 showed that the poly(ε-caprolactone) had the highest dynamic modulus at 40 °C, 900 MPa compared to 400 MPa and 500 MPa for the poly(ε-caprolactone) 90 %-silica composite and the cross-linked composite. Though at room temperature its modulus, 440 MPa was significantly lower than the cross-linked composite at 610 MPa and equivalent to the composite 480 MPa. It was also observed that the cross-linked composite had a noticeably higher softening temperature that the

two other materials. Finally, the tensile strength results showed that the poly(ε-caprolactone) had the highest strength, 17 MPa and the composite had the lower strength 8.1 ± 1. The composite was brittle compared to the pure poly(ε-caprolactone). The cross-linking of the composite leads to a lower ductility.

5.3.2. *In vitro* Apatite-forming ability tests

The composite material which had not been cross-linked with HMDI was tested for its *in vitro* osteoconductivity using the three methods described in chapter 4.

5.3.2.1. Dynamic Biomimetic Process (DBP)

The SEM and EDX results of the dynamic biomimetic process test carried out on the poly(ε-caprolactone) 90 %-silica composite are presented below.

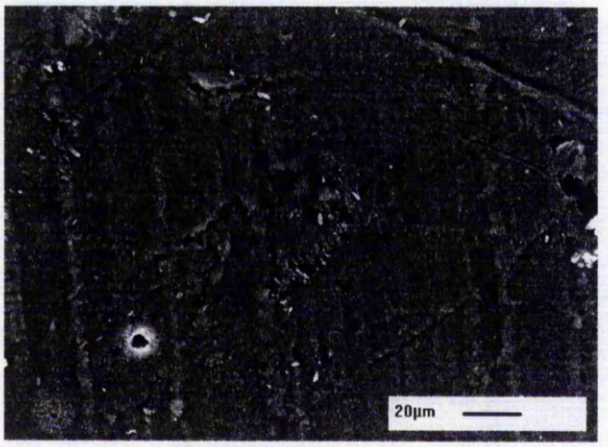

Figure 5.22 : SEM micrograph of poly(ε-caprolactone) 90 %-silica composite before *in vitro* DBP.

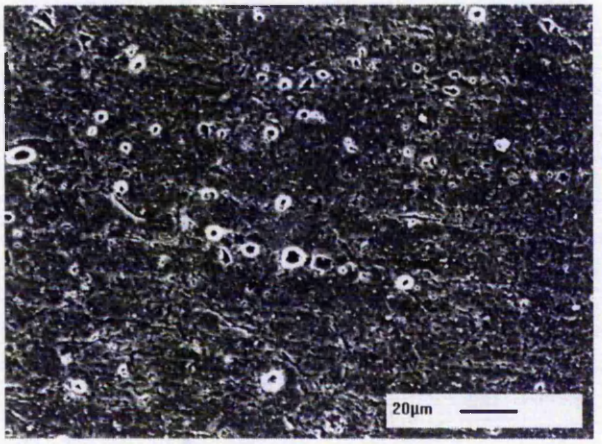

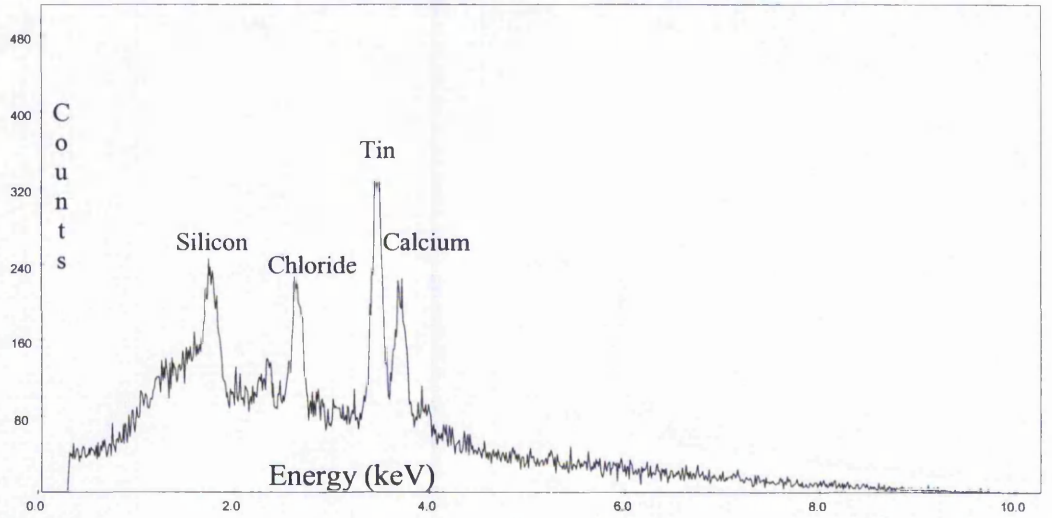

Figure 5.23 : SEM micrograph and EDXA graph of poly(ε-caprolactone) 90 %-silica composite after *in vitro* DBP (15 days).

The SEM-EDX analysis, Figures 5.22 and 5.23, showed that after 15 days of soaking in simulated body fluid (DBP), there was little or no calcium phosphate material precipitated on the surface of the materials. The X-ray analysis showed clearly the presence of silicon, chloride, calcium and tin but no phosphorus. It must be noticed that the strong signal intensity for tin, which was present in the material at only 0.02 mole percent, indicated that the calcium and chloride on the surface precipitated in a very small amount. The SEM photo, Figure 5.23, showed the surface of the composite and very little precipitated material. The apatite-forming ability of the composite was not apparent after 15 days of soaking in SBF in the dynamic biomimetic process. The static biomimetic process was also carried out to confirm the above result.

5.3.2.2. Static Biomimetic Process (SBP)

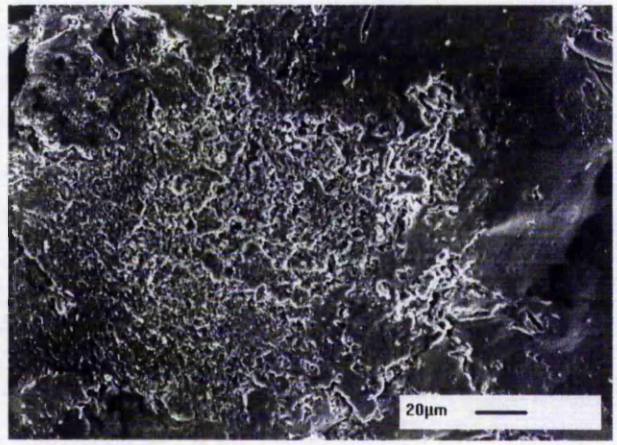

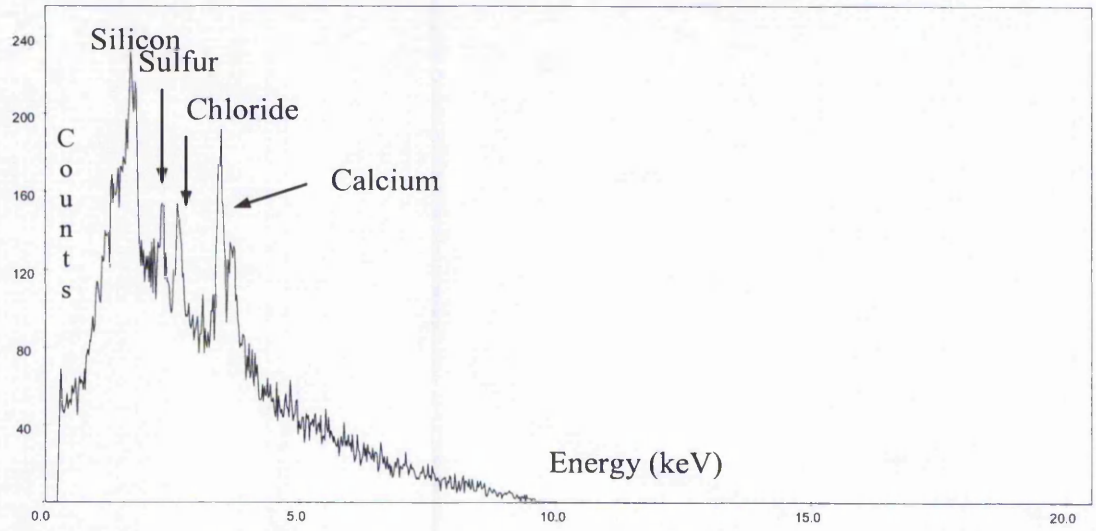

Figure 5 24 : SEM micrograph and EDXA graph of poly(ε-caprolactone) 90 %-silica composite after SBP (15 days).

As for the dynamic biomimetic process, the static biomimetic process carried out on the poly(ε-caprolactone) 90 %-silica composite was unsuccessful as the formation of an apatite layer was not observed, Figure 5.24, in the conditions of the apatite-forming ability tests. A recent paper reports that a PTMO-silica sol-gel hybrid with 30 % total weight silica precipitates calcium phosphate material in SBF but not before 28 days in a static biomimetic process[34].

5.3.2.3. Alternate Soaking Process (ASP)

Because of the negative results obtained from the SBP and DBP tests, the alternate soaking process test was carried out as described in the methods chapter and the poly(ε-caprolactone) and the poly(ε-caprolactone) 90 %-silica composite materials analysed after 20 ASP cycles by SEM-EDXA analysis. The number of ASP cycles was also extended to 60 cycles as it was expected that after 20 cycles that it would not be possible to observe a calcium phosphate precipitate on the surface of the composite in accordance with the biomimetic processes.

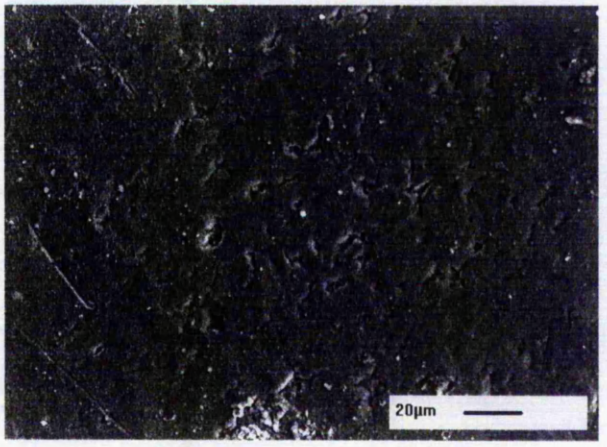

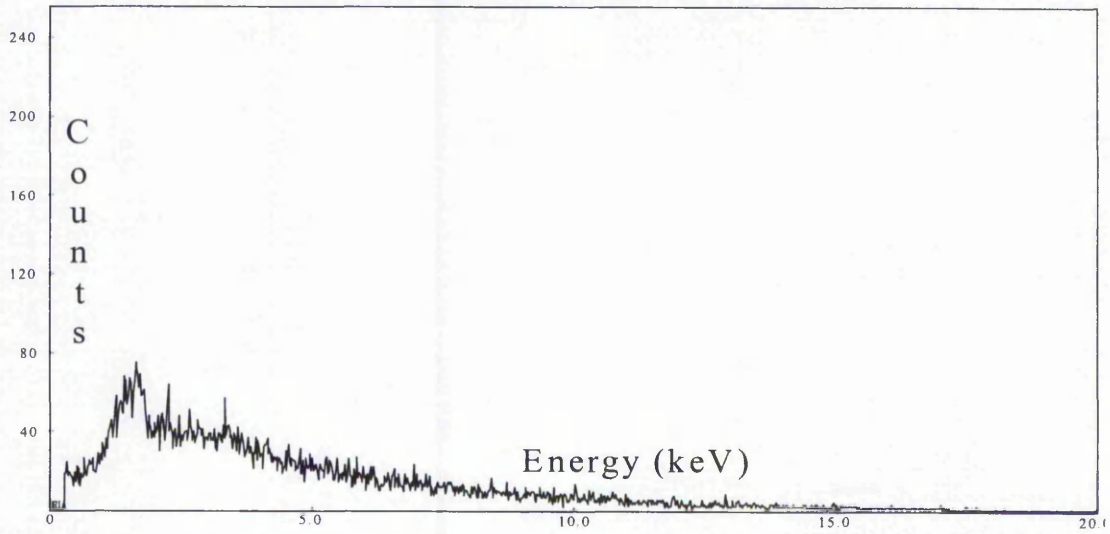

Figure 5.28 : SEM micrograph and EDX analysis of poly(ε-caprolactone) after 20 ASP cycles

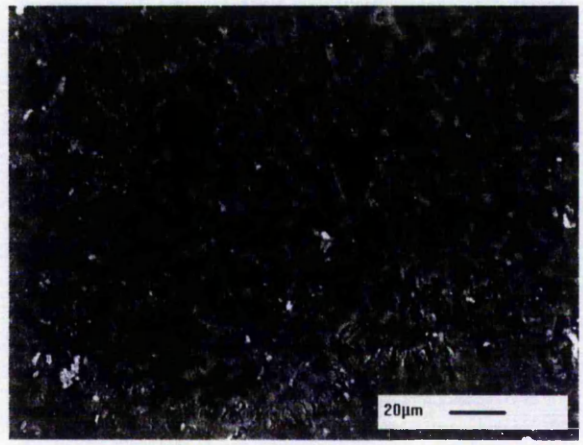

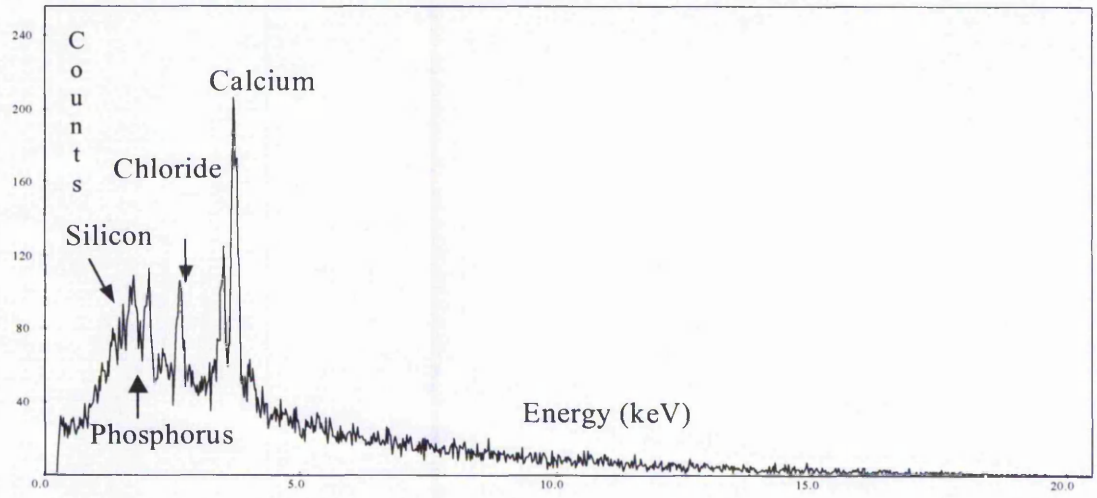

Figure 5.26 : SEM micrographs and EDX analysis of poly(ε-caprolactone) in ASP test after 60 ASP cycles.

The SEM micrograph of the poly(ε-caprolactone), Figure 5.25, did not show a precipitate of calcium phosphate on its surface after 20 ASP cycles. The EDXA graph confirmed that the surface of the polyester was free of calcium and phosphorous. After 60 ASP cycles the surface of the poly(ε-caprolactone), Figure 5.26, did not show the presence of precipitated material. The EDXA analysis indicated the presence of calcium, chloride and phosphorus but in very small quantity as their signal intensity was in the order of the tin present in the polymer in 0.02 mole percent. It was then considered that the poly(ε-caprolactone) did not precipitate calcium phosphate material on its surface under the conditions of the ASP test even after 60 cycles.

The poly(ε-caprolactone) 90 %-silica composite was also submitted to the 20 and 60 ASP cycles.

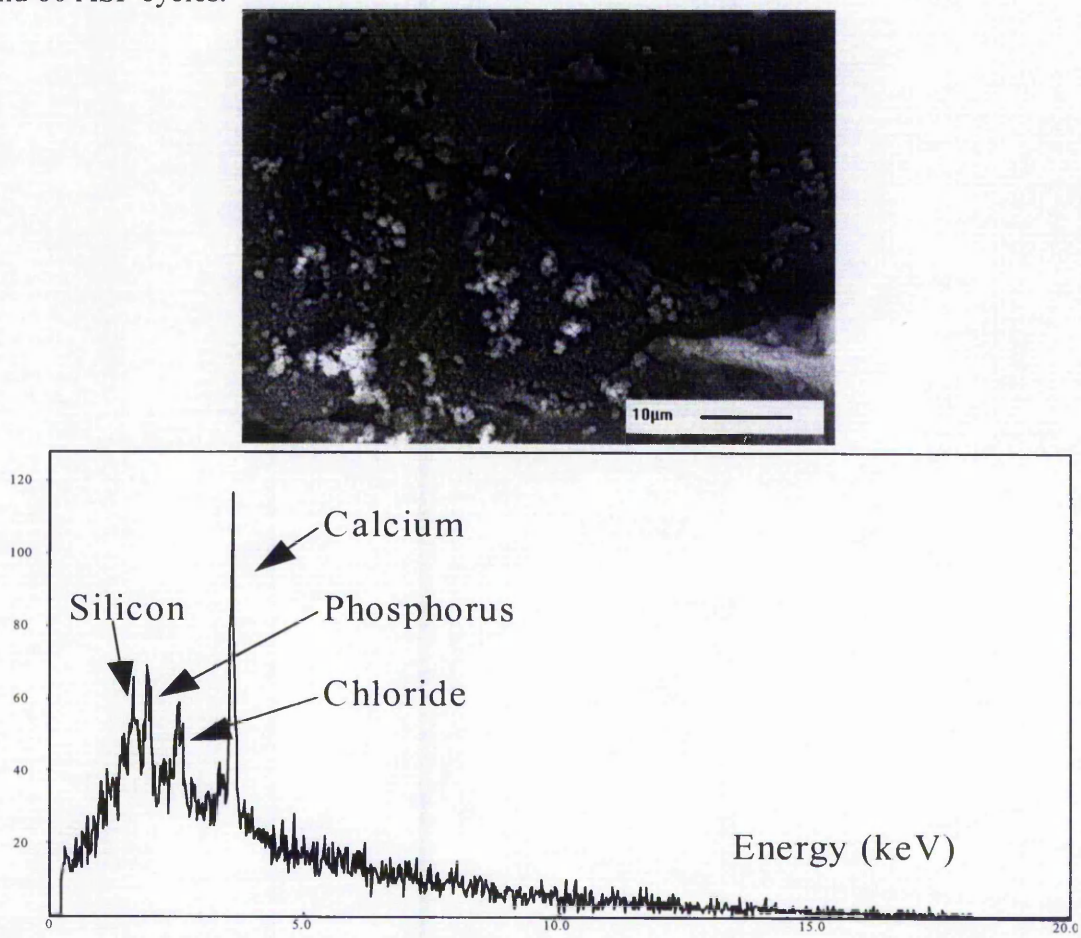

Figure 5.27 : SEM micrograph and EDX analysis of poly(ε-caprolactone) 90 %-silica composite after 20 ASP cycles.

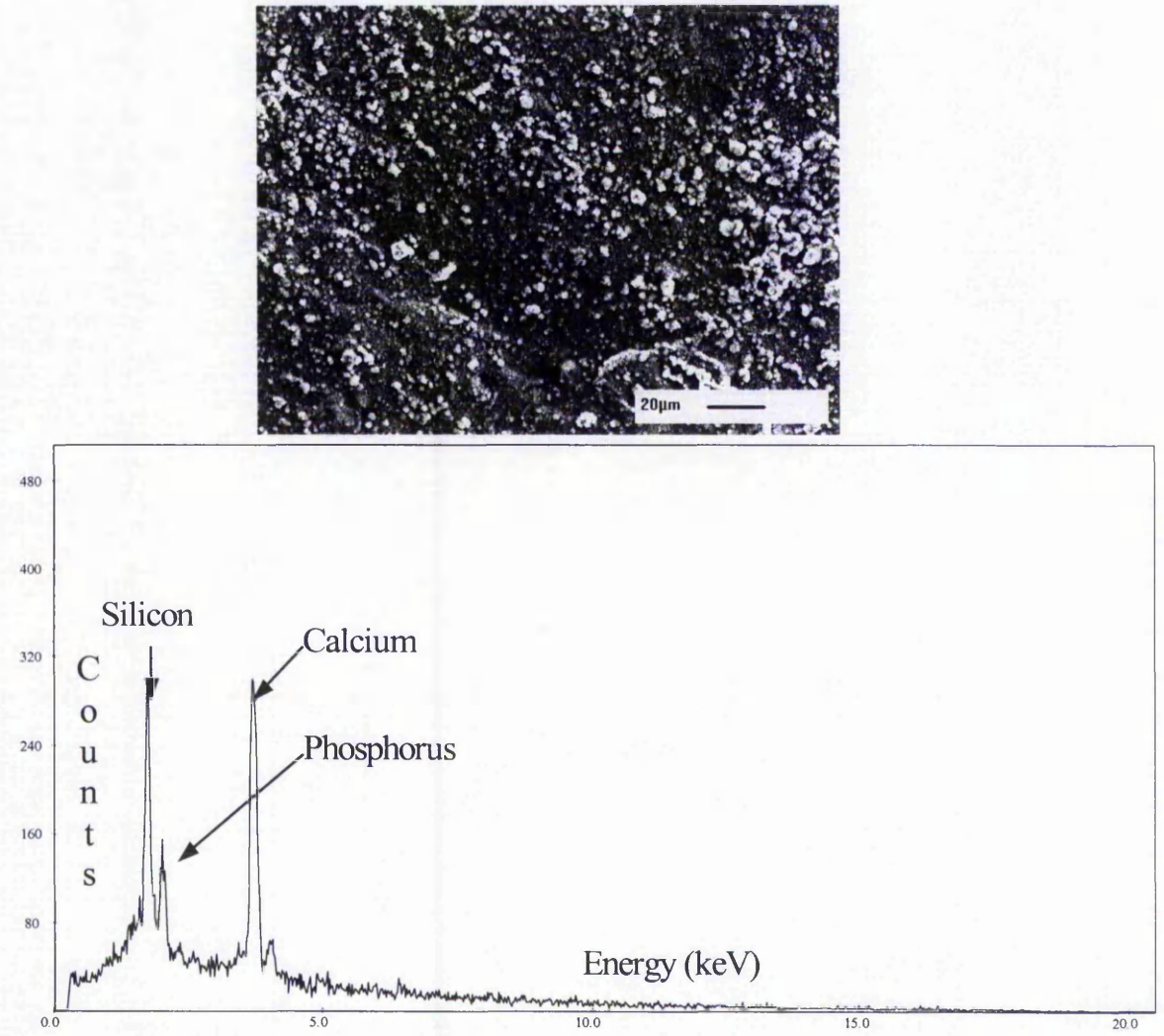

Figure 5.28 : SEM micrograph and EDX analysis of poly(ε-caprolactone) 90 %-silica composite after 60 ASP cycles.

Figures 5.27 and 5.28, showed the SEM-EDXA results of the ASP test for the poly(ε-caprolactone) 90 %-silica composite. The SEM micrographs after 20 and 60 cycles showed the presence of a precipitate on the surface of the composite. The amount of precipitate increased with the number of ASP cycles. The EDXA analysis showed that mostly calcium, phosphorus and chloride were detected in the precipitate on the surface of the material after 20 ASP cycles. After 60 ASP cycles, the precipitated material was composed of calcium and phosphorus without significant amount of chloride. The calcium to phosphorus ratio calculated from the EDXA analysis of the

composite sample after 60 ASP cycles was equal to 1.87 ± 1.0. The large standard deviation was due to error in the quantification because of the overlapping of the tin Kα and Kβ band at 3.38 keV and 3.49 keV respectively with the calcium Kα band at 3.60 keV.

5.3.3. Discussion

The *in vitro* apatite-forming ability of the poly(ε-caprolactone)-silica composite prepared was assessed by static and dynamic biomimetic processes. The scanning electron microscopy study showed that no apatite layer was formed under the conditions of the tests. Using the alternate soaking process the formation of an apatite layer was observed on the composite surface but only after 60 ASP cycles indicating a weak ability to form apatite *in vitro*. However, under the same conditions poly(ε-caprolactone) did not precipitate calcium phosphate on its surface. The poor bioactivity property of the composite material prepared in this chapter was not unexpected as poly(ε-caprolactone)-silica sol-gel composites with similar weight ratio of polyester and silica 9/1 also did not show *in vitro* apatite-forming ability (chapter 4).

The release of silicic acid from the material in the simulated body fluid during the static biomimetic process is plotted in the Figure 5.29.

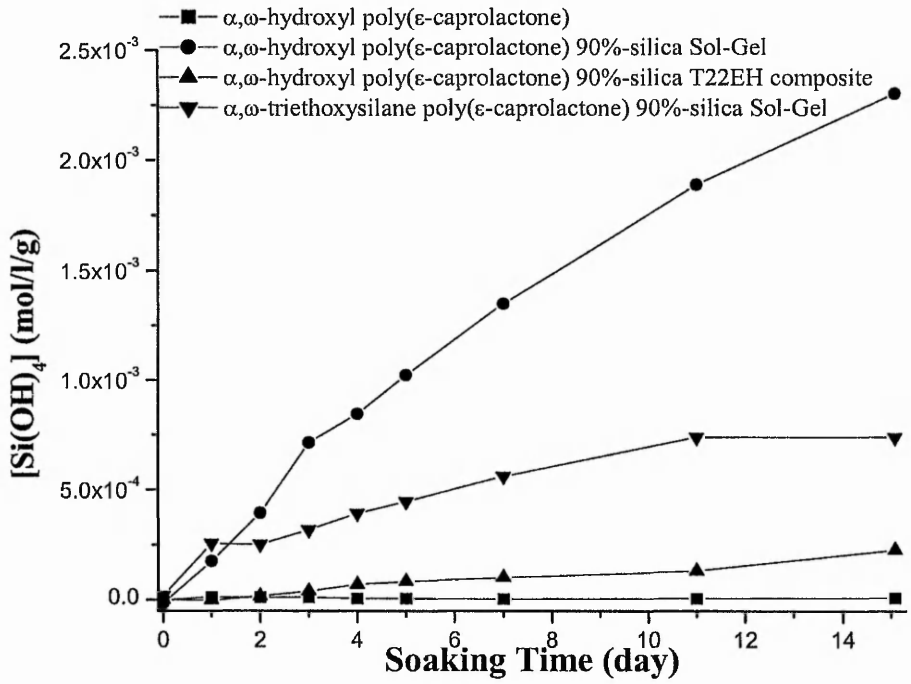

Figure 5. 29 : Plot of the concentration of silicic acid in simulated body fluid per gram of material as a function of the soaking time in the static biomimetic process.

The poly(ε-caprolactone) 90 %-silica materials prepared released silicic acid after 15 days of soaking in the following decreasing order; α,ω-hydroxyl poly(ε-caprolactone) 90 %-silica sol-gel, α,ω-triethoxysilane poly(ε-caprolactone) 90 %-silica sol-gel and α,ω-hydroxyl poly(ε-caprolactone) 90 %-silica-T22EH composite materials. The lower release of silicic acid from the last composite material indicates the probable higher bonding and therefore better interpenetration of the polyester and the silica phases compared to the sol-gel materials. The slower release of silicic acid may have also affected the speed of apatite precipitation.

5.4. Conclusion

In this chapter a new method for the preparation of poly(ε-caprolactone)-silica composite materials was investigated. An organotin catalyst, the tin(II) 2-ethylhexanoate was used to carry out the ring-opening polymerisation of the lactone, the condensation of hydrolysed alkoxysilane and the cross-linking between the hydroxyl functional polyester and the silica oligomers. Either, alkoxysilane or pre-hydrolysed alkoxysilanes were able to cross-link with the polyester. The formation of silicon-oxygen-carbon bonding was possibly confirmed by FTIR, and solid state ^{29}Si NMR analysis. The control of the water concentration in the reaction system is crucial. Water is necessary to activate the catalyst and to hydrolyse the alkoxysilanes, but a large amount of water will promote the hydrolysis and condensation reactions of the alkoxysilanes and be detrimental to the cross-linking with the hydroxyl functional poly(ε-caprolactone). The conditions of the cross-linking reactions catalysed by T22EH such as the temperature and the use of vacuum or not were important. Low temperature favours the condensation of hydrolysed alkoxysilane, high temperature and vacuum favours the cross-linking reaction between the organic and inorganic phases.

A poly(ε-caprolactone)-silica composite prepared by the catalysed cross-linking reaction was synthesised and characterised. The mechanical properties of the materials were characterised by dynamic mechanical thermal analysis. The DMTA analysis of poly(ε-caprolactone)-silica sol-gel materials have been reported[35] for weight percent polyester content of 50 % and lower. The conditions of the DMTA tests were different, notably the temperature range, than those used in this study and the polymer studied had different M_n and structure. Therefore, a strict comparison was not possible. Interestingly, it has been reported that the dynamic mechanical properties of the prepared hybrids were not very sensitive to variation of poly(ε-caprolactone) molecular weight and more sensitive to cross-interaction between the poly(ε-caprolactone) and the silica.

The *in vitro* apatite-forming ability of the composite was tested by biomimetic procedures and the alternate soaking process. Under the conditions of the dynamic and static biomimetic processes, the material did not form a calcium phosphate layer on its surface as shown by SEM and EDXA analysis. The alternate soaking process indicated

that the composite ability to form calcium phosphate material on its surface was low but higher that that of the pure polyester as only the composite had calcium phosphate precipitated on it after 60 ASP cycles. The poor *in vitro* apatite-forming ability of the composite can be explained by the quantity of silica in the material, 10 percent total weight, which was probably too low to induce nucleation of apatite as observed for composites with similar silica content prepared by the sol-gel method (chapter 4).

5.5. References

[1] K. M. Stridsberg, M. Ryner, A. C. Albertsson (2002), "Controlled ring-opening polymerisation: Polymers with designed macromolecular architecture.", *Advances in Polymer Science*, 157, 42-65.

[2] K. B. Aubrecht, M. A. Hillmyer, W. B. Tolman (2002), "Polymerization of lactide by monomeric Sn (II) alkoxide complexes.", *Macromolecules*, 35, 644-650.

[3] B. J. O'Keefe, M. A. Hillmyer, W. B. Tolman (2001), "Polymerization of lactide and related cyclic esters by discrete metal complexes.", *Journal of the Chemical Society. Dalton Transactions*, 15, 2215-2224.

[4] A. Duda, S. Penczek (1990), "Thermodynamics of L-lactide polymerisation.Equilibrium monomer concentration.", *Macromolecules*, 23 (6), 1636-1639.

[5] A. J. Nijenhuis, D. W. Grijpma, A. J. Pennings (1992), "Lewis acid catalysed polymerisation of L-lactide. Kinetics and mechanism of the bulk polymerisation.", *Macromolecules*, 25(24), 6419-6424.

[6] H. R. Kricheldorf (2000), "Tin-initiated polymerisations of lactones: mechanistic and preparative aspects.", *Macromolecular Symposium*, 153, 55-65.

[7] A. Kowalski, A. Duda, S. Penczek (2000) "Mechanism of cyclic ester polymerisation initiated with tin(II) octoate 2. Macromolecules fitted with tin(II) alkoxide species observed directly in MALDI-TOF spectra.", *Macromolecules*, 33, 689-695.

[8] A. Kowalski, A. Duda, S. Penvzek (2000), "Kinetics and mechanism of cyclic esters polymerisation initiated with tin(II) octoate. 3. Polymerization of L,L-dilactide.", *Macromolecules*, 33, 7359-7370.

[9] A. Duda, S. Penczek, A. Kowalski, J. Libiszowski (2000), "Polymerizations of ε-caprolactone and L,L-dilactide initiated with stannous octoateand stannous butoxide-A comparison.", *Macromolecular Symposium*, 153, 41-53.

[10] H. R. Kricheldorf, I. Kreiser-Saunders, A. Sticker (2000), "Polylactones 48. $SnOct_2$-initiated polymerisations of lactide: A mechanistic study.", *Macromolecules*, 33, 702-709.

[11] A. Schindler, Y. M. Hibionada, C.G. Pitt (1982), "Aliphatic polyesters. III. Molecular weight and molecular weight distribution in alcohol-initiated polymerisations of ε-caprolactone.", *Journal of Polymer Science: Polymer Chemistry Edition,* 20, 319-326.

[12] H. Korhonen, A. Helminen, J. V. Seppalla (2001), "Synthesis of polylactides in the presence of co-initiators with different numbers of hydroxyl groups.", *Polymer*, 42, 7541-7549.

[13] S. H. Kim, Y. K. Han, K. D Ahn, Y. H. Kim, T Chang (1993), "Preparation of star shaped polylactide with pentaerythrytol and stannous octoate.", *Makromolekulare Chemie. Macromolecular Chemistry and Physics*, 194, 3229-3236.

[14] K. Jamshidi, S. H. Hyon, Y. Ikada (1988), "Thermal characterization of polylactides.", *Polymer*, 29(12), 2229-2234.

[15] Y. K. Choi, Y. H. Bae, S. W. Kim (1998), "Star-shaped poly(ether-ester) block copolymers: Synthesis, characterization, and their physical properties.", *Macromolecules*, 31(25), 8766-8774.

[16] Y. J. Du, P. J. Lemstra, A. J. Nijenhuis, H. A. M. Van Aert, C. Bastiaansen (1995), "ABA type copolymers of lactide with poly(ethylene glycol)- Kinetic, mechanistic and model studies.", *Macromolecules*, 28(7), 2124-2132.

[17] D. Cohn, T. Stern, M. F. Gonzalez, J. Epstein (2001), "Biodegradable poly(ethylene oxide)/ poly(ε-caprolactone) multiblock copolymers.", *Journal of Biomedical Materials Research*, 59, 273-281.

[18] A. Breitenbach, T. Kissel (1998), "Biodegradable comb polyesters: Part 1 - Synthesis, characterization and structural analysis of poly(lactide) and poly(lactide-co-glycolide) grafted onto water-soluble poly(vinyl alcohol) as backbone.", *Polymer*, 39 (14), 3261-3271.

[19] M. Messori, M. Toselli, F. Pilati, L. Mascia, C. Tonelli (2002), "Synthesis and characterisation of silica hybrids based on poly(ε-caprolactone-b-perfluoropolyether-b-ε-caprolactone).", *European Polymer Journal*, 38, 1129-1136.

[20] J. Ma, H. Cao, Y. Li, Y. Li (2002), "Synthesis and characterization of poly(DL-lactide)-grafted gelatins as bioabsorbable amphilic polymers.", *Journal of Biomaterials Science. Polymer Edition*, 13(1), 67-80.

[21] I. Ydens, D. Rutot, P. Degee, J. L. Six, E. Dellacherie, P. Dubois (2000), "Controlled Synthesis of poly(ε-caprolactone)-grafted dextran copolymers as potential environmentally friendly surfactants.", *Macromolecules*, 33, 6713-6721.

[22] C. M. Dong, K. Y. Qiu, Z. W. Gu, X. D. Feng (2002), "Synthesis of star-shaped poly(D,L-lactic acid-alt-glycolic acid)-b-poly(L-lactic acid) with the poly(D,L-lactic acid-alt-glycolic acid) macroinitiator and stannous octoate catalyst.", *Journal of Polymer Science Part A-Polymer Chemistry*, 40 (3), 409-415.

[23] C. M. Dong, K. Y. Qiu, Z. W. Cu, X. D. Feng (2001), "Synthesis of star-shapee poly(epsilon-caprolactone)-b-poly(DL-lactic acid-alt-glycolic acid) with multifunctional initiator and stannous octoate catalyst.", *Macromolecules*, 34 (14), 4691-4696.

[24] H. R. Kricheldorf, D. Langanke (2001), "ABA triblock copolymers derived from ε-caprolactone or L-lactide and a central polysiloxane block.", *Macromolecular Bioscience*, 1, 364-369.

[25] F. W. Van Der Weij (1980), "The action of tin compounds in condensation-type RTV silicone rubbers.", *Makromolekular Chemie*, 181, 2541-2548.

[26] I. Yilgor, J. E. Mc Grath (1988), "Polysiloxane containing copolymers: A Survey of recent developments.", *Advances in Polymer Science*, 86, 1-86.

[27] N. Chiodini, F. Morazzoni, A. Paleari, R. Scotti, G. Spinolo (1999), "Sol-gel synthesis of monolithic tin-doped silica glass.", *Journal of Materials Chemistry*, 9(10), 2653-2658.

[28] C. Canevali, N. Chiodini, F. Morazzoni, J. Padovani, A. Paleari, R. Scotti, G. Spinolo (2001), "substitutional tin-doped silica glasses: an infrared study of the sol-gel transition.", *Journal of Non-Crystalline Solids*, 293-295, 32-38.

[29] B. M. Novak (1993), "Hybrid nanocomposite materials- Between inorganic glasses and organic polymers.", *Advanced Materials*, 5(6), 422-433.

[30] B. M. Novak, M. W. Ellsworth (1991), "Mutually interpenetrating inorganic organic networks. New routes into nonshrinking sol-gel composite materials.", *Journal of American Chemical Society*, 113(7), 2756-2758.

[31] H. U. Gottlieb, V. Kotlyar, A. Nudelman (1997), „NMR chemical shifts of common laboratory solvents as traces impurities.", *Journal of Organic Chemistry*, 62, 7512-7515.

[32] C. J. Brinker (1990) "Sol-Gel Science: The physics and chemistry of sol-gel processing.", eds. C. J. Brinker, G. W. Scherer (Academic Press) 152-169.

[33] Y. G. Hsu, I. L. Chiang, J. F. Lo (2000), "Properties of hybrid materials derived from hydroxyd-containing linear polyester and silica through sol-gel process. I. Effect of thermal treatment.", *Journal of Applied Polymer Science*, 78, 1179-1190.

[34] N. Miyata, K. –I. Fuke, Q. Chen, M. Kawashita, T. Kokubo, T. Nakamura (2002), "Apatite-forming ability and mechanical properties of PTMO-modified CaO-SiO2 hybrids prepared by sol-gel processing: Effect of CaO and PTMO contents.", *Biomaterials,* 23, 3033-3040.

[35] D. Tian, S. Blacher, Ph. Dubois, R. Jerome (1998), "Biodegradable and biocompatible inorganic-organic hybrid materials.", *Polymer,* 39(4), 855-864.

Poly(L-lactic acid) (PLLA) and poly(ε-caprolactone) (PCL) are biocompatible and resorbable poly(α-hydroxyacids). They represent an important class of materials for use in medicine. Uses of PLLA and PCL have been reported for replacement bone grafts[1], tissue regeneration[2], scaffolding for bone and cartilage[3] and drug delivery systems[4]. They are an attractive group of materials because of their biocompatibility and resorbability through natural pathways[5]. Their mechanical properties can be tailored through their synthesis and for example, very high molecular weight poly(L-lactic acid) has been prepared for load bearing devices[6]. Enhanced poly(α-hydroxyacid) composites have been extensively studied[7]. Materials have been made from blending or copolymerisation of PLLA with other polymers[8] such as PCL-PLLA[9] and a PGA-PLLA[10] copolymer has been used as a surgical suture since the1970's[11]. The control of the composite's mechanical and degradation properties has been obtained by varying the amount of each polymer in the blend. Another class of biomaterial are the polymer-calcium phosphate composites being an example of a ceramic composite. The aim is to introduce bioactivity to the polymeric material by blending the polymer with calcium phosphate materials such as hydroxyapatite, HAP[12], tri-calcium phosphate, α-TCP[13], or other calcium containing bioactive glass-ceramics[14]. The drawbacks of this type of composite are twofold in that a large amount of the inorganic phase is required and secondly, the size of the inorganic particles used can make the material more susceptible to mechanical fracture.

Silica is vital in bioactive silica based glass (bioglass®) for the mineralization of bone and formation of a bond with living tissue[15]. Silica induces calcium phosphate nucleation at the interface between the devices and the living tissue[16, 17]. Recently, Xynos et al.[18] have reported that bioactive glass dissolution products (e.g. silica) exert a genetic control over the osteoblast cell cycle and the rapid expression of genes that regulate osteogenesis and the production of growth factors. Others studies have also reported that silicic acid is involved in bone formation and interacts with osteoblasts[19, 20] but the exact biological mechanisms affected by silicic acid have not yet been identified.

The surface of an ethylene-vinyl alcohol copolymer modified with a silane coupling agent has been reported to have *in vitro* apatite-forming ability[21]. K. Tsuru and

co-workers[22] investigated the bioactivity of organically modified silicates starting from poly(dimethylsiloxane) and tetraethyl orthosilicate through sol-gel processing after J. D. Mackenzie[23] and G. L. Wilkes[24]. Those inorganic-organic composites containing silanol groups and Ca(II) ions were bioactive[25]. Other example of polymer-silica composite materials have been prepared and their *in vitro* apatite-forming ability studied[26, 27]. At the beginning of this study, the bioactivity of poly(α-hydroxyacid)-silica composites was unknown. Preliminary *in vitro* cell culture data had been reported and the attachment and spreading of fibroblasts observed on the surface of poly(ε-caprolactone)-silica ceramers[28]. The *in vitro* apatite-forming ability of poly(ε-caprolactone)-silica-calcium oxide sol-gel hybrids was first reported in 2002[29, 30] indicating the strong interest brought by this new type of material that could have biodegradation properties and potential bioactivity properties for the whole of their implantation life.

6.1. Aims

The aims of this work were to synthesise and study poly(α-hydroxyacid)-silica composite materials for potential biomedical applications.

The objectives of this work were several. First, the preparation and assessment of the *in vitro* apatite-forming ability of poly(α-hydroxyacid)-silica composites which was unknown at the beginning of this study was performed. Secondly, The development of a sol-gel composite model was carried out for the structural study of the effect of the silica content in the composite, the effect of the poly(α-hydroxyacid) modifications and the effect of procedure modifications. The sol-gel method and some of the structural characteristiation studies of poly(ε-caprolactone)-silica composites had already been initiated by R. Jerome's group[31]. The third objective was to develop the methods for study of the *in vitro* apatite-forming ability of the composites and elucidate the mechanism of apatite formation in simulated body fluid and possibly the effect of the material structure on its bioactivity properties. A fourth and final objective was the development of a new synthetic method different from the sol-gel method that could

potentially lead to useful poly(α-hydroxyacid)-silica materials for medical applications followed by the exploration of the mechanical and bioactivity properties of these materials.

6.2. Synthesis Methods

Silica has been used as filler in PMMA for dental applications for more than two decades[32, 33]. Biomaterial carrier PMMA-silica composites where proteins and enzymes are entrapped have been prepared by the blending of dispersed silica colloids and polymers[34] (bulk method) and more recently by using a sol-gel procedure[35]. To our knowledge, R. Jerome and co-workers published the first studies on the synthesis, structural characterization and *in vitro* biocompatibility of a poly(ε-caprolactone)-silica sol-gel hybrid materials[36, 37, 38]. In this study, the poly(ε-caprolactone)-silica sol-gel composites were used as model materials. The synthesis procedure described for the poly(ε-caprolactone)-silica sol-gel composites in the literature was modified for the preparation of poly(L-lactic acid)-silica sol-gels. Toluene instead of tetrahydrofuran was used as the co-solvent. A bulk method was also used to prepare α,ω-hydroxyl poly(ε-caprolactone)-silica composites. Poly(ε-caprolactone) and the poly(L-lactic acid) had their hydroxyl end-groups substituted by more reactive end-groups, triethoxysilane by reacting an excess of 3-isocyanatopropyltriethoxysilane with the linear hydroxyl terminated poly(α-hydroxyacids) and sol-gel composites were synthesised using these modified poly(α-hydroxyacids).

A new method was developed to prepare poly(ε-caprolactone)-silica composites. The procedure can be described as a reactive bulk where an organotin catalyst, tin(II) 2-ethylhexanoate is used to carry out the ring-opening polymerisation of ε-caprolactone, the condensation of hydrolysed alkoxysilanes and the cross-linking between the hydroxyl functional poly(ε-caprolactone) and the silica species. Hexamethyldiisocyanate (HMDI) was also used to cross-link further the prepared composites to improve their mechanical properties.

6.3. Structural Characterisation

Statistical experimental design was applied to the study of the effect of sol-gel reactants on the physical properties of the hydroxyl terminated poly(α-hydroxyacid)-silica composites. This statistical method allowed the simultaneous study of several factors and the optimization of the experimental work. The statistical analysis allowed assessment of the reproducibility of the materials synthesis and the error in the measurement of the physical property (crystallinity). A full 2^5 factorial design with 5 centre points was applied to the α,ω-hydroxyl poly(ε-caprolactone)-silica sol-gel analysis and a 2^5 fractional design with 5 centre points was designed for the study of α,ω-hydroxyl poly(L-lactic acid)-silica sol-gels.

Of the physical properties that can be measured, the crystallinity of a polymer is important in that it gives information on the structural state of the polymer whether alone or in the presence of another phase such as silica. Polymer crystallinity in confined environments has been mostly studied using the melting enthalpy of the hybrid from differential scanning calorimetry (DSC) analysis and the crystallite size calculated from line broadening analysis (Scherrer equation) performed on powder X-ray diffraction (XRD) spectra[39]. In chapter 3, DSC data and a graphical treatment of the powder X-ray diffraction analysis, two independent techniques, were used to measure the crystallinity of poly(α-hydroxyacid) in sol-gel materials. The graphical treatment of the powder X-ray diffraction was preferred over the crystallite size measurement because polymers can be described as paracrystals[40] and when they are analysed by X-rays some of the scattering from the crystalline domains of the polymer is diffuse and contributes to the amorphous background as well as to the diffraction reflections of the crystalline polymer. Substantial broadening of reflections due to this effect is observed. For crystallite size calculation using the Scherrer equation, the full width at half-height of the reflection is used but, for polymers, the lattice values obtained are distorted by contributions from background broadening. Thus estimates of the size of crystalline regions in polymers and composites such as poly(ε-caprolactone)-silica hybrids obtained using the Scherrer equation are unreliable. In fact, in chapter 2, the standard deviations of the poly(α-hydroxyacids) crystallite size in the statistical designs

compared to the crystallite size of the α-Al_2O_3 standard showed that their values were not significantly different in the conditions of the experiments and therefore any treatment of the crystallite size measurement using this method was considered meaningless.

Strict comparison of crystallinity measured by DSC and XRD was not possible because the meaning of the crystallinity measurement were different. However, it was found that the crystallinity measured by DSC and XRD gave concordant results.

The incorporation of poly(α-hydroxyacids) within a silica phase modified the vibrational bands observed by FTIR and vibrational spectroscopy is very sensitive to degree of order present in a polymer. Qualitative information was obtained from the infrared analysis; the presence of interactions such as hydrogen bonding and covalent bonding between the organic and inorganic phases and the "order" of the poly(α-hydroxyacids) (crystalline / amorphous) was observed. Thermogravimetric analysis results (residual weight) coupled with a Soxhlet experimental technique allowed us to find the amount of poly(α-hydroxyacid) incorporated either by covalent bonding or entrapment in the silica phase. Finally, transmission electron microscopy was used to tentatively observe the microstructure of the composites. The poor stability of the poly(α-hydroxyacids) (low melting temperature) under the electron beam and consequently, the difficulty in collecting good quality micrographs, did not allow the systematic study of the composites but the co-continuous structure of the composites could be observed for materials with 70 percent weight content of polyester as reported in the literature[31].

The materials studied can be described for high silica content as a co-continuous organic and inorganic structure[41] and for low silica content as a dispersed inorganic phase in an organic polymer. A measure of the crystallinity of the organic phase and its variation with synthesis variables was a good indicator of the incorporation of poly(α-hydroxyacids) into the silica network. The higher the extent of order of the poly(α-hydroxyacid) phase (high crystallinity), the lower the interaction of the silica phase with the organic polymer. The lower the crystallinity of the poly(α-hydroxyacid) phase, the

stronger the interaction between the two phases suggesting a more closed structure for the sol-gel composites.

For the poly(ε-caprolactone)-silica sol-gel statistical design, interaction effects of reactants were not significant in the limits of the experiments. For the poly(L-lactic acid)-silica sol-gel design, interaction effects were observed. These important observations reported chapter 3, would have been left undetected without the use of a statistical design approach. The results of the structural statistical studies carried out on both poly(α-hydroxyacid)-silica sol-gel composites showed that the modification of the poly(α-hydroxyacid) and the conditions of the sol-gel reaction modified the structure of the obtained sol-gels. Increasing the TEOS/poly(α-hydroxyacid) molar ratio decreased the poly(α-hydroxyacid) crystallinity and increased the incorporation of the organic polymer within the silica phase. For the poly(ε-caprolactone)silica sol-gels increasing the HCl/TEOS molar ratio increased the condensation of the silica phase and thus increased the incorporation or entrapment of the polyester in the silica network. The difference of solubility of the poly(ε-caprolactone) and poly(L-lactic acid) strongly affected the sol-gel reaction. This was a possible reason for the important effect of the co-solvent (toluene) on the hydrolysis-condensation reaction of tetraethyl orthosilicate in the poly(L-lactic acid)-silica sol-gels. The comparison of the two statistical designs was not straightforward. At the beginning of the sol-gel reaction, poly(α-hydroxyacid) and small silica oligomers can coexist in the sol-gel solution without specific interaction. With the progress of silica condensation, the poly(α-hydroxyacid) associated with the silica inhibits the condensation in the ageing and in the drying process[42]. Therefore, the strength of the interactions between the poly(α-hydroxyacid) and the silica controls the formation of the silica gel and the formation of the co-continuous structure. The poly(ε-caprolactone) and the poly(L-lactic acid) probably interacted differently with the silica oligomers in the sol-gel reaction but this has not been elucidated in this work.

Liquid and solid state ^{29}Si NMR analysis studies of the sol-gel reaction and the silica gel in the presence of both polyesters could allow determination of the type of

silica species present as a function of the reaction time and consequently provide information on how the silica gel formation is affected by the poly(α-hydroxyacids).

The results of the two statistical studies showed that the formation of the sol-gel, the structure or order of the poly(α-hydroxyacid) in silica composite materials was dictated by the physical constraints of putting the organic polymer into the open silica network. Comparison of the procedure used to obtain the poly(ε-caprolactone)-silica composites, Table 6.1, confirmed that the three composite preparation procedures and the modification of poly(α-hydroxyacid) end-groups reactivity had an effect on the incorporation of the poly(α-hydroxyacid) within the silica phase and the structure of the composites.

Table 6.1: Crystallinity measured by DSC, residual weight measured by TGA and Soxhlet experiment of α,ω-hydroxyl poly(ε-caprolactone), and poly(ε-caprolactone)-silica composites with 90% weight polyester (PCL 90% wt-SiO_2) prepared following three procedures (Bulk, Sol-gel and new method).

Material		**Residual weight (%)**	
	Cr_{DSC}	**TGA**	**Soxhlet experiment**
Poly(ε-caprolactone)			
M_n = 2,000 g.mol^{-1}	0.58	0.0	0.0
M_n = 60,000 g.mol^{-1}	0.39	0.0	0.0
PCL 90%wt-SiO_2			
Bulk	0.39	9.3	3.4
Sol-Gel			
α,ω-OH PCL	0.42	12.5	6.9
α,ω-$Si(OC_2H_5)_3$ PCL	0.00	11.0	60.2
New Method (M_n = 8,000 g.mol^{-1})	0.43	9.4	30.0

The chemical modification of the linear poly(α-hydroxyacids) by the substitution of hydroxyl end-groups by more reactive triethoxysilane end-groups increased the incorporation of the organic and inorganic phases by increasing the covalent bonding between the organic and inorganic phases. The residual weight measured by TGA and the Soxhlet experiment for the new composite preparation method using the tin(II) 2-ethylhexanoate for the cross-linking of the poly(ε-caprolactone) and the silica species, and the other sol-gel methods, Table 6.1 showed that the incorporation and bonding of the organic and inorganic phases in the composite prepared by the different procedures were in order of decreasing amount of residual weight measured by the Soxhlet experiment; triethoxysilane terminated poly(ε-caprolactone)-silica sol-gel procedure, new method, hydroxyl terminated poly(ε-caprolactone)-silica sol-gel procedure and hydroxyl terminated poly(ε-caprolactone)-silica bulk procedure.

To conclude, the structural studies carried out showed that the degree of crystallinity provided an indication of the confinement of the polyester in a composite material and yielded information on the formation of homogeneous composites. The incorporation of the poly(α-hydroxyacid) in an inorganic matrix of silica modifies their chemical and physical properties and could therefore lead to useful modifications of their biodegradability and possibly their biocompatibility[7]. The statistical study applied in conjunction with the measures of crystallinity could be extended to the measure of other physical, chemical or biological properties of the composite materials. For example, the effect of the reactants variation on the mechanical behaviour of the composite such as the dynamic modulus, or the degradation property could be assessed. This information could lead to an extensive comprehension of the behaviour of this type of materials and the possibility to tailor the properties of poly(α-hydroxyacid)-silica composites in response to specific applications. Such statistical design method has been applied recently for the optimisation of a polymeric carrier for controlled drug delivery[43], showing the usefulness of this experimental approach in the field of biomedical devices.

6.4. Mechanical Properties

The mechanical properties of poly(ε-caprolactone)-silica composite materials prepared by the new procedure, chapter 5 were characterised by dynamic mechanical thermal analysis. In Figures 6.1 and 6.2 are presented as an histogram plot, the modulus and the tensile strength of the poly(ε-caprolactone) (M_n equal to 60,000 $g.mol^{-1}$) and the poly(ε-caprolactone)-silica composites (PCL/(TMOS/MeOH/H_2O/HCl) and PCL/(TMOS/MeOH/H_2O/HCl) + HMDI). For comparison purposes the mechanical properties of cortical and cancellous bones, of poly(L-lactic acid), and poly(tetramethylene oxide)-silica sol-gel hybrids are also reported[44, 45].

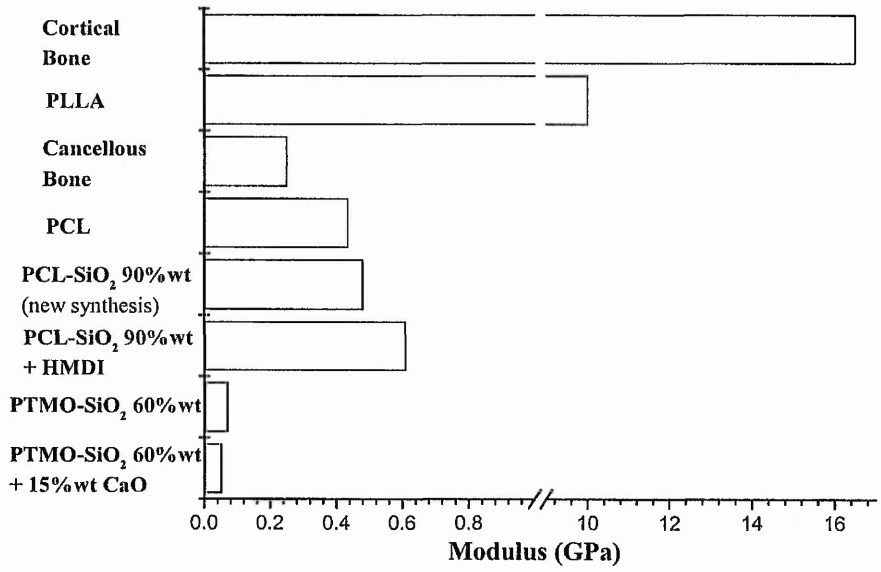

Figure 6.1 : Plot of the Young's modulus (GPa) for cortical and cancellous bone, poly(L-lactic acid) PLLA, poly(ε-caprolactone) PCL, poly(ε-caprolactone)-silica with 90% weight content of poly(ε-caprolactone) PCL-SiO_2 (new method), and poly(tetramethylene oxide)-silica with 60% weight content of polymer PTMO-SiO_2.

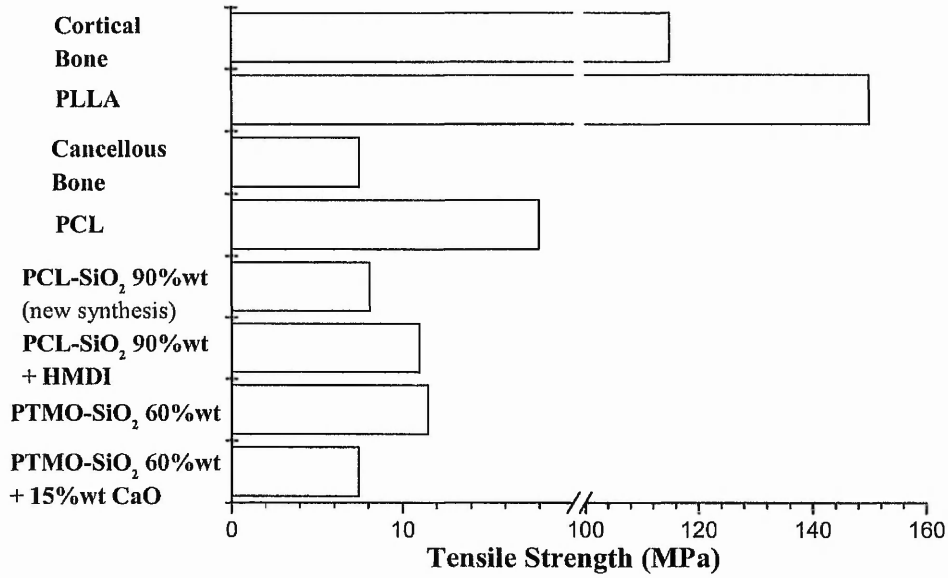

Figure 6.2 : Plot of the tensile strength (GPa) for cortical and cancellous bone, poly(L-lactic acid) PLLA, poly(ε-caprolactone) PCL, poly(ε-caprolactone)-silica with 90% weight content of poly(ε-caprolactone) PCL-SiO_2 (new method), and poly(tetramethylene oxide)-silica with 60% weight content of polymer PTMO-SiO_2.

The modulus and the tensile strength, Figures 6.1 and 6.2 of the poly(ε-caprolactone)-silica composite materials prepared by the new method were compared with these of cortical and cancellous bones. Mechanical properties close and even higher than cancellous bone have been achieved with the composites studied, but they are still far from the mechanical strength and the modulus of cortical bones. However, the composites have comparable mechanical properties of a high molecular weight poly(ε-caprolactone) and other polymer-silica hybrid materials reported[44].

The optimisation of the hydroxyl terminated poly(ε-caprolactone)-silica cross-linked with tin(II) 2-ethylhexanoate procedure would probably lead to an improvement in the mechanical properties of the composite. There are several ways to improve the mechanical properties of the composite. First, by increasing the molecular weight of the poly(ε-caprolactone). Secondly, the increase of cross-linking between the organic and inorganic phase should also improve the mechanical properties. The understanding of the effect of reaction parameters such as the reaction temperature, the catalyst and silica concentrations and the silica species introduced is important to control the structure of

the composite and should be studied. The increase of the hydroxyl end-group numbers on the poly(ε-caprolactone) by synthesising branched or star polymers by varying the type of co-initiator during the ring-opening polymerisation of the ε-caprolactone could also lead to better mechanical properties[46].

Finally, Figures 6.1 and 6.2 show that poly(L-lactic acid) has mechanical properties close to cortical bone. Therefore, the preparation of poly(L-lactic acid)-silica composites using tin(II) 2-ethylhexanoate may allow the preparation of materials with possible load bearing biomedical applications.

6.5. Biodegradation properties

The biodegradation properties of the poly(α-hydroxyacid)-silica composites have not been investigated yet. Poly(ε-caprolactone) and poly(L-lactic acid), both biodegradable polymers, degrade following a hydrolytic mechanism. The biodegradation rate of the poly(α-hydroxyacid) depends of the nature of the polymer chemical structure, the polymer water permeability (hydrophilicity/hydrophobicity), the polymer morphology (crystallinity), the glass transition temperatures and the molecular weight[47]. Poly(ε-caprolactone) has a degradation time of 2 to 5 years, poly(L-lactic acid) a degradation time of only a few months. The mechanisms of degradation for both polyesters have been extensively studied[48]. The *in vitro* and *in vivo* degradation of the poly(ε-caprolactone) and poly(L-lactic acid) proceed by the auto catalysis cleavage of the ester bonds in the presence of water[49]. A crystalline degradable polymer degrades more slowly than the corresponding amorphous polymer. This is explained by the slower diffusion of water and degradation products in the crystalline polymer than in the amorphous polymer.

Silica xerogels have been studied for use as biodegradable carriers for controlled drug delivery[50]. It has been reported that the weight loss of a silica gel matrix soaked in a simulated body fluid (pH 7.4) for 99 hours at 37°C was about 65 percent of the original weight[51]. The *in vivo* degradation of silica is an erosion-dissolution process, and silicic acid is released[55].

In composite materials the degradation of the poly(α-hydroxyacid) and silica phase will be probably modified. The poly(α-hydroxyacids) crystallinity decreased with the incorporation of silica. Consequently, the diffusion of water will be facilitated and polyesters will probably have a higher degradation rate in the composites. Also, the presence of silicic acid as a degradation product of the silica phase may possibly act as a catalyst for the cleavage of ester bonds and speed up the kinetics of degradation. The cross-linking of the organic and inorganic phases may have a retardant effect on the degradation of the polyesters in composites as the cleavage reaction is initiated primarily by the polymer end-groups. A preliminary *in vitro* biodegradation study could be carried out as follows. Material samples soaked in deionised water at 37 °C or higher temperature to increase the rate of degradation could be collected at desired times and their weight loss measured, the polyester M_n and polydispersity measured by GPC analysis and the amount of silica in the composite calculated from the TGA residual weight. This preliminary *in vitro* biodegradation study is a necessary step before the *in vivo* assessment of the composites behaviour.

6.6. Apatite-Forming Ability

The *in vitro* biocompatibility of the prepared materials was assessed by the seeding of osteoblasts on the surface of prepared samples. After 24 hours, a cytotoxic assay allowed observation of the attachment and spreading of cells, indicating that the materials did not have an adverse effect on the viability of cells *in vitro*. The biocompatibility property of the poly(α-hydroxyacids) was preserved in the poly(α-hydroxyacid)-silica composites.

A common and general method for the study of the *in vitro* apatite-forming ability of materials does not exist. However, the most widespread methods are the static biomimetic method followed by the dynamic biomimetic process. Both, the static and dynamic biomimetic processes showed the *in vitro* apatite-forming ability of some of the prepared poly(α-hydroxyacid)-silica composites. In the condition of the experiments, the formation of an apatite layer on the surface was faster in the static than in the dynamic system. It was probably due to the release of silicic acid from the

materials into the simulated body fluid medium and the possible building up of a silicic acid concentration in the static biomimetic process that led to the speeding up of calcium phosphate precipitation[52]. However, because of the formation of an apatite layer in the dynamic biomimetic process, it was concluded that the build up of a silicic acid concentration in the static biomimetic process was not the major factor inducing apatite formation of the composites. The circulation and renewing of the medium solution during the test mimicked the best *in vivo* conditions. It must be noticed that the experimental set up for a dynamic biomimetic process and the time scale (15 days) for this experimentation made it difficult to perform an extensive and quantitative study of materials. That is why an alternate soaking process was developed to get quick, reproducible, quantitative measures of the *in vitro* apatite-forming ability of the materials. Also, the results of the alternate soaking process test had to be correlated with the biomimetic process to be meaningful as materials which are non-bioactive in the biomimetic processes can form calcium phosphate material on their surface in the conditions of the alternate soaking process[53].

The *in vitro* apatite forming ability studies of the poly(α-hydroxyacid)-silica sol-gels showed that composite with a weight content of polyester equal to 70 percent precipitates calcium phosphate material on their surface under the conditions of the biomimetic tests. Triethoxysilane terminated poly(ε-caprolactone)-silica sol-gel with 70 percent weight content of polyester precipitated calcium phosphate material on its surface *in vitro*. The modification of the hydroxyl by triethoxysilane end-groups on the poly(α-hydroxyacids) did not significantly influence the *in vitro* apatite forming ability of the corresponding sol-gel composites. The poly(L-lactic acid)-silica sol-gel composites precipitated less calcium phosphate materials on their surface than the poly(ε-caprolactone)-silica sol-gels under the same conditions. The reason was not elucidated but poly(α-hydroxyacids) influenced the formation of the co-continuous sol-gel structures. Thus, the modified chemical and /or physical properties of the sol-gel probably influenced the apatite-forming ability.

To elucidate the effect of the composite structure on the *in vitro* osteoconductivity property, poly(ε-caprolactone)-silica sol-gel composites selected from the statistical design experiment were introduced in the *in vitro* static biomimetic

process. As reported in chapter 5, only material samples containing 30 percent weight silica precipitated calcium phosphate material on their surface. Moreover, it has been observed that a poly(ε-caprolactone)-silica sol-gel composite prepared with HCl/TEOS molar ratio equal to 0.1 precipitated more calcium phosphate material than one prepared with HCl/TEOS molar ratio equal to 0.025. The measure of the silicic acid concentration released from the composite discs to the solution medium after 15 days of soaking were not significantly different for both materials with HCl/TEOS molar ratio equal to 0.1 and 0.025, chapter 5. It was then considered that the difference observed could be due to the different porosity of the materials. An initial nitrogen gas adsorption experiment was carried out on those two materials and the obtained results are presented in Figure 6.3.

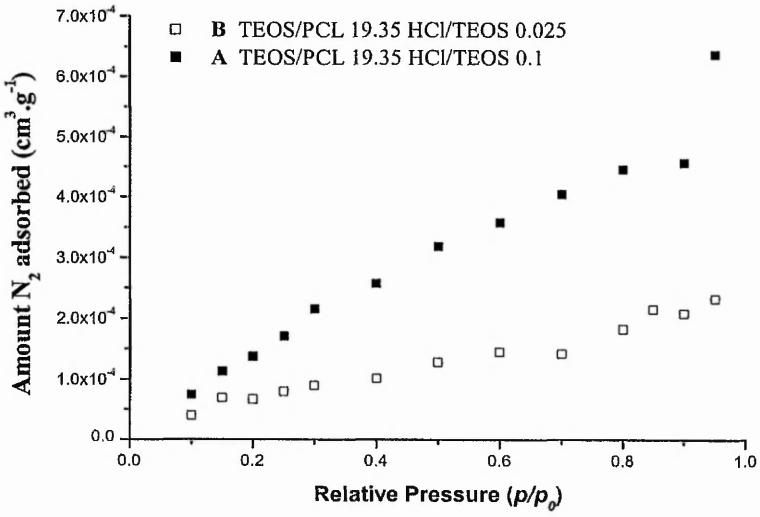

Figure 6.3 : Nitrogen adsorbed as a function of the relative pressure for two poly(ε-caprolactone)-silica sol-gel composites.

The amount of nitrogen adsorbed on the poly(ε-caprolactone)-silica sol-gel composites with a TEOS/PCL molar ratio of 19.35 and HCl/TEOS molar ratio of respectively 0.1 and 0.025 plotted as a function of the relative pressure, Figure 6.3,

showed that at a relative pressure of 0.9 the amount of N_2 adsorbed was in the order $2x10^{-4}$ to $4.5x10^{-4}$ $cm^3.g^{-1}$. These values are typical of non-porous materials. A porous silica gel for example, has a value of N_2 adsorbed in the order of the $cm^3.g^{-1}$. It was then concluded that the apatite-forming ability of the poly(ε-caprolactone)-silica sol-gel composites was not dependent of the material porosity. Interestingly, the rapid kinetics of apatite formation on the surface of bioactive glasses and ceramics has been reported to be partly dependent of the presence of pores (pore size > 2 nm)[54]. The same authors reported that the concentration of hydroxyl groups on the surface of silica surface does not control the rate of hydroxyapatite formation and that the involvement of silanol groups in the nucleation process although possible was not supported by any evidence. Other authors suggested that a silica gel layer is the important factor for the apatite nucleation on bioactive glass and silica sol-gels[55].

Figure 6.4 presents the contact angles (average contact angle of 5 measurements) of poly(ε-caprolactone)-silica sol-gel composites with TEOS/PCL molar ratio equal to 19.35 and 3.226 and HCl/TEOS molar ratio equal to 0.1 and 0.025.

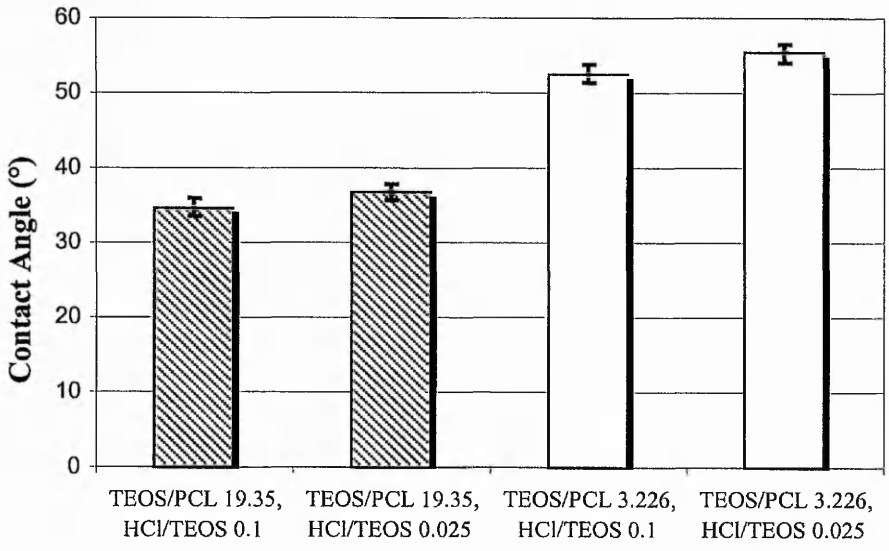

Figure 6.4 : Contact angle measurement on poly(ε-caprolactone)-silica sol-gel composites with 70% and 95% weight content of poly(ε-caprolactone) using deionized water.

The measure of contact angle for the poly(ε-caprolactone)-silica sol-gel composites, Figure 6.4, showed that materials prepared with a TEOS/PCL molar ratio equal to 19.35 (70% wt poly(ε-caprolactone)) had a contact angle lower than those prepared with TEOS/PCL molar ratio equal to 3.226 (95% wt poly(ε-caprolactone)). The value of the contact angle measured for the poly(ε-caprolactone)-silica 70% wt sol-gel composites were slightly lower than the values reported in the literature[29, 38], respectively 40° and 62° for similar composites with 60% and 50% weight content of poly(ε-caprolactone). The contact angle value decreased with the increase of the TEOS/PCL molar ratio (increase of silica content) indicating that the composite surface became more hydrophilic. This is due to an increase of the silanol groups on the composite surface[28]. The obtained results suggested that a minimum amount of silanol groups was necessary to induce apatite formation on the surface of the poly(ε-caprolactone)-silica sol-gel composites. This was in accordance with the proposed mechanism that apatite formation is triggered by a silica gel layer[59].

The contact angle measurement on composite surfaces with constant TEOS/PCL molar ratio and HCl/TEOS molar ratio equal to 0.1 and 0.025 were also collected, Figure 6.4. The average difference in value of the contact angle between the materials with HCl/TEOS molar ratio equal to 0.1 and 0.025 equal to 2.46° was significant compared to the average contact angle standard deviation of five measures for the a same sample composition (equal to 0.87°). The slightly lower value of the contact angle observed for the materials with HCl/TEOS molar ratio equal to 0.1 compared to materials with HCl/TEOS molar ratio equal to 0.025, indicated a more hydrophilic surface for the composites with 0.1 HCl/TEOS molar ratio. From the structural study carried out chapter 3, it was found that increasing the HCl/TEOS molar ratio from 0.025 to 0.1 decreased the measured poly(ε-caprolactone) crystallinity. This suggested that a change of the poly(ε-caprolactone)-silica sol-gel structure properties influenced the surface chemistry and topography of the sol-gel composites. The measurement of contact angle reflected these variations. Also, it was not possible to attribute the variation of contact angle specifically to a topographic or a chemical effect. It must be mentioned that the processing of the materials to obtain analysable surfaces may have

influenced the contact angle measurements. The difference of the *in vitro* apatite-forming ability of the poly(ε-caprolactone)-silica sol-gel composites (molar ratios TEOS/PCL 19.35 and HCl/TEOS 0.1 and 0.025) could possibly be attributed to the variations of the composite surface properties. The increase of composites wettability with the increase of the TEOS/PCL and HCl/TEOS molar ratios was connected with the better *in vitro* osteoconductivity of the materials. This suggested that the contact angle measurement could be used to optimize the bioactive property of the composites.

The study of the effect on the poly(α-hydroxyacid)-silica composites *in vitro* apatite-forming ability on the surface chemistry and topography would allow us to elucidate the mechanisms involved in the nucleation and growth of calcium phosphate materials. Surface defects in silica gel, such as metastable trisiloxane rings, are likely to be associated with apatite nucleation[56] but have not yet been identified experimentally. A recent paper reported that the silica speciation plays an important role in the bioactivity behaviour of glasses[57]. Q^0 species observed by solid state ^{29}Si NMR analysis in some bioglass ®[58] being more active in promoting the formation of a silica gel layer than other silica species because they are more easily leached out. The presence of Q^0 species was due to the disruption of the Si-O-Si bonds in the bioglass by the addition of magnesium oxide. In the poly(α-hydroxyacid)-silica composite, the silica speciation was influenced by the polyester interaction with the silica oligomers. The studies of silicic acid released from poly(α-hydroxyacid)-silica sol-gels, chapter 4, showed that silicic acid (Q^0) leached out more rapidly in poly(L-lactic acid)-silica sol-gels than the corresponding poly(ε-caprolactone)-silica sol-gels prepared with the same TEOS/Poly(α-hydroxyacid) molar ratio. The results in our study are in accordance with the *in vitro* bioactivity mechanism proposed for the bioglass® material[59]; slower release of the silicic acid leads to a slower formation of the silica sol-gel and apatite layers.

The effect of the surface topography may be studied by preparing poly(α-hydroxyacid)-silica sol-gel composites in mould with different and controlled patterns. Then, the prepared sol-gels could be subject to *in vitro* apatite-forming ability tests and the kinetics of apatite formation measured. The use of a quartz crystal microbalance (QCM) coated with the composite, equipped with a flow cell could be a very interesting way to study the kinetics of apatite formation on the surface of the hybrid materials[60, 61].

A QCM quartz coated with a bioactive material in a cell with a simulated body fluid medium may allow the study in real time of the apatite precipitation and give information on the reaction mechanisms. Also, the poly(ε-caprolactone)-silica composites are complex biodegradable materials. Therefore, such a study could be particularly difficult as compared with the QCM studies of protein and cell attachment on biomaterial surfaces[62].

Finally, poly(α-hydroxyacid)-silica composites are potentially very interesting materials for biomedical applications. *In vitro* biocompatibility and apatite-forming properties have been demonstrated. The novel synthesis procedure for the preparation of poly(ε-caprolactone)-silica composite has not yet been fully explored but it could potentially be applied to other hydroxyl terminated poly(α-hydroxyacids) and even other hydroxyl containing macromolecules and lead to a large range of composite materials. Figure 6.5 presents the time of formation of apatite layer on the surface of bioglass ®[16], silica sol-gel[63] and several polymer-silica sol-gel materials[26, 29, 22] *in vitro*.

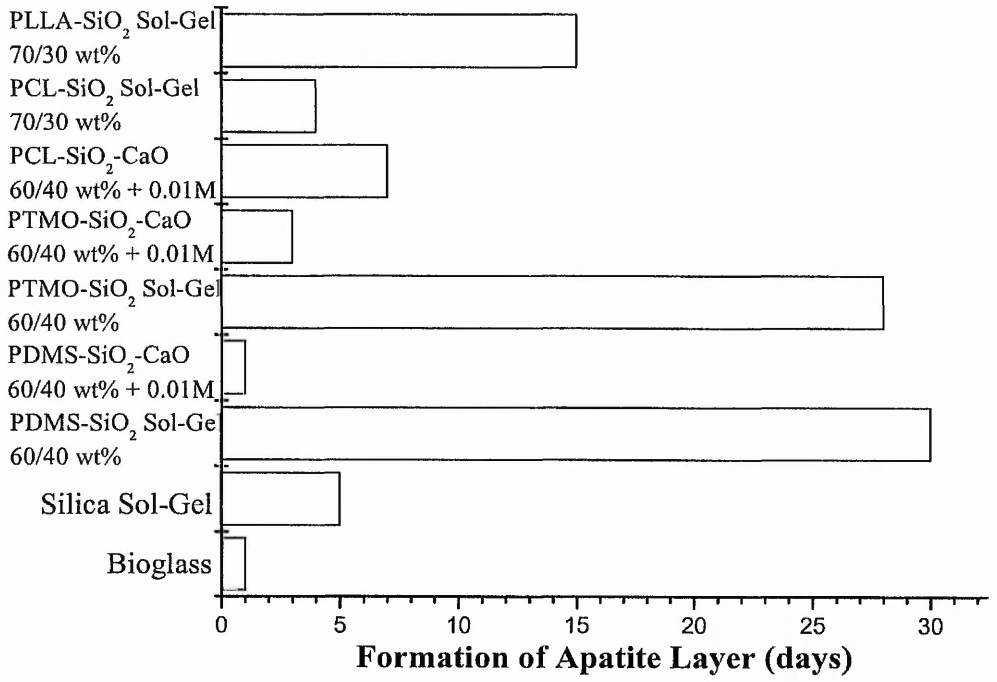

Figure 6.5 : Histogram plot of the time of formation of apatite layer on the surface of bioactive materials *in vitro*.

Figure 6.5 shows that the time of soaking in simulated body fluid necessary for the formation of an apatite layer on the surface of organic polymer-silica sol-gels was higher or equal to the soaking time of a silica sol-gel. *In vivo* and *in vitro* osteoconductivity of the poly(α-hydroxyacid)-silica composites could be improved by the incorporation of calcium oxide during the sol-gel reaction for the formation of the sol-gel composites as already reported for other silica sol-gel composites[44, 64] or during the pre-hydrolysis reaction of alkoxysilanes in the new procedure.

N. Miyata and co-workers reported that the addition of calcium ions in poly(tetramethylene oxide)-silica sol-gel composite decreased the time for apatite layer formation in the static biomimetic process and decreased the tensile strength and Young's modulus of the composite[44]. Therefore, the optimisation of the bioactivity, biodegradation and mechanical properties of the poly(α-hydroxyacid)-silica composites may prove to be challenging.

6.7. References

[1] A. J. Domb, J. Kost, D. M. Wiseman (1997), "Handbook of Biodegradable Polymers", (Harwood Academic).

[2] K. P. Andriano, T. Pohjonen, P. Tormala (1994), "Processing and characterization of absorbable polylactide polymers for use in surgical implants.", *Journal of Applied Biomaterials,* 5(2), 133-140.

[3] G. Schwach, M. Vert (1999), "In vitro and in vivo degradation of lactic acid-based interference screws used in cruciate ligament reconstruction.", *International Journal of Biological Macromolecules,* 25(1-3), 283-291.

[4] T. V. Chirila, P. E. Rakoczy, K. L. Garrett, X. Lou, I. J. Constable (2002), "The use of synthetic polymers for delivery of therapeutic antisense oligodeoxynucleotides.", *Biomaterials,* 23(2), 321-342.

[5] M. Vert, G. Schwach, R. Engel, J. Coudane (1998), "Something new in the field of PLA/GA bioresorbable polymers?", *Journal of Controlled Release,* 53(1-3), 85-92.

[6] J. W. Leenslag, A. J. Pennings, R. R. M. Bos, F. R. Rozema, G. Boering (1987), "Resorbable materials of poly(L-lactide). 6. Plates and screwsfor internal fracture fixation.", *Biomaterials* 8(1), 70-73.

[7] S. Ramakrishna, J. Mayer, E. Wintermantel, K. W. Leong (2001), "Biomedical applications of polymer-composite materials: a review.", *Composites Science and Technology* 61(9), 1189-1224.

[8] J. C. Middleton, A. J. Tipton (2000), "Synthetic biodegradable polymers as orthopedic devices.", *Biomaterials,* 21(23), 2335-2346.

[9] R. Dell'Erba, G. Groeninckx, G. Maglio, M. Malinconico, A. Migliozzi (2001), "Immiscible polymer blends of semicrystalline biocompatible components: thermal properties and phase morphology analysis of PLLA/PCL blends.", *Polymer* 42(18), 7831-7840.

[10] D. K. Gilding, A. M. Reed (1979), "Biodegradable polymers for use in surgery-polyglycolic/poly(lactic acid) homo- and copolymers.", *Polymer*, 20, 1459-1464.

[11] M. Moukwa (1997), "The development of polymer –based biomaterials since 1920s.", *JOM*, 49, 46-50.

[12] N. Ignjatovic, S. Tomic, M. Dakic, M. Miljkovic, M. Plavsic, D. Uskokovic (1999), "Synthesis and properties of hydroxyapatite/poly-L-lactide composite biomaterials.", *Biomaterials*, 20, 809-816.

[13] T. Kasuga, S. Ozaki, T. Hayakawa, M. Nogami, Y. Abe (1999), "Mechanical properties of polylactic acid composites containing ss-Ca(PO3)(2) fibers in simulated body fluid.", *Journal of Materials Science Letters,* 18(24), 2021-2023.

[14] H. Schliephake, T. Kage (2001), "Enhancement of bone regeneration using resorbable ceramics and a polymer-ceramic composite material.", *Journal of Biomedical Materials Research*, 56, 128-136.

[15] L. L. Hench, J. Wilson (1986), "Ciba Foundation Symposium 121. Silicon Biochemistry.Biocompatibility of silicates for medical use.", (Wiley, Chichester), 231-246.

[16] T. Kokubo (1992), "Bone Bonding. Bioactivity of glasses and glass ceramics.", Eds. Ducheyne, T. Kokubo, Van Blitterswijk (Reed Healthcare Communications) 31-46.

[17] S. Radin, S. Falaize, H. L. Mark, P. Ducheyne (2002), "In vitro bioactivity and degradation behavior of silica xerogels intended as controlled release materials.", *Biomaterials,* 23, 3113-3122.

[18] I. D Xynos, A. J. Edgar, L. D. K. Buttery, L. L. Hench, J. M. Polak (2001), "Gene-expression profiling of human osteoblasts following treatment with the ionic products of bioglass.", *Journal of Biomedical Materials Research*, 55, 151-157.

[19] T. Gao, H. T. Aro, H. Ylanen, E. Vuorio (2001), "Silica-based bioactive glasses modulate expression of bone morphogenetic protein-2 mRNA in Saos-2 osteoblasts in vitro." *Biomaterials*, 22, 1475-1483.

[20] S. I. Anderson, S. Downes, C. C. Perry, A. M. Caballero (1998), "Evaluation of the osteoblast response to a silica gel in vitro.", *Journal of Materials Science. Materials in Medicine*, 9, 731-735.

[21] A. Oyane, M. Minoda, T. Miyamoto, K. Nakanishi, M. Kawashita, T. Kokubo, T. Nakamura (2001), "Apatite formation on ethylene-vinyl alcohol copolymer modified with silane coupling agent and calcium silicate.", *Key Engineering Materials*, 192-195, 713-716.

[22] K. Tsuru, C. Ohtsuki, A. Osaka, T. Iwamoto, J. D. Mackenzie (1997), "Bioactivity of sol-gel derived organically modified silicates.", *Journal of Materials Sciences: Materials in Medicine*, 8, 157-161.

[23] J. D. Mackenzie, Y. J. Chung, Y. Hu (1992), "Rubbery ormosils and their applications.", *Journal of Non-Crystalline Solids*, 147&148, 271-279.

[24] G. L. Wilkes, B. Orler, H. H. Huang (1985), "Ceramers: Hybrid materials incorporating polymeric/oligomeric species into inorganic glasses utilizing a sol-gel approach.", *Polymer Preparation*, 26, 300-302.

[25] K. Tsuru, Y. Aburatani, T. Yabuta, S. Hayakawa, C. Ohtsuki, A. Osaka (2001), "Synthesis and in vitro behavior of organically modified silicate containing Ca ions.", *Journal of Sol-Gel Science and Technology*, 21, 89-96.

[26] N. Miyata, K. –I. Fuke, Q. Chen, M. Kawashita, T. Kokubo ,T. Nakamura (2002), "Apatite formation ability and mechanical properties of PTMO-modified CaO-SiO_2 Hybrids prepared by sol-gel processing: Effect of CaO and PTMO contents.", *Biomaterials*, 23, 3003-3040.

[27] S. H. Rhee, J. Y. Choi (2002), "Synthesis of bioactive poly(methyl methacrylate)/silica hybrid.", *Key Engineering Materials.*, 218-220, 433-436.

[28] D. Tian, Ph. Dubois, C. Grandfils, R. Jerome, P. Viville, R. Lazzaroni, J. L. Bredas, P. Leprince (1997), "A novel biodegradable and biocompatible ceramer prepared by the sol-gel process.", *Chemistry of Materials*, 9(4), 871-874.

[29] S. H. Rhee, H. M. Kim (2002), "Preparation of a bioactive polycaprolactone/silica nanocomposite.", *Key Engineering Materials*, 218-220, 453-456.

[30] S. H. Rhee, J. Y. Choi, H. M. Kim (2002), "Preparation of a bioactive and degradable poly(ε-caprolactone)/silica hybrid through a sol-gel method.", *Biomaterials*, 23(24), 4915-4921.

[31] D. Tian, Ph. Dubois, R. Jerome (1996), "A new poly(ε-caprolactone) containing hybrid creamer prepared by the sol-gel process.", *Polymer*, 37(17), 3983-3987.

[32] S. C. Bayne, H. O. Heymann, E. J. Swift, (1994), "Update on dental composite restorations.", *Journal of the American Dental Association, 125(6), 687-701.*

[33] M. L. Cannon (1988), "in Encyclopaedia of dental devices and instrumentation. Composite resins.", ed. J.G. Webster (Wiley & Sons, New-York).

[34] K. Yoshinaga, K. Kondo, A. Kondo (1997), "Capabilities of polymer-modified monodisperse colloid silica particles as biomaterial carrier.", *Colloid Polymers Science*, 275, 220-226.

[35] Y. Wei, K. Qiu (2000), "Synthesis and biotechnological applications of vinyl polymer-inorganic hybrid and mesoporous materials.", *Chinese Journal of Polymer science*, 18(1), 1-7.

[36] D. Tian, Ph. Dubois, R. Jerome (1997), "Biodegradable and biocompatible inorganic-organic hybrids materials I. Synthesis and characterization.", *Journal of Polymer Science. Part A. Polymer Chemistry*, 35, 2295-2309.

[37] D. Tian, S. Blacher, Ph. Dubois, R. Jerome (1998), "Biodegradable and biocompatible inorganic-organic hybrid materials. 2. Dynamic mechanical properties, structure and morphology.", *Polymer*, 39(4), 855-864.

[38] D. Tian, Ph. Dubois, C. Grandfils, R. Jerome, P. Viville, R. Lazzaroni, J. L. Bredas, P. Leprince (1997), "A novel biodegradable and biocompatible ceramer prepared by the sol-gel process.", *Chemistry of Materials*, 9(4), 871-874.

[39] S. Jiang, X. Ji, L. An, B. Jiang (2001), "Crystallization behavior of PCL in hybrid confined environment" *Polymer,* 42(8), 3901-3907.

[40] L. E. Alexander, (1952), "X-ray Diffraction Procedures for polycrystalline and amorphous materials" eds Klug H. P., Alexander L. E., John Wiley and Sons.

[41] M. R. Landry, B. K. Coltran, C. J. T. Landry, J. M. O'Reilly (1995), "Structural models for homogeneous organic-inorganic hybrid materials. Simulations of small angle X-ray scattering profiles.", *Journal of Polymer Science: Part B: Polymer Physics* 33(4), 637-655.

[42] R. Takahashi, K. Nakanishi, N. Soga (2000), "Aggregation behavior of alkoxide-derived silica in sol-gel process in presence of poly(ethylene oxide).", *Journal of Sol-Gel Science and Technology*, 17, 7-18.

[43] J. Fu, J. Fiegel, E. Krauland, J. Hanes (2002), "New polymeric carrier for controlled drug delivery following inhalation or injection.", *Biomaterials*, 23, 4425-4433.

[44] N. Miyata, K. Fuke, Q. Chen, M. Kawashita, T. Kokubo, T. Nakamura (2002), "Apatite-forming ability and mechanical properties of PTMO-modified CaO-SiO_2 hybrids prepared by sol-gel processing: effect of CaO and PTMO contents." *Biomaterials*, 23, 3033-3040.

[45] Y. G. Hsu, I. L. Chiang, J. F. Lo (2000), "Properties of hybrid materials derived from hydroxyl-containing linear polyester and silica through sol-gel process. I. Effect of thermal treatment.", *Journal of Applied Polymer Science*, 78, 1179-1190.

[46] H. Korhonen, A. Helminen, J. V. Seppala (2001), "Synthesis of polylactides in the presence of co-initiators with different numbers of hydroxyl groups.", *Polymer*, 42, 7541-7549.

[47] W. P. Ye, F. S. Du, W. H. Jin, J. Y. Yang, Y. Xu (1997), "In vitro degradation of poly(caprolactone), poly(lactide) and their block copolymers: influence of composition, temperature and morphology.", *Reactive & Functional Polymers*, 32, 161-168.

[48] M. Vert, G. Schwach, R. Engel, J. Coudane (1998), "Something new in the field of PLA/GA bioresorbable polymers?", *Journal of Controlled Release*, 53, 85-92.

[49] C. G. Pitt, F. I. Chasalow, Y. M. Hibionada, D. M. Klimas, A. Schindler (1981), "Aliphatic polyesters. I. The degradation of poly(ε-caprolactone) *in vivo*.", *Journal of Applied Polymer Science*, 26, 3779-3787.

[50] S. Radin, S. Falaize, M. H. Lee, P. Ducheyne (2002), "In vitro bioactivity and degradation behaviour of silica xerogels intended as controlled release materials.", *Biomaterials*, 23, 3113-3122.

[51] P. Kortesuo, M. Ahola, S. Karlsson, I. Kangasniemi, A. Yli-Urpo, J. Kiesvaara (2000), "Silica xerogel as an implantable carrier for controlled drug delivery. Evaluation of drug distribution and tissue effects after implantation.", *Biomaterials*, 21, 193-198.

[52] J. J. M. Damen, J. M. Ten Cate (1989), "The effect of silicic acid on calcium phosphate precipitation.", *Journal of Dental Research*, 68(9), 1355-1359.

[53] T. Karita, K. Imachi, T. Taguchi, A, Kishida, M. Akashi (2000), "*In vitro* calcification model. Part 1. Apatite formation on segmented polyurethane containing silicone using an alternate soaking process.", *Journal of Bioactive and Compatible Polymers*, 15, 72-84.

[54] M. M. Pereira, L. L. Hench (1996), "Mechanisms of hydroxyapatite formation on porous Gel-silica Substrates.", *Journal of Sol-Gel Science and Technology,* 7, 59-68.

[55] P. Li, C. Ohtsuki, T. Kokubo, K. Nakanishi, N. Soga (1992), "Apatite formation induced by silica gel in simulated body fluid.", *Journal of The American Ceramics Society*, 75, 2094-2107.

[56] N. Sahai, J. A. Tossell (2000), "Molecular orbital study of apatite ($Ca_5(PO_4)_3OH$) nucleation at silica bioceramic surfaces.", *Journal of Physic Chemistry. Part B*, 104, 4322-4314.

[57] J. M. Oliveira, R. N. Correia, M. H. Fernández (2002), "Effects of Si speciation on the in vitro bioactivity of glasses.", *Biomaterials*, 23, 371-379.

[58] J. M. Oliviera, R. N. Correia, M. H. V. Fernándes, J. Rocha (2000), "Influence of the CaO/MgO ratio on the structure of phase-separated glasses: a solid state ^{29}Si and ^{31}P MAS NMR study.", *Journal of Non-crystalline Solids*, 265, 221-229.

[59] L. L. Hench (17 July 1995), "Bioactive implants.", *Chemistry and Industry*, 547-550.

[60] P. X. Zhu, Y. Masuda, K. Koumoto (2001), "Site-selective adhesion of hydroxyapatite microparticles on charged surfaces in a supersaturated solution.", *Journal of Colloid and Interface Science*, 243(1), 31-36.

[61] M. Tanahashi, T. Matsuda (1997), "Surface functional group dependence on apatite formation on self-assembled monolayers in a simulated body fluid.", *Journal of Biomedical Materials Research*, 34(3), 305-315.

[62] F. Hook, J. Voros, M. Rodahl, R. Kurrat, P. Boni, J. J. Ramsden, M. Textor, N. D. Spencer, P. Tengvall, J. Gold, B. Kasemo (2002), "A comparative study of protein adsorption on titanium oxide surfaces using in situ ellipsometry, optical waveguide lightmode spectroscopy, and quartz crystal microbalance/dissipation.", *Colloids and Surfaces B. Biointerfaces*, 24, 155-170.

[63] P. Li, K. Nakanishi, T. Kokubo, K. De Groot (1993), "Induction and morphology of hydroxyapatite, precipitated from metastable simulated body fluids on sol-gel prepared silica.", *Biomaterials*, 14(13), 963-968.

[64] Q. Chen, F. Miyaji, T. Kokubo, T. Nakamura (1999), "Apatite formation on PDMS-modified $CaO-SiO_2-TiO_2$ hybrids prepared by sol-gel process.", *Biomaterials*, 20, 1127-1132.